

GROUP RESISTANCE OF RECYCLED PLASTIC PIN IN
SUSTAINABLE SLOPE STABILIZATION

by

MOHAMMAD REZAUL HAQUE BHUIYAN

Presented to the Faculty of the Graduate School of
The University of Texas at Arlington in Partial Fulfillment
of the Requirements
for the Degree of

MASTER OF SCIENCE IN CIVIL ENGINEERING

THE UNIVERSITY OF TEXAS AT ARLINGTON

May 2014

Copyright © by Mohammad Rezaul Haque Bhuiyan 2014

All Rights Reserved



Acknowledgements

I would like to express my heartiest gratitude to Dr. Sahadat Hossain for his constant support and guidance throughout my time at the University of Texas at Arlington. My appreciation extends to Dr. Xinbao Yu and Dr. Laureano R. Hoyos for their instruction, wisdom and guidance.

I greatly appreciate the contribution of Dr. Xinbao Yu and Dr. Mohammad Najafi to improve my thesis with their valuable advice and suggestions, and for devoting their time in my committee.

A special thanks needs to be extended to Dr. Mohammad Sadik Khan. Without the help, instruction, guideline and support from him I could not have completed my Master's thesis.

I am thankful to my wife Ayesha Aman, daughter Rukayat Reza and my parents for being with me as the source of my inspiration. I am truly blessed to them in my life.

I appreciate all the help and support from my fellow classmates and friends, namely Golam Kibria, Depak Tiwari, Alejandro and Brett DeVries.

I am thankful to almighty ALLAH for giving me the courage, strength and patience to achieve my goal.

April 16, 2014

Abstract

GROUP RESISTANCE OF RECYCLED PLASTIC PIN IN SUSTAINABLE SLOPE STABILIZATION

Mohammad Rezaul Haque Bhuiyan

The University of Texas at Arlington, 2014

Supervising Professor: MD. Sahadat Hossain

Slope failure is a common phenomenon in areas with slope constructed on high plasticity clay and shallow slope failure is predominant in North Texas. The cumulative maintenance cost of minor slides is equal or greater than major landslides. But, cost associated with post failure maintenance can be reduced significantly if an appropriate stabilization method is adopted. Thus, selection of appropriate and economically viable slope stabilization method has got great importance for the geotechnical engineers.

Recently, a new approach of shallow slope stabilization technique is introduced using Recycled Plastic Pin (RPP). RPP used in shallow slope stabilization should pass beyond the slip surface to pin the sliding surface with the stiff soil.

An extensive study based on the field performance of RPP installed for shallow slope stabilization was carried out by Loehr and Boders in Missouri, and Khan in Texas. In most of the cases, the horizontal displacement of RPP reinforced slope was about 3 inches both in Missouri and in Texas. The field investigation of the RPP reinforced slopes leads researchers to develop two new design protocols. They are limit resistance method by Loehr and Boders and performance based method by Khan. The limit resistance design method did not consider the effects of creep of RPP. This limitation was taken into account and a new performance based design method is proposed by Khan. But,

instead of considering group resistance of RPP, only resistance of single RPP is considered in performance based method.

Thus, the objective of this study is to determine the group resistance of RPP in sustainable slope stabilization. To attain the goal, number of RPP required forming an effective group at different spacing is determined. In order to fulfill the objective, an extensive study has been conducted based on numerical modeling and supported by field data. Thereby, a new design chart is proposed considering group resistance of RPP, where maximum horizontal displacement and flexural stress of RPP are taken into account.

Parametric study is carried out to determine the variation of resistance between group of RPP and single RPP at different loading condition, soil strength parameters, spacing and depth of slip surface, where the horizontal displacement of single RPP and group of RPP is determined and plotted graphically. The graphical representation shows the difference of resistance between group of RPP and single RPP with increasing load, soil strength, spacing and depth of slip surface. Thus, the design charts for group of RPP at different spacing are developed considering different types of soil for different slope, where the horizontal displacement and/or flexural stress is shown with increasing applied load.

Similar conditions of Interstate 70-Emma Site, as presented in the literature by Loehr and Borders is plotted on developed design chart for 4-ft deep slip surface. The interpolated horizontal displacement according to the developed design chart for RPP at 3-ft spacing is 0.51 and is in good agreement with Interstate 70-Emma Site.

Finally, a multiplication factor is introduced to establish a relationship between the developed design charts to performance based method.

Table of Contents

Acknowledgements	iii
Abstract	iv
List of Illustrations	xi
List of Tables	xvi
Chapter 1 Introduction.....	1
1.1 Background.....	1
1.2 Problem Statement.....	2
1.3 Research Objective	3
1.4 Organization of the Study	3
Chapter 2 Literature Review	5
2.1 Introduction	5
2.2 Types of Slope Failure.....	6
2.3 Shallow Slope Failure	7
2.4 Remedies to Prevent Shallow Slope Failure	8
2.4.1 Unloading	8
2.4.2 Buttreassing	8
2.4.2.1 Soil and Rock Fill	8
2.4.2.2 Shear Keys	9
2.4.2.3 Counterberms	9
2.4.2.4 Pneusol (tiresoil)	9
2.4.2.5 Mechanically Stabilized Embankments (MSE)	9
2.4.3 Drainage.....	11
2.4.3.1 Surface Drainage	11
2.4.3.2 Subsurface Drainage	11

2.4.4 Vegetation	12
2.4.5 Retaining Walls	12
2.4.5.1 Conventional Gravity or Cantilever Retaining Wall	12
2.4.5.2 Drilled Shaft Walls	12
2.4.5.3 Driven Piles	13
2.4.5.4 Tieback Walls	14
2.4.5.5 Gabion Walls	15
2.4.6 Surface Slope Protection	15
2.4.7 Soil Hardening	16
2.4.7.1 Grouting	16
2.4.7.2 Compacted Soil-Cement Fill	16
2.4.7.3 Electro-osmosis	16
2.4.7.4 Lime Injection	18
2.4.7.5 Preconsolidation	18
2.4.7.6 Thermal Treatment	18
2.4.8 Reinforcement	18
2.4.8.1 Geosynthetically Reinforced Slopes	19
2.4.8.2 Stone Columns	19
2.4.8.3 Soil Nailing	20
2.4.8.4 Reticulated Micropiles	21
2.4.8.5 Plate Piles	22
2.4.8.6 Recycled Plastic Pins	23
2.5 Recycled Plastic Pin	23
2.5.1 Engineering Properties of RPP	23
2.5.2 Creep of RPP	26

2.5.2.1 Compression Creep of RPP	26
2.5.2.2 Flexural Creep	27
2.5.2.3 Estimation of Creep Life.....	29
2.6 Slope Stabilization with Recycled Plastic Pin	30
2.6.1 Field Performance of RPP	31
2.6.1.1 Interstate 70-Emma Site	31
2.6.1.2 US 36 Highway Site	33
2.6.1.3 US 287 Highway Site	35
2.6.1.4 Loop 12 Highway Site	36
2.6.2 Design Methods	38
2.6.2.1 Limit Resistance Method (Loehr and Borders, 2007)	38
2.6.2.2 Performance Based (Khan, 2013)	42
2.7 Limitations of Previous Studies	47
2.7.1 Limit Resistance Method	47
2.7.2 Performance Based Method	48
2.7.3 Room for Future Studies	48
Chapter 3 Methodology	49
3.1 Introduction	49
3.2 Soil and Reinforcement Parameters.....	50
3.3 Model Configuration	51
3.4 Selection of Number of RPP.....	52
3.5 Parametric Study on the Group Effect of RPP	57
3.6 Development of Design Chart	58
3.7 Comparison with Field Data	61
3.8 Effect of Spacing.....	61

3.9 Determination of Multiplication Factor	62
Chapter 4 Results and Discussions	63
4.1 Introduction	63
4.2 Effects of Spacing	63
4.2.1 Effect of Spacing of RPP at different Loading Condition	63
4.2.2 Effect of Spacing at different Slip Surface	65
4.2.3 Effect of Soil Strength on RPP Spacing	66
4.2.4 Effect of Spacing on Flexural Stress	68
4.2.5 Most Efficient Spacing	68
4.3 Effect of Loading	69
4.4 Effect of Depth of Slip Surface	71
4.4.1 Depth of Slip Surface 3 ft	71
4.4.2 Depth of Slip Surface 5 ft	73
4.4.3 Depth of Slip Surface 7 ft	75
4.5 Effect of Soil Strength	77
4.5.1 Effect of Cohesion	78
4.5.2 Effect of Friction Angle	80
4.6 Development of Design Chart considering Group Effect	82
4.7 Comparison	83
4.7.1 Comparison with Field Data	83
4.7.2 Comparison with Performance based Method proposed by Khan (2013)	86
4.8 Multiplication Factor	91
4.9 Factor of Safety Calculation	95

Chapter 5 Conclusions and Recommendations for Future Research	97
5.1 Summary and Conclusions.....	97
5.2 Recommendations for Future Works.....	99
Appendix A Effect of Load on Increasing Number of RPP	100
Appendix B Design Chart for Group Resistance of RPP	117
Appendix C Multiplication Factors for Horizontal Displacement and Flexural stress.....	184
Appendix D Calculation of Factor of Safety for RPP Reinforced Slope using Multiplication Factors	195
Appendix E Calculation of Factor of Safety for RPP Reinforced Slope using Group Resistance Design Charts	197
References.....	202
Biographical Information	205

List of Illustrations

Figure 2.1 Geometry of slip circle analysis (Abramson et al., 2002).	5
Figure 2.2 Types of movement in clay slopes. (redrawn after Abramson et al., 2002).	7
Figure 2.3 Rock buttress (Abramson et al., 2002).	10
Figure 2.4 Weight at toe provided by Counterberm (Abramson et al., 2002).	10
Figure 2.5 Slope stabilized with Pneusol buttressing (Abramson et al., 2002).....	10
Figure 2.6 Stabilized slope with MSE (Abramson et al., 2002).....	11
Figure 2.7 Conventional gravity or cantilever retaining wall (Abramson et al., 2002).	13
Figure 2.8 Drilled shaft wall stabilized slope (Abramson et al., 2002).	13
Figure 2.9 Driven piles stabilized slope (Abramson et al., 2002).....	14
Figure 2.10 Schematic showing tieback walls (Abramson et al., 2002).	14
Figure 2.11 Rip-rap to protect erosion at toe of a slope (Abramson et al., 2002).	15
Figure 2.12 Slope reinforced with geosynthetic materials (Abramson et al., 2002).	19
Figure 2.13 Stone columns stabilized unstable slope (Abramson et al., 2002).	20
Figure 2.14 Schematic diagram of soil nailing system (Abramson et al., 2002).	21
Figure 2.15 Schematic of reticulated micropiles (Abramson et al., 2002).	22
Figure 2.16 Stabilization of Slope using plate pile (McCormick and Short, 2006).	22
Figure 2.17 Typical deflection of RPP under constant axial stress with time (Chen et al., 2007).	26
Figure 2.18 RPP testing setup for flexural creep (Chen et al., 2007).	28
Figure 2.19 Deflection of RPP under 222 N loads with respect to time (Chen et al., 2007).	28
Figure 2.20 Method to estimate time of failure due to flexural creep of RPP (redrawn after Chen et al., 2007).....	30
Figure 2.21 Schematic of slide areas on I-70 Emma site (Loehr and Border, 2007).	32

Figure 2.22 Plan view of stabilized sections of slide area S3 (Loehr and Borders, 2007).	33
Figure 2.23 Plan Views of stabilized sections of US36 Highway (Loehr and Borders, 2007).	34
Figure 2.24 RPP layouts on US287 Highway slope (Khan M. S., 2013).	36
Figure 2.25 Layouts of stabilized sections of Loop 12 Highway (Khan, M. S., 2013).	37
Figure 2.26 Resisting force due to installed RPP on an individual slice in Method of Slices (Loehr and Borders, 2007).	38
Figure 2.27 Schematic and Limit Resistance Curve for Failure Mode 1 (Loehr and Borders, 2007).	39
Figure 2.28 Schematic and Limit Resistance Curve for Failure Mode 2 (Loehr and Borders, 2007).	40
Figure 2.29 Schematic and Limit Resistance Curve for Failure Mode 3a (Loehr and Borders, 2007).	41
Figure 2.30 Schematic and Limit Resistance Curve for Failure Mode 3b (Loehr and Borders, 2007).	41
Figure 2.31 Composite Limit Resistance Curve for all Failure Modes (Loehr and Borders, 2007).	42
Figure 2.32 Soil model for determination of maximum horizontal displacement and flexural stress of RPP due to mobilized load (Khan, 2013).	46
Figure 2.33 Limit Resistance Curve for RPP, a. load vs horizontal displacement, b. load vs maximum flexural stress (Khan, 2013).	47
Figure 3.1 Representative model with all structural elements.	51
Figure 3.2 Generated mesh for a slope ratio of 2H:1V at initial condition.	52
Figure 3.3 Flow chart for selection of number of RPP to form an effective group.	54

Figure 3.4 Representative Model of increasing RPP at 2 ft spacing for 2H:1V slope and 3-ft deep slip surface.	55
Figure 3.5 Influence of mobilized load on increasing number of RPP spaced at, a. 2-ft, b.3-ft, c. 4-ft.	56
Figure 3.6 Influence of mobilized load on increasing number of RPP spaced at, a. 5-ft, b. 6-ft.	57
Figure 3.7 Representative model for development of design chart considering group resistance for, a. slope 2H:1V, b. slope 3H:1V, c. slope 4H:1V.....	59
Figure 3.8 Flow chart showing sequential development of design chart.	60
Figure 3.9 Seven feet deep slip surface stabilized with RPP at 2-ft spacing for a slope of 2H:1V showing, a. horizontal displacement of RPP, b. bending moment diagram of RPP.	61
Figure 3.10 Effect of spacing on horizontal displacement of RPP due to 500 psf horizontal load.....	62
Figure 4.1 Influence of small mobilized load on increasing spacing of RPP	64
Figure 4.2 Influence of different loading condition on increasing spacing of RPP.	64
Figure 4.3 Effect of RPP spacing for 3-ft deep slip surface.	65
Figure 4.4 Effect of RPP spacing for 5-ft deep slip surface.	66
Figure 4.5 Effect of soil strength on RPP spacing for a soil of, a. $c=300$ psf and, $\phi=30^\circ$, b. $c=100$ psf and, $\phi=10^\circ$	67
Figure 4.6 Effect of spacing on flexural stress for different slip surface	68
Figure 4.7 Influence of lower mobilized load (100 psf) on increasing number of RPP.	70
Figure 4.8 Effect of mobilized load on group of RPP and single RPP.....	70
Figure 4.9 Influence of different loading condition on different slip surface.....	72

Figure 4.10 Influence of 500 psf load on RPP at 2-ft spacing in terms of, a. bending moment diagram and b. horizontal displacement, for 3-ft deep slip surface (slope 2H:1V).	72
Figure 4.11 Influence of 500 psf load on RPP at 2-ft spacing in terms of, a. bending moment diagram and b. horizontal displacement, for 5-ft deep slip surface (slope 2H:1V).	74
Figure 4.12 Influence of 500 psf load on RPP at 2-ft spacing in terms of, a. bending moment diagram and b. horizontal displacement, for 7-ft deep slip surface (slope 2H:1V).	76
Figure 4.13 Group Resistance of RPP with respect to soil strength.....	77
Figure 4.14 Influence of cohesive strength on horizontal displacement for a soil having, a. friction angle of 0° , b. friction angle of 30°	79
Figure 4.15 Influence of friction angle on horizontal displacement for a soil having, a. cohesive strength of 200 psf, b. cohesive strength of 300 psf.....	81
Figure 4.16 Limit Resistance Curve for group of RPP, a. load versus horizontal displacement, b. load vs maximum flexural stress.	82
Figure 4.17 Limit Resistance Curves of RPP at 2 ft spacing for, a. flexural stress, b. horizontal displacement.	84
Figure 4.18 Limit Resistance Curves of RPP at 4 ft spacing for, a. flexural stress, b. horizontal displacement.	85
Figure 4.19 Limit Resistance Curves showing horizontal displacement of group versus single RPP for, a. 3-ft, b. 5-ft, c. 7-ft deep slip surface, for a soil of $c=200$ psf and, $\phi=0^\circ$	87
Figure 4.20 Limit Resistance Curves of group versus single RPP for flexural stress of, a. 3-ft, b. 5-ft, c. 7-ft deep slip surface, in case of a soil having $c=200$ psf and, $\phi=0^\circ$	88

Figure 4.21 Limit Resistance Curves showing horizontal displacement of group versus single RPP for, a. 3-ft, b. 5-ft, c. 7-ft deep slip surface, for a soil of $c=300$ psf and, $\phi=30^\circ$.	89
Figure 4.22 Limit Resistance Curves of group versus single RPP for flexural stress of, a. 3-ft, b. 5-ft, c. 7-ft deep slip surface, in case of a soil having $c=300$ psf and, $\phi=30^\circ$.	90
Figure 4.23 Determination of Multiplication factor for, a. Horizontal Displacement, b. Flexural Stress.	92

List of Tables

Table 2.1 Triaxial strength (28 curing days) and cement content.	17
Table 2.2 Summary and detailed results of tested RPP (Chen et al., 2007).	24
Table 2.3 Results of Four Point Bending Test (Bowders et al., 2003).	25
Table 2.4 Weathering effect on typical RPP (Krishnaswamy and Francini, 2000).	25
Table 2.5 Summary of results on compressive creep of RPP (Chen et al., 2007).	27
Table 2.6 Summarized results of flexural creep tests on RPPs (Chen et al., 2007).	29
Table 2.7 Creep rate for I 70-Emma site slide area S3 (Loehr and Borders, 2007).	33
Table 2.8 Summary of Failure Modes (Loehr and Borders, 2007).	39
Table 2.9 Numerical model matrix for Parametric study (Khan, 2013).	44
Table 2.10 Consideration for development of graphical design chart (Khan, 2013).	44
Table 2.11 Soil and RPP strength parameters used for FEM analysis (Khan, 2013).	45
Table 2.12 Soil parameters used for development of design chart (Khan, 2013).	45
Table 3.1 Numerical modeling parameters.	50
Table 3.2 Reinforcement parameters.	50
Table 4.1 Multiplication Factor between RPP Grouped at Different Spacing vs Single RPP for Slope Ratio of 2H:1V	93
Table 4.2 Soil parameters (Khan, 2013).	96
Table 4.3 Factor of Safety of RPP reinforced slope for allowable horizontal displacement of 2 inch (Khan, 2013).	96
Table 4.4 Calculation of Multiplication Factors for RPP at 3-ft spacing.	96

Chapter 1

Introduction

1.1 Background

Slope failure is a geological phenomenon which is known as landslide or landslip. It is a great concern as it includes downward movement of top soil causing loss of lives, properties and disruptions of communications. Slope failure generally occurs due to gravitational force triggered by excessive rainfall. The recent estimated cost per year to maintain and repair landslides involving US major highways exceeds \$100 million (Loehr and Borders, 2007). A large amount of maintenance and repair budget is depleted to maintain and repair shallow slope failures. The depth of shallow slope failure varies from 3-ft to 6-ft and it is known as surficial slope failure.

Though shallow slope failure is not usually hazardous for human life but it can disrupt the communication system by creating road block on the road surface and attribute financial loss by damaging the guardrails, shoulders, road surface, drainage facilities, utility poles (Titi and Helwany, 2007). In order to mitigate surficial slide problems \$1 million per year on average is needed for Missouri Department of Transportation (Loehr and Borders, 2007). On the other hand, the cumulative maintenance cost of minor slides is equal or greater than major landslides (Turner and Schuster, 1996). Therefore, to resist shallow slope failure various methods have been adopted.

Presently, slope failure is prevented by installing soilnails, retaining wall, drilled shafts, lime injection, MSE wall, geosynthetics, etc. The selection of appropriate type of remedial measure depends on various factors such as technical constraints, site constraints, environmental constraints, aesthetic constraints, schedule constraints and cost (Abramson et al., 2002).

Recent use of recycled plastic pin (RPP) to stabilize shallow slope opens a new arena to resist shallow slope failure. Recycled plastic pins are manufactured from plastic wastes. Basically, it is composed of High Density Polyethylene, HDPE (55%-70%), Low Density Polyethylene, LDPE (5%-10%), Polystyrene, PS (2%-10%), Polypropylene, PP (2%-7%), Polyethylene-terephthalate, PET (1%-5%), and varying amount of additives. Sawdust and fly ash (0%-5%) used as additives. That's why, it provides an additional market for recycled plastic and will reduce the volume of non degradable waste entering the landfill. Transportation and installation of RPP is comparatively less as it is a lightweight material. Thus using RPP in slope stabilization has got great economic advantages over other traditional methods. Moreover, it is also environmental friendly as it is not susceptible to environmental degradation due to chemical and biological attack. RPPs are already utilized in Missouri and Texas, and found to be effective in shallow slope stabilization.

1.2 Problem Statement

In order to estimate the resistance offered by RPP used in stabilizing shallow slope failure, different design chart is developed as an outcome of different research. Loehr and Borders (2007) developed a limit resistance design chart but did not consider the effect of creep of RPP. Then, Khan (2013) proposed a new design method to determine the horizontal displacement considering the effect of creep under sustained load. This design method is developed based on Numerical modeling in conjunction with field data obtained from US287 highway and Loop 12 Highway. But Khan (2013) only considers single RPP under sustained load instead of considering the group resistance of RPP, though RPPs are always installed in group to stabilize a slope. Thus, the group resistance of RPP should be evaluated considering horizontal displacement and flexural stress induced on RPP due to mobilized load.

1.3 Research Objective

The main objective of this study is to determine the group resistance offered by RPP used in shallow slope stabilization. To accomplish the objective, the steps listed subsequently were conducted.

1. Determination of number of RPP needed to form an effective group.
2. Development of design chart considering spacing between RPP for different type of soil and slope condition using FEM analysis.
3. Analyzing effect of spacing of RPP considering horizontal displacement and flexural stress at different loading condition, depth of slip surface and soil strength parameters.
4. Comparison of group resistance of RPP with resistance offered by single RPP.
5. Introducing a new multiplication factor comparing group resistance of RPP with resistance of single RPP.
6. To study the influence of group resistance of RPP on Factor of Safety of RPP reinforced slope.

1.4 Organization of the Study

The subject matter of the thesis divided into five chapters and the following provides a brief summary of each chapter.

Chapter 1 provides an introduction with scope of this study.

Chapter 2 presents different techniques found in literature applied to resist shallow slope failure. Moreover, usage of RPP in shallow slope stabilization and developed design chart to use RPP in shallow slope stabilization is also included in this chapter.

Chapter 3 describes the chronological steps followed to select the number of RPP required to simulate an effective group considering 2-ft, 4-ft and 6-ft spacing of RPP within a group. Finally develop a new design chart considering group resistance of RPP at different spacing.

Chapter 4 analyses the effect of loading, depth of slip surface, soil strength, spacing of RPP to evaluate and compare the group resistance of RPP with respect to single RPP. Hence, propose a multiplication factor for horizontal displacement and flexural stress considering RPP spaced at 2-ft or 4-ft or 6-ft apart for different soil and slope.

Chapter 5 is the chapter where general conclusions about the results from the study are provided.

Appendix A shows the influence of mobilized load on increasing number of RPP.

Appendix B presents the developed design charts considering group resistance at different spacing of RPP.

Appendix C represents the Multiplication Factors for horizontal displacement and flexural stress of RPP grouped at different spacing for different soil and slope.

Appendix D portrays a sample calculation of Factor of Safety using Multiplication Factors.

Appendix E shows a sample calculation of Factor of Safety using developed design charts considering group resistance of RPP.

Chapter 2

Literature Review

2.1 Introduction

Slope failure is a geological phenomenon which is also known as landslide or landslip. It is a great concern for the geotechnical engineers and it includes ground movement causing loss of lives, properties and communication disruptions. Gravitational force is the driving force for slope failure. But there are other factors causing slope failure like excessive rainfall for prolonged period, additional overburden pressure on a slope caused due to huge snow fall, steepness of the slope, strength of the soil, scouring and earth quake can be another triggering factor for slope failure. Thus, slope stability is a great challenge for the geotechnical engineer till today.

Slope stability is expressed in terms of Factor of Safety, the ratio between resisting force or moment offered by the soil to acting/driving force or moment applied on the soil. Typically, factor of safety should be 1.25 to 1.5 for a stable slope (Abramson et al., 2002). The resisting force offered by the soil due to its cohesive strength and frictional resistance, and can be expressed according to Mohr-Coulomb theory as $S = c + \sigma_n \tan \phi$ (Abramson et al., 2002).

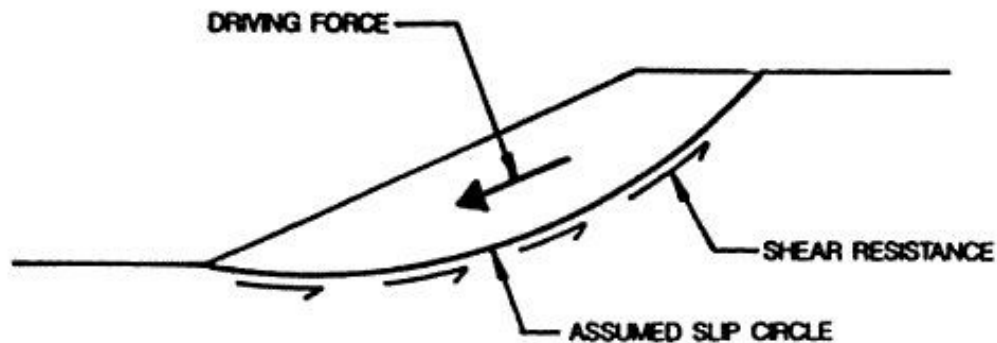


Figure 2.1 Geometry of slip circle analysis (Abramson et al., 2002).

Where, T = shearing stress along the assumed failure surface

S = shear strength of the soil

Factor of Safety = S / T

2.2 Types of Slope Failure

The rate of slope movement ranges from less than 6 inches per year to more than 5 ft per second according to Cruden and Varnes (1992) and post failure movement on existing slip surface varies from 8 inches to 20 ft per year (Abramson et al., 2002).

Slope failure is a downward movement of top soil on failure surface and usually shows a sign of crack in the original ground surface. The slope movement might be transitional or rotational or combination of both, known as compound slide. Transitional movement occurs along predefined discontinuities or planes of weakness and along existing failure surface, whereas rotational movement occurs along concave upward failure surface mostly in an intact soil mass (Abramson et al., 2002). Different types of slope failure are portrayed in Figure 2.2.

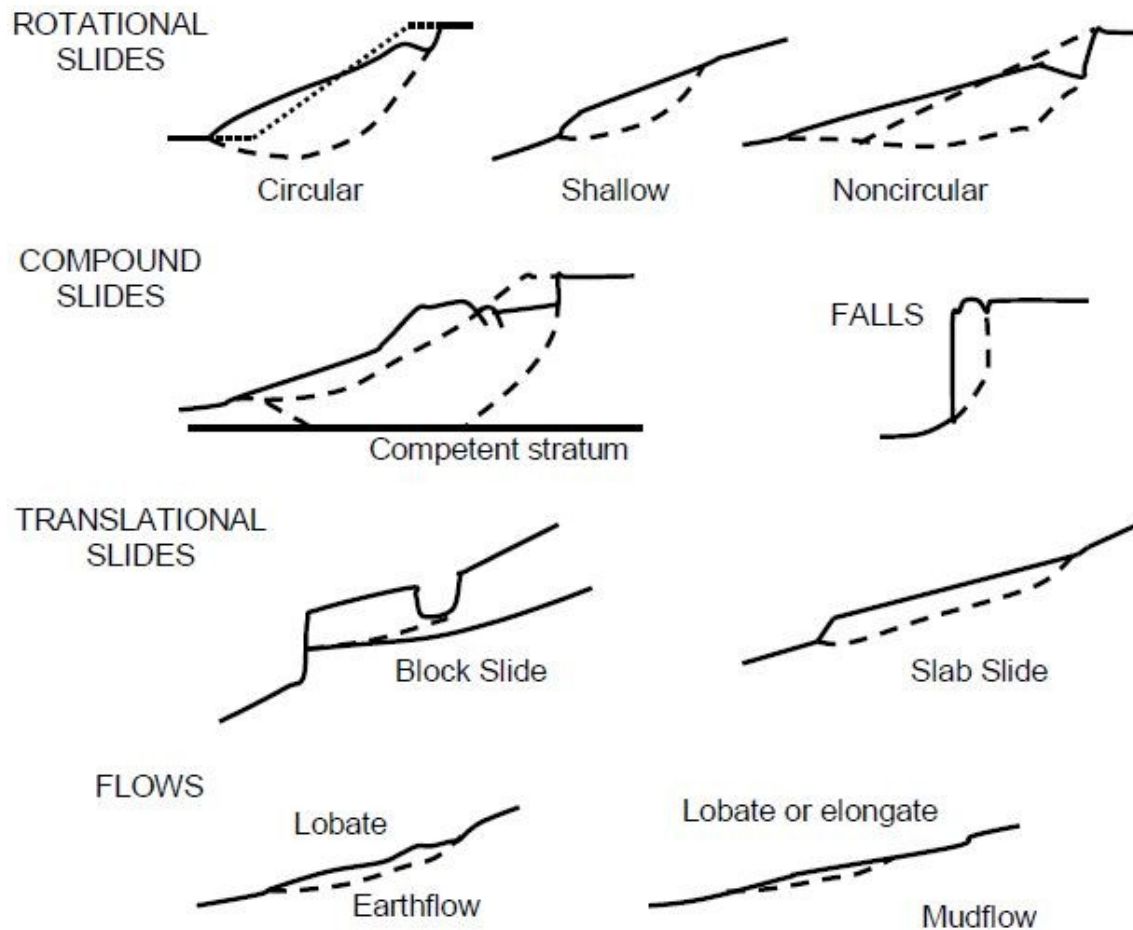


Figure 2.2 Types of movement in clay slopes. (redrawn after Abramson et al., 2002).

2.3 Shallow Slope Failure

Shallow landslide is associated with the sliding of top soil surface located within the soil mantle. Thus, shallow slope failure can be termed as surficial slope failure. It occurs generally along highway cut slopes and embankments commonly in case of fine grained soil triggered by excessive rainfall as trapped rain water makes the soil saturated and heavy. Moreover, failure might occur if the pore water pressure is increased sufficiently to reduce the effective normal stress to a critical level (Abramson et al., 2002). Slip surface in case of shallow slope failure is often parallel to the slope surface and typically, depth of slip surface is less than 1.2 m or less (Day, R. W. et al., 1989). According to WisDOT field observations depth of slip surface varies from 2 to 4 ft.

Though shallow slope failure is not usually hazardous for human life but it can disrupt the communication system by creating road block on the road surface and attribute financial loss by damaging the guardrails, shoulders, road surface, drainage facilities, utility poles (Titi and Helwany, 2007). Therefore, to resist shallow slope failure various methods have been applied to determine the most effective solution.

2.4 Remedies to Prevent Shallow Slope Failure

Slope can be made stable by increasing the resisting force or by reducing the driving force or combination of both. But, most economic and effective means of slope stabilization method for prevention of slope failure or appropriate repair work selection method depends on various factors such as technical constraints, site constraints, environmental constraints, aesthetic constraints, schedule constraints and cost (Abramson et al., 2002).

2.4.1 *Unloading*

Unloading is done by excavation or by replacing the top soil with light weight materials to reduce the driving force in order to make the slope stable. Excavation includes removal of upper part of the slope and unstable materials, flattening of slopes and benching. Replacement of top soil with light weight fill materials such as slag, encapsulated sawdust, expanded shale, cinders, shredded rubber tires, polystyrene foam and seashell (Abramson et al., 2002) is also effective method of slope stability

2.4.2 *Buttressing*

It is a technique to increase the resisting force to counter the driving force in order to make the slope stable. It can be consist of soil and rock fill, counterberms, shear keys, mechanically stabilized embankments and pneusol (Abramson et al., 2002).

2.4.2.1 Soil and Rock Fill

Buttressing can be provided by soil and rock fill to apply additional weight near the toe of an unstable slope shown in Figure 2.3.

2.4.2.2 Shear Keys

Shear keys is another method for buttressing in order to provide additional resistance against sliding. Critical slip circle is pushed deeper into underlying stronger soil. It's a very effective method, if the underlying strong soil stratum is very close to the overlying soft soil.

2.4.2.3 Counterberms

Buttressing can be consisting of counterberms by providing weight at the toe of a slope and there by shear strength below the toe of the slope is increased and presented in Figure 2.4.

2.4.2.4 Pneusol (tiresoil)

Pneusol (tiresoil) is a technique of buttressing where automobile tires are used instead of metal strips or geosynthetics materials. Internal and external stability has to be ensured like a MSE slopes while designing a pneusol. Schematic of pneusol is shown in Figure 2.5.

2.4.2.5 Mechanically Stabilized Embankments (MSE)

Mechanically stabilized embankments (MSE) is another technique of buttressing where the strength of the backfill soil is increased by using metal strips, mesh or geosynthetics to withstand large imposed loads and depicted in Figure 2.6. Internal and external stability should be ensured while designing a MSE. If there is possibility of future extension, it should be extensible means geosynthetic materials should be used instead of metal strips.

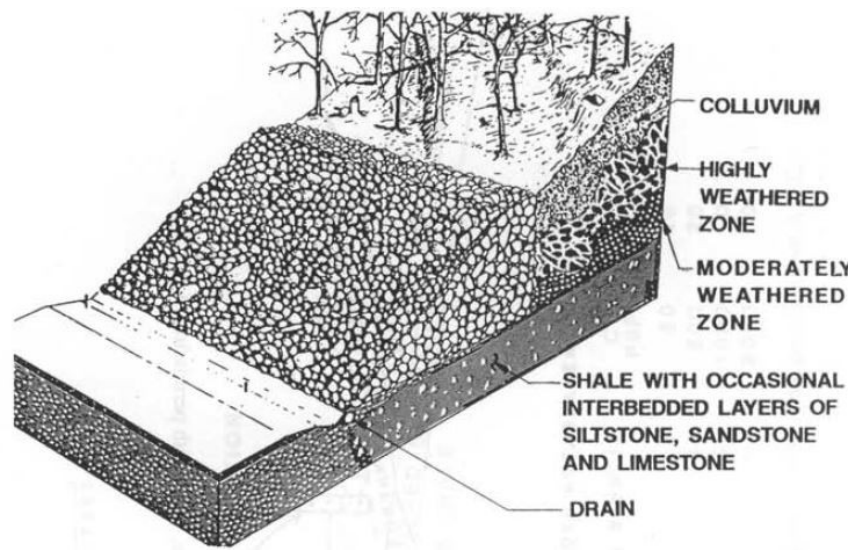


Figure 2.3 Rock buttress (Abramson et al., 2002).

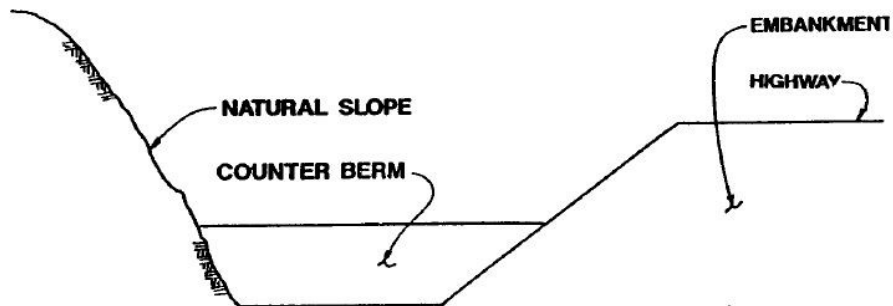


Figure 2.4 Weight at toe provided by Counterberm (Abramson et al., 2002).

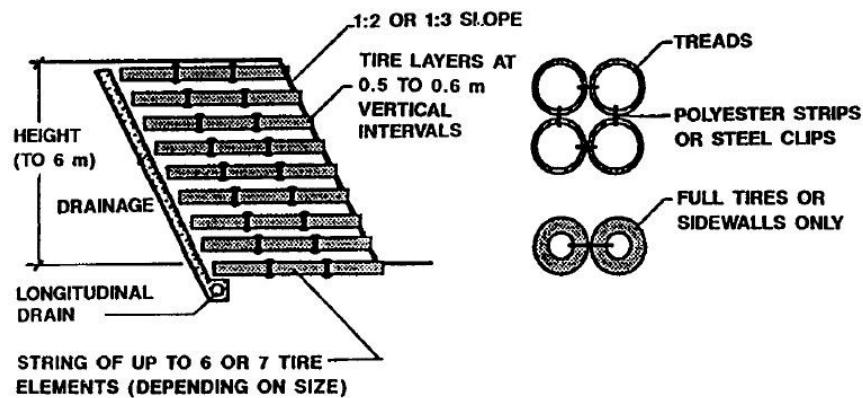


Figure 2.5 Slope stabilized with Pneusol buttressing (Abramson et al., 2002).

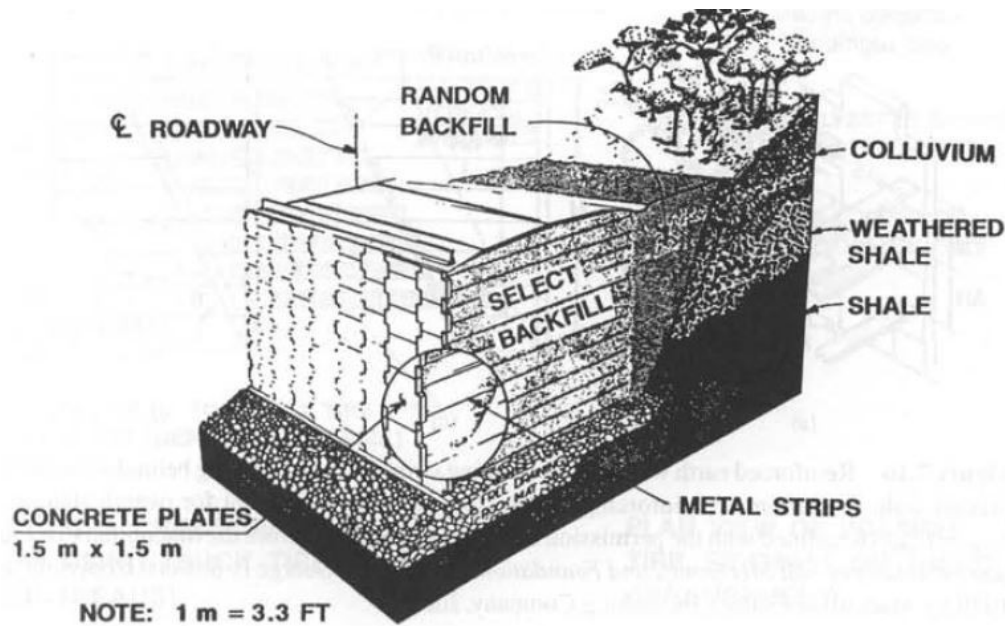


Figure 2.6 Stabilized slope with MSE (Abramson et al., 2002).

2.4.3 Drainage

Drainage system plays a vital role to maintain a stable slope as excessive rainfall for a prolonged period acts as one of the triggering factors for landslide. Proper drainage reduces the probability of erosion and piping. Drainage can be surface or subsurface.

2.4.3.1 Surface Drainage

Surface drainage is designed to carry away the surface run off from the slope to prevent seeping. To divert the surface run off sandbags can be used and cracks should be sealed with shotcrete, lean concrete or bitumen to prevent infiltration.

2.4.3.2 Subsurface Drainage

Subsurface drainage is a dewatering system that increases the stability of the slope. Subsurface drainage can be ensured by providing drain blankets, tranches, cut-off drains, horizontal drains, relief drains and drainage tunnels (Abramson et al., 2002).

2.4.4 Vegetation

Vegetation is an easy and cost effective method to control erosion due to surface run off and wind attack. Roots of vegetation hold the soil together, which increase the slope stability. Moreover, vegetations minimizes run off velocity and seepage by intercepting rainfall. Deep rooted vegetation absorbs moisture from ground and thereby reduces the moisture of the soil. Plantation provides good aesthetic view and it's not expensive, though it is susceptible to weather change and unable to withstand sever scouring action (Abramson et al., 2002).

2.4.5 Retaining Walls

Slope stability can be ensured by a retaining wall if there is space constraint. The wall should be deep enough to withstand the active pressure caused by the soil. The retaining wall should be internally and externally stable. Retaining wall can be various types such as conventional gravity or cantilever retaining wall, driven piles, drilled shaft walls and tieback walls (Abramson et al., 2002).

2.4.5.1 Conventional Gravity or Cantilever Retaining Wall

Gravity retaining wall should be designed considering its internal and external stability. Internal stability is required to withstand shear stress and bending moment induced by the backfill materials. Whereas, external stability is required to resist overturning moment, sliding forces and bearing capacity failure of the gravity retaining wall. Schematic of conventional gravity or cantilever retaining wall is presented in Figure 2.7.

2.4.5.2 Drilled Shaft Walls

Drilled shaft walls are very effective in urban areas where space constraint is a great challenge. Drilled shafts should be embedded beyond the potential critical slip surface into a strong soil stratum to gain enough strength due to its tip friction and skin friction to withstand the driving force or moment. Drilled shafts should be 2 to 5 feet in diameter and spacing between them should be three pile diameters (Abramson et al., 2002). Drilled shaft wall is portrayed in Figure 2.8.

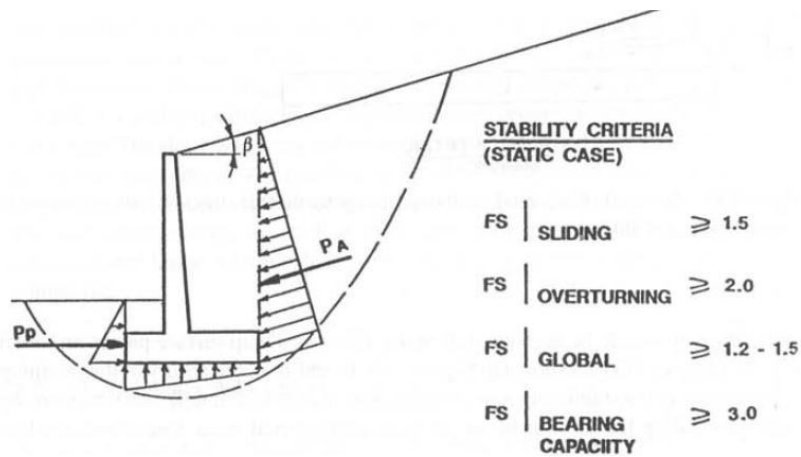


Figure 2.7 Conventional gravity or cantilever retaining wall (Abramson et al., 2002).

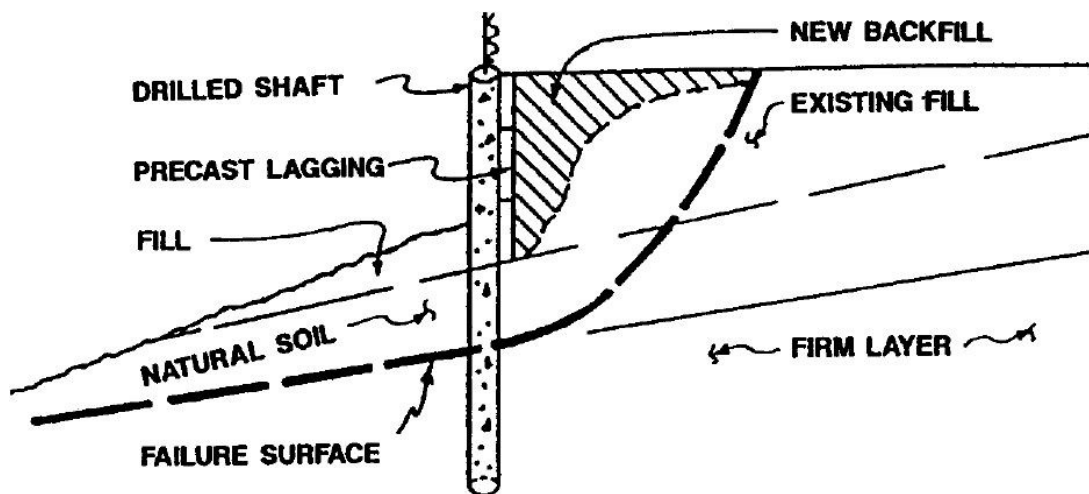


Figure 2.8 Drilled shaft wall stabilized slope (Abramson et al., 2002).

2.4.5.3 Driven Piles

Driven piles provide slope stability to withstand shallow landslide against hillside and engineered slopes. This method is not suitable for deep seated slides and for soil, which will flow between the piles. Piles should be embedded into strong soil to gain enough strength in order to resist being uprooted or overturned. This method is not as effective as other methods to resist the sliding of soil mass in case of an unstable slope. A major setback of driving piles is development of high pore water pressure, which might initiate slope failure. Schematic of driven piles stabilized slope is shown in Figure 2.9.

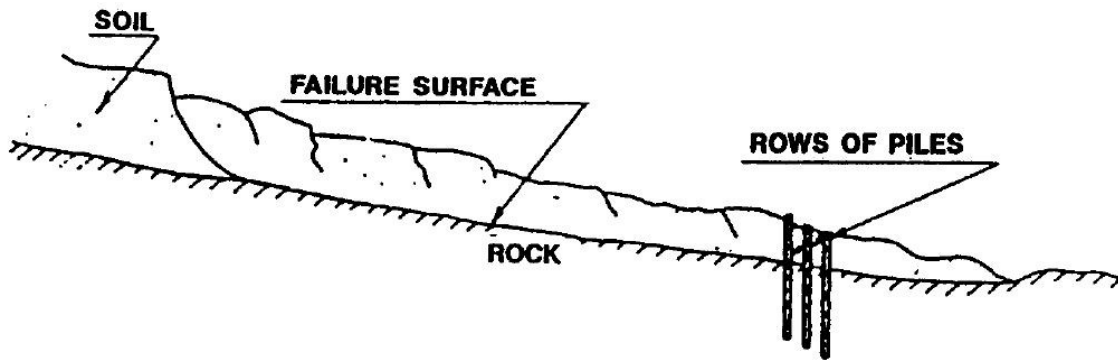


Figure 2.9 Driven piles stabilized slope (Abramson et al., 2002).

2.4.5.4 Tieback Walls

Tieback walls can be constructed if there is restraint imposed due to location or space limitations for excavation of footing. The wall is secured to a deadmen or grouted to a firm, strong bearing stratum and the acting load on the wall is transferred with post tensioned steel cables, rods or wires behind the potential or existing slip plane to ensure satisfactory resistance. Schematic of driven piles stabilized slope is shown in Figure 2.10.

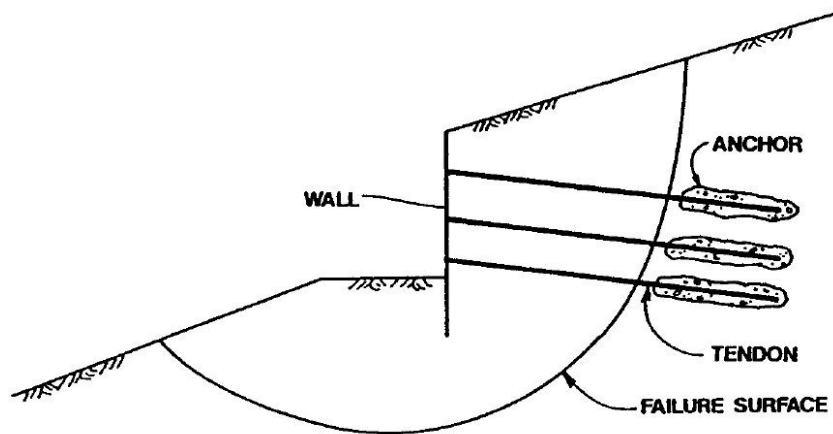


Figure 2.10 Schematic showing tieback walls (Abramson et al., 2002).

2.4.5.5 Gabion Walls

Gabion walls can be constructed in situ by assembling the gabion baskets and then filled up with rocks. Due to mechanical interlocking between stones, strength is gained to resist the driving force causing failure of a slope though gabion walls are unbounded structures (Fay et al., 2012). As, the gabion baskets are filled with stones, they provide drainage through the walls. They are placed at the toe of a cut slope or top of a fill slope.

2.4.6 Surface Slope Protection

The aim of surface slope protection is to maintain a dry or partially dry slope by preventing infiltration of rain water. By providing a near-impermeable layer on top of soil, slope is protected from failure due to excessive rainfall for a prolonged period. Slope surface protection can be provided by shotcrete or chunam plaster, masonry blocks or rip-rap. This method is quite labor intensive and does not provide any resisting forces to the slope like buttresses or retaining walls. To ensure good performance in slope protection proper drainage system is need when this method is used. Masonry blocks, shotcrete or chunam plaster are susceptible to weather and loose strength due to seasonal variation. Rip-rap is an effective method to prevent scouring of toe of slope at river or stream bank, which can eventually cause slope failure. The schematic of rip-rap is depicted in Figure 2.11.

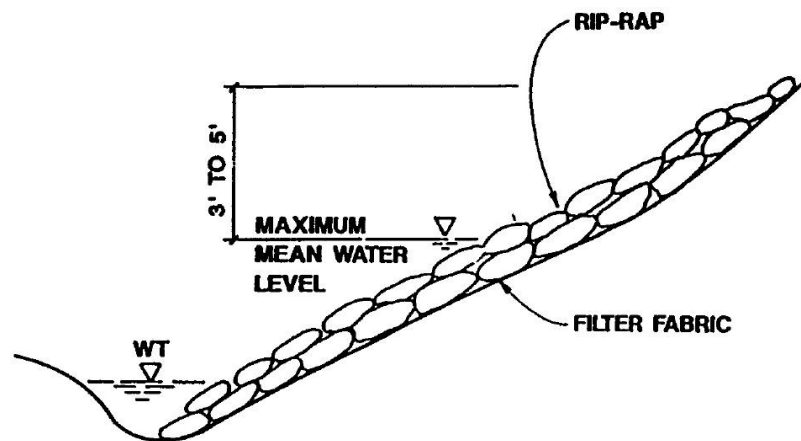


Figure 2.11 Rip-rap to protect erosion at toe of a slope (Abramson et al., 2002).

2.4.7 Soil Hardening

This is a technique to stabilize a slope by increase the strength of soil. In case of cohesive soil when drainage is not effective, soil hardening methods can be adopted by cement fill, electro-osmosis, thermal treatment, grouting, lime injection or preconsolidation (Abramson et al., 2002).

2.4.7.1 Grouting

Grouting is an effective stabilizing method to ensure slope stability in case of shallow landslide. Though, granular soils can be grouted, but it is more suitable for stiff materials like clay shale or stiff clay. Grouting is not suitable for slaked materials. It is done by filling the fissures or pores with cement mortar and thus removes water from pores or fissures. Drilled bore holes for grouting should be spaced at a distance of 10 to 15 feet (Abramson et al., 2002) and cement mortar injection should be started from the lowest row to increase support near the toe.

2.4.7.2 Compacted Soil-Cement Fill

Cement is mixed with soil to increase the shear strength of soil in order to enhance slope stability. Soil-cement fill is very useful to rebuild a failed slope. The ratio of soil-cement mix is determined in the laboratory based on required strength to be provided. Usually, 1 to 10 percent cement by weight of soil produces cohesive strength of 25 to 125 pound per square inch (Table 2.1). This method is more suitable for cohesionless soils (sand) than cohesive soils (clay to silty clays) as cement mixes better and thoroughly with in situ cohesionless soils.

2.4.7.3 Electro-osmosis

Electro-osmosis is a slope stability method where despite the gravitational force water moves towards the cathode due to potential difference between electrodes located within the generated electric field and thus accumulated water inside the perforated cathode pipe is removed by pumping. This method is suitable for silty soil having particles size ranging from

0.0002 to 0.002 inch. It is not a suitable method for fine sand. As electro-osmosis is an expensive method, it is not commonly used.

Table 2.1 Triaxial strength (28 curing days) and cement content.

Soil (AASHTO)	Percent Cement (by Weight)	Cohesion (psi)	Slope Angle (degree)	Remarks
A-2-4	0	20	29	Silty or clayey gravel and sand with maximum 35 percent passing No. 200 sieve.
	2	50	41	
	3	58	44	
	4	70	44	
	6	90	48	
	8	100	49	
A-1-b	0	10	38	Gravelly sand or sandy gravel with maximum 25 percent passing No. 200 sieve.
	1	27	45	
	2	37	49	
	3	50	51	
	4	72	52	
	5	95	55	
A-4	0	5	37	Silty soil with minimum 36 percent passing No. 200 sieve.
	2.5	30	46	
	5.5	65	45	
	7.5	85	45	
	9.5	125	45	

Source: Nusbaum and Colley (1971)

2.4.7.4 Lime Injection

Lime columns can be injected into clayey or silty soil to improve the slope stability. Injected lime increases the shear strength of soil. These lime columns should pass beyond the slip surface. Lime columns are more feasible than driven piles, if there is any possibility of slope failure due to pile driving. Lime columns also act as vertical drains, which cause rapid dissipation of excess pore water pressure. The shear strength of stabilized soil increases with time and it is observed that undrained shear strength can be as much as 5 to 10 tons per square foot after 1 year in case of stabilized clay (Broms, 1991). This method is not suitable for sandy soil. Minimum 80 days required for the lime columns of stabilized soil to gain enough strength before subjected to loading.

2.4.7.5 Preconsolidation

Consolidation of clayey soil is an effective method of increasing its strength and thus, it is an effective method for slope stabilization. To expedite the consolidation, surcharge can be applied or sand drains or wick drains can also be an efficient method. This process can even be more expedited by using surcharge in combination with wick drains or sand drains.

2.4.7.6 Thermal Treatment

Permanent drying of the embankment or cut slope is induced by high temperature in thermal treatments and thus enhanced slope stability is obtained. This method is used only in Romania (Beles and Stanculescu, 1958) and the United States (Hausmann, 1990). This method is not commonly used due to its undesirable environmental effects and high energy demands.

2.4.8 Reinforcement

Reinforced slope design is a conservative method (Elias et al., 2001) as they are more stable. Due to added reinforcement the slope can be steeper than unreinforced slope and more stable than a flatter slope having same factor of safety. The application of reinforcement makes the slope less susceptible to differential settlement and incorporation of vegetation on the slope is another advantage against erosion control.

2.4.8.1 Geosynthetically Reinforced Slopes

Reinforcement of soil with Geosynthetic is one of the most effective methods to stabilize a slope which has already failed or in a state of near its failure. Slope reinforced with geosynthetic material can be made steeper than its unreinforced state ensuring desired factor of safety. Moreover, use of geosynthetic materials decrease the tendency for surface sloughing due to compaction at the edge of the slope. Many researchers proposed simplified charts for designing reinforced slope using geosynthetic materials such as Christopher and Holtz, Jewll and Woods, Christopher and Leschinsky (Abramson et al., 2002). Figure 2.12 portrays a schematic diagram of reinforced slope using geosynthetic materials.

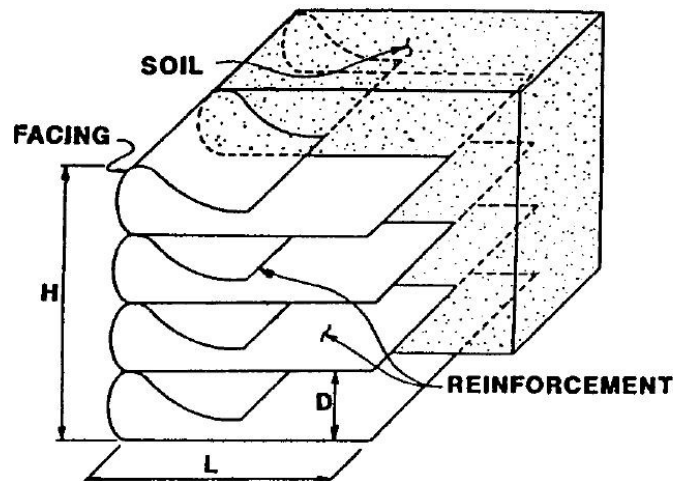


Figure 2.12 Slope reinforced with geosynthetic materials (Abramson et al., 2002).

2.4.8.2 Stone Columns

Stone columns increase the average shear resistance of soil along a potential slip surface and thereby stabilize or prevent landslide. Numbers of large diameter of compacted stone columns are spaced closely and increase the stability of slope by replacing in situ soil. These stone columns act as vertical drains like sand drains and expedite the consolidation process by dissipating the excess pore water pressure. Thus, increases the strength of surrounding clayey soils. This method is more suitable for subsurface soil whose shear strength is 200 to 1000 pounds per square foot (Abramson et al., 2002). Amount of vibration should be

minimized in case of organic or sensitive soil and for that the construction process of stone columns should be expedited. Stone columns stabilized unstable slope is depicted in Figure 2.13.

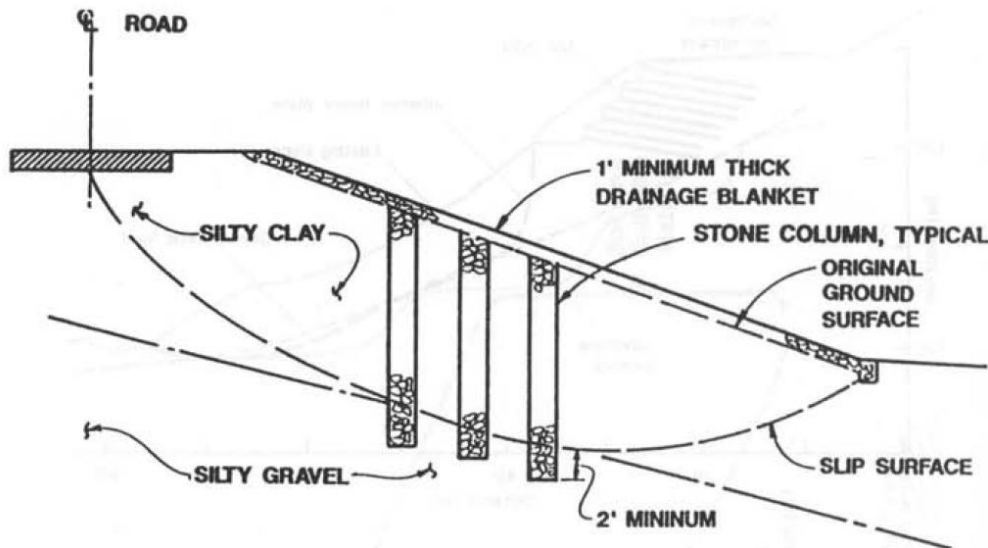


Figure 2.13 Stone columns stabilized unstable slope (Abramson et al., 2002).

2.4.8.3 Soil Nailing

Soil nailing is an in situ soil reinforcement technique where nails are driven or grouted into predrilled boreholes. Usually steel bars, metal tubes or other metal rods are used for soil nailing. The closely spaced reinforcement driven into the soil improves slope stability by resisting tensile stresses, shear stresses, and bending moments. Surface skin provides the stability of the ground surface between nails. A thin layer of shotcrete (4 to 6 inches thick) reinforced with wire mesh or intermittent rigid elements analogous to large washers can serve as a surface skin. This in situ slope stabilization method can also be used to retain excavations.

Spacing, size and length of the nails and design of the wall facing should be considered while designing soil nailing system based on global and internal stability. Corrosion protection should be considered while designing soil nailing system for slope stability as reinforcement members are steel bars. Low cost, requirement of light construction equipment, adaptability to different soil conditions, flexibility and reinforcement redundancy are the advantages of soil

nailing system (Abramson et al., 2002). A schematic diagram of soil nailing system is presented in Figure 2.14.

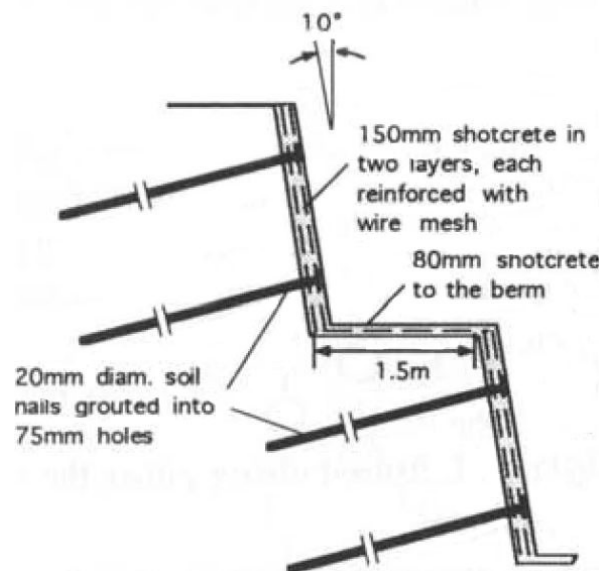


Figure 2.14 Schematic diagram of soil nailing system (Abramson et al., 2002).

2.4.8.4 Reticulated Micropiles

Slope stability is ensured by reticulated micropiles by creating a monolithic rigid block of reinforced soil. Reticulated micropiles should pass beyond the critical failure surface. This method was developed in Italy (Abramson et al., 2002). Reticulated micropiles system is similar to soil nailing but their behavior differs from soil nailing as they are influenced by their geometric arrangement. Reticulated micropiles method offer higher load bearing and shearing capacities than closely spaced vertical piles (Lizzi, 1985).

Reticulated micropiles method has many advantages such as micropiles do not require large soil excavation, suitable for any soil type, can be arranged to counteract many patterns of internal forces and do not obstruct water circulation in the subsoil. The setbacks are that they are susceptible to corrosion and also they need to be driven into stable soil strata, which might be located deep below the slip zone (Abramson et al., 2002). Figure 2.15 represents a schematic of reticulated micropiles.

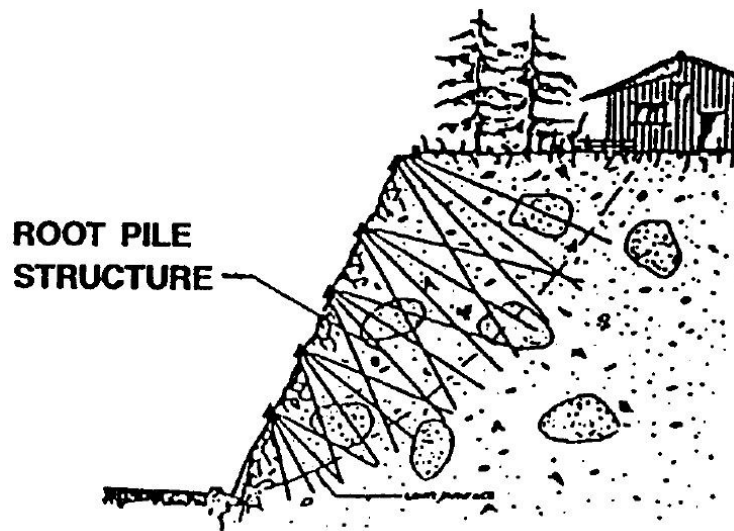


Figure 2.15 Schematic of reticulated micropiles (Abramson et al., 2002).

2.4.8.5 Plate Piles

Plate piles are installed vertically into the slope to resist shallow landslide, where weak top soil is resting over strong soil stratum. Typically plate piles are 2.1 meter long and 9.5 mm thick steel angle iron. Top of the pile is attached to a 0.3 meter by 0.6 meter rectangular steel plate. The driving forces of the upper slope mass is obstructed by the plates and thereby reduced and transferred to the stiffer subsurface soil. Static factor of safety against slide can be increased by 20% or greater by using plate piles. The slope stabilization cost can be reduced by 6 to 10 times compared to conventional slope stabilization methods (McCormick and Short, 2006). A schematic of plate pile is presented in Figure 2.16.

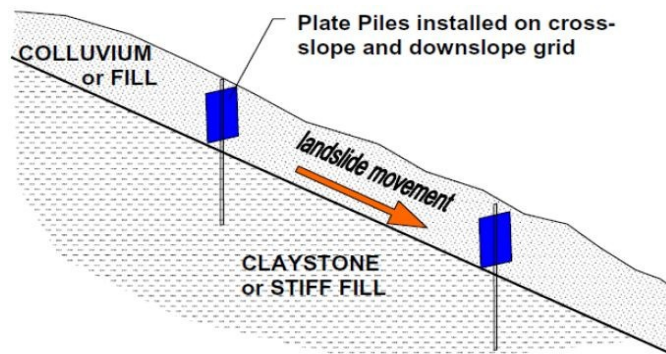


Figure 2.16 Stabilization of Slope using plate pile (McCormick and Short, 2006).

2.4.8.6 Recycled Plastic Pins

Recycled Plastic Pins (RPPs) are commercially known as recycled plastic lumber. RPP apply the similar technique of slope stabilization like soil nails or micropiles. RPPs are low susceptible to environmental degradation and manufactured from plastic waste. Thereby, using RPPs for stabilizing minor slope instabilities can be economically a viable option. To evaluate the potentiality of RPPs, an extensive investigation is ongoing as this method is a new scheme for shallow slope stabilization (Loehr et al.,2000).

2.5 Recycled Plastic Pin

Recycled plastic pins are manufactured from plastic wastes, thus using RPP in slope stabilization has got great economic advantages over other traditional methods and this method is environment friendly as well. Shallow slope failure can be resisted using RPPs as it is a durable product with respect to environmental degradation. RPPs are utilized in Missouri and found to be effective to stabilize surficial failure of embankment. Polymeric materials along with sawdust, fly ash and other byproducts are usually used to manufacture RPP (Chen et al., 2007). Compression molding and extrusion forming are the commonly used methods for manufacturing RPP. Creep rates of RPP can be higher compared to timber, concrete or steel as it is a polymeric compound. Thus, its ability to withstand deformation due to acting lateral forces is a crucial factor to determine its utility in slope stabilization. Therefore, more and detailed study should be conducted on RPP.

2.5.1 *Engineering Properties of RPP*

To analyze the capacity and suitability of RPP to withstand surficial slope failure, its properties should be defined accurately. Chen et al. (2007) carried out a study on specimens provided by three different manufacturers. The samples from different manufacturers are denoted as A, B and C respectively. All of them were 3.5 inch by 3.5 inch in cross section and 8 feet long. To understand the different engineering properties of RPP, the test result is shown in Table 2.2 along with their composition and manufacturing processes. It was found that the

compressive strength of RPP ranges from 11 to 20 MPa and compressive moduli from 580 MPa to 1280 MPa at 1% strain. On the other hand, Flexural strength ranged from 9 to 25 MPa and flexural moduli from 620 to 1675 MPa at 1% strain. According to Bowders et al. (2003), four point bending test results shown in Table 2.3 represent the resemblance with test results of Chen et al. (2007).

Table 2.2 Summary and detailed results of tested RPP (Chen et al., 2007).

Specimen batch	Principal constituent	Manufacturing process	Unit weight (KN/m ³)	Uniaxial compression strength (MPa)	Secant compression modulus, E _{1%} (MPa)	Flexural strength (MPa)	Secant flexural modulus, E _{1%} (MPa)
A1	LDPE	Compression	10	19	924	11	710
A2	LDPE	Compression	10	20	1269	-	-
A3	LDPE	Compression	10	19	1131	-	-
A4	LDPE	Compression	10	18	1282	18	1469
A5	LDPE	Extruded	9	11	579	11	676
A6	HDPE	Extruded	10	11	641	9	655
A10	HDPE	Extruded	11	15	786	11	848
B7	HDPE	Extruded	8	14	600	10	621
B8	HDPE+ fiberglass	Extruded	8	17	952	25	1675
C9	HDPE	Extruded	11	16	600	12	738

Table 2.3 Results of Four Point Bending Test (Bowders et al., 2003).

Specimen batch	No. of Specimen Tested	Nom. Def. Rate (mm/min)	Flexural strength (MPa)	Secant flexural modulus, $E_{1\%}$ (MPa)	Secant flexural modulus, $E_{5\%}$ (MPa)
A1	13	-	11	779	662
A4	3	4.27	18	1388	-
A5	3	5.74	11	711	504
A6	4	3.62	10	634	443
B7	1	4.05	9	544	425
B8	1	5.67	-	816	-
C9	2	3.21	12	691	553

Plastic is a polymeric compound and thus with increase of temperature it becomes weaker and ductile. To observe the weathering and environmental effects, a study was conducted by Krishnaswamy and Francini (2000), which includes the degradation due to UV radiation, thermal expansion and combined effect of moisture and temperature on mechanical behavior of RPP. The variation of flexural modulus and strength of RPP was insignificant compared to before and after hydrothermal cycling and shown in Table 2.4.

Table 2.4 Weathering effect on typical RPP (Krishnaswamy and Francini, 2000).

Hydrothermal Cycling	Secant Modulus (psi)	Stress at 3% strain (psi)
Before cycling	97,800±6400	1900±120
After cycling	113,600±14,400	2400±400

2.5.2 Creep of RPP

Rate of loading greatly influence the properties of plastic materials (Birley et al., 1991). RPP behaves like strong and stiffer material when loaded more rapidly as it is a viscoelastic material (McLaren, 1995). On the other hand under static loading, it is susceptible to creep and increased deflection with time. Creep can be due to compression or flexural stress.

2.5.2.1 Compression Creep of RPP

According to Chen et al. (2007), test results shown in Figure 2.17 reveals that the primary creep of RPPs were completed within one day and on the other hand secondary creep was prolonged about one year at a steady rate after primary creep. The compressive creep ranged from 690 KPa to 827 KPa creep. The ratio of compressive creep stress to compressive strength varies from 4% to 6%. None of the specimens were ruptured during this test as the applied stress was low. Maximum deflection was divided by the initial height of the specimen to determine the maximum creep strain. The compressive creep test results are represented in Table 2.5.

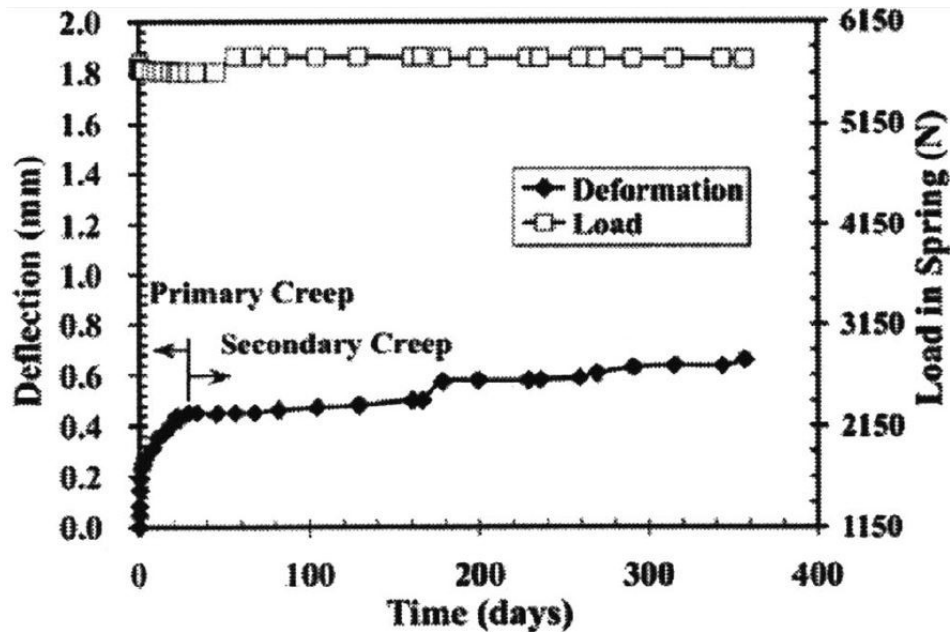


Figure 2.17 Typical deflection of RPP under constant axial stress with time (Chen et al., 2007).

Table 2.5 Summary of results on compressive creep of RPP (Chen et al., 2007).

Manufacturing batch	Number of Specimen	Creep Stress (KPa)	Ration of Creep Stress to Compressive Strength (%)	Maximum Creep Strain (%)
A3	2	724	3.7	0.1
A6	2	690	6.3	0.1
B7	1	758	5.3	0.4
C9	1	827	5.1	0.4

2.5.2.2 Flexural Creep

Tests at different temperature conducted by Chen et al. (2007) depict the behavior of typical RPP under a sustained bending load. At the free end of a simple cantilever, specimens were loaded with 222 N (50 lb) at 21°C, 56°C, 68°C and 80°C shown in Figure 2.18. All specimens tested above 21°C failed after the final data point. Specimens at 21°C were under load for more than 5 years and did not fail, whereas specimens at 56°C, 68°C and 80°C temperature failed due to breakage under four types of loading conditions. The graphical representation of the test results are shown in Figure 2.19 and in summarized form shown in Table 2.6. The test results reveals that the creep behavior of RPP influenced by loading condition along with temperature. With increasing temperature, failure time reduces though the loading condition is same. On the other hand, higher the load level faster the creep rate and thus failure time reduces. Therefore, life time of RPP considering maximum probable load and temperature it might undergo while used as reinforcement for slope stabilization should be considered.

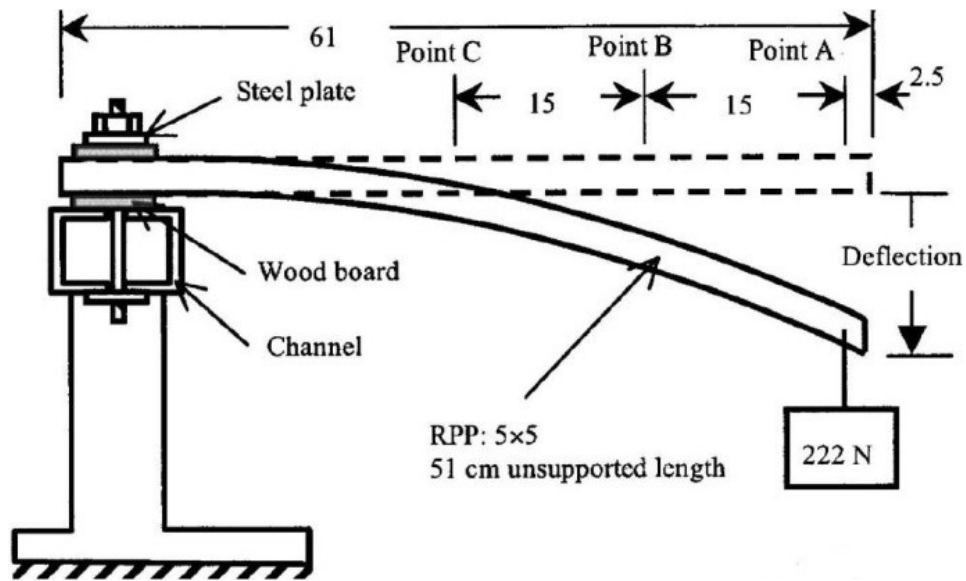


Figure 2.18 RPP testing setup for flexural creep (Chen et al., 2007).

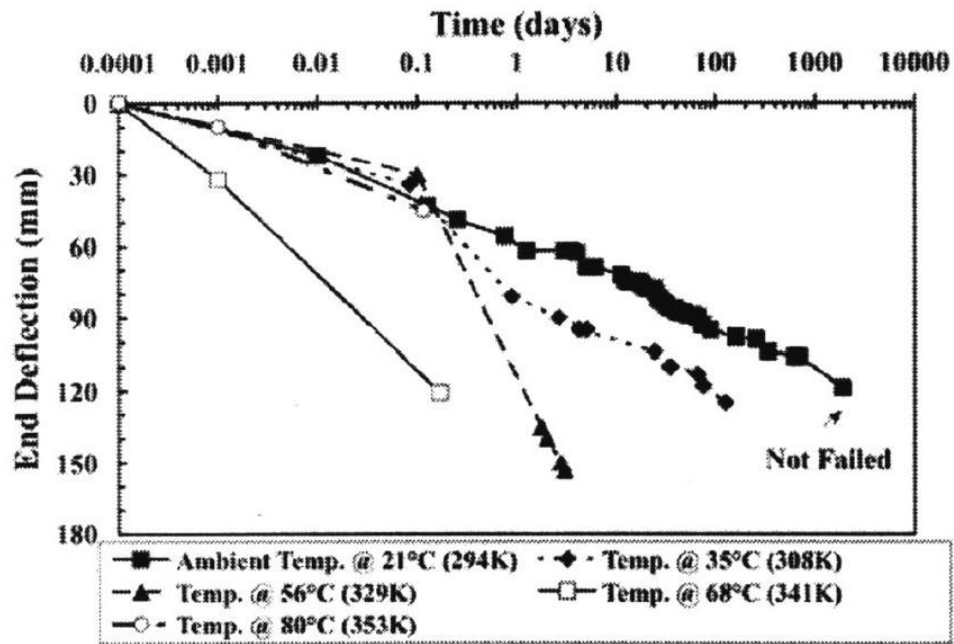


Figure 2.19 Deflection of RPP under 222 N loads with respect to time (Chen et al., 2007).

Table 2.6 Summarized results of flexural creep tests on RPPs (Chen et al., 2007).

Loading Condition	Temperature (°C)	Number of Specimens Tested	Average Time to Reach Failure (days)	Comments
44-N at 5 points	21	2	1,185	Not Failed
	56	2	195	Failed
	68	2	3.5	Failed
	80	2	0.8	Failed
93-N Single Load	21	2	1,185	Not Failed
	56	2	574	Failed
	68	2	17.5	Failed
	80	2	8.5	Failed
156-N Single Load	21	2	1,185	Not Failed
	56	2	71.5	Failed
	68	2	0.6	Failed
	80	2	0.8	Failed
222-N Single Load	21	2	1,185	Not Failed
	35	2	200	Failed
	56	2	3.1	Failed
	68	2	0.4	Failed
	80	2	0.8	Failed

2.5.2.3 Estimation of Creep Life

To predict the effective creep life time of an RPP in the field, a graphical chart is developed by Chen et al. (2007) and shown in Figure 2.20. To develop the graphical chart only the results for single-load tests were included as the loading type effects the moment distribution in the member and subsequently affects the creep rate. Since the loading conditions in the field are much closer to distributed loading instead of single-point loading, this method to predict the life time of RPP in the field is probably a conservative method.

Life time of RPP can be increased in the field by reducing the stress level in the RPP used for slope stabilization. Reduction of stress in RPPs can be achieved by increasing the number of RPP, increasing moment of inertia of RPP by changing the cross section or by changing the constituent blend in the RPP to reduce the creep susceptibility (Chen et al., 2007).

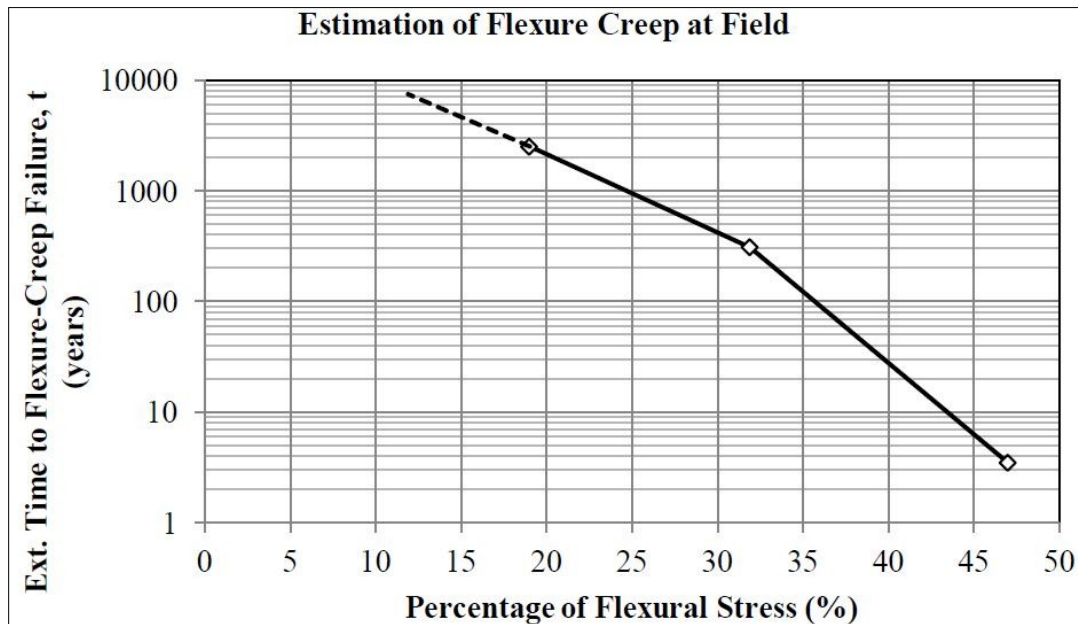


Figure 2.20 Method to estimate time of failure due to flexural creep of RPP (redrawn after Chen et al., 2007).

2.6 Slope Stabilization with Recycled Plastic Pin

RPP provides the needed resistance for long-term slope stability as they are installed in the slope beyond the potential sliding surface for shallow slope stabilization. RPPs are light weight materials, thus its installation and transportation cost is comparatively less. On the other hand, they are more stable than other slope reinforcement materials as they are less susceptible to degradation due to chemical and biological attack. In case of future construction, which might traverse a RPP stabilized site would offer less obstruction. Moreover, manufacture of RPPs will provide an additional market for recycled plastic and will reduce the volume of non degradable waste entering the landfill. Thus, stabilizing slopes with RPPs have lot of

advantages over commonly used civil engineering materials. Thereby, its field performance needs to be studied to determine the suitability of RPP in shallow slope stabilization.

2.6.1 Field Performance of RPP

RPPs are already used in Missouri (Loehr and Borders, 2007) and Texas to study the field performance of RPP with a view to determine its suitability in shallow slope stabilization. For better understanding two case studies of Missouri presented by Loehr and Border (2007) and two case studies of Texas presented by Khan (2013) are briefly discussed below.

2.6.1.1 Interstate 70-Emma Site

This site is located approximately 1 mile north of the city of Emma Missouri on I-70. The failure occurred in an embankment that forms the eastbound entrance ramp of I-70 and height of the embankment is 22 feet with side slopes varying from 2.5H:1V to 2.2H:1V. The boring logs revealed that the failed sites of the embankment composed of mixed lean and fat clays with scattered gravel, cobbles, and construction rubbles. The slide areas are denoted as S1, S2, S3, and S4. A schematic of the site area is shown in Figure 2.21. Shallow land slide occurred in those sites repeatedly over a decade though those sites were stabilized by dumping concrete rubble over the crest of the embankment and replacing the toe with construction rubble.

Slope stabilization of slide areas S1 and S2 were accomplished in October and November 1999 during phase I. The RPP used for slope stabilization were 8 feet long and 3.5 inch by 3.5 inch in cross section. In both the sites RPPs were installed at 3 feet by 3 feet staggered grid. Reinforcement members at S2 were installed vertically, whereas members at S1 were installed perpendicularly to the face of the slope and found to be effective to stabilize the slope in area S1 and S2. On the other hand, control area S3 failed on June 2001. Performance of the stabilized slope of slide areas S1 and S2 were quite satisfactory as it was found that the overall movement of the slope ranged from 0.5 inch to 1.5 inch at the end of 2003.

Phase II was started in October 2000 and completed in December 2003. Slide area S3 was stabilized in January 2003 during phase II. It was divided into four Sections A, B, C and D

based on the spacing of installed RPP during slope stabilization. The spacing of RPP members was 4.5 ft by 3 ft (longitudinal by transverse), 4.5 ft by 6 ft, 6 ft by 6 ft and 6 ft by 4.5 ft in Section A, B, C and D respectively, shown in Figure 2.22. Sections B and C of slide area S3 failed between November 2004 and January 2005, whereas Sections A and D did not fail as they were heavily reinforced though the lateral displacement was more than slide areas S1 and S2. Post-failure investigations revealed that the reinforcing members of those two sections failed structurally. According to observation of performance, during stabilizing slopes with RPP creep may play a role and rate of creep increase with RPP spacing shown in Table 2.7.

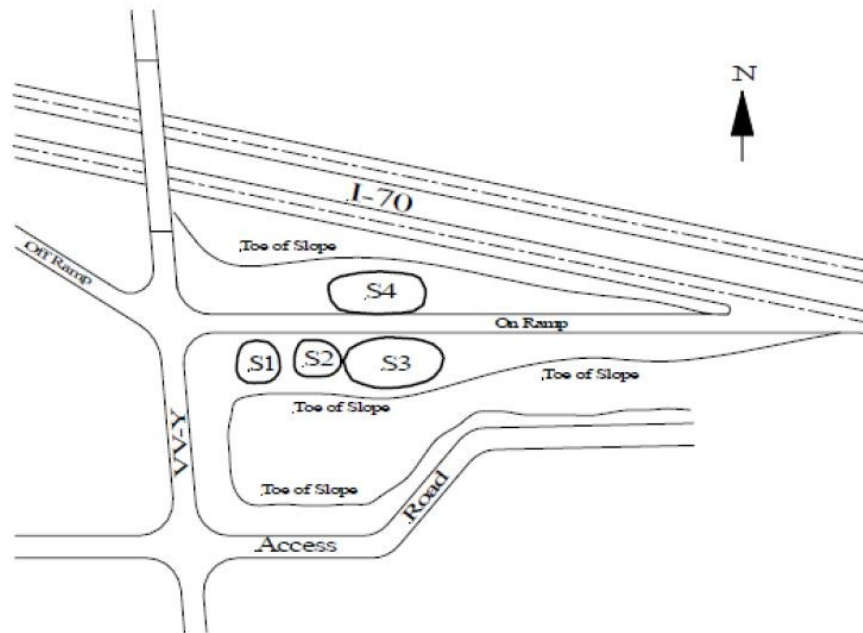


Figure 2.21 Schematic of slide areas on I-70 Emma site (Loehr and Border, 2007).

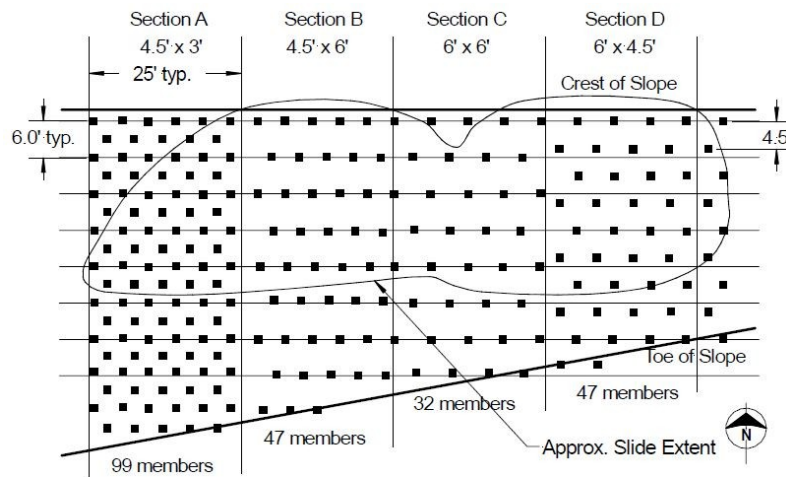


Figure 2.22 Plan view of stabilized sections of slide area S3 (Loehr and Borders, 2007).

Table 2.7 Creep rate for I 70-Emma site slide area S3 (Loehr and Borders, 2007).

Slide Area	Section	RPP Spacing	Estimated Creep Rate (in/yr)		
			2 ft Depth	4 ft Depth	6 ft Depth
S3	A	4.5 ft by 3 ft	0.51	0.29	0.29
	B	4.5 ft by 6 ft	0.69	0.62	0.51
	C	6 ft by 6 ft	0.69	0.51	0.47
	D	6 ft by 4.5 ft	1.02	1.06	0.84

2.6.1.2 US 36 Highway Site

The selected site for slope stabilization using RPP was located in the median of US36 between the eastbound sections of the roadway. The slope ratio is 2H:1V and height is 29 ft, where slide event involved approximately 150 ft. Boring and sampling of the site performed by MoDOT in June 2001 and revealed that the slope is consists of stiff to hard fat clay underlying a 3-ft to 5-ft thick surficial layer of soft to medium clay. The slope is not an embankment fills rather an excavated slope and no ground water was observed during site investigation in any of the

bore holes. Another slide area was selected as a control slope located approximately 100-ft west of the main slide area.

Slope stabilization of slide area was accomplished in April 30 to May 7, 2002. The RPPs used for slope stabilization were 8 feet long and 3.5 inch by 3.5 inch in cross section. It was divided into four Sections A, B, C and D based on the spacing of installed RPP during slope stabilization. The spacing of RPP members was 4.5-ft by 3-ft (longitudinal by transverse), 6-ft by 6-ft, 6-ft by 4.5-ft and 4.5-ft by 6-ft in Section A, B, C and D respectively, shown in Figure 2.23. All reinforcement members were installed vertically and in staggered grid.

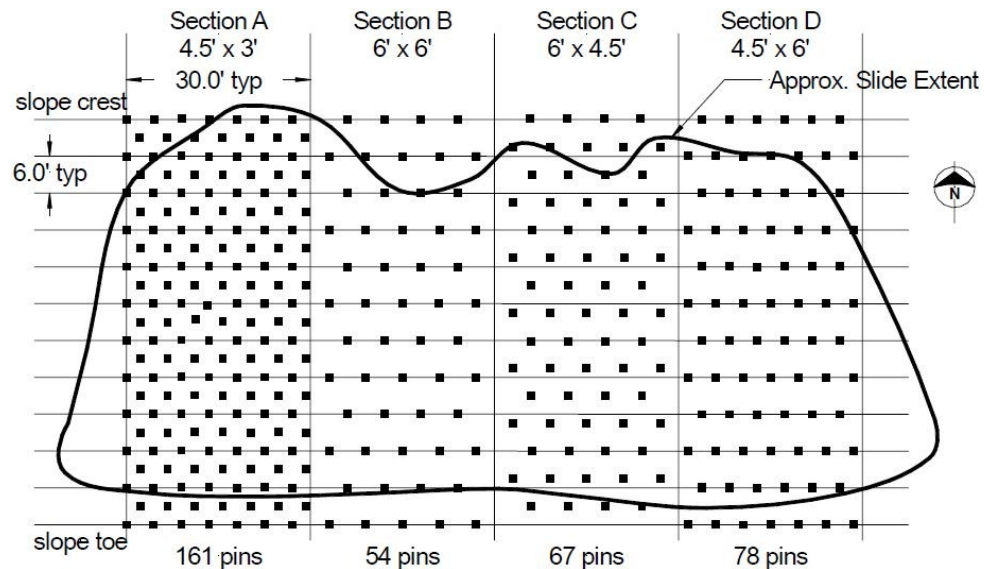


Figure 2.23 Plan Views of stabilized sections of US36 Highway (Loehr and Borders, 2007)..

The selected site was observed from July 2002 to February 2005 with a view to determine the field performance of RPP used for slope stabilization. The control area of the slope failed sometime between July to September 2004. On the other hand, the reinforced slope sections were stable and maximum measured movements of the slope was 1.5 inch to 2 inch. Moreover, only the upper 6 feet of the slope experienced the deformations.

2.6.1.3 US 287 Highway Site

This site is located in Midlothian Texas on US 287 highway. The slope was constructed in 2003 to 2004. The slope ratio is 3H:1V and height is 30-ft to 35-ft. Boring logs revealed that the slope was constructed on high plastic clay and dominant mineral of the soil is montmorillonite. Therefore, the soil was highly susceptible to swelling and shrinking upon hydrothermal cycling, which leads to develop fully soften strength and in fully soften state cohesion of the soil almost disappears (Saleh and Wright, 1997). The cracks were observed in September 2010 along the shoulder of the road and till now slope has not yet failed though cracks are indication of initiation of failure. The top 7 feet of the soil was considered as sliding surface.

The slope area was divided into five sections and width of each section is 50-ft. Three sections were stabilized with RPP and two sections were kept as control section without any reinforcement. Different length and spacing of RPPs were used in Section 1, uniform spacing with different length of RPPs were used in section 2, and uniform length with different spacing of RPPs were used in section 3. RPPs were installed perpendicularly in a staggered grid. A schematic of the reinforced slope is shown in Figure 2.24.

A drastic improvement was observed due to reinforcement. Slope of Section 1 moved 1.3 inches and Section 2 moved 1.8 inches downward as on July 2013. Section 1 was heavily reinforced with closely spaced RPPs and thus horizontal displacement of the top soil was less compared to Section 2. Similar phenomenon was observed in Missouri, where heavily reinforced slope section moved comparatively less. On the other hand, the controlled sections were settled by 9 inches and 12 inches respectively and a new crack zone was observed over the shoulder in June 2012.

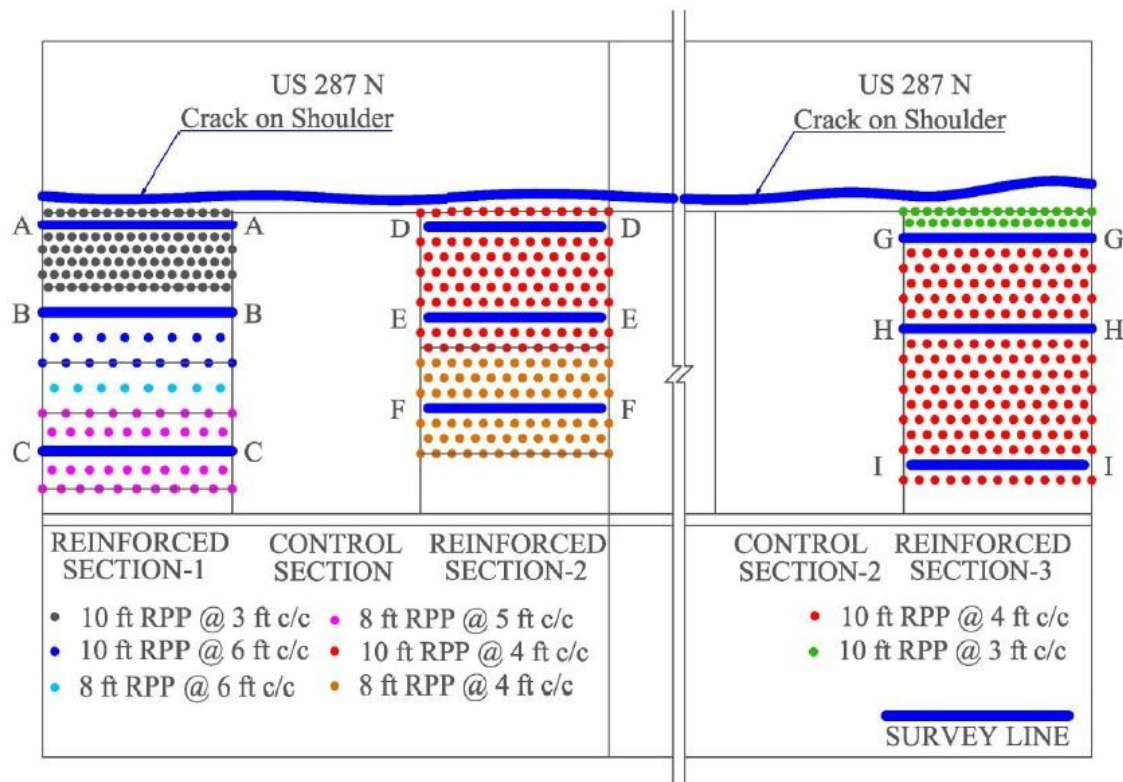


Figure 2.24 RPP layouts on US287 Highway slope (Khan M. S., 2013).

2.6.1.4 Loop 12 Highway Site

The site is located near the UP RP overpass on Loop 12 Highway in Dallas, Texas. A concrete retaining wall divided the slope into top slope and bottom slope. A crack in the retaining wall near the joint was observed on August 2011 during site visit due to 12 inches settlement at the crest of the slope. Soil boring results revealed that the soil is medium to high plastic clay. This type of soil is susceptible to shrinkage and swelling due to hydrothermal cycling and leads to develop fully soften state. Moreover, perched water zone might develop due to water intrusion through the shrinkage cracks during rainfall. Thus increased lateral pressure force the retaining wall to move downward and crack was developed near the construction joint of the retaining wall. Site investigation revealed that the failure occurred at the top of the slope.

The slope was reinforced with RPP in February, 2012 and installation of RPP started from bottom of the slope to avoid further reduction of factor of safety caused by vibration of drilling rig. At the bottom of the slope 4 rows of RPP at spacing of 4-ft center to center in staggered grid was installed over a 100-ft section, though two rows of RPP were at a longitudinal distance of 2-ft c/c along a 24-ft long section near the cracked area of wall. In order to resist the sliding of the retaining wall, first row of RPP was installed along the edge of the footing of retaining wall. The 50-ft failed section of the top slope was reinforced by installing 4 rows of 10 feet long RPP placed at 3-ft c/c staggered grid. The layout of the stabilized sections is shown in Figure 2.25.

The field performance results revealed that 4 inch horizontal displacement took place where the RPP spacing was 4-ft c/c. On the other hand, horizontal displacement was 1 inch to 3 inches in case of 2-ft c/c RPP spacing. It means, heavily reinforced slope is more stable like Interstate 70-Emma Site. The slope stability analysis results revealed that the reinforcement increase the factor of safety from 1.01 to 1.19. Thus, it is obvious that the retaining wall would fail if not the slope was stabilized by RPP.

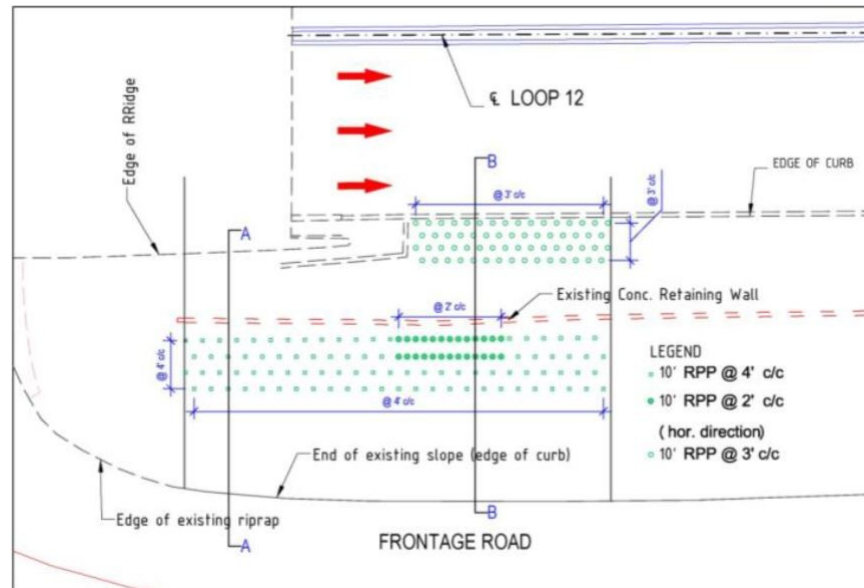


Figure 2.25 Layouts of stabilized sections of Loop 12 Highway (Khan, M. S., 2013).

2.6.2 Design Methods

An extensive study based on the field performance of RPP installed for shallow slope stabilization was carried out by Loehr and Boders (2007) in Missouri, and Khan (2013) in Texas. Thereby Limit Resistance method by Loehr and Boders (2007), and Performance based method by Khan (2013) are introduced. Both the methods are briefly discussed below.

2.6.2.1 Limit Resistance Method (Loehr and Borders, 2007)

According to limit resistance method the stability of reinforced or unreinforced slope assumes a potential sliding surface to determine the factor of safety. Sliding body is divided into number of vertical slices in case of method of slices, where the equilibrium of each slice is considered to determine the normal and shear forces on the sliding surface and thus the factor of safety is calculated using Mohr Coulomb failure envelop. This process is repeated assuming numbers of failure surface until the lowest factor of safety is obtained and that is the calculated factor of safety of the slope.

Similar concept is used to calculate the reinforced slope stability. An additional force because of reinforcing member, F_R is added to the other resisting forces on the slices that are intersected by RPP. Thus, the factor of safety of the slope is increased. Figure 2.26 illustrates this concept.

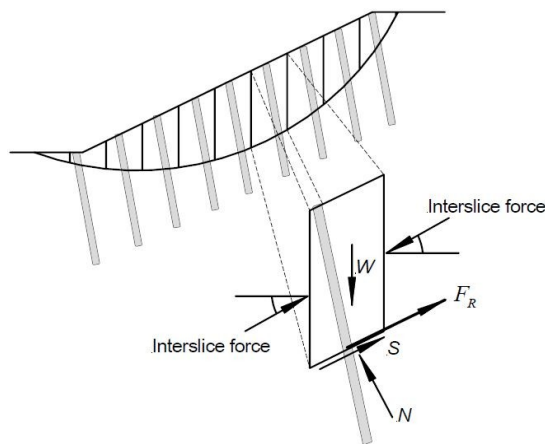


Figure 2.26 Resisting force due to installed RPP on an individual slice in Method of Slices

(Loehr and Borders, 2007).

The increased resisting force due to reinforcing member is termed as limit resistance. To calculate the limit resistance Loehr and Borders (2007) proposed two soil failure modes and two structural failure modes shown in Table 2.8. Therefore, based on the limit soil pressure the limit resistance corresponding to each failure modes is calculated.

Table 2.8 Summary of Failure Modes (Loehr and Borders, 2007).

Failure Mode	Description
Mode 1	Failure of soil above sliding surface around or between reinforcing members
Mode 2	Failure of soil below sliding surface due to insufficient anchorage length
Mode 3	Structural failure of member in bending
Mode 4	Structural failure of member in shear

By flowing between or around the reinforcing members the soil above the sliding surface is assumed to fail according to failure mode 1. On the other hand, soil below the sliding surface is stable where the reinforcing members are assumed sufficiently anchored. Figure 2.27 depicts failure mode 1.

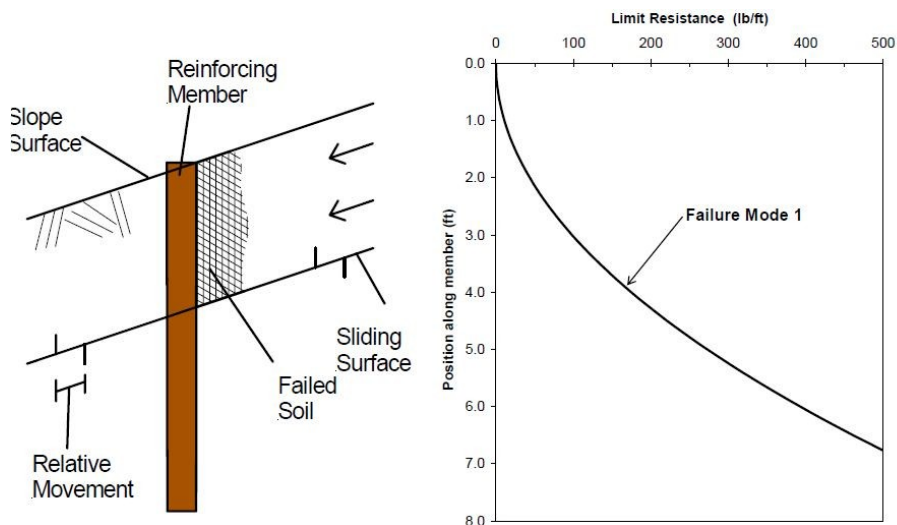


Figure 2.27 Schematic and Limit Resistance Curve for Failure Mode 1 (Loehr and Borders, 2007).

Similar method is used to calculate the resistance for Failure Mode 2. Only exception is that the soil below the sliding surface adjacent to the reinforcing member is assumed to fail though the members is sufficiently anchored in the moving soil above the sliding surface. Figure 2.28 portrays the Failure Mode 2.

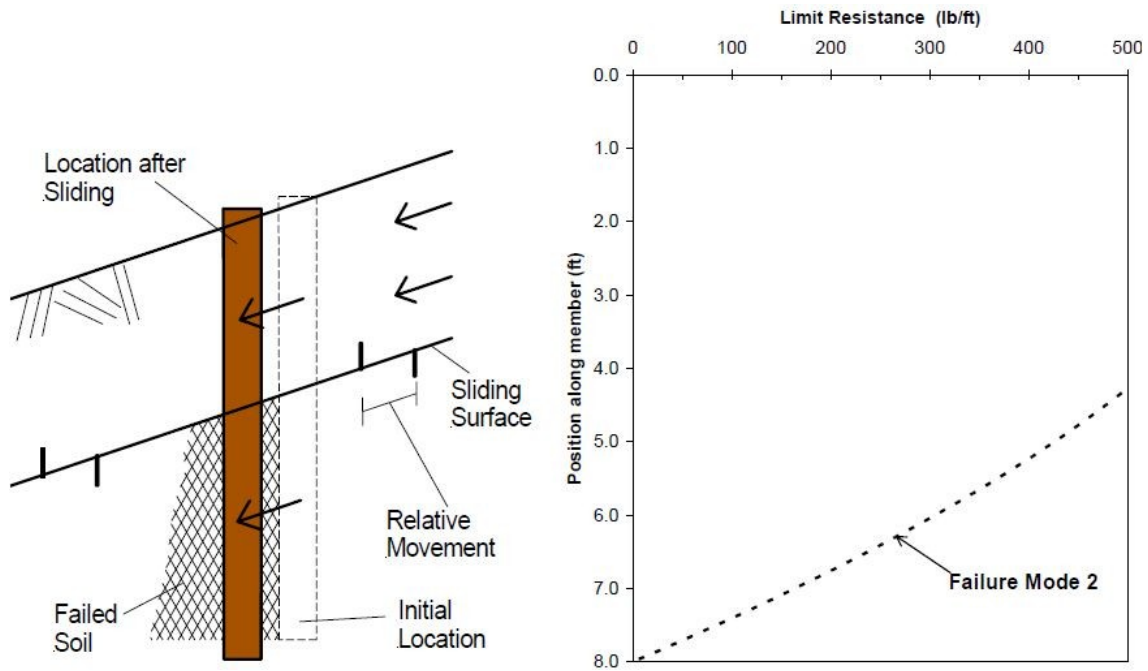


Figure 2.28 Schematic and Limit Resistance Curve for Failure Mode 2 (Loehr and Borders, 2007).

Failure mode 3 is subdivided into 2 categories as Failure Mode 3a and Failure Mode 3b. Failure due to excessive moments from the applied soil pressure above sliding surface is termed as Failure Mode 3a and shown in Figure 2.29. On the other hand, failure due to excessive moments from the soil pressure below the sliding surface is termed as Failure Mode 3b and shown in Figure 2.30

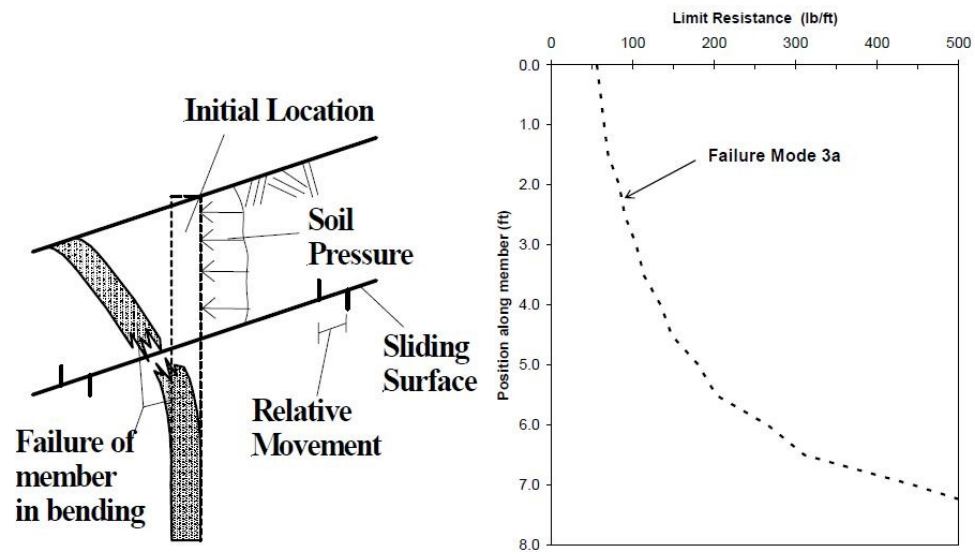


Figure 2.29 Schematic and Limit Resistance Curve for Failure Mode 3a (Loehr and Borders, 2007).

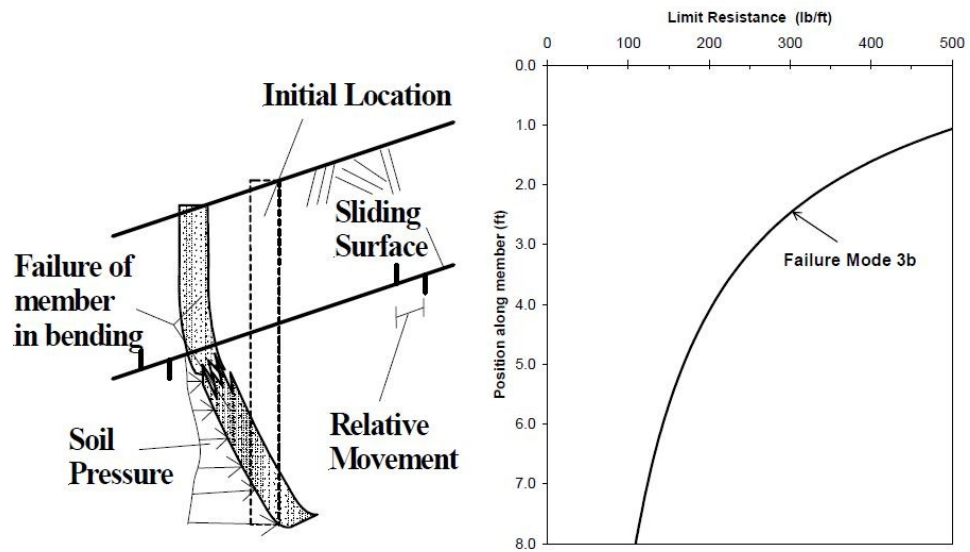


Figure 2.30 Schematic and Limit Resistance Curve for Failure Mode 3b (Loehr and Borders, 2007).

A composite limit resistance curve is developed combining the limit resistance curves due to soil failure and the failure of the reinforcing member, and by taking the least resistance of all failure modes. Thus, the developed composite limit resistance curve accounts for all failure modes.

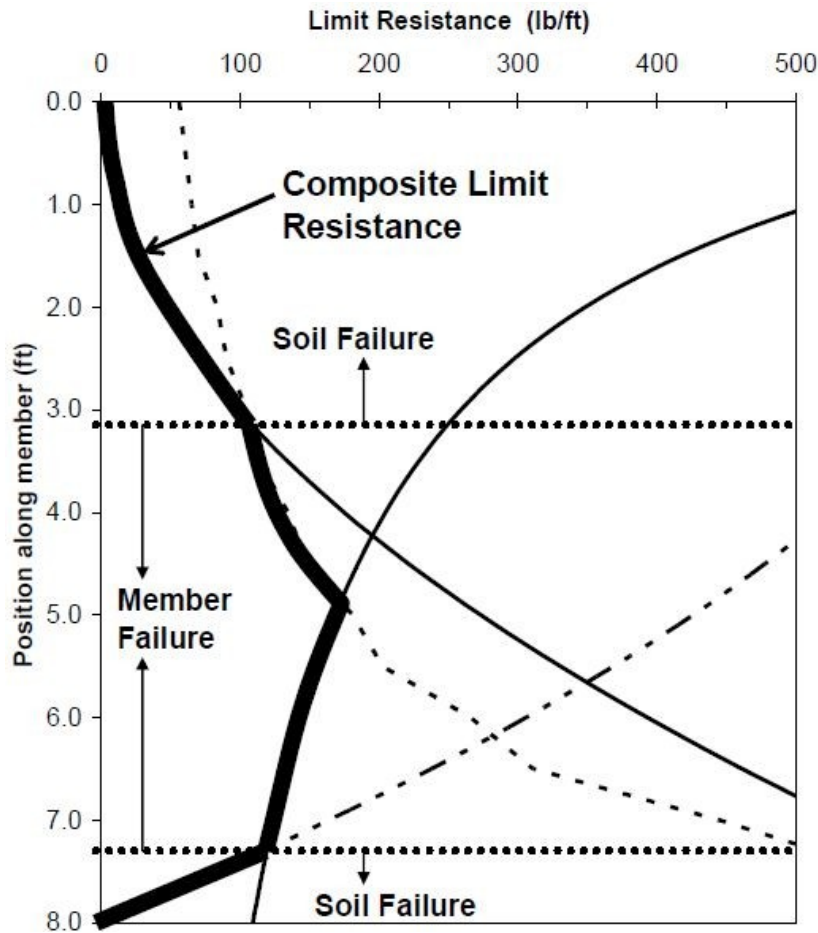


Figure 2.31 Composite Limit Resistance Curve for all Failure Modes (Loehr and Borders, 2007).

2.6.2.2 Performance Based (Khan, 2013)

This method analyzes the slope stability with finite element (FE) program PLAXIS 2D using elastic perfectly plastic Mohr-Coulomb model and also 15 node triangular elements was utilized for better accuracy. For initial FE model calibration, identical soil parameters for the control section of US287 Highway slope were used and the deformation analysis of reinforced section 1 and reinforced section 2 were carried out. PLAXIS generated horizontal displacement

was 3.2 inches and settlement was 2.3 inches for section 1, which commensurate with the field data. On the other hand horizontal displacement was 3.25 inches and settlement was 2.62 inches in case of section 2. The results do not match the obtained field data due to propagation effect of crack which cannot be simulated by 2D FEM analysis. The bending moment along the length of RPP for first seven rows of section 1 and 2 was determined with FEM analysis, and it was found that maximum bending moment is acting on the first row of RPP. Similar phenomenon is observed from the obtained field data.

Parametric study was conducted to evaluate the numerical model for reinforced section 1 and 2. The parametric study was performed using the above mentioned calibrated model where RPPs were modeled as plate element with 0.85 interface element strength for all models. The numerical modeling matrix used for parametric study is shown in Table 2.9. According to the study, it was found that 10 ft long RPP with spacing of 2 ft to 5 ft gives the most ideal results and these results also match the obtained field data of US 287 Highway. But, to develop the performance based method only individual effect of RPP was considered instead of considering group of RPP at a particular spacing.

The approach also considers the limit resistance based on the adjacent soil. Moreover, limiting resistance of RPP based on the deformation criteria of RPP and limiting criteria for creep was considered.

Installed RPP for slope stabilization is subjected to active and passive resistance of soil in addition to soil pressure above the slip surface due to sliding of the slope which causes the displacement of RPP. Thus, this method considered the limit horizontal displacement approach. For this reason, the capacity of RPP was evaluated based on the anticipated displacement as a result of soil movement.

Limiting the percentage of flexural stress in RPP is also taken into account in this method to limit the creep failure time of RPP. According to Chen et al. (2007) the estimated time to flexural-creep failure is 100 years at 35% of flexural stress. Therefore, flexural stress of RPP

was restricted to 35% of its ultimate capacity, while developing the design method by Khan (2013).

According to Loehr and Borders (2007), depth of shallow failure ranged between 3-ft to 7-ft and geometry of the slope varied from 2H:1V to 4H:1V. Thus, the developed design chart by Khan (2013) considered wide range of slip surface depth, mobilized load, slope ratio and soil strength parameters, shown in Table 2.9 and 2.10.

Table 2.9 Numerical model matrix for Parametric study (Khan, 2013).

Length of RPP (ft)	Spacing of RPP (ft)	Type of Analysis
12 ft	2 ft, 3 ft, 4 ft, 5 ft, 6 ft, 7 ft and 8 ft	Plastic Deformation
		Factor of Safety
10 ft	2 ft, 3 ft, 4 ft, 5 ft, 6 ft, 7 ft and 8 ft	Plastic Deformation
		Factor of Safety
8 ft	2 ft, 3 ft, 4 ft, 5 ft, 6 ft, 7 ft and 8 ft	Plastic Deformation
		Factor of Safety

Table 2.10 Consideration for development of graphical design chart (Khan, 2013).

Slope Inclination	Depth of Slip Surface (ft)	Lateral Pressure on RPP (psf)
2H:1V, 3H:1V, 4H:1V	3, 4, 5, 6, 7	10, 20, 30, 40, 50, 60, 70, 80, 90, 100, 200, 300, 400, 500

The FEM analysis was performed considering two layer of soil, where top layer above the slipping surface was considered as soft soil overlying on a stiff foundation soil. The strength parameters of soft soil (for example, $c=200$ psf and $\phi=10^\circ$), stiff soil and RPP are shown in Table 2.11. The slope and depth of slip surface varied according to Table 2.10, soil strength parameters of top soil varied according to Table 2.12 and stiff foundation soil parameters were kept constant. Soil model used for performing the FEM analysis is shown in Figure 2.32.

Table 2.11 Soil and RPP strength parameters used for FEM analysis (Khan, 2013).

Soil Type	Friction angle ϕ	Cohesion c	Unit Weight γ	Elastic Modulus E	Poisson Ratio ν	RPP properties	Unit	Parameters
-	$^\circ$	psf	pcf	psf	-			
Top Soil	10	200	125	2025	0.35	EA	lb/ft	857500
						EI	lbft ² /ft	255300
Foundation Soil	30	500	125	37140	0.30	d	ft	1.89
						w	lb/ft/ft	4.4

Table 2.12 Soil parameters used for development of design chart (Khan, 2013).

Cohesion (psf)	Friction Angle, ϕ (degree)			
100	0	10	20	30
200	0	10	20	30
300	0	10	20	30
400	0	10	20	30
500	0	10	20	30

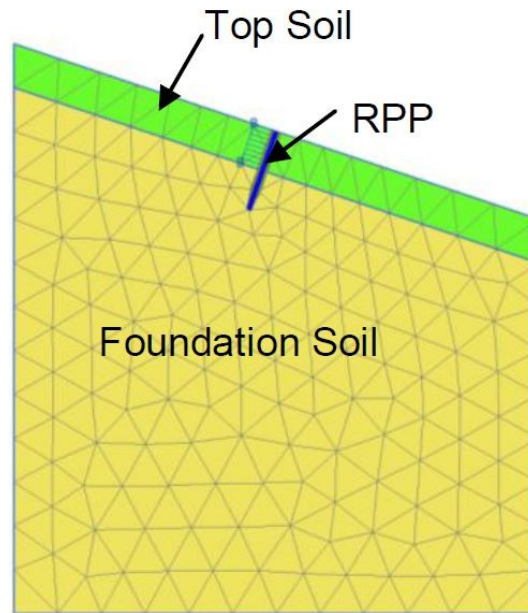
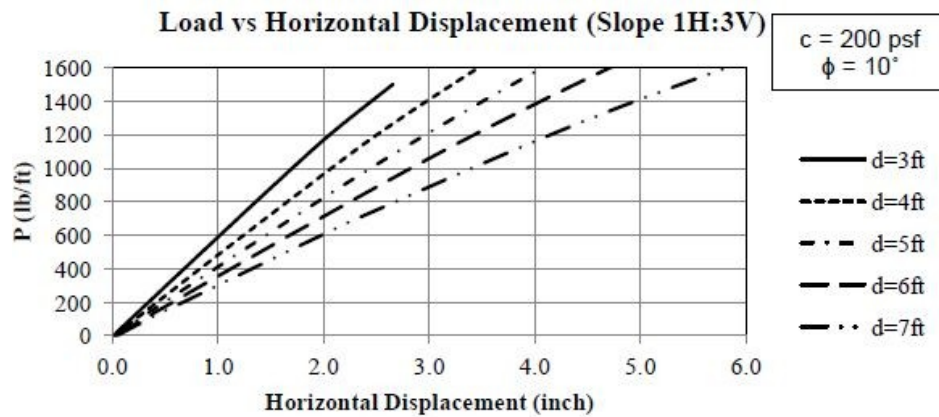
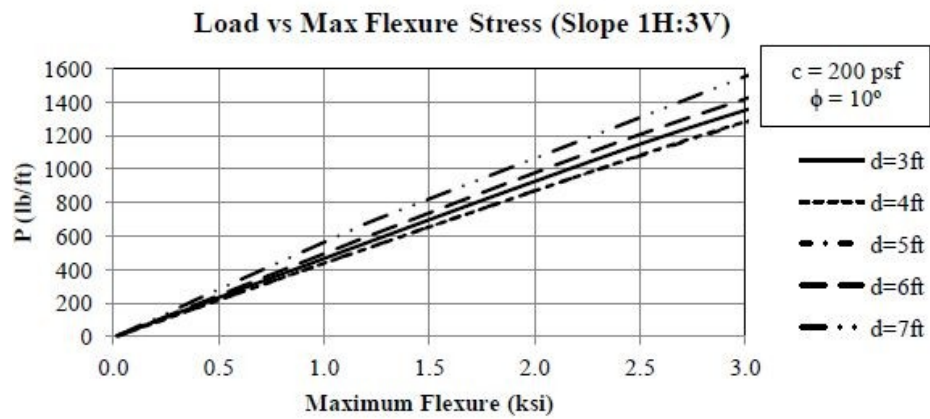


Figure 2.32 Soil model for determination of maximum horizontal displacement and flexural stress of RPP due to mobilized load (Khan, 2013).

Finally, the design chart was developed to evaluate the load carrying capacity of RPP by applying series of load over the installed RPP and the corresponding maximum horizontal displacement and maximum bending moment due to the load were determined. The obtained maximum bending moment was converted into flexural stress. Then the maximum horizontal displacement and flexural stress were represented graphically with respect to applied load for a specific slope, slip surface and soil type. One of the developed design charts by Khan (2013) is shown in Figure 2.33.



(a)



(b)

Figure 2.33 Limit Resistance Curve for RPP, a. load vs horizontal displacement, b. load vs maximum flexural stress (Khan, 2013).

2.7 Limitations of Previous Studies

2.7.1 Limit Resistance Method

According to Loehr and Borders (2007), all test sections at Emma Missouri on I-70 stabilized by installing RPP at 4.5 ft or less spacing were stable, whereas two sections stabilized with RPP spaced at 6 ft apart failed. It was found that the reinforcing members of those two sections failed structurally and observations of performance suggest that creep may play a role in case of stabilizing slopes with RPP. But the design method by Loehr and Borders (2007) did not consider the effect of creep of RPP in shallow slope stabilization.

2.7.2 Performance Based Method

Khan (2013) proposed a new design method to determine the horizontal displacement considering the effect of creep under sustained load. Numerical modeling with finite element software PLAXIS was used to develop the design method in conjunction with field data obtained from US287 highway and Loop 12 Highway. RPPs are always installed in a group, but this method only considers single RPP under sustained load instead of considering the group resistance of RPP in stabilizing shallow slope.

2.7.3 Room for Future Studies

Effect of mobilized load causing shallow slope failure acting over a group of RPP can be a new room for future studies, which might include the horizontal displacement and flexural creep of RPP installed in a group. Thus, the objective of this study is to determine the group resistance of RPP in stabilizing shallow slope failure, which will improve the design method proposed by Khan (2013).

Chapter 3

Methodology

3.1 Introduction

The objective of this study is to determine the group resistance of RPP used in sustainable slope stabilization. RPPs were found to be effective in shallow slope stabilization according to the field study carried out in Missouri and Texas. Based on the field study, Loehr and Borders (2007) introduced limit resistance curves and Khan (2013) proposed performance based design methods. Loehr and Borders (2007) did not consider the effect of creep of RPP in their design method. On the other hand Khan (2013) considered the creep effect in his design chart, but it was developed considering the resistance offered by single RPP. Thus, the design method proposed by Khan (2013) can be improved by considering the group resistance of RPP.

The proposed design method is developed using the finite element software PLAXIS 2D. It's a two dimensional finite element (FE) program for various types of geotechnical applications used in deformation and stability analysis. To develop the new design method elastic perfectly plastic Mohr-Coulomb soil model with 15 node triangle elements was used to attain accuracy during stability analysis. The FE model was calibrated by using the identical soil parameters of the control section of US 287 Highway slope.

Required number of RPP to simulate an effective group in shallow slope stabilization was determined at the beginning of the study considering spacing of RPP ranged from 2-ft to 6-ft. Then, the proposed design chart was developed based on parametric study with PLAXIS 2D, where the group resistance of RPP was considered. The proposed design method considers the horizontal displacement of RPP along with flexural creep effect under sustained load like Khan (2013). Three design charts at 2-ft, 4-ft and 6-ft spacing of RPP were developed for each type of soil and then the group resistance of RPP is compared with resistance of single RPP. Finally, a multiplication factor is introduced to evaluate the group resistance of RPP with respect to individual resistance of RPP.

3.2 Soil and Reinforcement Parameters

The parametric study to develop the proposed design chart was performed using the calibrated model. According to Loehr and Borders (2007), depth of shallow slope failure ranged between 3-ft to 7-ft and geometry of the slope ratio varied from 2H:1V to 4H:1V. Moreover, usually the US highway embankment slopes varies from 2H:1V to 4H:1V. Thus, the proposed design chart considers wide range of slip surface depth, mobilized load, and slope ratio and soil strength parameters, shown in Table 3.1. The slope is stabilized using RPP and the RPPs were modeled as plate element with 0.85 interface element strength for all models. According to the study conducted by Khan (2013), it was found that 12/10 ft long RPP at a spacing of 2-ft to 5-ft yields the most ideal result. Therefore, the chosen dimensions of RPPs were 3.5 inch by 3.5 inch and 10-ft long and spacing between them ranged from 2-ft to 6-ft. The strength parameters of the RPP are presented in Table 3.2.

Table 3.1 Numerical modeling parameters.

Soil Parameters	Top Soil	Foundation Soil	Slope Ratio	Mobilized Load (psf)	Depth of Slip Surface (ft)
Unit weight of Soil (pcf)	125	125	2H:1V, 3H:1V, 4H:1V	10, 30, 50, 70, 90, 100, 200, 300, 400, 500	3, 5 and 7
Cohesion (psf)	100 to 300	500			
Friction Angle (degree)	0 to 30	30			
Interface	0.85	0.85			

Table 3.2 Reinforcement parameters.

Recycled Plastic Pin Properties	Parameters
EA (lb/ft)	857500
EI (lb-ft ² /ft)	255300
d (ft)	1.89
w (lb/ft/ft)	4.4

3.3 Model Configuration

The modeling configuration used for reinforced slope simulation and stability analysis is presented with a representative model for 2H:1V slope ratio, shown in Figure 3.1. Standard fixities have been used as boundary condition, where the two vertical boundaries were free to move vertically and were considered fixed in the horizontal direction. The bottom boundary was modeled as fixed. The generated model is elastic perfectly plastic Mohr-Coulomb soil model with 15 node triangle elements.

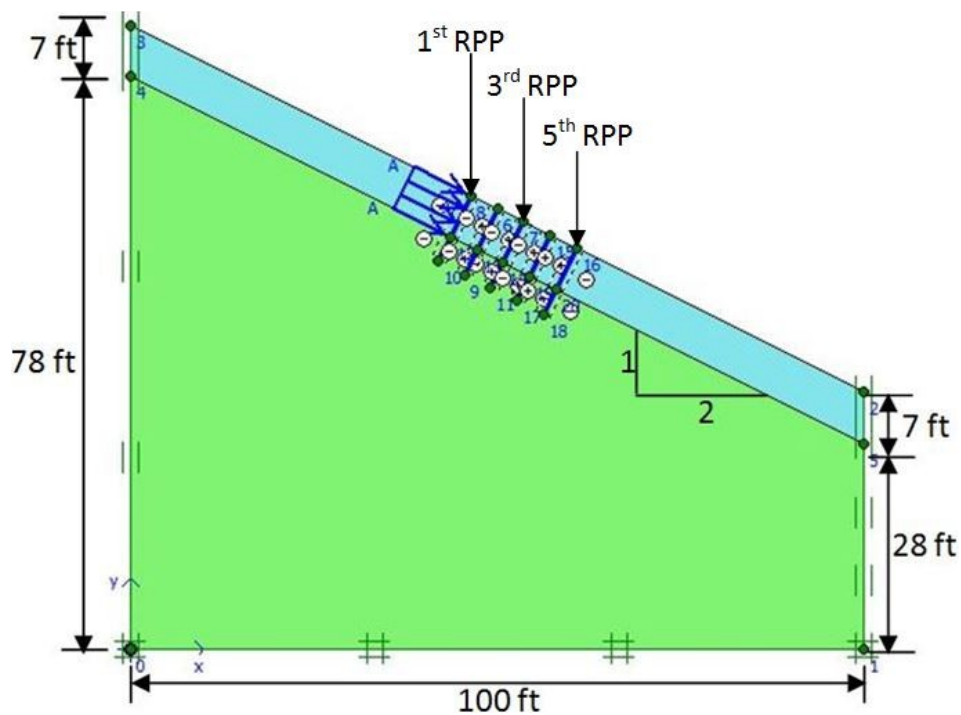


Figure 3.1 Representative model with all structural elements.

The geometry has been divided into finite elements to perform finite element analysis after the model geometry is fully defined and material properties are assigned to all clusters and structural objects. Mesh is a composition of interconnected finite elements and PLAXIS allows for a fully generation of finite element meshes. The developed meshes are triangular and unstructured based on robust triangulation procedure. Very fine mesh is generated in order to

obtain more accurate results. The generated mesh of a representative model used for the analysis is shown in Figure 3.2.

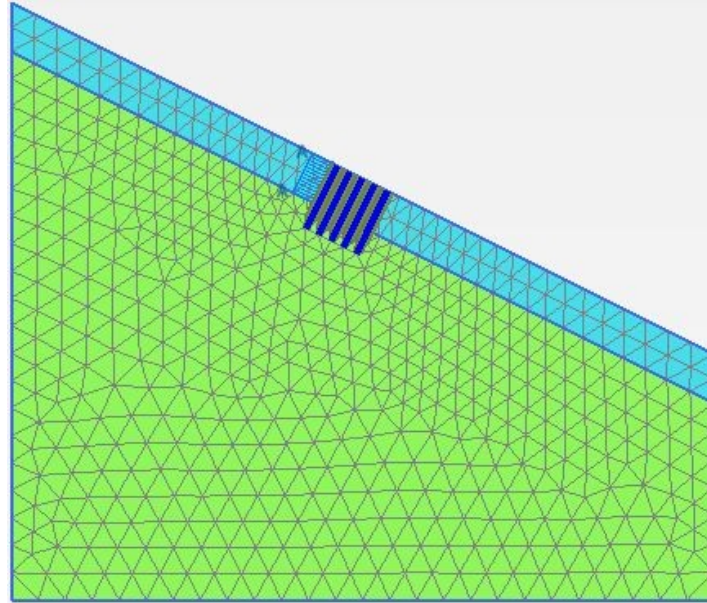


Figure 3.2 Generated mesh for a slope ratio of 2H:1V at initial condition.

Gravity loading is considered for the initial phase as the model deals with a slope and after that the structural elements (RPP) were activated. Then the deformation analysis is done assuming stage construction by applying series of load over the installed RPP.

3.4 Selection of Number of RPP

It is important to determine the number of required RPP to simulate an efficient group in sustainable slope stabilization at the beginning of the study. A detailed numerical study is conducted chronologically following Figure 3.3 to simulate the most effective group.

At first, slope ratio of 2H:1V is considered, where 100 psf, 300 psf, 500 psf and 1000 psf load was applied consecutively on single RPP installed in a 3-ft deep slip surface and the maximum horizontal displacement is noted. Then the number of RPP is increased gradually up to 8 at constant spacing of 2-ft and maximum horizontal displacement of first RPP under 100 psf, 300 psf, 500 psf and 1000 psf load is recorded for each increment. Similarly, the maximum horizontal displacement of first RPP is determined and recorded in each case under same

loading condition in case of increasing number (up to 8) of RPP at different spacing ranging from 3-ft to 6-ft for a 3 feet deep slip surface. Similar technique is followed for 5-ft and 7-ft deep slip surface. Figure 3.4 depicts the above mentioned idea.

Same concept is adopted for slope ratio of 3H:1V to determine the number of RPP required to simulate an effective group in case of different slip surface. This study is conducted for a soil having cohesion of 100 psf and friction angle of 20° . The obtained horizontal displacements for each case are plotted graphically with respect to increment of RPP and shown in Appendix A.

Finally, the maximum horizontal displacement of first RPP in all cases was plotted graphically. Maximum horizontal displacement caused due to 500 psf load in case of 2H:1V slope ratio is shown in Figure 3.5 and Figure 3.6 for 3-ft, 5-ft and 7-ft deep slip surface. The graphical representation in Appendix A shows that the horizontal displacement of first RPP decreases with increasing number of RPP. The propagation of applied load is maximum in case of 7-ft deep slip surface and become almost constant after installation of 5th RPP in case of even higher applied load. Thus, a group of 5 RPP is chosen to simulate an effective group for sustainable shallow slope (3-ft to 7-ft) stabilization with PLAXIS 2D considering the most critical condition (slope ratio of 2H:1V and depth of slip surface is 7-ft with a top soil having cohesion of 100 psf and friction angle of 20° withstanding mobilized load of 500 psf).

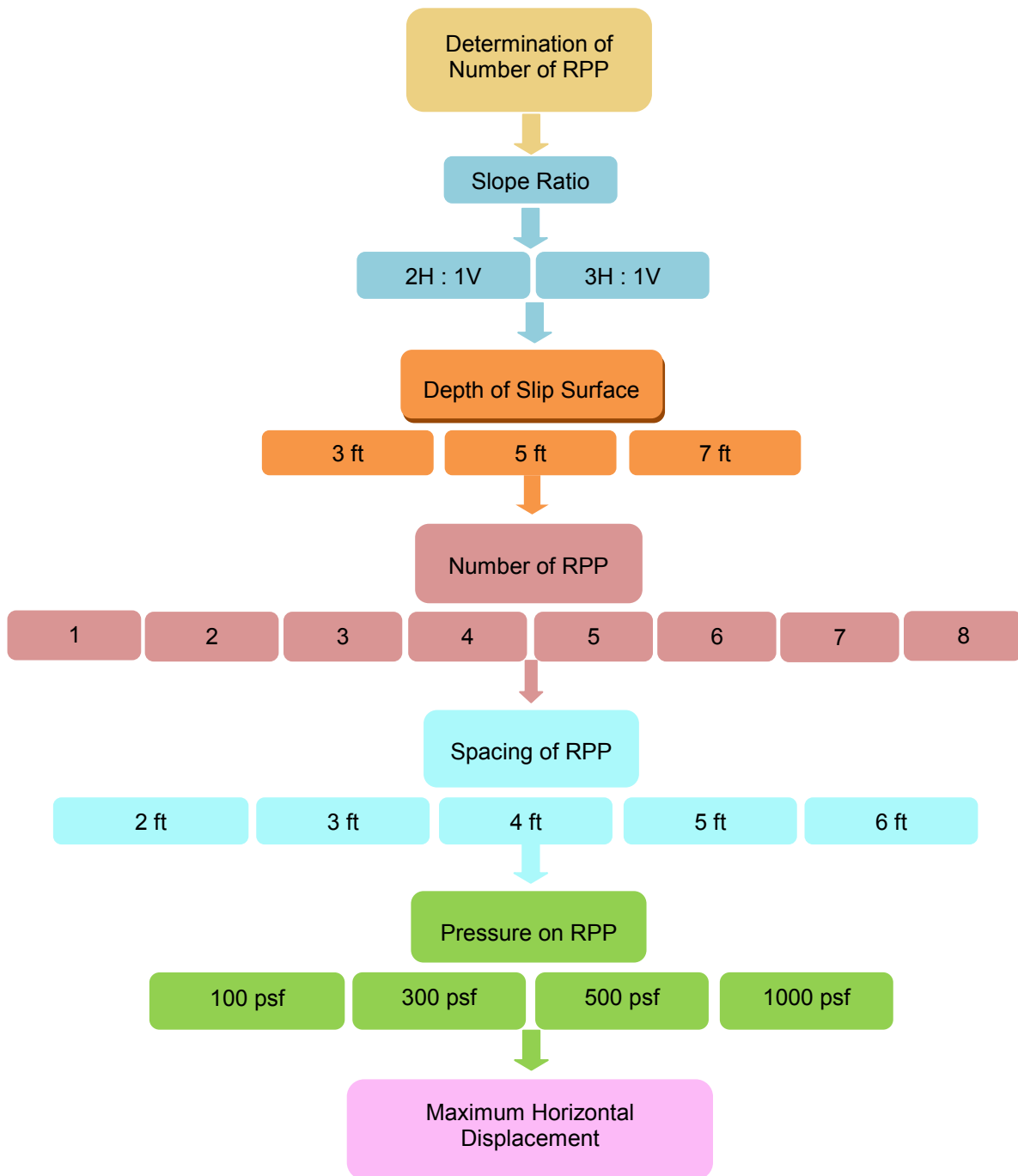


Figure 3.3 Flow chart for selection of number of RPP to form an effective group.

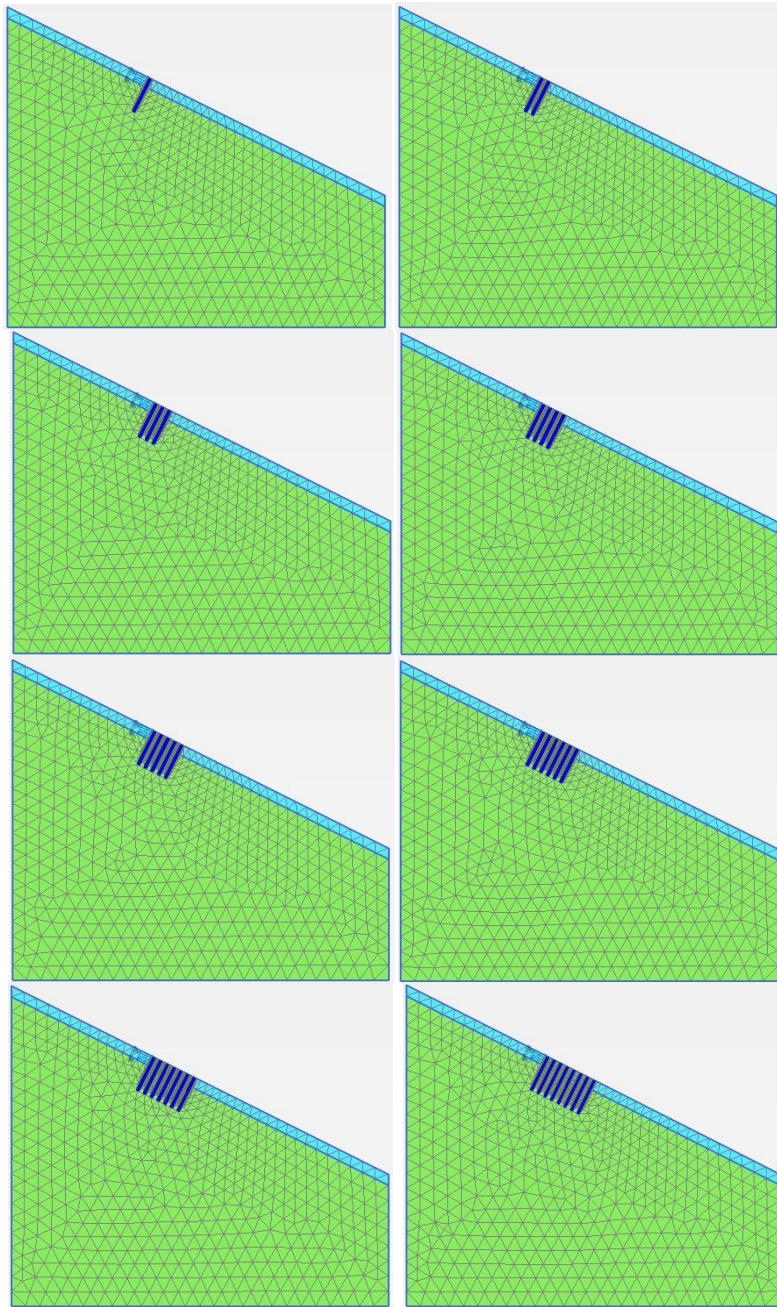
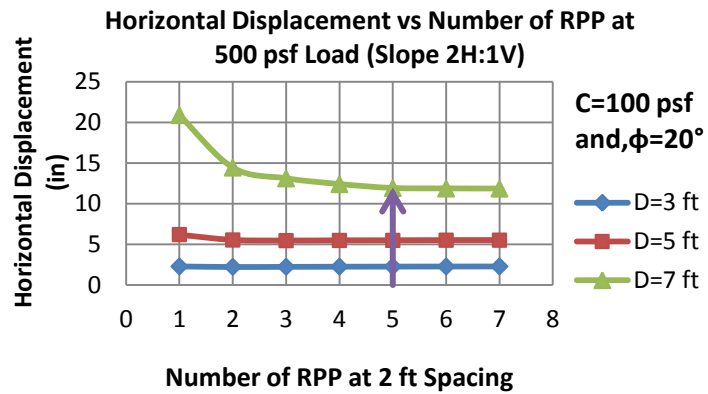
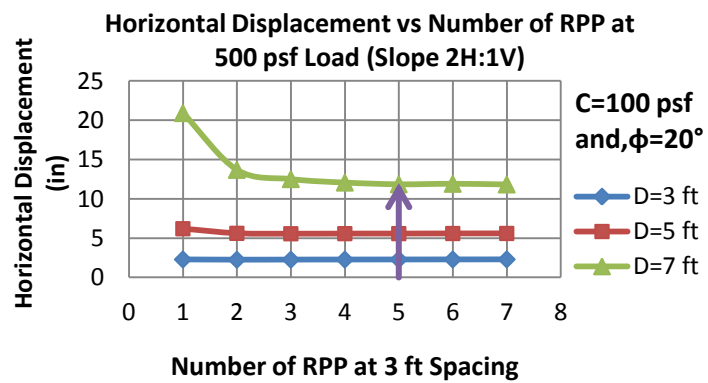


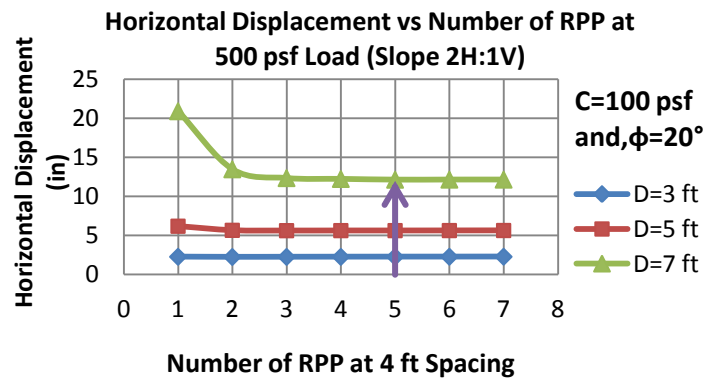
Figure 3.4 Representative Model of increasing RPP at 2 ft spacing for 2H:1V slope and 3-ft deep slip surface.



(a)

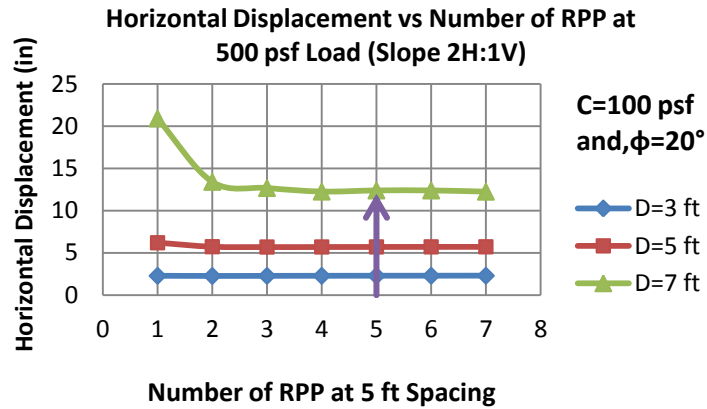


(b)

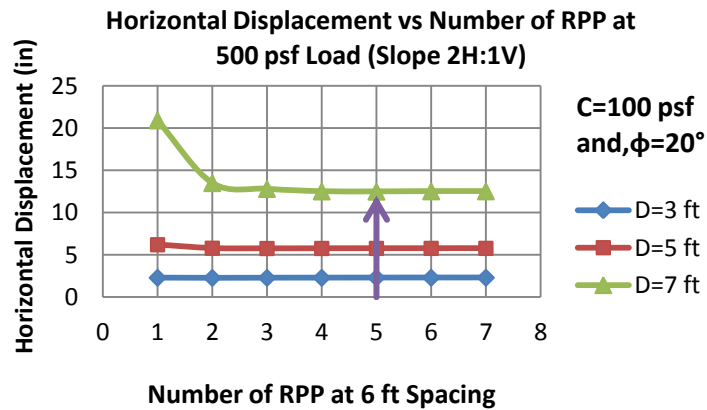


(c)

Figure 3.5 Influence of mobilized load on increasing number of RPP spaced at,
a. 2-ft, b.3-ft, c. 4-ft.



(a)



(b)

Figure 3.6 Influence of mobilized load on increasing number of RPP spaced at, a. 5-ft, b. 6-ft.

3.5 Parametric Study on the Group Effect of RPP

Parametric study is carried out to determine the variation of resistance between group of RPP and single RPP at different loading condition, soil strength parameters, spacing and depth of slip surface, where the horizontal displacement of single RPP and group of RPP is determined and plotted graphically. The graphical representation shows the difference of resistance between group of RPP and single RPP with increasing load, soil strength, spacing and depth of slip surface. Thus, the design charts for group of RPP at different spacing are

developed considering different types of soil for different slope, where the horizontal displacement and/or flexural stress is shown with increasing applied load.

3.6 Development of Design Chart

The design chart is developed to evaluate the load carrying capacity of group of RPP considering 5 RPP as a group, shown in Figure 3.7. According to Loehr and Borders (2007), depth of shallow slope failure ranged between 3-ft to 7-ft and geometry of the slope varied from 2H:1V to 4H:1V. Moreover, usually the US highway embankment slopes varies from 2H:1V to 4H:1V. Thus, the proposed design chart considers wide range of slip surface depth, mobilized load, and slope ratio and soil strength parameters, shown in Figure 3.8. On the other hand, 10-ft long RPP at three different spacing is considered to form a group as 12/10 ft long RPP at a spacing of 2-ft to 5-ft yields the most ideal result according to field data obtained from US 287 Highway (Khan, 2013). Therefore, the group of RPP installed at a spacing of 2-ft, 4-ft and 6-ft was considered in order to develop the design charts. A series of mobilized load (shown in Figure 3.8) applied over the group of RPP installed at a spacing of 2-ft, 4-ft or 6-ft and the corresponding maximum horizontal displacement and maximum bending moment of the first RPP forming the group is determined for a particular (2-ft or 4-ft or 6-ft) spacing of RPP. Figure 3.9 represents the maximum bending moment and horizontal displacement diagram induced on first RPP due to sustained load. Then obtained maximum bending moment is converted into flexural stress. Finally, the maximum horizontal displacement and flexural stress are plotted graphically with respect to applied load for a specific spacing of RPP, slope, slip surface and soil type. The study was conducted in order to develop the design chart following the flow chat shown in Figure 3.8. Therefore, three design charts are developed considering 2-ft, 4-ft and 6-ft spacing for each type of soil, slope and slip surface. The developed charts are shown in Appendix B.

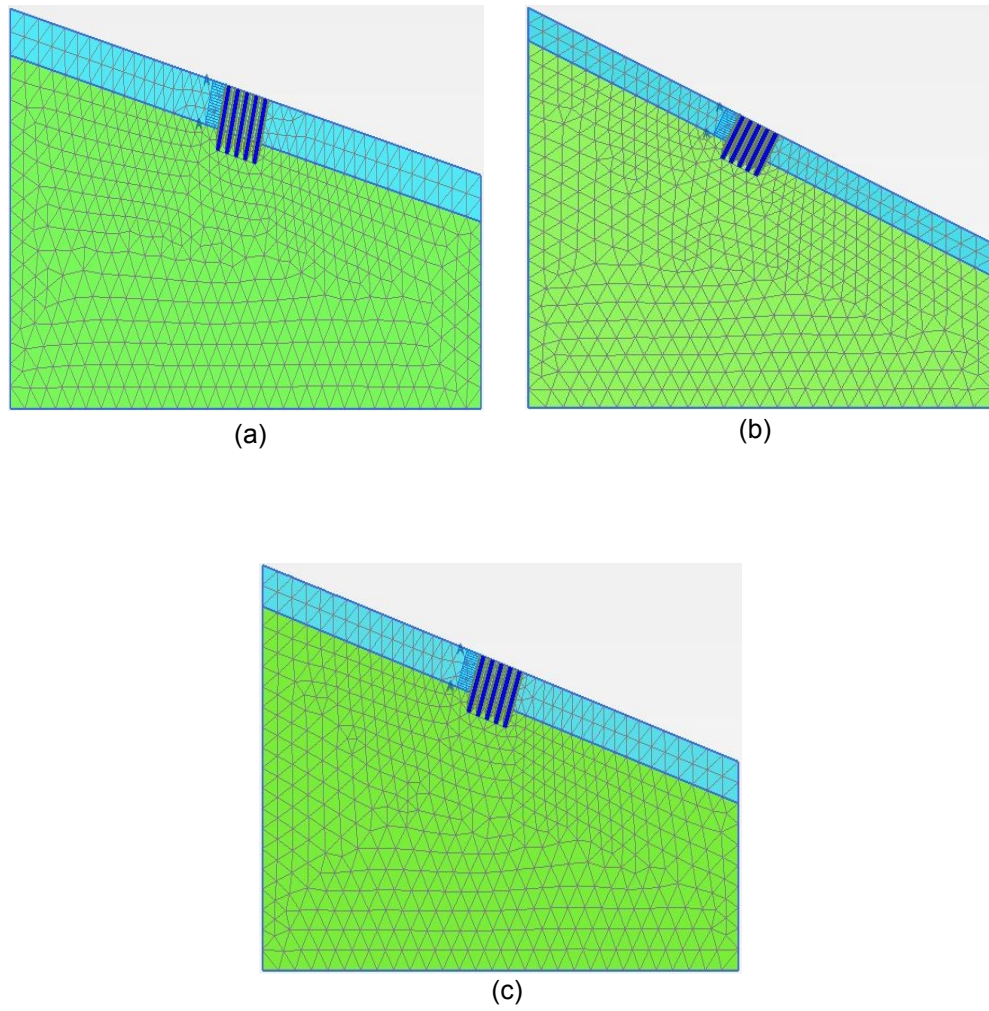


Figure 3.7 Representative model for development of design chart considering group resistance
for, a. slope 2H:1V, b. slope 3H:1V, c. slope 4H:1V.

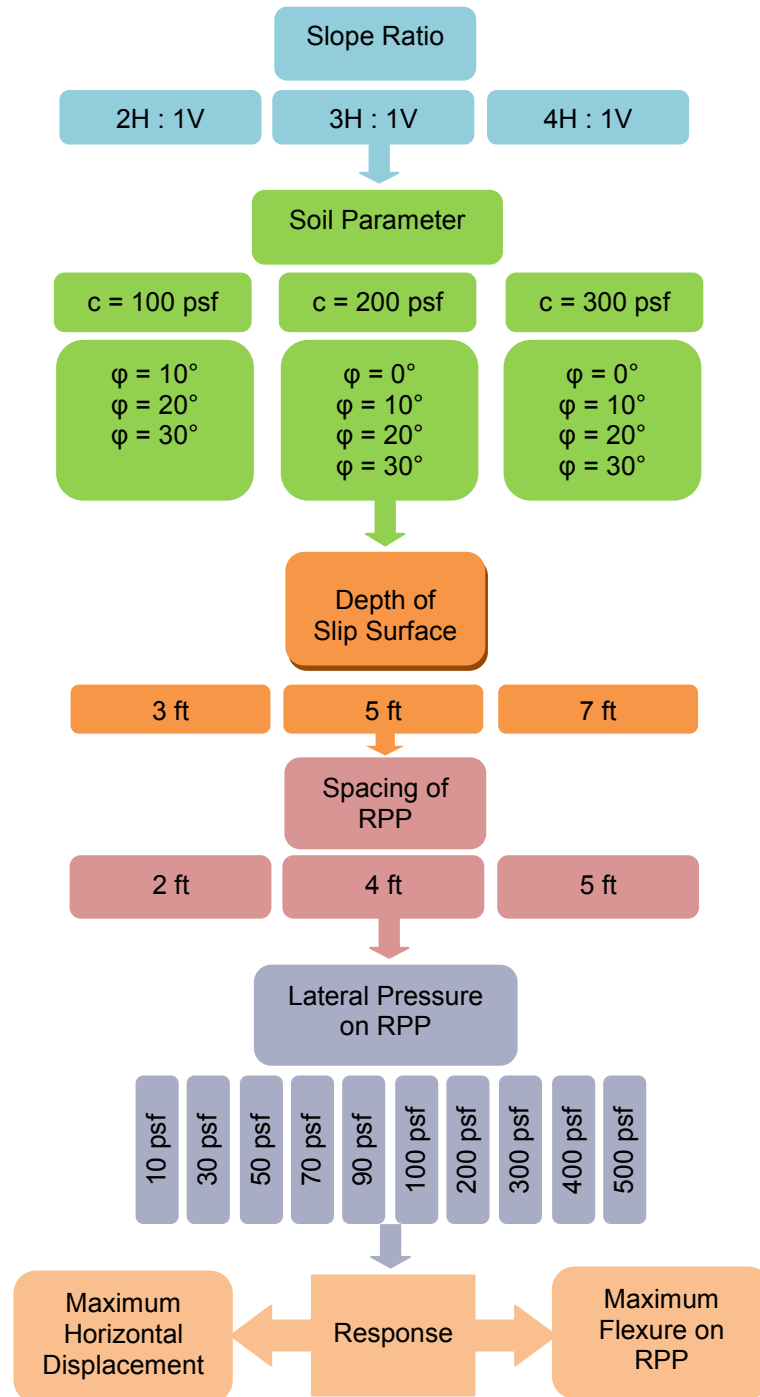


Figure 3.8 Flow chart showing sequential development of design chart.

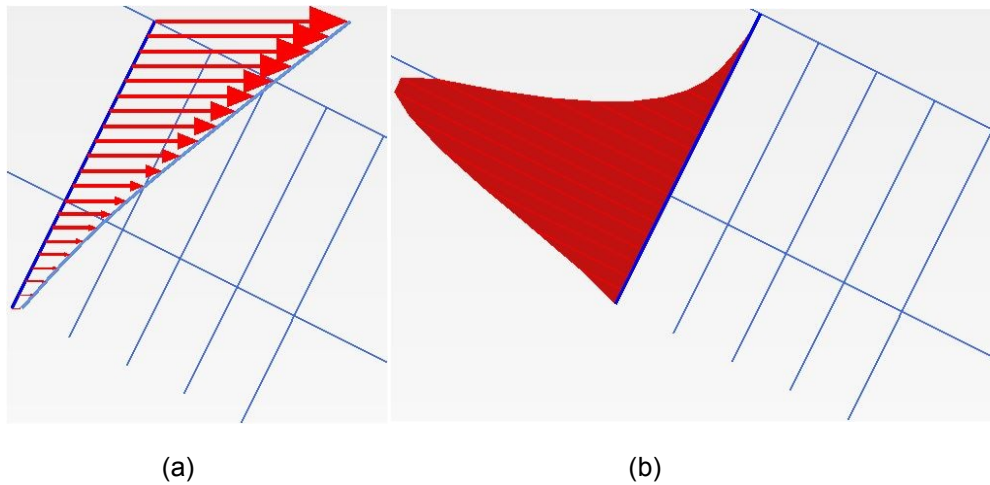


Figure 3.9 Seven feet deep slip surface stabilized with RPP at 2-ft spacing for a slope of 2H:1V showing, a. horizontal displacement of RPP, b. bending moment diagram of RPP.

3.7 Comparison with Field Data

It is necessary to validate the developed chart with field data. To determine the effectiveness of the developed design chart obtained field data from Interstate 70-Emma site is considered, where the slope ratio of the embankment is 2.2H:1V. According to Loehr and Borders (2007), the maximum bending moment induced on instrumented RPP installed in Interstate 70-Emma site was 350 ft-lb. The calculated maximum mobilized flexural stress of RPP is 500 psi due to the induced bending moment. The developed design chart for similar condition is used to determine the mobilized load causing same amount of flexural stress using Load vs Flexural Stress chart. Then the horizontal displacement due to the mobilized load is determined using Load vs Horizontal Displacement design chart. Hence, the obtained horizontal displacement is compared with the actual horizontal displacement occurred in the field.

3.8 Effect of Spacing

The effect of spacing is studied in terms of horizontal displacement and flexural stress at different loading conditions. The horizontal displacement due to 500 psf load at increasing spacing ranged from 2-ft to 6-ft for each type of soil, slope and slip surface is obtained by numerical modeling and analyzed to determine the effect of spacing on group resistance of

RPP. Figure 3.10 represents the horizontal displacement at increasing spacing due to 500 psf horizontal load for a soil having cohesion of 100 psf and friction angle of 10° , where slope ratio is 3H:1V.

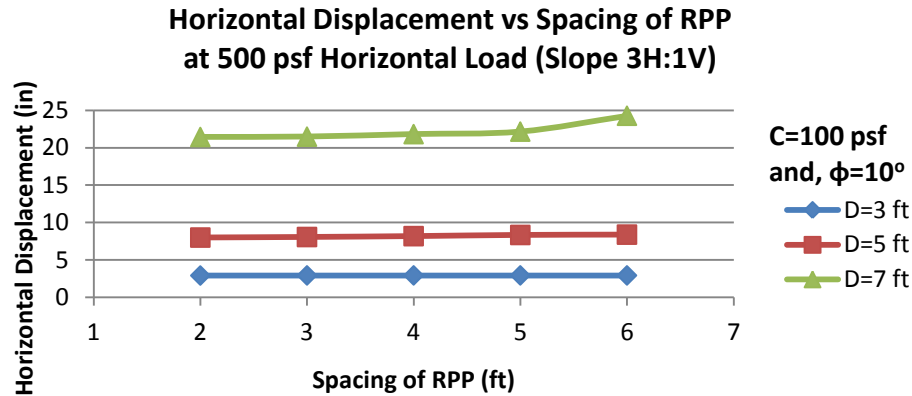


Figure 3.10 Effect of spacing on horizontal displacement of RPP due to 500 psf horizontal load.

3.9 Determination of Multiplication Factor

Finally, the performance of group of RPP at (2-ft/4-ft/6-ft) different spacing over single RPP under applied load is evaluated according to the following ratio. Then, the performance of group of RPP compared to single RPP under sustained load is expressed as a factor. Thus, the resistance in terms of horizontal displacement of RPP grouped at different spacing is evaluated as a multiplication factor, which will adjust the under estimated resistance of RPP proposed by Khan (1013).

(a) Factor for Allowable Horizontal Displacement =

$$\frac{\text{Load causing horizontal displacement of Grouped RPP}}{\text{Load causing same amount of horizontal displacement of Single RPP}}$$

(b) Factor for Allowable Flexural Stress =

$$\frac{\text{Load causing Flexural Stress on Group of RPP}}{\text{Load causing same amount of Flexural Stress on Single RPP}}$$

Chapter 4

Results and Discussions

4.1 Introduction

The application of RPP in reinforcing slope affirms to be an effective and economic solution for sustainable shallow slope stabilization. The load acting on the sliding surface transferred to the firm soil strata through the installed RPP and resists the imminent slope failure. Therefore, it is crucial to investigate the group resistance of RPP as they are always installed in a group with a view to find out their suitability. Thus, aim of this study is to determine the group resistance of RPP at different spacing considering maximum horizontal displacement and flexural creep of RPP. After deliberate and meticulous study, five RPPs are chosen to simulate an effective group and based on that three different design charts are developed considering different spacing between RPP ranging from 2-ft to 6-ft for each type of soil of a slope. So, it is important to determine the most effective spacing in order to choose the appropriate design chart. Keeping this point in mind, following analysis and comparison has been carried out.

4.2 Effects of Spacing

Three design charts at 2-ft, 4-ft and 6-ft spacing for each type of soil, slope and slip surface are developed to determine the group resistance of RPP. Then the most efficient spacing resulting minimum horizontal displacement and flexural stress from developed charts are evaluated graphically.

4.2.1 Effect of Spacing of RPP at different Loading Condition

Spacing effect is very less in case of small mobilized load irrespective of depth of slip surface shown in Figure 4.1, where 100 psf horizontal load is applied on RPP grouped together with variable spacing ranged from 2-ft to 6-ft. The variation of horizontal displacement with increasing spacing is not noticeable. Thus, the effect of spacing is

insignificant on group of RPP at lower mobilized load. But, at higher mobilized load (500 psf) variation in horizontal displacement is observed with different spacing of RPP. In Figure 4.2, the horizontal displacement of RPP at 2-ft spacing is 11.85 inch and at 6-ft spacing is 12.48 inch in case of 7 feet deep slip surface.

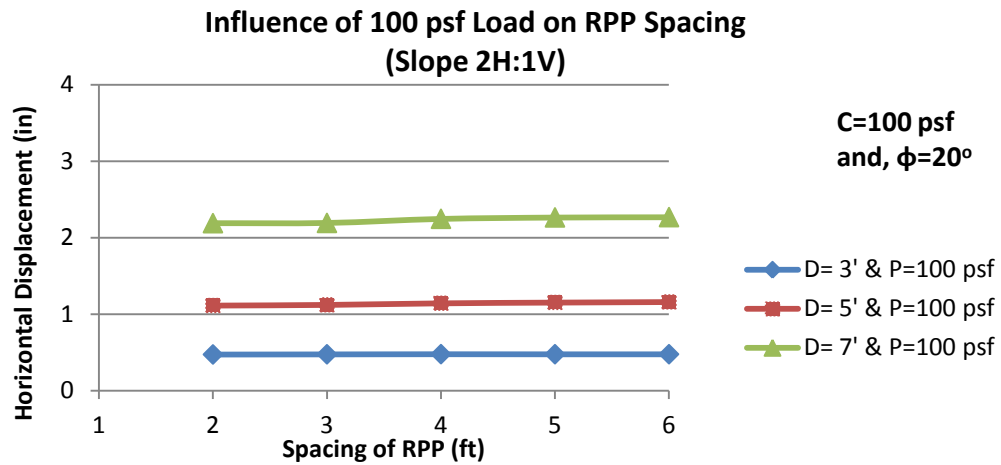


Figure 4.1 Influence of small mobilized load on increasing spacing of RPP

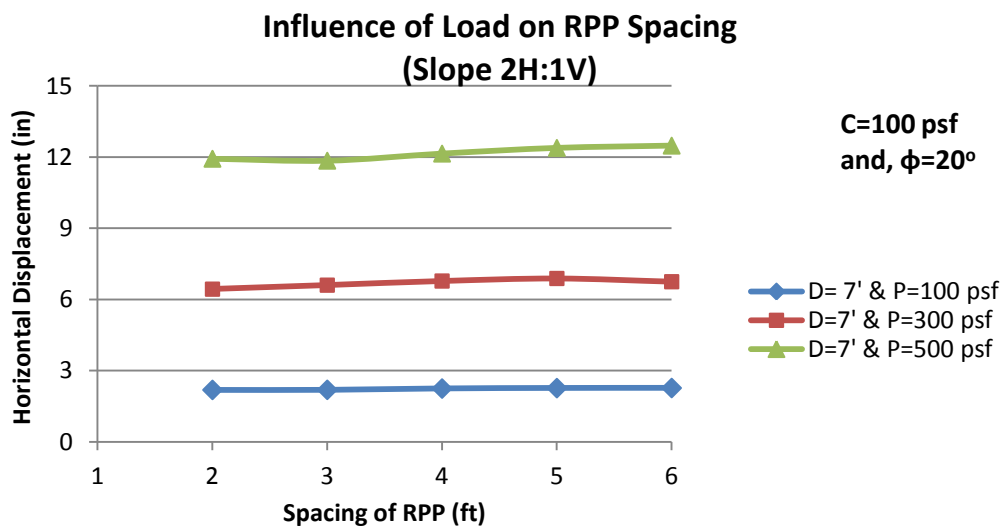


Figure 4.2 Influence of different loading condition on increasing spacing of RPP.

4.2.2 Effect of Spacing at different Slip Surface

According to Figure 4.3 and 4.4, the observed horizontal displacement variation is very less in case of 3-ft and 5-ft deep slip surface because of higher embedded depth of RPP into stiff soil. Thus, the spacing effect is very less in case of 3-ft and 5-ft deep slip surface irrespective of mobilized load.

On the other hand, the variation of horizontal displacement of group of RPP for 7-ft deep slip surface is already observed in Figure 4.2, where the minimum horizontal displacement occurs at 2-ft spacing and increases gradually with increment of RPP spacing.

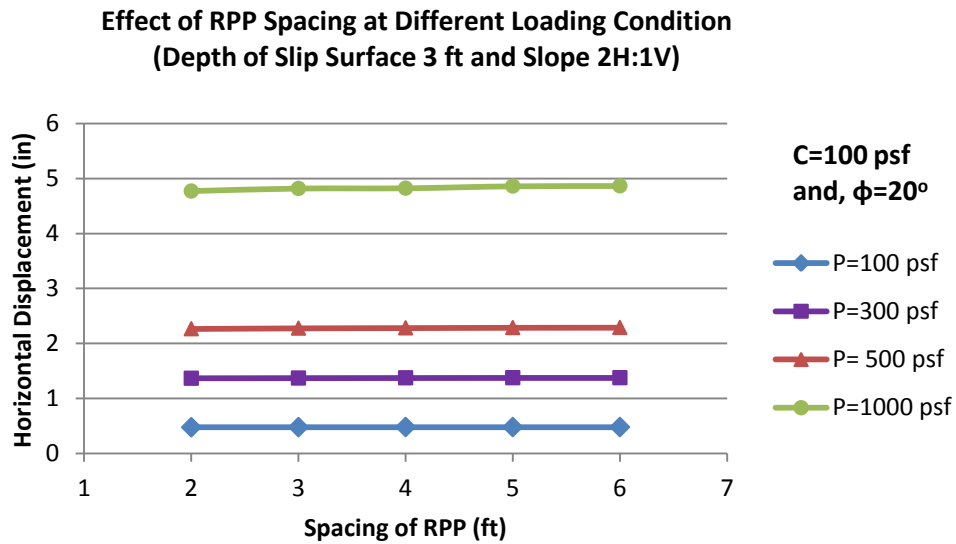
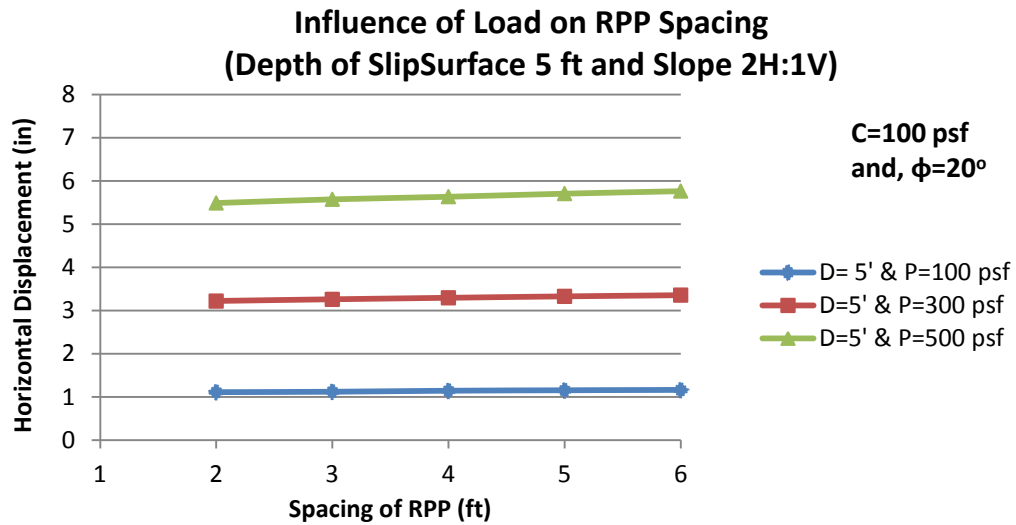


Figure 4.3 Effect of RPP spacing for 3-ft deep slip surface.

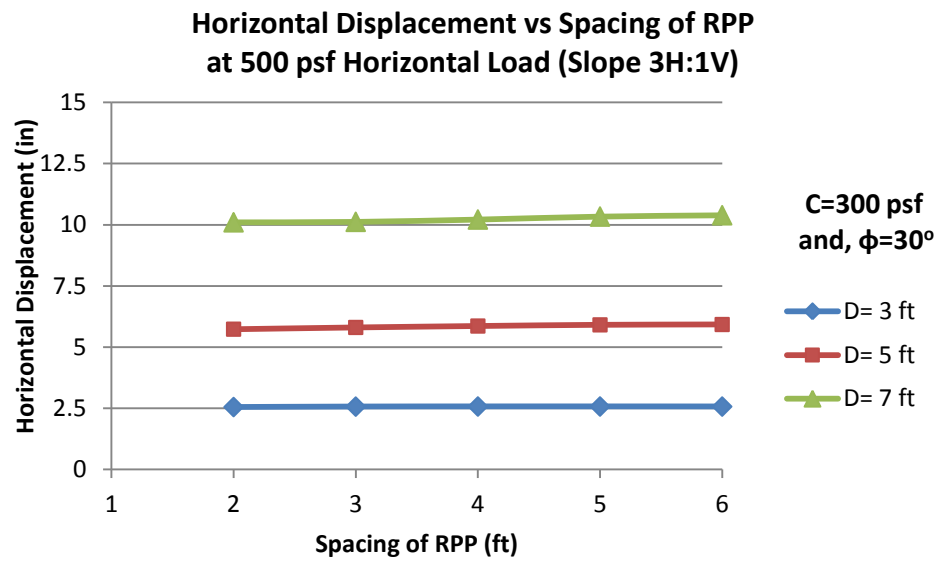


(b)

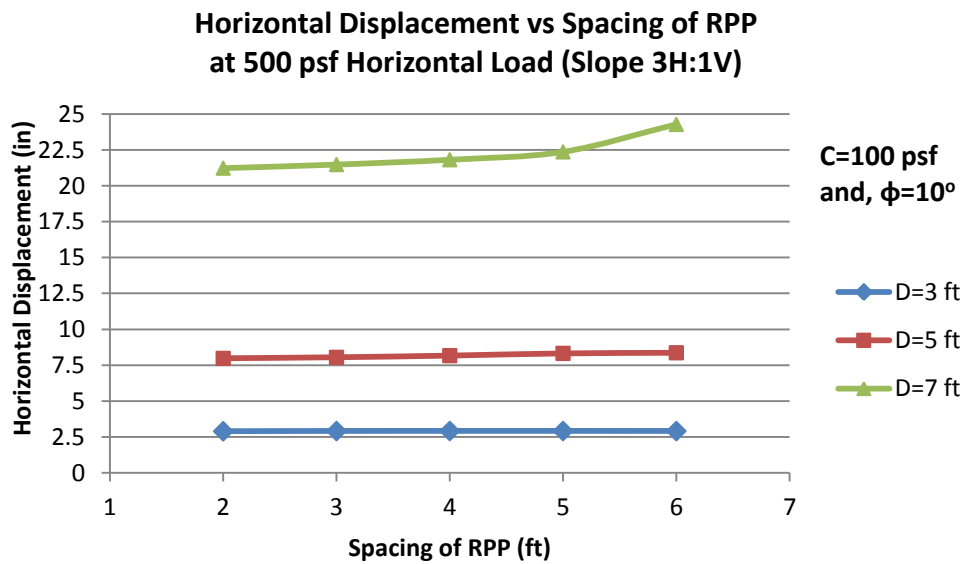
Figure 4.4 Effect of RPP spacing for 5-ft deep slip surface.

4.2.3 Effect of Soil Strength on RPP Spacing

Stability of a slope increases with increment of soil strength. Thus the effect of spacing between RPP is also reduced. The influence of soil strength can be studied from Figure 4.5, where the horizontal displacements at different soil strength parameters are studied for 3-ft, 5-ft and 7-ft deep slip surface at constant horizontal mobilized load of 500 psf. Considering both the figures, the variation of observed horizontal displacement due to increasing spacing of RPP is higher in case of the weak soil and lower for the soil having higher strength parameters. Therefore, it can be concluded that the effect of spacing decreases with increase of soil strength and minimum horizontal displacement occurs at 2-ft spacing RPP spacing.



(a)



(b)

Figure 4.5 Effect of soil strength on RPP spacing for a soil of, a. $c=300$ psf and, $\phi=30^\circ$,
b. $c=100$ psf and, $\phi=10^\circ$

4.2.4 Effect of Spacing on Flexural Stress

Group effect in terms of flexural stress induced on group of RPP is studied with increment of RPP spacing for different slip surface and shown in Figure 4.6. Influence of spacing is insignificant in case of 3-ft deep slip surface and it is quite less in case 5-ft deep slip surface. But, the influence of spacing in terms of flexural stress has conspicuous effect in case of 7-ft deep slip surface. Minimum flexural stress is induced at 2-ft spacing and thus group of RPP at 2-ft spacing is capable of withstanding higher mobilized load than group of RPP at 4-ft or 6-ft spacing.

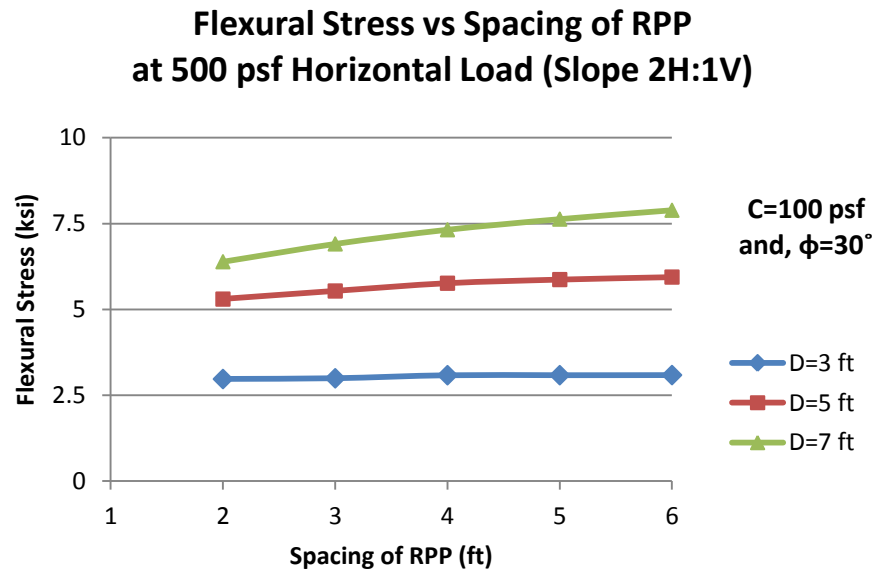


Figure 4.6 Effect of spacing on flexural stress for different slip surface

4.2.5 Most Efficient Spacing

The minimum horizontal displacement occurs at 2-ft spacing observed in Figure 4.5. Similarly, induced flexural stress on group of RPP at 2-ft spacing is minimum shown in Figure 4.6. Same phenomenon is observed for any types of soil considered to develop the design charts. Hence, it can be concluded that the most efficient spacing of RPP is

2-ft considering horizontal displacement and flexural stress. Thus, RPP can be installed at 2-ft spacing to achieve higher factor of safety if necessary.

4.3 Effect of Loading

The difference between resistance offered by group of RPP and single RPP is very less in terms of horizontal displacement in case of small mobilized load irrespective of depth of slip surface. Thus, the group effect is not noticeable for small mobilized load shown in Figure 4.7. The horizontal displacement of single RPP is 0.45 inch, 1.19 inch and 2.62 inch for 3-ft, 5-ft and 7-ft deep slip surface respectively caused due to 100 psf load. Similar horizontal displacement is observed at 100 psf load irrespective of slip surface in case of group of RPP group at 2-ft spacing. The obtained horizontal displacements of group of RPP at different spacing are also similar at 100 psf load and shown graphically in Appendix A.

The mobilized load was increased in order to compare the resistance offered by group of RPP with single RPP. The applied load was increased chronologically to 300 psf, 500 psf and 1000 psf as shown in Figure 4.8. In case of 1000 psf load, the horizontal displacement of RPP grouped at 2-ft spacing is 12.8 inch and 39 inch for 5-ft and 7-ft deep slip surface respectively. The obtained result is way beyond the acceptable limit in case of 5-ft and 7-ft deep slip surface and thus disregarded. According to Figure 4.8, difference of resistance between group of RPP and single RPP is very less in case of 3-ft and 5-ft deep slip surface at 300 psf and 500 psf applied load. But in case of 7-ft deep slip surface the resistance offered by group of RPP is higher than resistance of single RPP as single RPP experience more horizontal displacement than group of RPP.

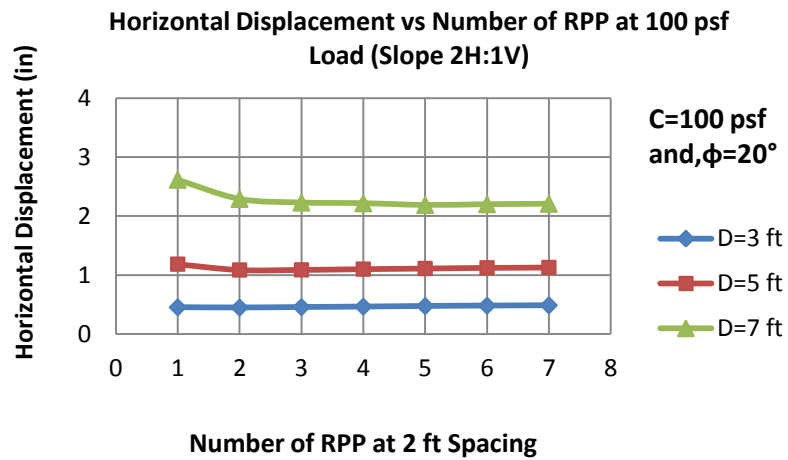


Figure 4.7 Influence of lower mobilized load (100 psf) on increasing number of RPP.

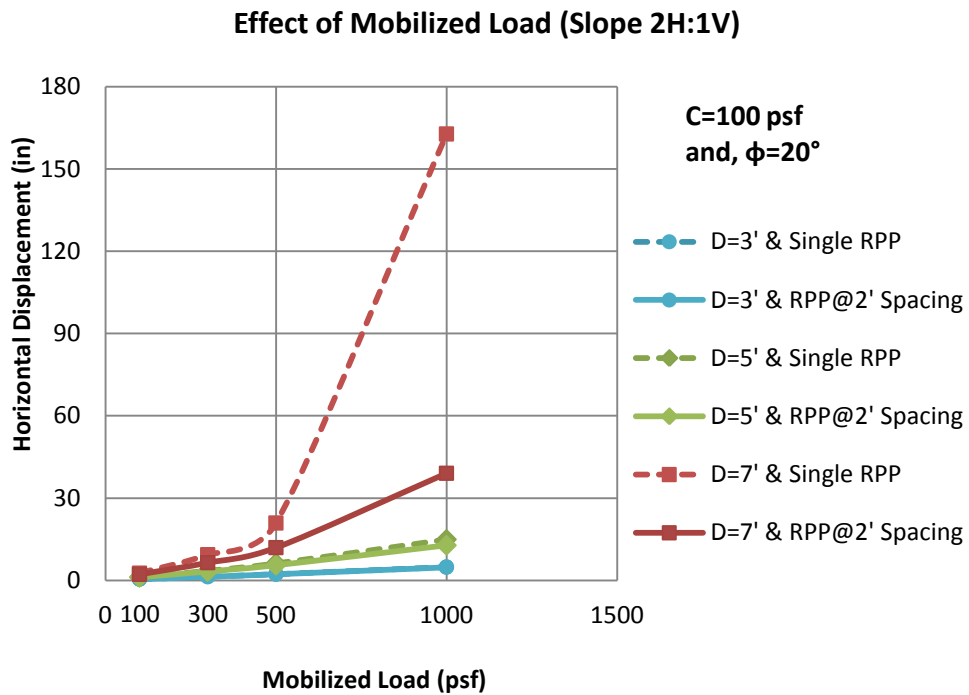


Figure 4.8 Effect of mobilized load on group of RPP and single RPP.

4.4 Effect of Depth of Slip Surface

4.4.1 *Depth of Slip Surface 3 ft*

The difference of resistance between group of RPP and single RPP is very less for 3-ft deep slip surface considering the variation of horizontal displacement between them. Thus, the variation in resistance between group of RPP and single RPP is not noticeable in case of 3-ft deep slip surface irrespective of mobilized load as major portion of RPP is embedded into the stiff soil. This phenomenon is represented in Figure 4.9 and according to the Figure for 3-ft deep slip surface, the horizontal displacement experienced by group of RPP is similar to single RPP, though the applied load was increased from 100 psf to 500 psf.

The effect of mobilized load decreases with increment of RPP. PLAXIS generated horizontal displacement and bending moment diagrams due to 500 psf load portrayed in Figure 4.10 shows the similar phenomenon in case of 3-ft deep slip surface. The induced bending moments are 1662.038 lb-ft/ft, 269.217 lb-ft/ft, 69.56 lb-ft/ft, 16.43 lb-ft/ft, 24.90 lb-ft/ft, 26.80 lb-ft/ft, 27.29 lb-ft/ft and 33.726 lb-ft/ft and horizontal displacements are 2.174 inch, 1.174 inch, 0.832 inch, 0.644 inch, 0.516 inch, 0.419 inch, 0.344 inch and 0.281 inch respectively. Though the reduction of horizontal displacement is less remarkable with increasing number of RPP but induced bending moment reduces drastically in the 2nd RPP. Therefore, it can be concluded that the influence of mobilized load is observed up to 2nd RPP in case of higher mobilized load for 3-ft deep slip surface.

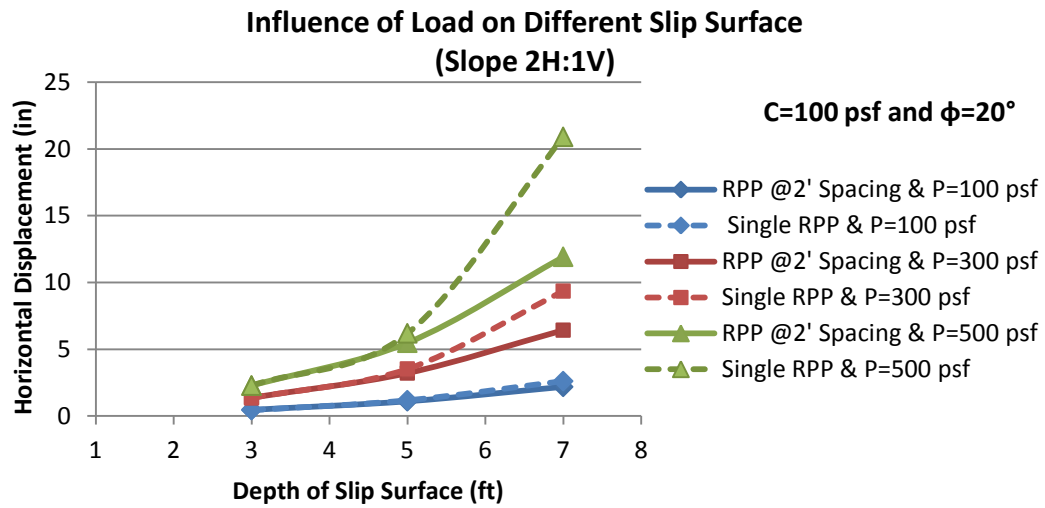
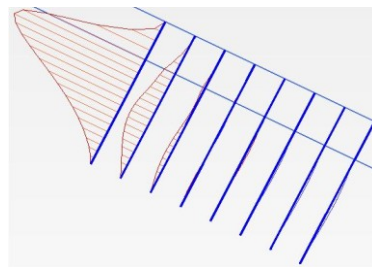
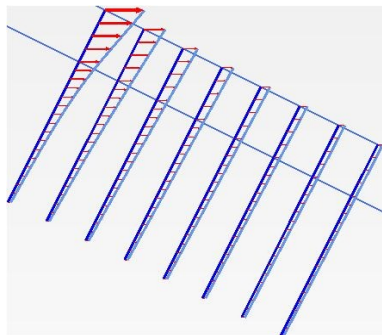


Figure 4.9 Influence of different loading condition on different slip surface.



(a)



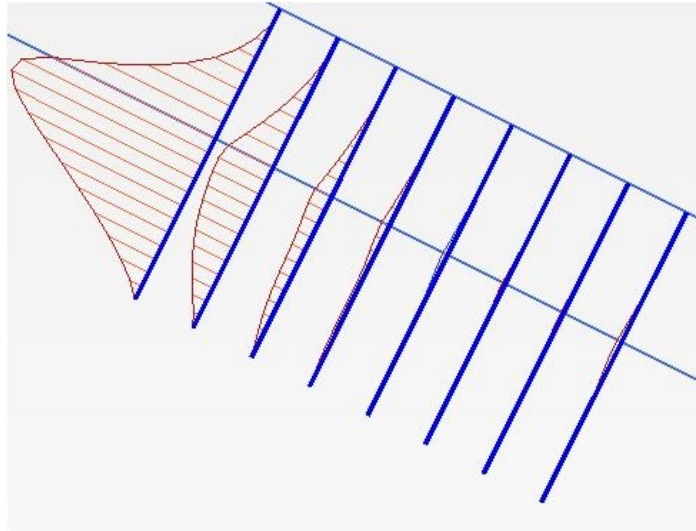
(b)

Figure 4.10 Influence of 500 psf load on RPP at 2-ft spacing in terms of, a. bending moment diagram and b. horizontal displacement, for 3-ft deep slip surface (slope 2H:1V).

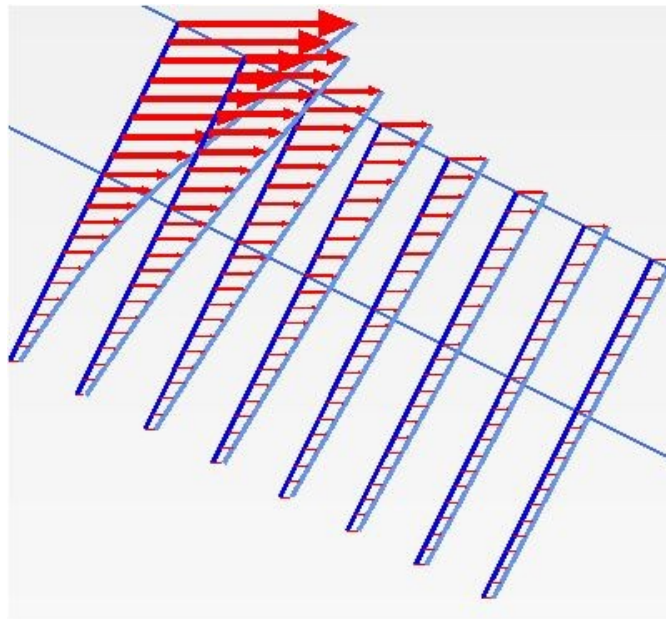
4.4.2 Depth of Slip Surface 5 ft

The difference of resistance between group of RPP and single RPP is also less for 5-ft deep slip surface considering the variation of horizontal displacement between them. Thus, the group effect is quite small in case of 5-ft deep slip surface as half of the length of RPP is embedded into the stiff soil. This phenomenon is already represented in Figure 4.9, where the variation in horizontal displacement between group of RPP and single RPP is small, though the applied load was increased from 100 psf to 500 psf.

PLAXIS generated horizontal displacement and bending moment diagrams due to 500 psf load portrayed in Figure 4.11. The induced bending moments are 3282 lb-ft/ft, 818.2 lb-ft/ft, 280.3 lb-ft/ft, 130.6 lb-ft/ft, 76.15 lb-ft/ft, 52.33 lb-ft/ft, 46.22 lb-ft/ft and 75.15 lb-ft/ft, and horizontal displacements are 5.645 inch, 3.281 inch, 2.208 inch, 1.612 inch, 1.231 inch, 0.967 inch, 0.779 inch and 0.651 inch respectively. The induced bending moment and horizontal displacement reduce drastically up to 3rd RPP. After the 3rd RPP, the horizontal displacement and bending moment due to applied load become almost similar. Therefore, it can be concluded that the influence of mobilized load is observed up to 3rd RPP in case of 500 psf (2500 lb/ft) mobilized load for 5-ft deep slip surface.



(a)



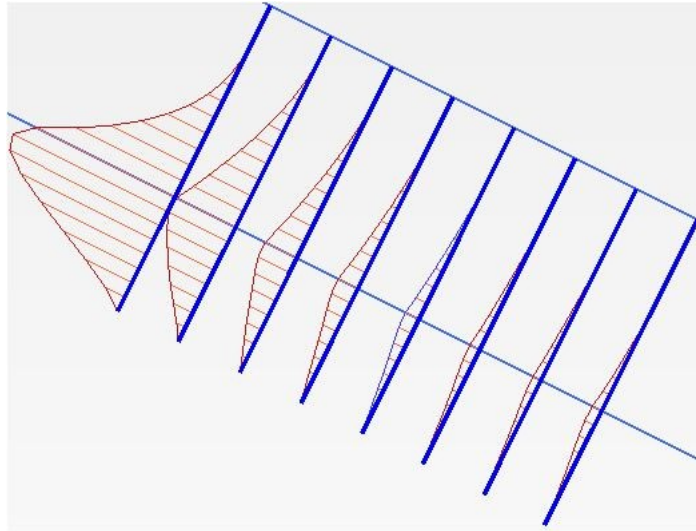
(b)

Figure 4.11 Influence of 500 psf load on RPP at 2-ft spacing in terms of, a. bending moment diagram and b. horizontal displacement, for 5-ft deep slip surface (slope 2H:1V).

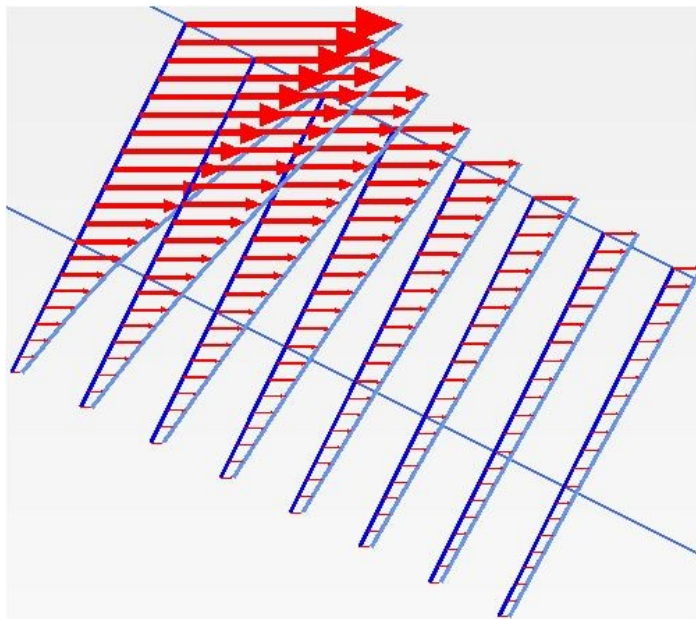
4.4.3 Depth of Slip Surface 7 ft

According to Figure 4.9, the variation in resistance offered by group of RPP compared to single RPP is vividly exposed in case of 7-ft deep slip surface as the horizontal displacement of single RPP is much higher than group of RPP. This condition prevails, in case of 300 psf and 500 psf applied load. But, the difference of horizontal displacement between group of RPP and single RPP is insignificant at lower mobilized load (100 psf) for 7-ft deep slip surface.

PLAXIS generated horizontal displacement and bending moment diagrams due to 300 psf load portrayed in Figure 4.12. The induced bending moments are 2536 lb-ft/ft, 970.9 lb-ft/ft, 521.3 lb-ft/ft, 323.2 lb-ft/ft, 217.9 lb-ft/ft, 157.5 lb-ft/ft, 129.6 lb-ft/ft and 157.8 lb-ft/ft, and horizontal displacements are 6.65 inch, 4.49 inch, 3.16 inch, 2.31 inch, 1.74 inch, 1.33 inch, 1.05 inch and 0.86 inch respectively. The induced bending moment and horizontal displacement reduce drastically up to 5th RPP. Hence, it can be concluded that the influence of mobilized load is observed up to 5th RPP in case of 300 psf (2100 lb/ft) mobilized load for 7-ft deep slip surface.



(a)



(b)

Figure 4.12 Influence of 500 psf load on RPP at 2-ft spacing in terms of, a. bending moment diagram and b. horizontal displacement, for 7-ft deep slip surface (slope 2H:1V).

4.5 Effect of Soil Strength

Strength of soil plays a vital role in case of slope failure besides gravitational force. Increment of soil strength reduces the susceptibility of slope failure. Similar phenomenon is observed in Figure 4.13, where the horizontal displacement of RPP acting in a group is reduced gradually with increasing soil strength at 400 psf applied load though the observed horizontal displacement in case of 3-ft deep slip surface is very less due to higher embedment of RPP into stiff soil. The horizontal displacement in case of 5-ft deep slip surface also not remarkable, but reduction of horizontal displacement of RPP is vividly exposed for 7-ft deep slip surface. Thus, the difference of horizontal displacement between group of RPP and single RPP should be studied at different soil parameters to examine the group resistance of RPP.

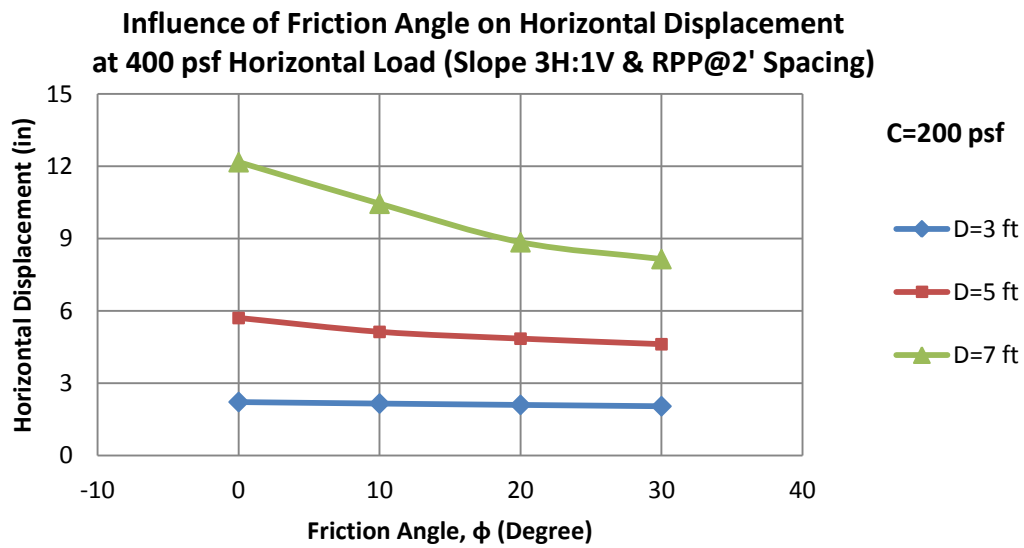


Figure 4.13 Group Resistance of RPP with respect to soil strength.

4.5.1 *Effect of Cohesion*

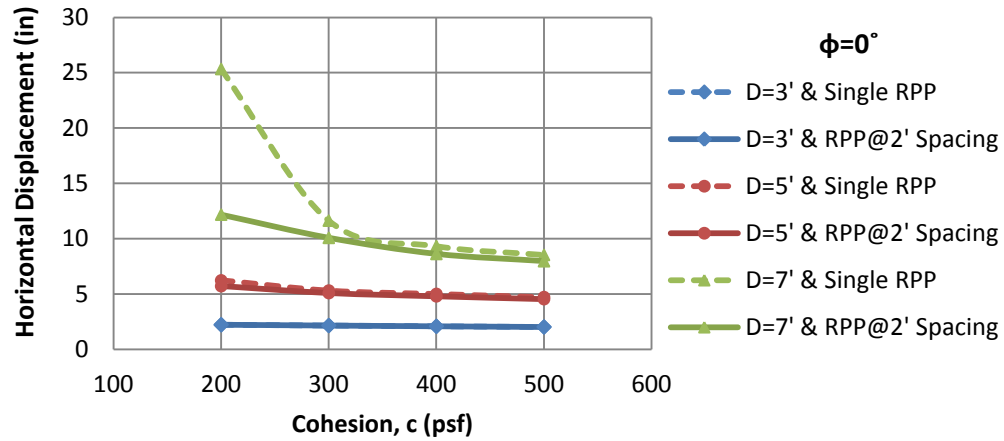
The graphical representation depicted in Figure 4.14 shows the effect of cohesion. For this reason pure clayey soil with friction angle of 0° and granular soil with friction angle 30° is considered with increasing cohesive strength, where resistance offered by group of RPP and single RPP under 400 psf horizontal load is portrayed.

In case of 3-ft deep slip surface, the horizontal displacement of group of RPP and single RPP is similar at 0° or 30° friction angle with increasing cohesion. Thus, the variation of resistance between group of RPP and single RPP is insignificant irrespective of soil strength for 3-ft deep slip surface shown in Figure 4.14(a) and 4.14(b).

In case of 5-ft deep slip surface, the horizontal displacement of group of RPP and single RPP is closer at different friction angle with increasing cohesion. Thus, the variation of resistance between group of RPP and single RPP is also not remarkable for different types of soil in case of 5-ft deep slip surface shown in Figure 4.14(a) and 4.14(b).

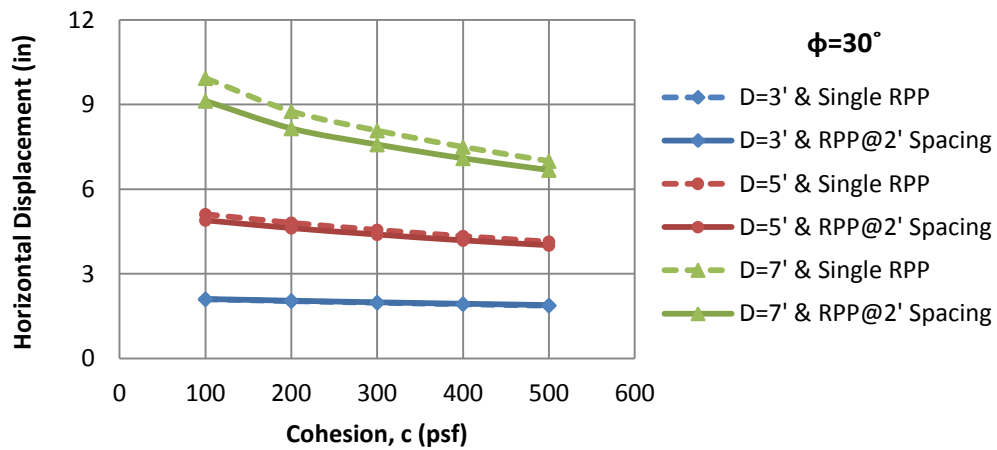
The maximum horizontal displacement of single RPP is quite higher than group of RPP in case of 7-ft deep slip surface for a soil having friction angle of 0° and cohesion of 200 psf, shown in Figure 4.14(a). On the other hand, the difference between the horizontal displacements of group of RPP and single RPP is less in case of a soil having higher friction angle, shown in Figure 4.14(b). At higher strength, resistance offered by group of RPP and Single RPP is almost similar. Thus, the group effect reduces with increase of soil strength.

**Influence of Cohesion on Horizontal Displacement
at 400 psf Horizontal Load (Slope 3H:1V)**



(a)

**Influence of Cohesion on Horizontal Displacement
at 400 psf Horizontal Load (Slope 3H:1V)**



(b)

Figure 4.14 Influence of cohesive strength on horizontal displacement for a soil having, a. friction angle of 0° , b. friction angle of 30° .

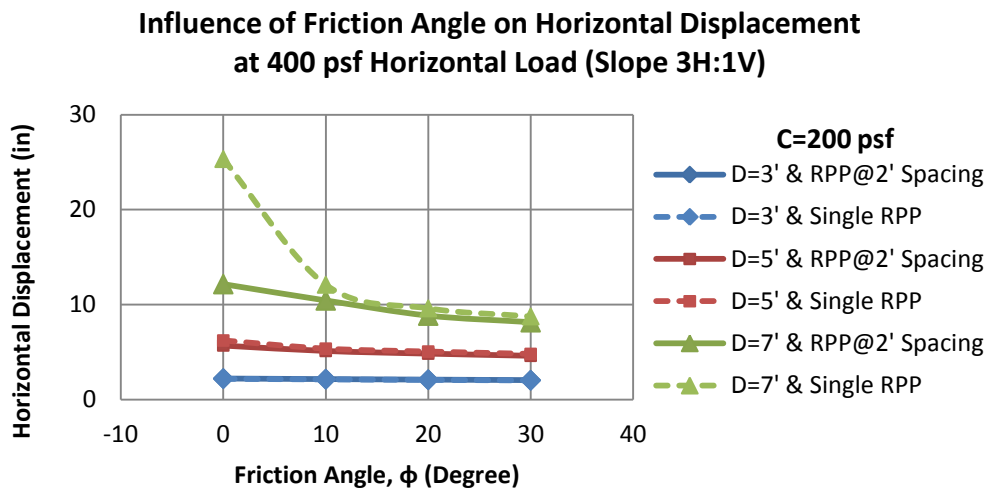
4.5.2 Effect of Friction Angle

The resistance offered by group of RPP and single RPP under 400 psf horizontal load is depicted in terms of horizontal displacement in Figure 4.15 for clayey soil with increment of friction angle ranging from 0° to 30° .

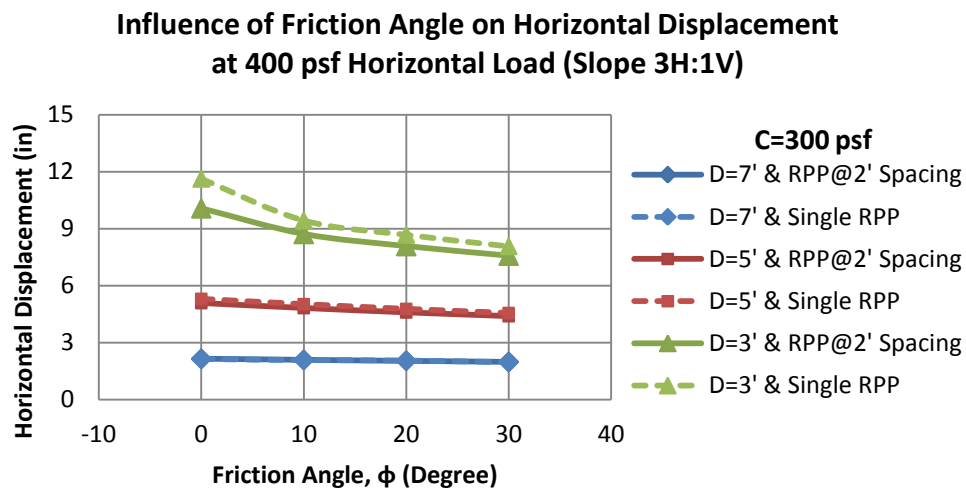
In case of 3-ft deep slip surface, the horizontal displacement for group of RPP and single RPP is similar, shown in Figure 4.15(a) and 4.15(b). It implies that the resistance of group of RPP and single RPP is same in case of 3-ft deep slip surface irrespective of soil strength.

Similar phenomenon is observed in case of 5-ft deep slip surface in Figure 4.15. It means that the soil strength parameters have very less influence on horizontal displacement of group of RPP and single RPP. Thus the resistance offered by group of RPP is closer to the resistance offered by single RPP in case of 5-ft deep slip surface at any types of soil.

In case of 7-ft deep slip surface, the difference in horizontal displacement of group of RPP and single RPP is conspicuous for a soil having friction angle of 0° and cohesion of 200 psf (or below) shown in Figure 4.15 (a). The variation of horizontal displacement reduces sharply with increment of friction angle. On the other hand, the difference between the horizontal displacement of group of RPP and single RPP is less irrespective of friction angle in case of a soil having cohesive strength of 300 psf or above shown in Figure 4.15(b). Thus, the difference of resistance between group of RPP and single RPP is less in case of a soil having higher cohesive strength irrespective of its friction angle and variation is higher for weak soil in case of 7-ft deep slip surface.



(a)

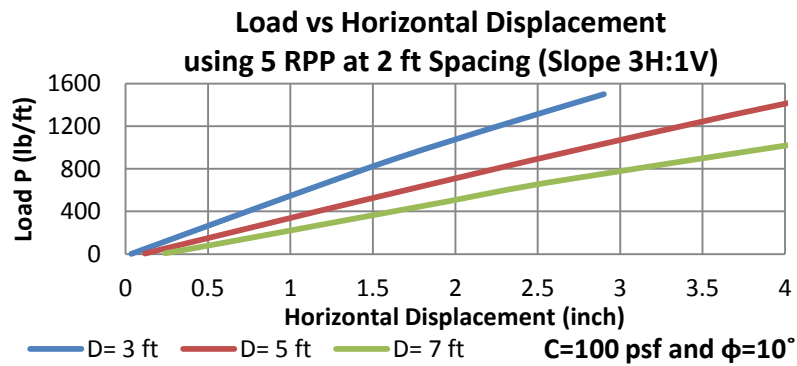


(b)

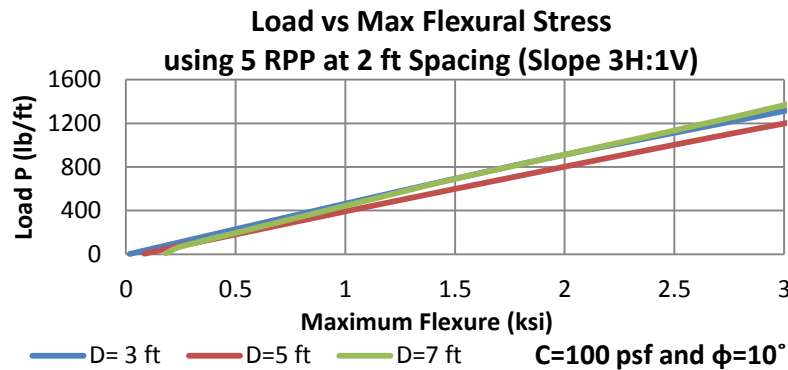
Figure 4.15 Influence of friction angle on horizontal displacement for a soil having, a. cohesive strength of 200 psf, b. cohesive strength of 300 psf.

4.6 Development of Design Chart considering Group Effect

It is vividly exposed that the minimum horizontal displacement and flexural stress occurs in case of RPP grouped at 2-ft spacing and required number of RPP to simulate an effective group is five. Same phenomenon is observed irrespective of soil type, slope and slip surface. But, stabilizing a slope using RPP at 2-ft spacing may not be economically viable. Thus, for each type of soil and slope, three design charts are developed considering 2-ft, 4-ft and 6-ft RPP spacing. The developed design charts are shown in Appendix B and Figure 4.16 represents a design chart for 2-ft spacing.



(a)



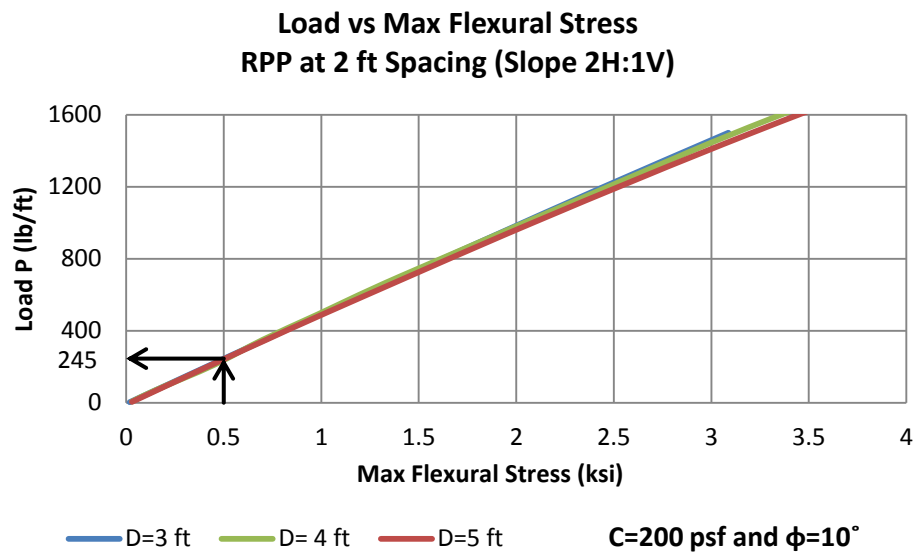
(b)

Figure 4.16 Limit Resistance Curve for group of RPP, a. load versus horizontal displacement, b. load vs maximum flexural stress.

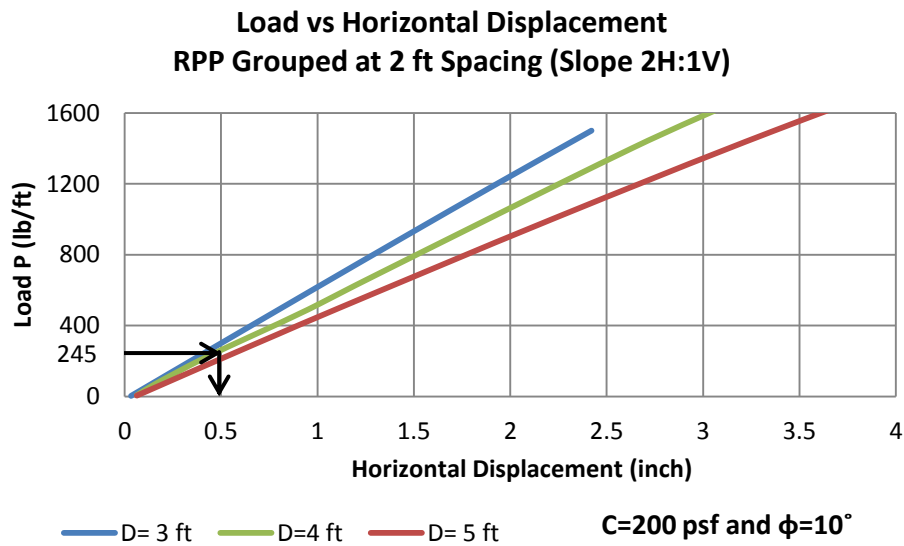
4.7 Comparison

4.7.1 *Comparison with Field Data*

Based on the study conducted by Loehr and Borders (2007), the Interstate 70-Emma Site, Missouri, highway embankment has a slope ratio of 2.5H:1V to 2.2H:1V. The depth of slip surface of the slope is 4-ft. Cohesive strength of soil is 202 psf and friction angle is 14° (according to direct shear test). The slope was reinforced with RPP at 3-ft spacing. The mobilized flexural stress induced on instrumented RPP was 500 psi (0.5 ksi) and the horizontal displacement observed after 2 years was 0.5 inch to 1.5 inch. Similar conditions of Interstate 70-Emma Site is plotted on developed chart for slope ratio of 2H:1V with cohesion of 200 psf and friction angle of 10° . The 4-ft deep slip surface is shown by interpolation in the design chart. The horizontal displacement according to the developed design chart for RPP at 2-ft spacing is 0.5 inch, shown in Figure 4.17 and the horizontal displacement for RPP at 4-ft spacing is 0.52 inch, shown in Figure 4.18. The interpolated horizontal displacement for 3-ft spacing of RPP is 0.51 inch. Hence, the obtained result is in good agreement with Interstate 70-Emma Site.

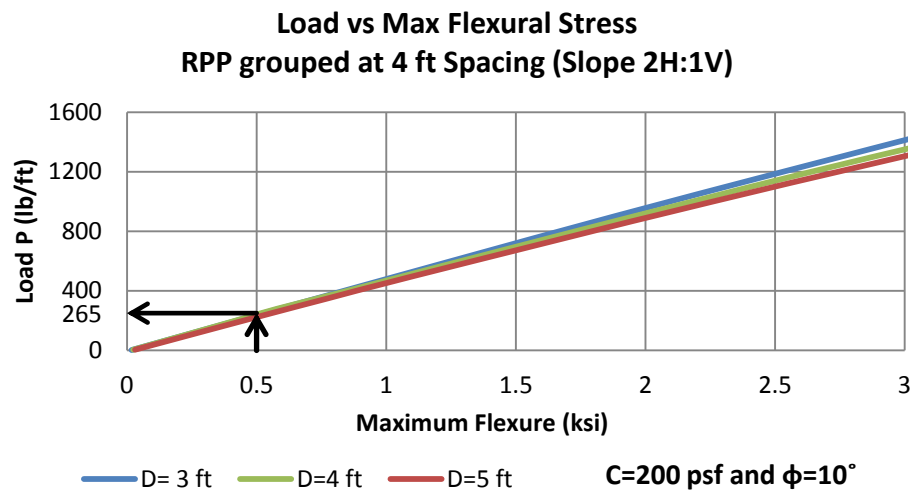


(a)

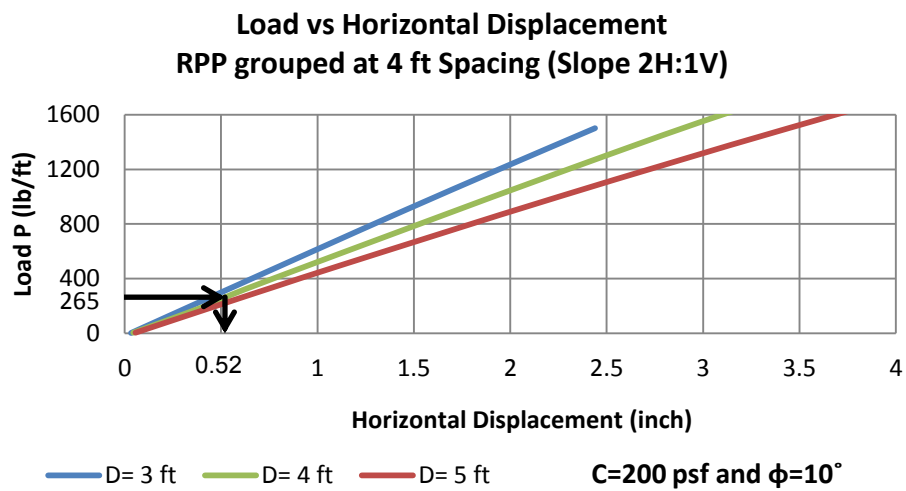


(b)

Figure 4.17 Limit Resistance Curves of RPP at 2 ft spacing for, a. flexural stress, b. horizontal displacement.



(a)



(b)

Figure 4.18 Limit Resistance Curves of RPP at 4 ft spacing for, a. flexural stress, b. horizontal displacement.

4.7.2 Comparison with Performance based Method proposed by Khan (2013)

The proposed limit resistance curves of single RPP developed by Khan (2013) is compared with the developed limit resistance curves for RPP grouped at 2ft/4-ft/6-ft spacing and shown in Figure 4.19, 4.20, 4.21 and 4.22 for different soil parameters. The comparison is done graphically by plotting the limit resistance curves of RPP grouped at different spacing and single RPP for a particular slip surface in terms of load versus horizontal displacement/flexural stress for each type of soil. Thus, the resistance of group of RPP at 2-ft/4-ft/6-ft spacing with single RPP is compared in terms of horizontal displacement and flexural stress.

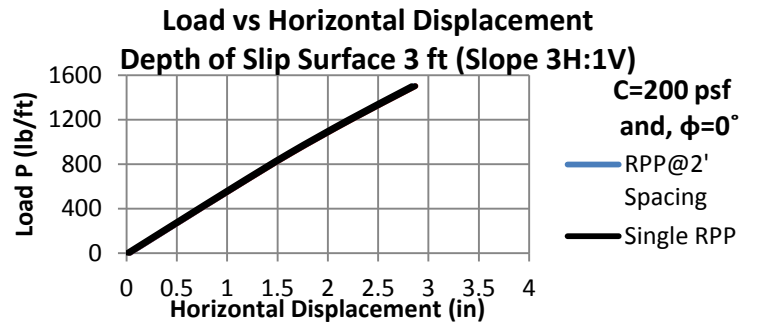
In case of 3-ft deep slip surface, it is already observed that the difference of resistance between group of RPP and single RPP is insignificant in terms of horizontal displacement and flexural stress, shown in Figure 4.19(a), 4.20(a), 4.21(a) and 4.22(a). Thus, it can be concluded that the resistance offered by group of RPP is almost equivalent to resistance offered by single RPP for 3-ft deep slip surface.

In case of 5-ft deep slip surface, it is already observed that the difference in resistance is less in terms of horizontal displacement, shown in Figure 4.19(b) and 4.21(b). But the flexural stress induced on group of RPP is lesser than single RPP for a particular amount of load, shown in Figure 4.20(b) and 4.22(b). Thus, the group capacity of RPP increases while withstanding mobilized load.

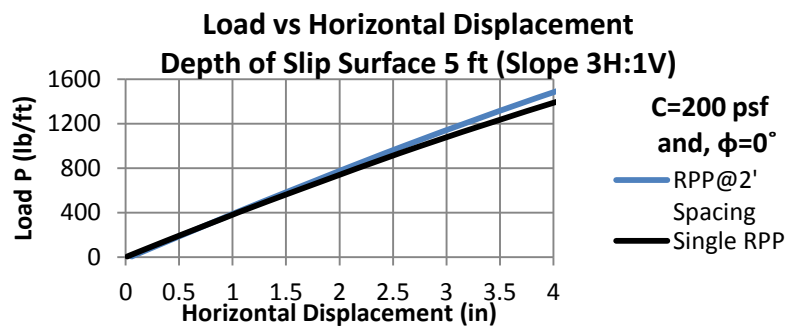
In case of 7-ft deep slip surface, the resistance offered by group of RPP is much higher than the resistance offered by single RPP in terms of horizontal displacement and flexural stress, shown in Figure 4.19(c) and Figure 4.20(c).

The variation of resistance in terms of horizontal displacement between group of RPP and single RPP decreases with increment of soil strength shown in Figure 4.21(c). Though, the difference of flexural stress between group of RPP and single RPP in case

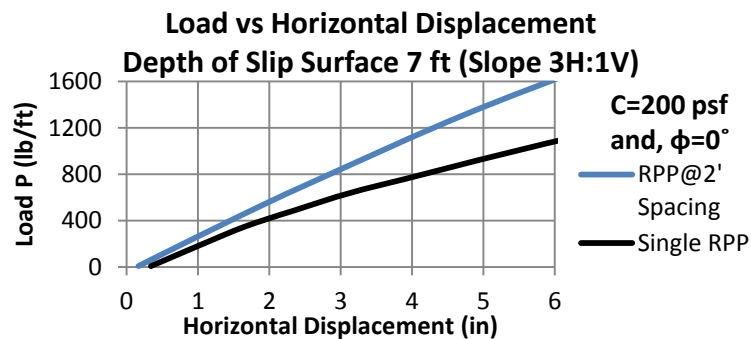
of 7-ft and 5-ft deep slip surface is quite higher for a soil having cohesion 300 psf and friction angle of 30° and shown in Figure 4.22(b) and 4.22(c).



(a)

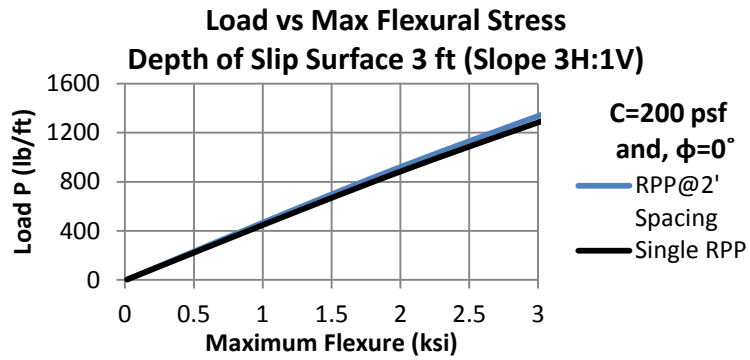


(b)

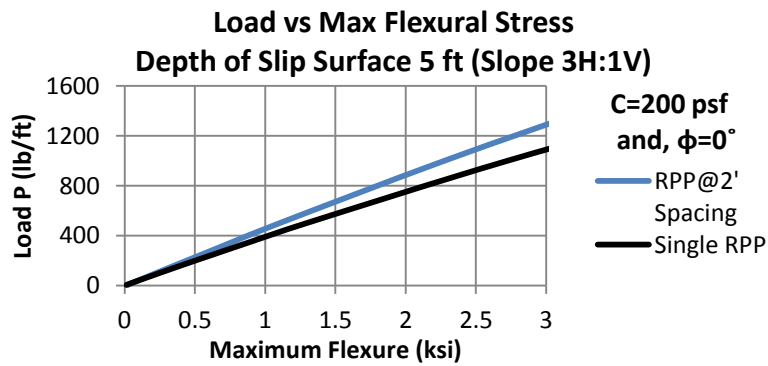


(c)

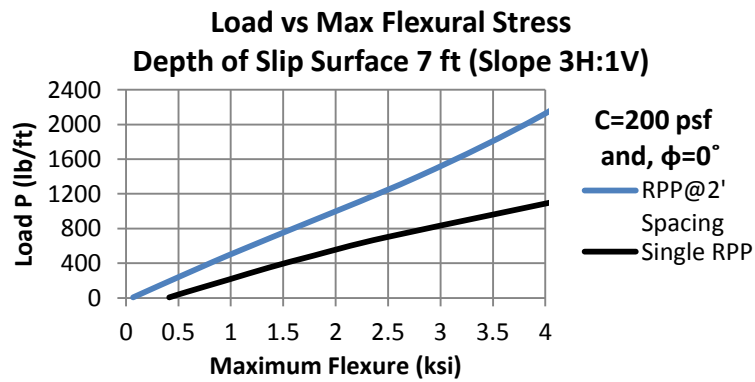
Figure 4.19 Limit Resistance Curves showing horizontal displacement of group versus single RPP for, a. 3-ft, b. 5-ft, c. 7-ft deep slip surface, for a soil of $c=200$ psf and, $\phi=0^\circ$.



(a)

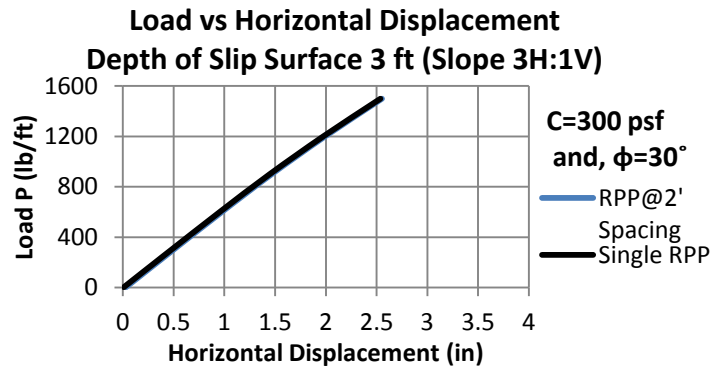


(b)

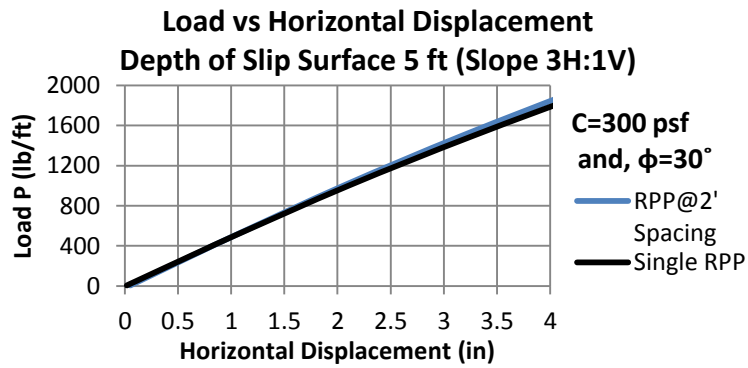


(c)

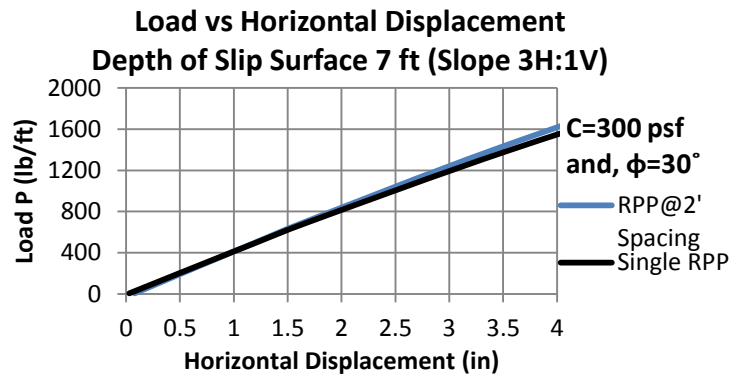
Figure 4.20 Limit Resistance Curves of group versus single RPP for flexural stress of, a. 3-ft, b. 5-ft, c. 7-ft deep slip surface, in case of a soil having $c=200$ psf and, $\phi=0^\circ$.



(a)

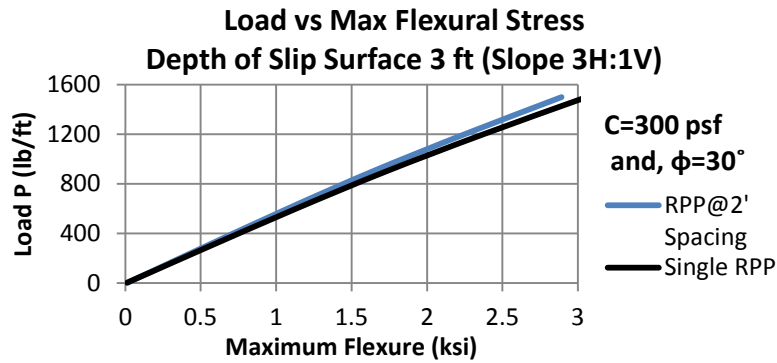


(b)

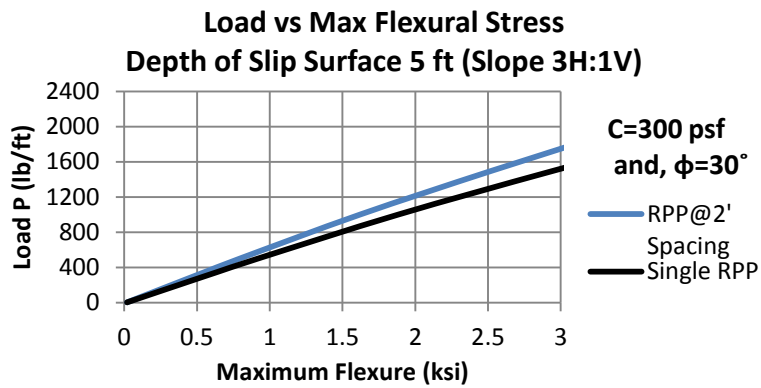


(c)

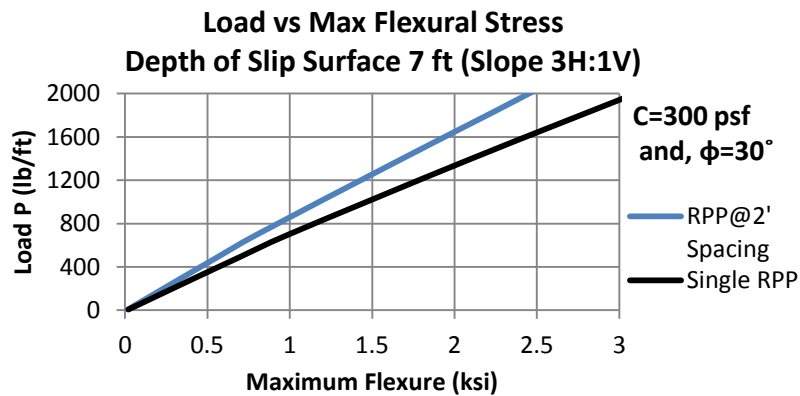
Figure 4.21 Limit Resistance Curves showing horizontal displacement of group versus single RPP for, a. 3-ft, b. 5-ft, c. 7-ft deep slip surface, for a soil of $c=300$ psf and, $\phi=30^\circ$.



(a)



(b)



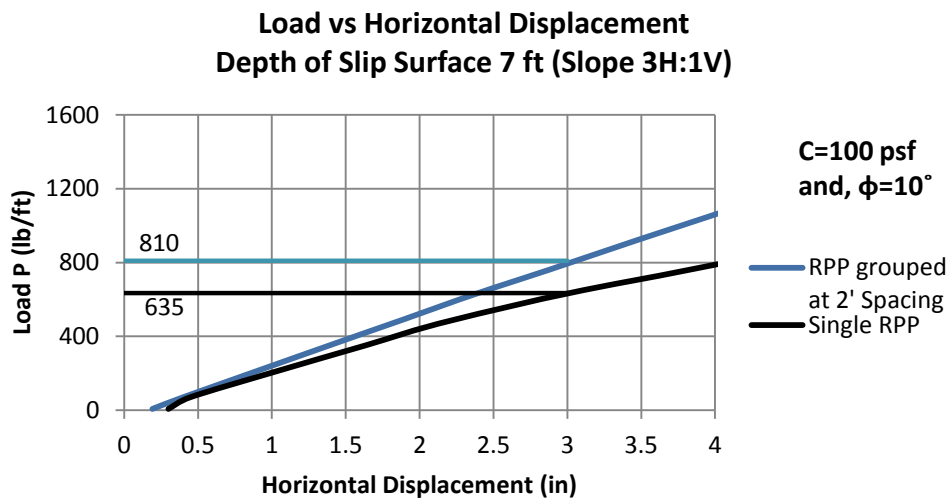
(c)

Figure 4.22 Limit Resistance Curves of group versus single RPP for flexural stress of, a.

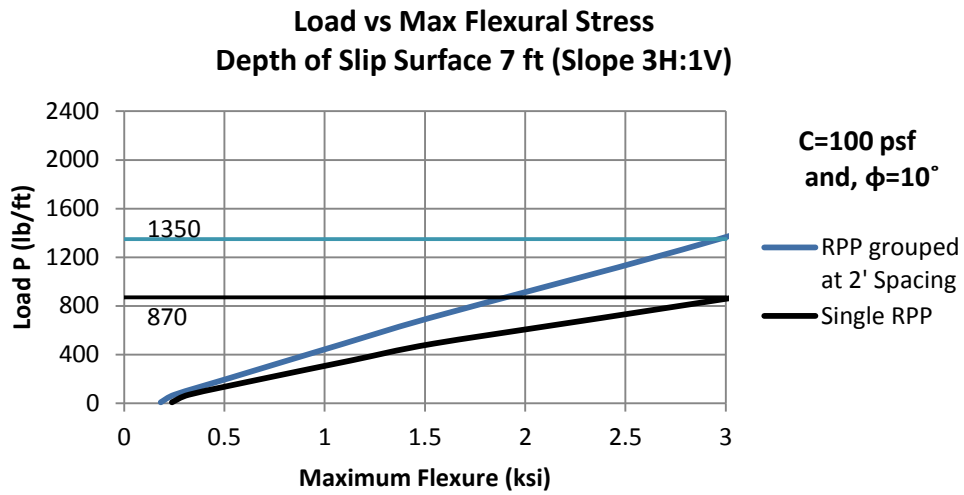
3-ft, b. 5-ft, c. 7-ft deep slip surface, in case of a soil having $c=300$ psf and, $\phi=30^\circ$.

4.8 Multiplication Factor

Based on the comparison between the horizontal displacement and/or flexural stress of group of RPP and single RPP, a multiplication factor is introduced as a ratio between them, shown in section 3.9 (chapter 3). The ratio is determined considering a specific allowable horizontal displacement or flexural stress for each type of soil considering RPP grouped at 2-ft/4-ft/6-ft spacing, shown in Figure 4.23. The ratio in terms of horizontal displacement is termed as multiplication factor for allowable horizontal displacement and in terms flexural stress is termed as multiplication factor for allowable flexural stress. Table 4.1 represents the multiplication factors for horizontal displacement for slope ratio of 2H:1V . The evaluated performance of group of RPP over single RPP for horizontal displacement and flexural stress is represented as a multiplication factor for different slope in tabular form in Appendix C. The introduced multiplication factor for a particular (2-ft/4-ft/6-ft) spacing of RPP will adjust the under estimated resistance of RPP proposed by Khan (2013).The group resistance of RPP compared to single RPP decreases with increment of soil strength as already observed. Thus, the multiplication factor in terms of horizontal displacement and/or flexural stress for weak soil is quite higher and for strong soil is very less.



(a)



(b)

Figure 4.23 Determination of Multiplication factor for, a. Horizontal Displacement, b.
Flexural Stress.

Table 4.1 Multiplication Factor between RPP Grouped at Different Spacing vs Single

RPP for Slope Ratio of 2H:1V

Slip Surface Soil Parameters	Allowable Horizontal Displacement (in)	Multiplication Factor for Horizontal Displacement (Single RPP vs Grouped RPP)								
		Depth of Slip Surface 3 ft			Depth of Slip Surface 5 ft			Depth of Slip Surface 7 ft		
		Spacing of RPP 2 ft	Spacing of RPP 4 ft	Spacing of RPP 6 ft	Spacing of RPP 2 ft	Spacing of RPP 4 ft	Spacing of RPP 6 ft	Spacing of RPP 2 ft	Spacing of RPP 4 ft	Spacing of RPP 6 ft
C=100 psf and $\phi=20^\circ$	1	1	1	1	1.09	1.06	1.03	1.28	1.20	1.13
	2	1	1	1	1.09	1.07	1.04	1.27	1.18	1.14
	3	1	1	1	1.1	1.07	1.05	1.26	1.19	1.14
	4				1.09	1.07	1.05	1.27	1.21	1.15
C=100 psf and $\phi=30^\circ$	1	1	1	1	1.04	1.02	1	1	1	1
	2	1	1	1	1.03	1.02	1.01	1.05	1.04	1.04
	3	1	1	1	1.04	1.02	1.01	1.08	1.07	1.04
	4				1.03	1.01	1	1.09	1.08	1.05
C=200 psf and $\phi=0^\circ$	1	1	1	1	1.10	1.06	1.04			
	2	1	1	1	1.11	1.06	1.03			
	3	1	1	1	1.11	1.07	1.04			
	4				1.13	1.09	1.06			
C=200 psf and $\phi=10^\circ$	1	1	1	1	1	1	1	1.21	1.14	1.10
	2	1	1	1	1.03	1.02	1	1.22	1.13	1.10
	3	1	1	1	1.04	1.02	1	1.23	1.15	1.11
	4				1.04	1.02	1	1.23	1.15	1.11
C=200 psf and $\phi=20^\circ$	1	1	1	1	1	1	1	1	1	1
	2	1	1	1	1	1	1	1	1	1
	3	1	1	1	1.03	1.02	1	1.05	1.05	1.02
	4				1.03	1	1	1.06	1.04	1.03
C=200 psf and $\phi=30^\circ$	1	1	1	1	1	1	1	1	1	1
	2	1	1	1	1	1	1	1	1	1
	3	1	1	1	1.03	1	1	1.05	1.04	1
	4				1.03	1	1	1.05	1.03	1.02
C=300 psf and $\phi=0^\circ$	1	1	1	1	1	1	1	1.32	1.13	1.05
	2	1	1	1	1.03	1.02	1	1.28	1.11	1.04
	3	1	1	1	1.04	1.03	1	1.29	1.12	1.05
	4				1.04	1.03	1	1.29	1.11	1.06
C=300 psf and $\phi=10^\circ$	1	1	1	1	1	1	1	1	1	1.02
	2	1	1	1	1.04	1.03	1	1.04	1.03	1.02
	3	1	1	1	1.04	1.03	1	1.04	1.03	1.02
	4				1.04	1.03	1	1.05	1.03	1.02

Table 4.1-Continued

C=300 psf and $\phi=20^\circ$	1	1	1	1	1	1	1	1	1	1
	2	1	1	1	1.04	1	1	1.04	1.03	1
	3	1	1	1	1.04	1	1	1.04	1.03	1.02
	4				1.04	1	1	1.04	1.03	1.02
C=300 psf and $\phi=30^\circ$	1	1	1	1	1.03	1	1	1	1	1
	2	1	1	1	1.03	1	1	1.04	1	1
	3	1	1	1	1.03	1	1	1.04	1.03	1.02
	4				1.03	1	1	1.04	1.03	1.02

4.9 Factor of Safety Calculation

The performance based method introduced by Khan (2013) underestimates the resistance of RPP in shallow slope stabilization as it is developed based on the resistance of single RPP. Therefore, the calculated factor of safety based on performance based method is also comparatively less. So, this method is conservative.

Khan (2013) calculated the factor of safety based on the soil parameters shown in table 4.2. Then obtained results are compared with PLAXIS and GSTABL7 calculated factor of safety. The obtained factors of safety values are smaller than PLAXIS and GSTABL generated results in case of slope 1 and slope 3, shown in table 4.3.

The factor of safety of same slopes is calculated using newly introduced Multiplication Factors and shown in Appendix D. The calculated results are found to be in good agreement with PLAXIS generated results in case of slope 1 and slope 3, and shown in column f of table 4.3. The Multiplication Factors for 3-ft spacing (shown in table 4.4) is determined by interpolation as it is determined for 2-ft, 4-ft and 6-ft spacing.

Without using the Multiplication Factors, similar calculation can be performed using the newly developed design charts of Appendix B. According to the sample calculation shown in Appendix E, the obtained factor of safety for 2 inch allowable horizontal displacement is 2.29 and PLAXIS generated factor of safety is 2.27. So, the obtained result using the newly developed design chart for slope 2 is in good agreement with PLAXIS generated result.

Thus, it can be concluded that the underestimated resistance of RPP according to performance based method can be aptly addressed by the Multiplication Factors or by the newly developed design charts.

Table 4.2 Soil parameters (Khan, 2013).

Soil Type	Slope Height (ft)	Top Soil			Foundation Soil		
		c (psf)	ϕ (degree)	γ (pcf)	c (psf)	ϕ (degree)	γ (pcf)
Slope 1 (2H:1V)	40	250	10	125	300	20	125
Slope 2 (3H:1V)	40	250	10	125	400	10	125
Slope 3 (4H:1V)	40	250	10	125	400	10	125

Table 4.3 Factor of Safety of RPP reinforced slope for allowable horizontal displacement of 2 inch (Khan, 2013).

Slope Type (a)	Limit Resistance (lb/ft) (b)	PLAXIS (c)	GSTABL7 (d)	Performance based method (e)	Group resistance (f)
Slope 1 (2H:1V)	600	1.55	2.27	1.52	1.57
Slope 2 (3H:1V)	725	2.27	3.05	2.35	2.38
Slope 3 (4H:1V)	730	3.14	4.14	3.05	1.13

Table 4.4 Calculation of Multiplication Factors for RPP at 3-ft spacing.

Slope Type	C=200 psf and $\phi=10^\circ$		C=300 psf and $\phi=10^\circ$		C=250 psf and $\phi=10^\circ$
	RPP at 2-ft Spacing	RPP at 4-ft Spacing	RPP at 2-ft Spacing	RPP at 4-ft Spacing	RPP at 3-ft Spacing (by interpolation)
Slope 1 (2H:1V)	1.19	1.16	1.04	1.03	1.11
Slope 2 (3H:1V)	1.07	1.04	1.06	1.04	1.05
Slope 3 (4H:1V)	1.07	1.06	1.06	1.04	1.06

Chapter 5

Conclusions and Recommendations for Future Research

Expansive clay develop fully soften state in course of time due to hydro-thermal cycling, and thus the slope failure is triggered due to excessive and prolonged rainfall in case of expansive clay. Therefore, shallow slope failure is a common phenomenon, which needs an economically viable stabilizing solution. Recycled plastic pin is an environmental friendly and economic reinforcing member, which can be used for in situ shallow slope stabilization. Therefore, it draws the attention of the researchers and extensive field study had been carried out during past few years. The limit resistance curve and performance based method are the outcomes.

The objective of this study is to determine the group resistance of RPP in sustainable slope stabilization. To attain the goal, number of RPP required forming an effective group and the spacing of RPP within a group is determined. An extensive study has been conducted based on numerical modeling and supported by field data. Thus, a new design chart is proposed considering group resistance of RPP. Finally the group resistance is compared with performance based design chart (Khan, 2013), which has been developed considering individual resistance of RPP and a multiplication factor is introduced to evaluate the group resistance of RPP with respect to individual resistance.

5.1 Summary and Conclusions

Based on the current study, the findings can be summarized as follows:

1. Variation of resistance between group of RPP and single RPP increases with depth of slip surface. It is insignificant in case of 3-ft deep slip surface, where resistance offered by group of RPP is equal to resistance offered by single RPP. But, in case of 7-ft deep slip surface the resistance offered by group of

RPP is much higher than single RPP. Thus, it can be concluded that the group effect in terms of resistance increases with depth of slip surface.

2. Variation of resistance between group of RPP and single RPP decreases with increment of soil strength. Resistance offered by group of RPP is much higher than single RPP in case of weak soil, but it is very less for stiff soil and/or granular soil with higher friction angle.
3. Variation of resistance between group of RPP and single RPP increases with increment of loading condition. At lower loading condition single RPP is capable enough to withstand the load, thus the resistance offered by group of RPP is similar to single RPP.
4. Group resistance of RPP varies with spacing of RPP. It decreases with increment of RPP spacing. Group resistance is higher at lower spacing of RPP.
5. Effect of RPP spacing on group resistance is more in case of weak soil and quite less in case of stiff soil. In case of stiff soil, single RPP offer almost similar resistance to group of RPP. Thus, effect of spacing of RPP is very less considering horizontal displacement.
6. The induced flexural stress on group of RPP is much lower than single RPP irrespective of soil strength for 5-ft and 7-ft deep slip surface, though the horizontal displacement variation is quite less in case of stiff soil.
7. Spacing of RPP has drastic effect on flexural stress compared to horizontal displacement. Thus, the structural strength of RPP is more at lower spacing and reduces with increment of spacing.
8. Variation of resistance between group of RPP and single RPP for a particular type of soil is more in case of a steep slope. Vertical component of the

mobilized load is higher in case of a steep slope than a gentle slope. So, its influence on single RPP is more than group of RPP in case of a steep slope compared to a gentle slope. Thus, it can be concluded that the variation of resistance between group of RPP and single RPP increases with increment of soil slope.

9. The Multiplication Factors decreases with increasing soil strength and RPP spacing. Moreover, it is quite small in case of 3-ft deep slip surface because of higher embedded depth of RPP.
10. Factor of Safety obtained by performance based method is lower as this method is developed considering resistance of single RPP. On the other hand, calculated Factor of Safety considering group resistance is higher.

5.2 Recommendations for Future Works

1. The numerical modeling was done with PLAXIS 2D, where the displacement and strains in the z-direction is assumed to be zero. Thus, the modeling can be revised using PLAXIS-3D to investigate the influence of loading in z-direction.
2. Determination of suitable dimension (cross section area and length) of RPP required for different depth of slip surface considering embedded depth into stiff soil.
3. Slope stabilization using RPP is a new concept. Thus, the developed design methods should be verified with respect to different types of soil considering long term performance.

Appendix A

Effect of Load on Increasing Number of RPP

List of Figures

Figure No	Spacing of RPP	Applied Load	Slope Ratio
A 1	2	100	2H:1V
A 2	3	100	2H:1V
A 3	4	100	2H:1V
A 4	5	100	2H:1V
A 5	6	100	2H:1V
A 6	2	300	2H:1V
A 7	3	300	2H:1V
A 8	4	300	2H:1V
A 9	5	300	2H:1V
A 10	6	300	2H:1V
A 11	2	500	2H:1V
A 12	3	500	2H:1V
A 13	4	500	2H:1V
A 14	5	500	2H:1V
A 15	6	500	2H:1V
A 16	2	1000	2H:1V
A 17	3	1000	2H:1V
A 18	4	1000	2H:1V
A 19	5	1000	2H:1V
A 20	6	1000	2H:1V
A 21	2	100	3H:1V
A 22	3	100	3H:1V
A 23	4	100	3H:1V
A 24	5	100	3H:1V
A 25	6	100	3H:1V
A 26	2	300	3H:1V
A 27	3	300	3H:1V
A 28	4	300	3H:1V
A 29	5	300	3H:1V
A 30	6	300	3H:1V
A 31	2	500	3H:1V
A 32	3	500	3H:1V
A 33	4	500	3H:1V
A 34	5	500	3H:1V
A 35	6	500	3H:1V
A 36	2	1000	3H:1V
A 37	3	1000	3H:1V

A 38	4	1000	3H:1V
A 39	5	1000	3H:1V
A 40	6	1000	3H:1V

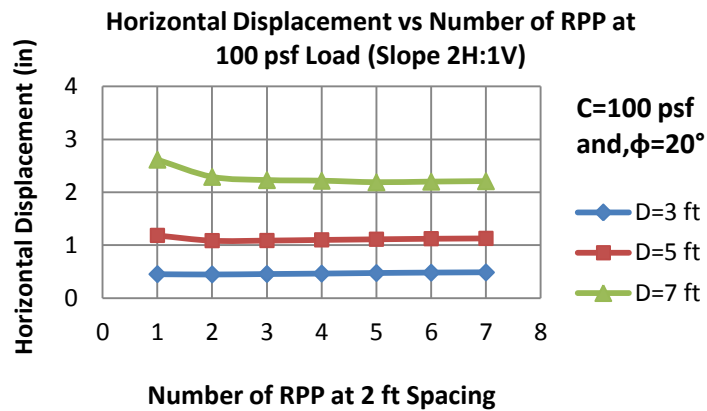


Figure A 1: Influence of 100 psf load on increment of RPP at 2-ft spacing (slope 2H:1V).

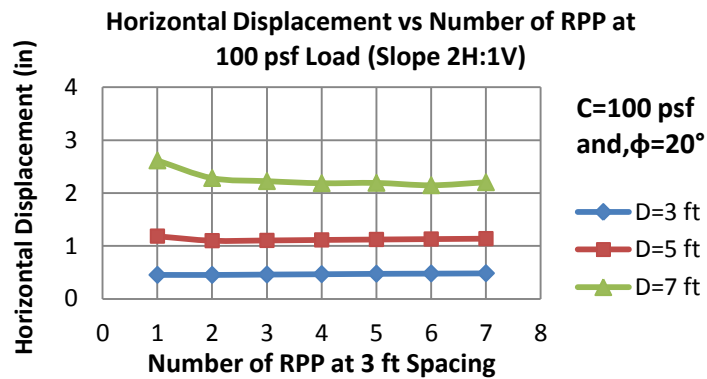


Figure A 2: Influence of 100 psf load on increment of RPP at 3-ft spacing (slope 2H:1V).

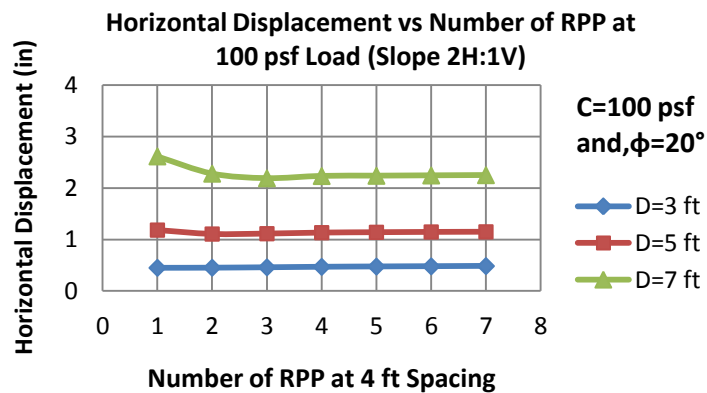


Figure A 3: Influence of 100 psf load on increment of RPP at 4-ft spacing (slope 2H:1V).

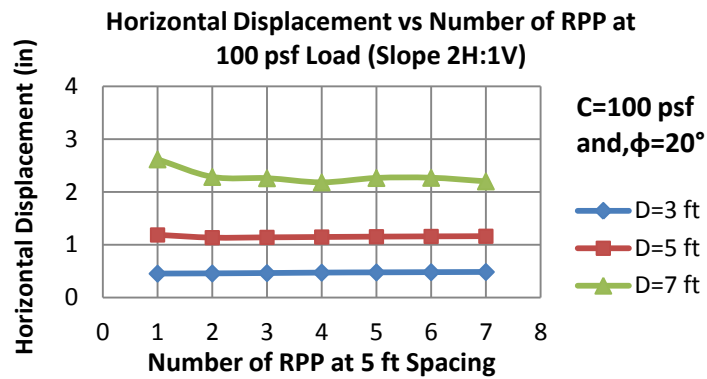


Figure A 4: Influence of 100 psf load on increment of RPP at 5-ft spacing (slope 2H:1V).

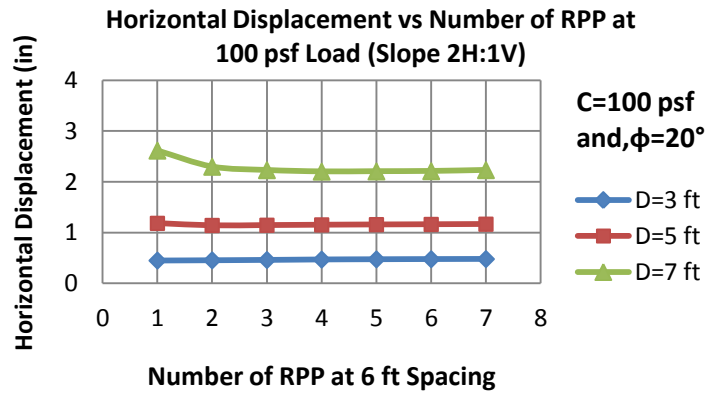


Figure A 5: Influence of 100 psf load on increment of RPP at 6-ft spacing (slope 2H:1V).

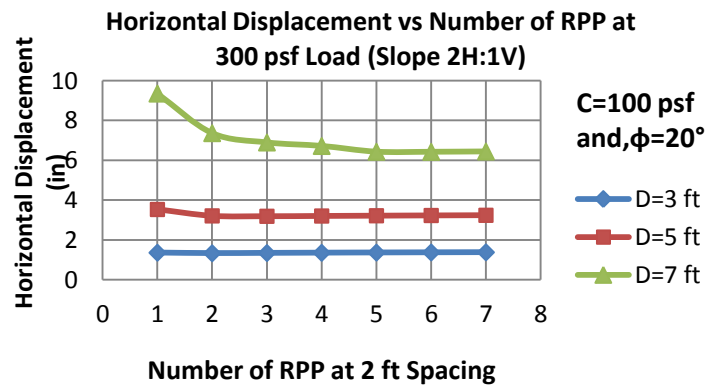


Figure A 6: Influence of 300 psf load on increment of RPP at 2-ft spacing (slope 2H:1V).

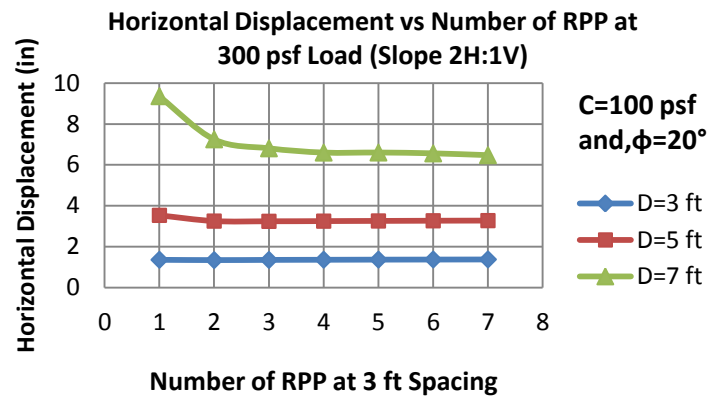


Figure A 7: Influence of 300 psf load on increment of RPP at 3-ft spacing (slope 2H:1V).

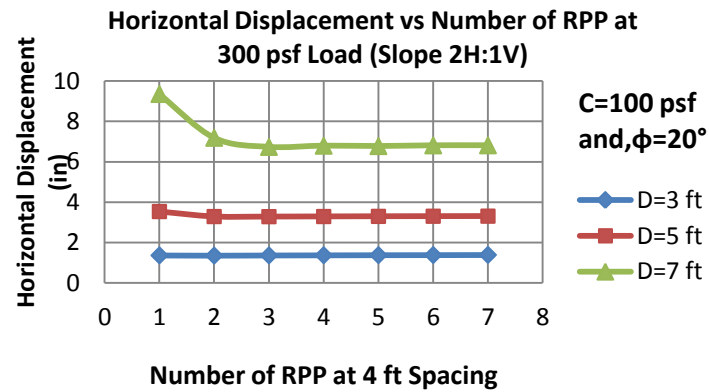


Figure A 8: Influence of 300 psf load on increment of RPP at 4-ft spacing (slope 2H:1V).

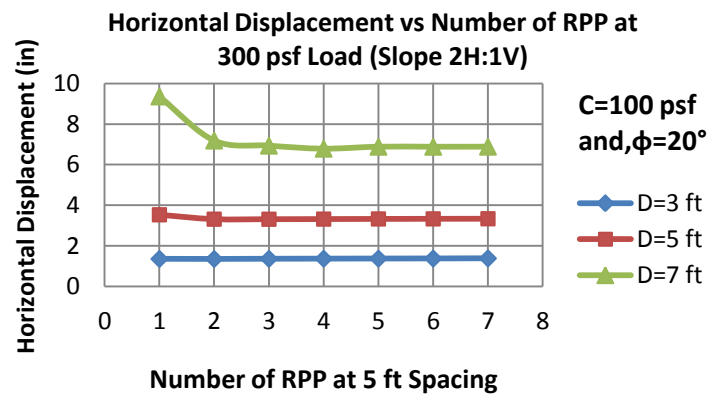


Figure A 9: Influence of 300 psf load on increment of RPP at 5-ft spacing (slope 2H:1V).

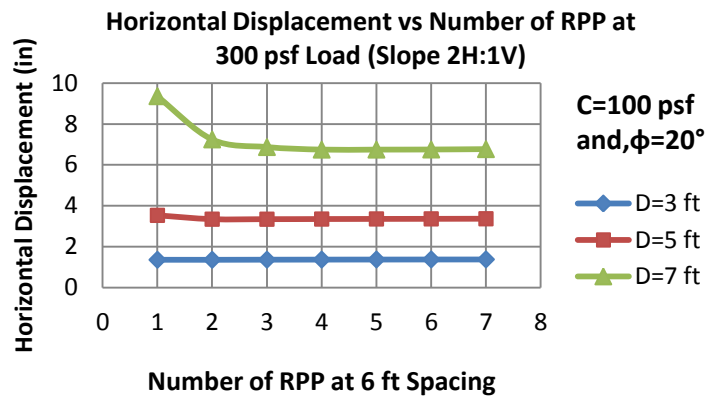


Figure A 10: Influence of 300 psf load on increment of RPP at 6-ft spacing (slope 2H:1V).

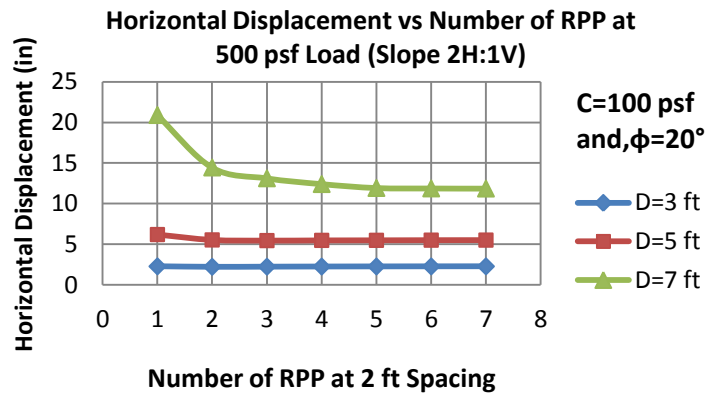


Figure A 11: Influence of 500 psf load on increment of RPP at 2-ft spacing (slope 2H:1V).

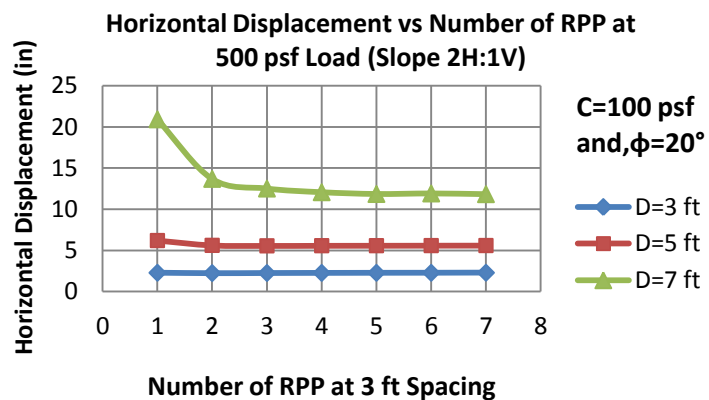


Figure A 12: Influence of 500 psf load on increment of RPP at 3-ft spacing (slope 2H:1V).

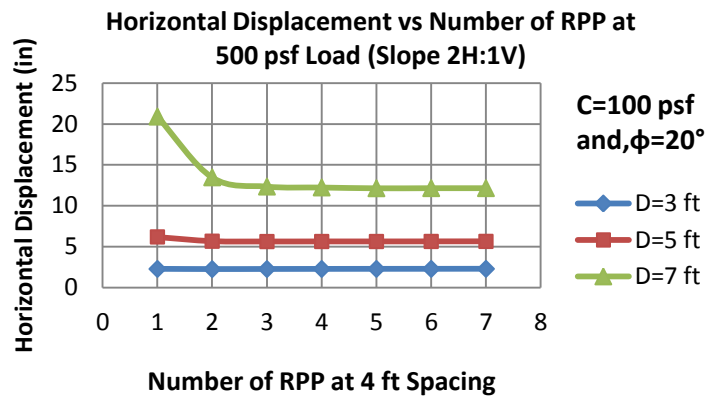


Figure A 13: Influence of 500 psf load on increment of RPP at 4-ft spacing (slope 2H:1V).

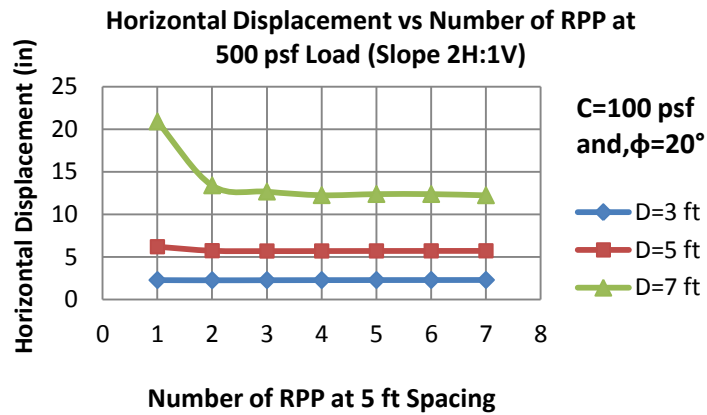


Figure A 14: Influence of 500 psf load on increment of RPP at 5-ft spacing (slope 2H:1V).

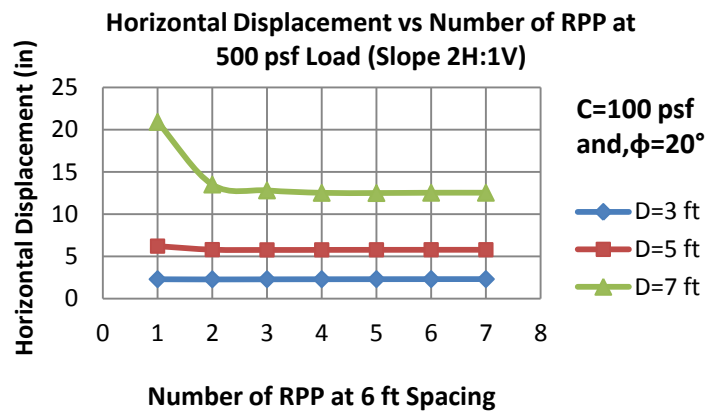


Figure A 15: Influence of 500 psf load on increment of RPP at 6-ft spacing (slope 2H:1V).

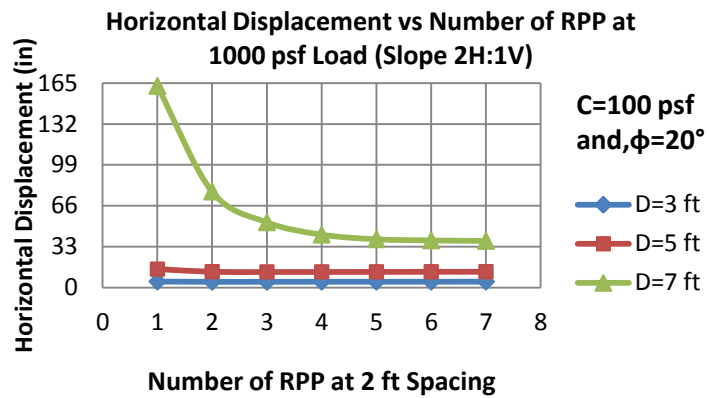


Figure A 16: Influence of 1000 psf load on increment of RPP at 2-ft spacing (slope 2H:1V).

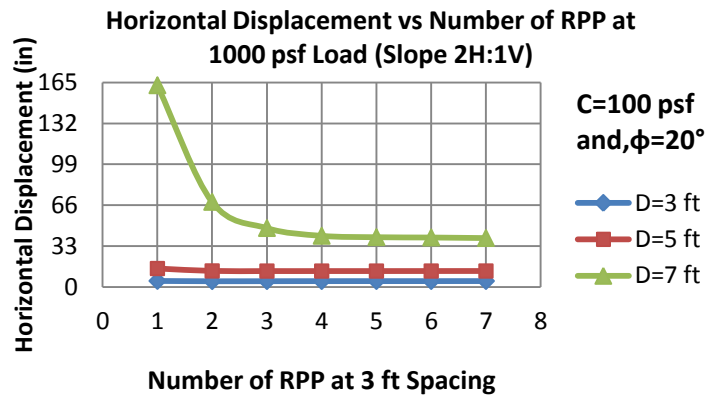


Figure A 17: Influence of 1000 psf load on increment of RPP at 3-ft spacing (slope 2H:1V).

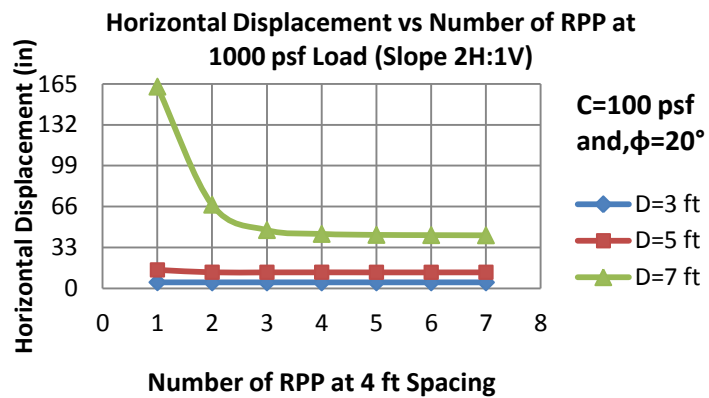


Figure A 18: Influence of 1000 psf load on increment of RPP at 4-ft spacing (slope 2H:1V).

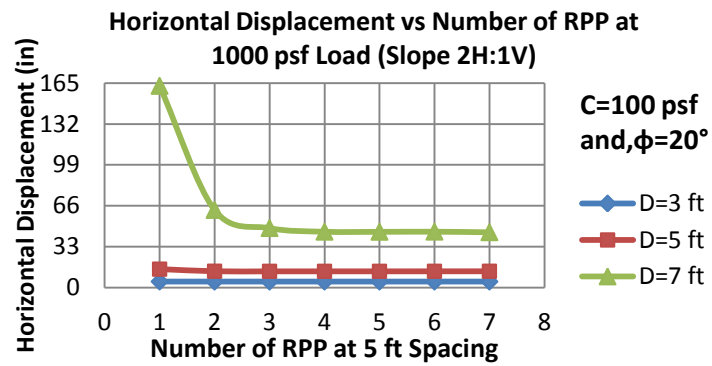


Figure A 19: Influence of 1000 psf load on increment of RPP at 5-ft spacing (slope 2H:1V).

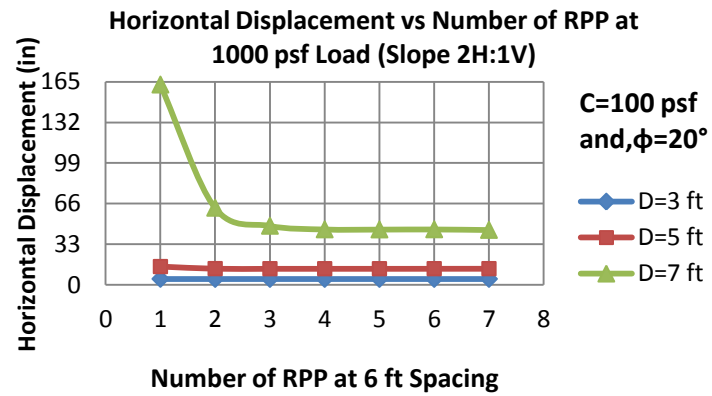


Figure A 20: Influence of 1000 psf load on increment of RPP at 6-ft spacing (slope 2H:1V).

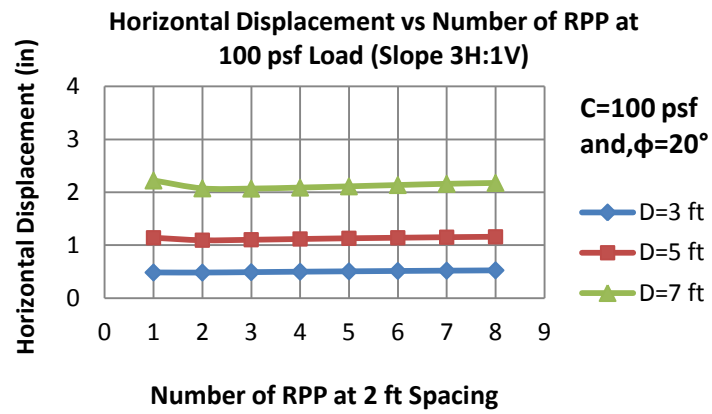


Figure A 21: Influence of 100 psf load on increment of RPP at 2-ft spacing (slope 3H:1V).

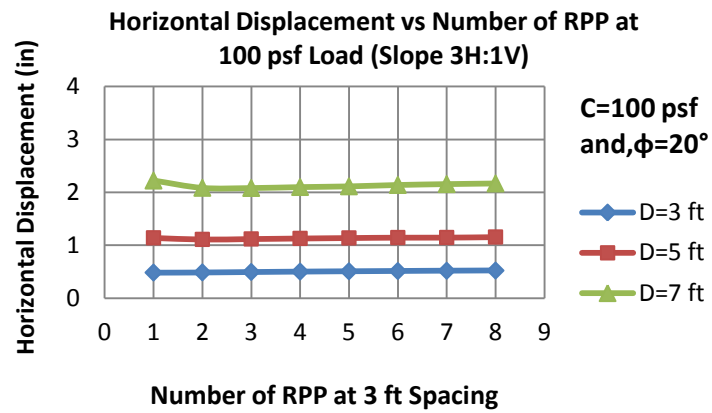


Figure A 22: Influence of 100 psf load on increment of RPP at 3-ft spacing (slope 3H:1V).

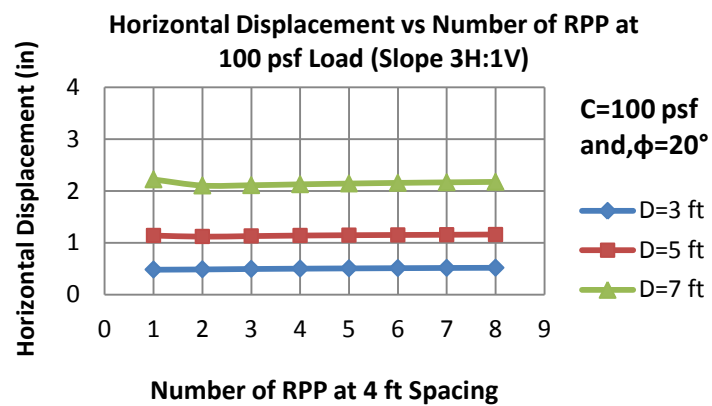


Figure A 23: Influence of 100 psf load on increment of RPP at 4-ft spacing (slope 3H:1V).

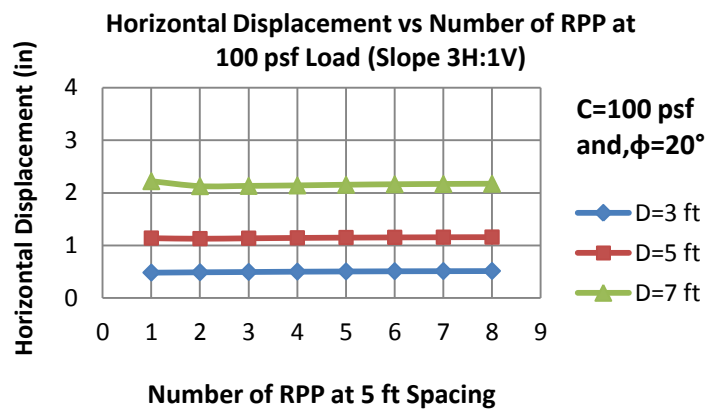


Figure A 24: Influence of 100 psf load on increment of RPP at 5-ft spacing (slope 3H:1V).

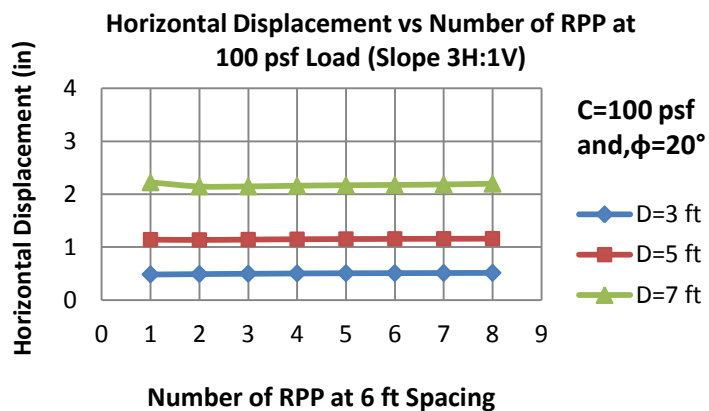


Figure A 25: Influence of 100 psf load on increment of RPP at 6-ft spacing (slope 3H:1V).

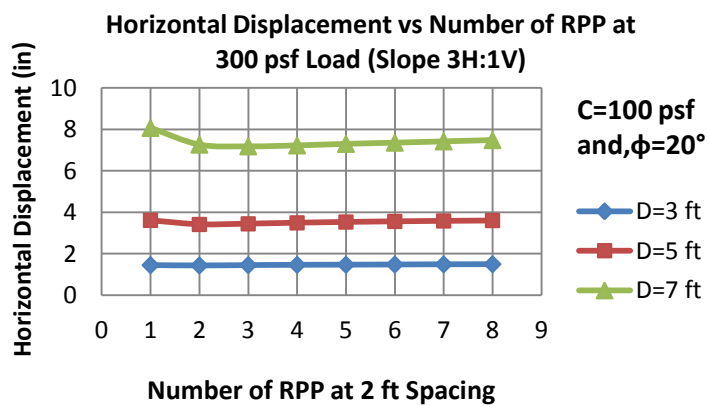


Figure A 26: Influence of 300 psf load on increment of RPP at 2-ft spacing (slope 3H:1V).

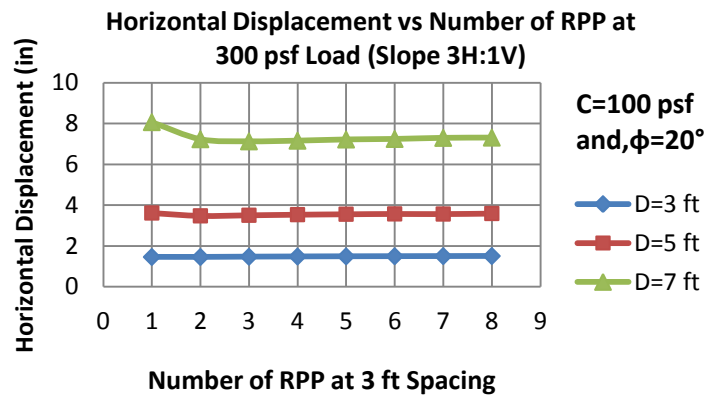


Figure A 27: Influence of 300 psf load on increment of RPP at 3-ft spacing (slope 3H:1V).

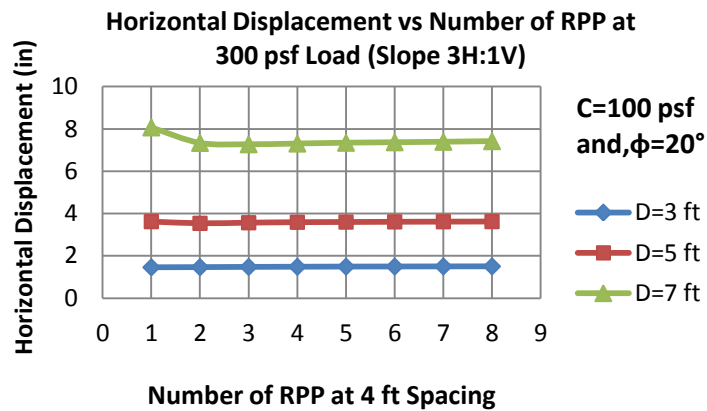


Figure A 28: Influence of 300 psf load on increment of RPP at 4-ft spacing (slope 3H:1V).

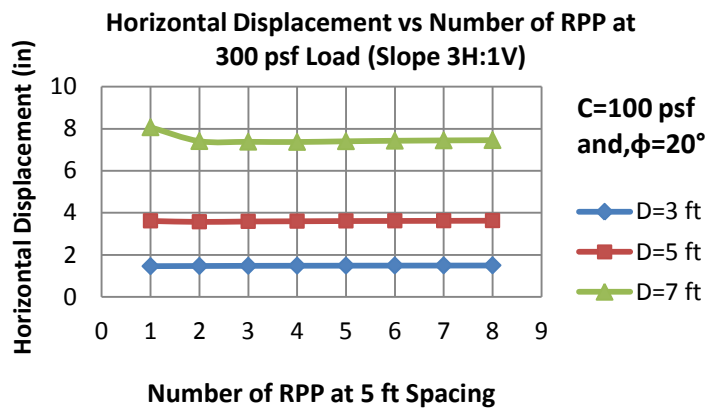


Figure A 29: Influence of 300 psf load on increment of RPP at 5-ft spacing (slope 3H:1V).

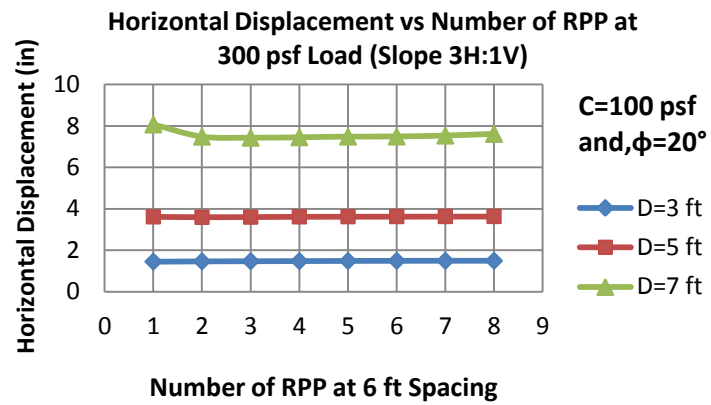


Figure A 30: Influence of 300 psf load on increment of RPP at 6-ft spacing (slope 3H:1V).

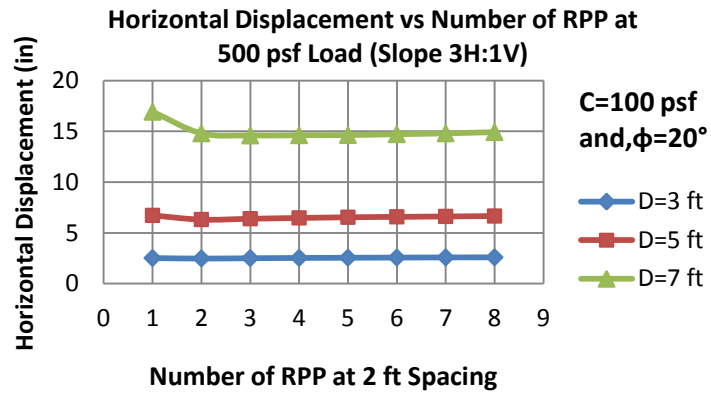


Figure A 31: Influence of 500 psf load on increment of RPP at 2-ft spacing (slope 3H:1V).

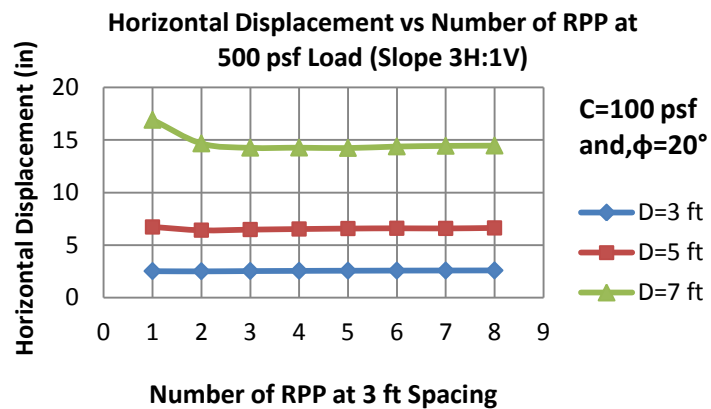


Figure A 32: Influence of 500 psf load on increment of RPP at 3-ft spacing (slope 3H:1V).

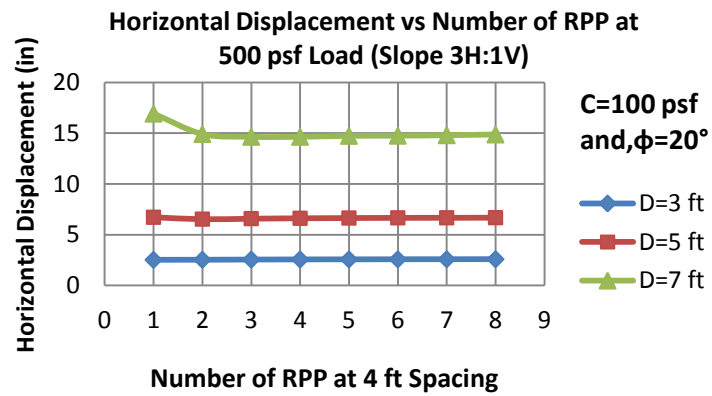


Figure A 33: Influence of 500 psf load on increment of RPP at 4-ft spacing (slope 3H:1V).

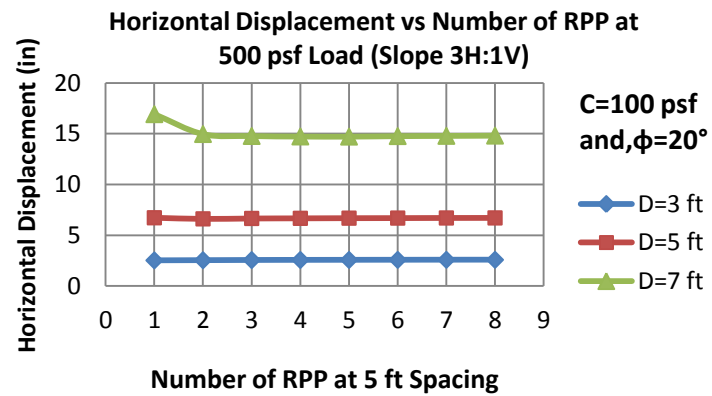


Figure A 34: Influence of 500 psf load on increment of RPP at 5-ft spacing (slope 3H:1V).

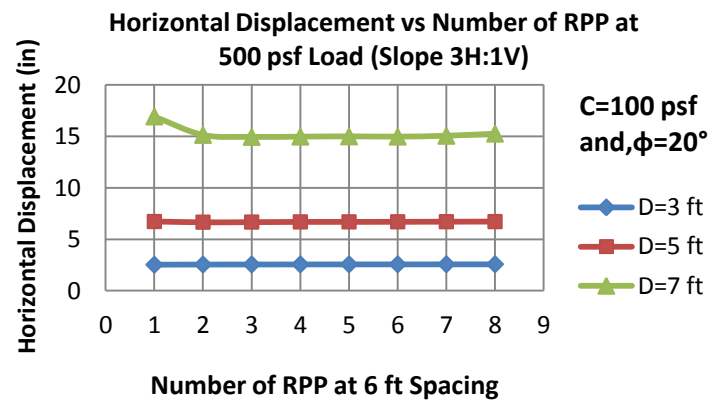


Figure A 35: Influence of 500 psf load on increment of RPP at 6-ft spacing (slope 3H:1V).

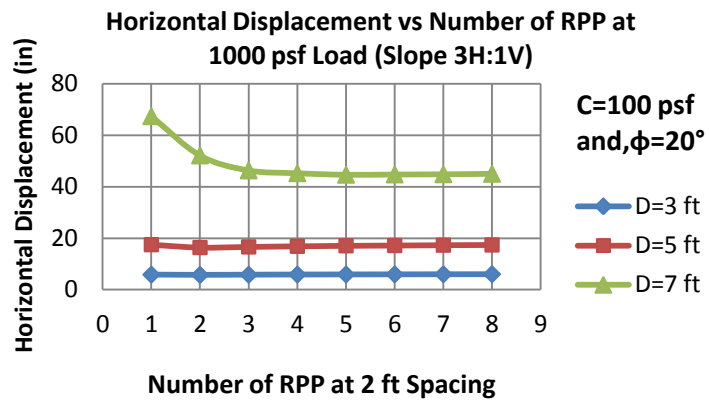


Figure A 36: Influence of 1000 psf load on increment of RPP at 2-ft spacing (slope 3H:1V).

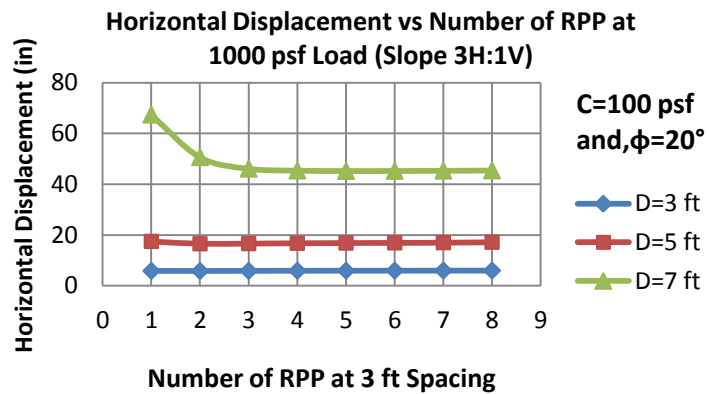


Figure A 37: Influence of 1000 psf load on increment of RPP at 3-ft spacing (slope 3H:1V).

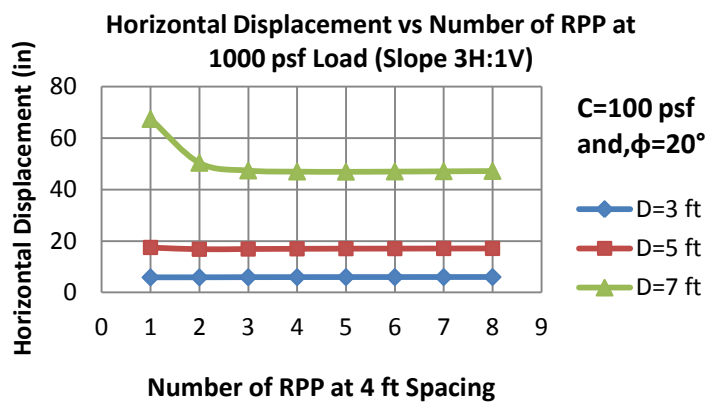


Figure A 38: Influence of 1000 psf load on increment of RPP at 4-ft spacing (slope 3H:1V).

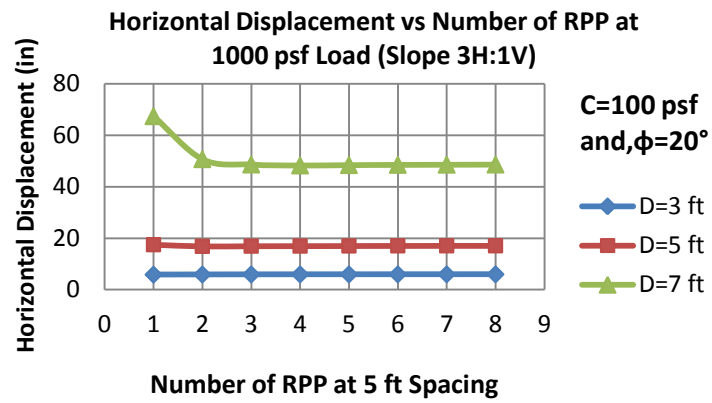


Figure A 39: Influence of 1000 psf load on increment of RPP at 5-ft spacing (slope 3H:1V).

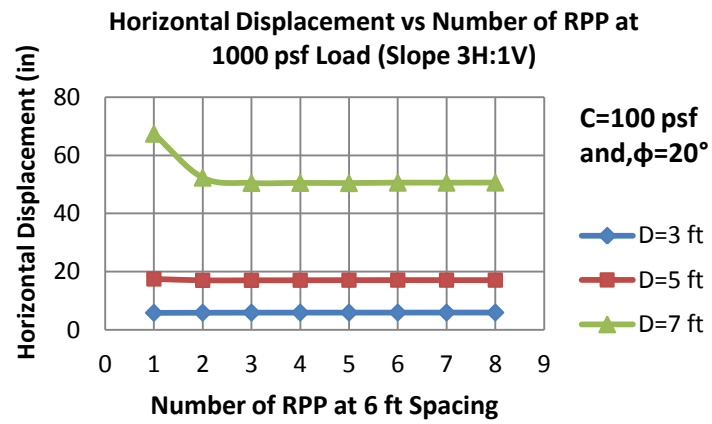


Figure A 40: Influence of 1000 psf load on increment of RPP at 6-ft spacing (slope 3H:1V).

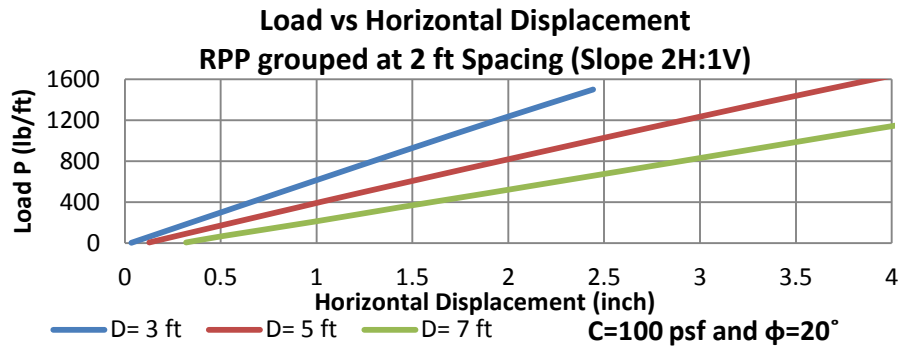
Appendix B

Design Chart for Group Resistance of RPP

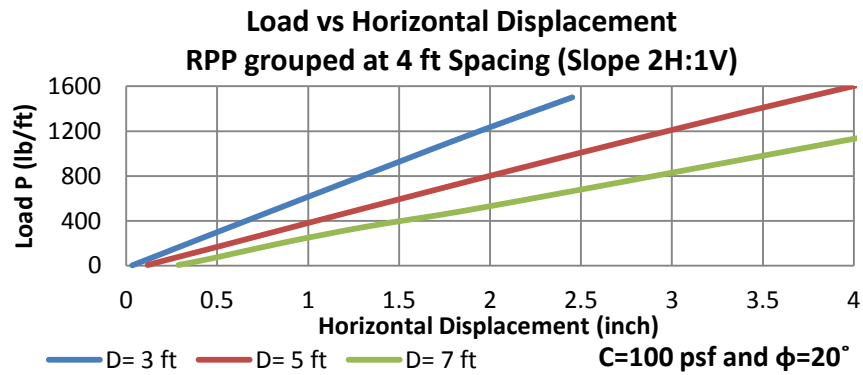
List of Figures

Figure No	Types of Design Chart	Cohesion (psf)	Friction Angle (Degree)	Slope Ratio
B 1	Load vs Horizontal Displacement	100	20	2H:1V
B 2	Load vs Flexural Stress	100	20	2H:1V
B 3	Load vs Horizontal Displacement	100	30	2H:1V
B 4	Load vs Flexural Stress	100	30	2H:1V
B 5	Load vs Horizontal Displacement	200	0	2H:1V
B 6	Load vs Flexural Stress	200	0	2H:1V
B 7	Load vs Horizontal Displacement	200	10	2H:1V
B 8	Load vs Flexural Stress	200	10	2H:1V
B 9	Load vs Horizontal Displacement	200	20	2H:1V
B10	Load vs Flexural Stress	200	20	2H:1V
B 11	Load vs Horizontal Displacement	200	30	2H:1V
B 12	Load vs Flexural Stress	200	30	2H:1V
B 13	Load vs Horizontal Displacement	200	0	2H:1V
B 14	Load vs Flexural Stress	300	0	2H:1V
B 15	Load vs Horizontal Displacement	300	10	2H:1V
B 16	Load vs Flexural Stress	300	10	2H:1V
B 17	Load vs Horizontal Displacement	300	20	2H:1V
B 18	Load vs Flexural Stress	300	20	2H:1V
B 19	Load vs Horizontal Displacement	300	30	2H:1V
B 20	Load vs Flexural Stress	300	30	2H:1V
B 21	Load vs Horizontal Displacement	100	10	3H:1V
B 22	Load vs Flexural Stress	100	10	3H:1V
B 23	Load vs Horizontal Displacement	100	20	3H:1V
B 24	Load vs Flexural Stress	100	20	3H:1V
B 25	Load vs Horizontal Displacement	100	30	3H:1V
B 26	Load vs Flexural Stress	100	30	3H:1V
B 27	Load vs Horizontal Displacement	200	0	3H:1V
B 28	Load vs Flexural Stress	200	0	3H:1V
B 29	Load vs Horizontal Displacement	200	10	3H:1V
B 30	Load vs Flexural Stress	200	10	3H:1V
B 31	Load vs Horizontal Displacement	200	20	3H:1V
B 32	Load vs Flexural Stress	200	20	3H:1V
B 33	Load vs Horizontal Displacement	200	30	3H:1V
B 34	Load vs Flexural Stress	200	30	3H:1V
B 35	Load vs Horizontal Displacement	200	0	3H:1V
B 36	Load vs Flexural Stress	300	0	3H:1V
B 37	Load vs Horizontal Displacement	300	10	3H:1V

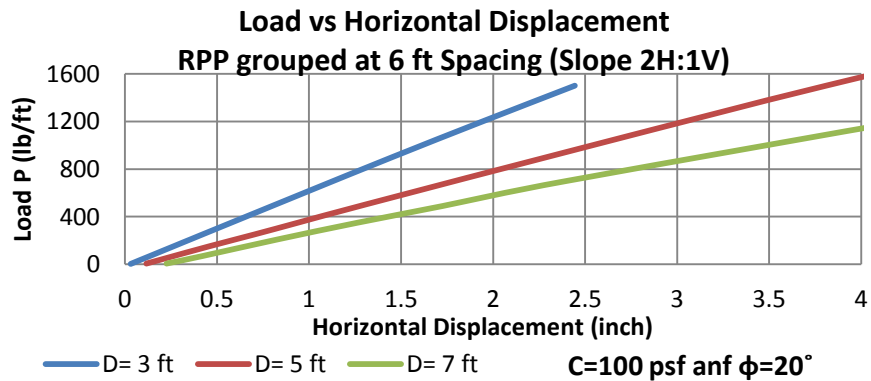
B 38	Load vs Flexural Stress	300	10	3H:1V
B 39	Load vs Horizontal Displacement	300	20	3H:1V
B 40	Load vs Flexural Stress	300	20	3H:1V
B 41	Load vs Horizontal Displacement	300	30	3H:1V
B 42	Load vs Flexural Stress	300	30	3H:1V
B 43	Load vs Horizontal Displacement	100	10	4H:1V
B 44	Load vs Flexural Stress	100	10	4H:1V
B 45	Load vs Horizontal Displacement	100	20	4H:1V
B 46	Load vs Flexural Stress	100	20	4H:1V
B 47	Load vs Horizontal Displacement	100	30	4H:1V
B 48	Load vs Flexural Stress	100	30	4H:1V
B 49	Load vs Horizontal Displacement	200	0	4H:1V
B 50	Load vs Flexural Stress	200	0	4H:1V
B 51	Load vs Horizontal Displacement	200	10	4H:1V
B 52	Load vs Flexural Stress	200	10	4H:1V
B 53	Load vs Horizontal Displacement	200	20	4H:1V
B 54	Load vs Flexural Stress	200	20	4H:1V
B 55	Load vs Horizontal Displacement	200	30	4H:1V
B 56	Load vs Flexural Stress	200	30	4H:1V
B 57	Load vs Horizontal Displacement	200	0	4H:1V
B 58	Load vs Flexural Stress	300	0	4H:1V
B 59	Load vs Horizontal Displacement	300	10	4H:1V
B 60	Load vs Flexural Stress	300	10	4H:1V
B 61	Load vs Horizontal Displacement	300	20	4H:1V
B 62	Load vs Flexural Stress	300	20	4H:1V
B 63	Load vs Horizontal Displacement	300	30	4H:1V
B 64	Load vs Flexural Stress	300	30	4H:1V



(a)

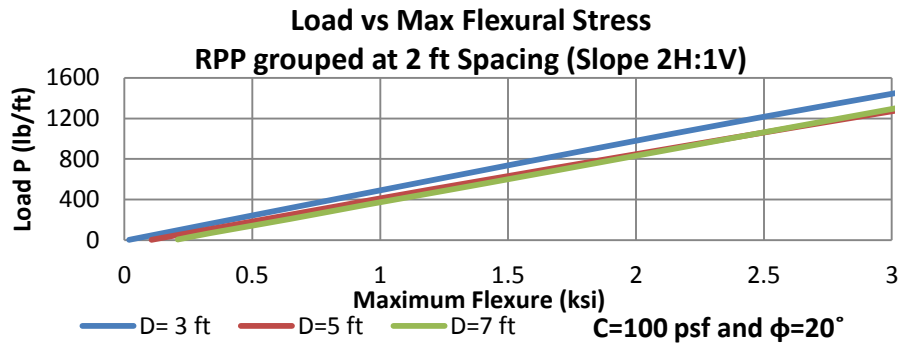


(b)

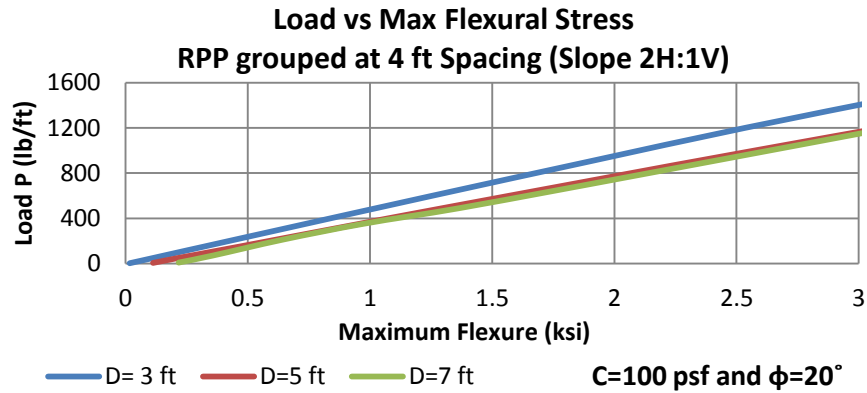


(c)

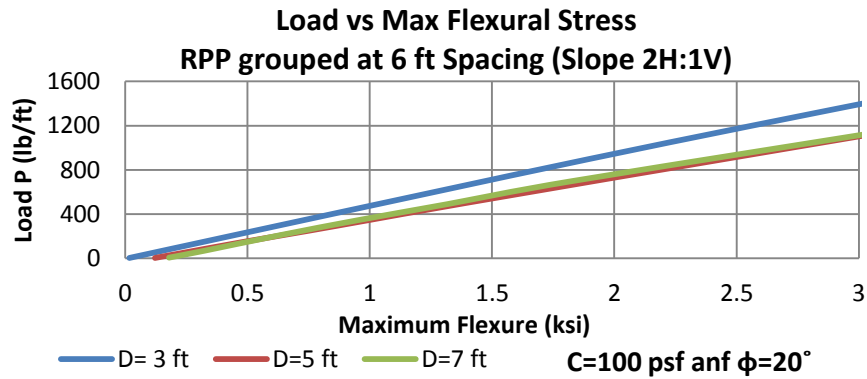
Figure B 1: Design Chart for Load versus Horizontal Displacement of RPP grouped at, a. 2-ft, b. 4-ft, c. 6-ft spacing for a soil of $c=100$ psf, $\phi=20^\circ$ and slope 2H:1V.



(a)

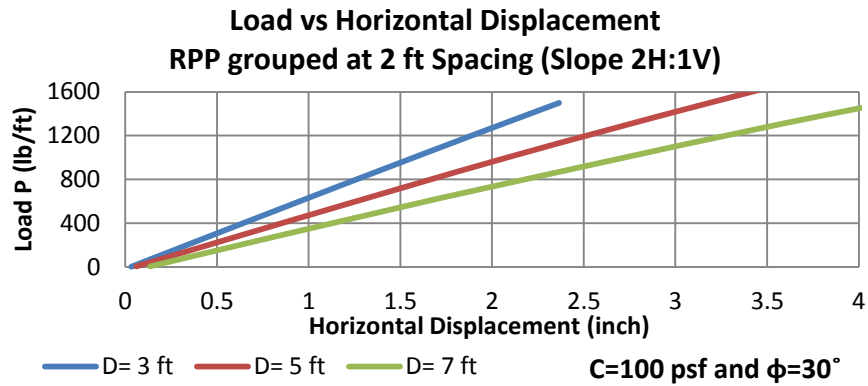


(b)

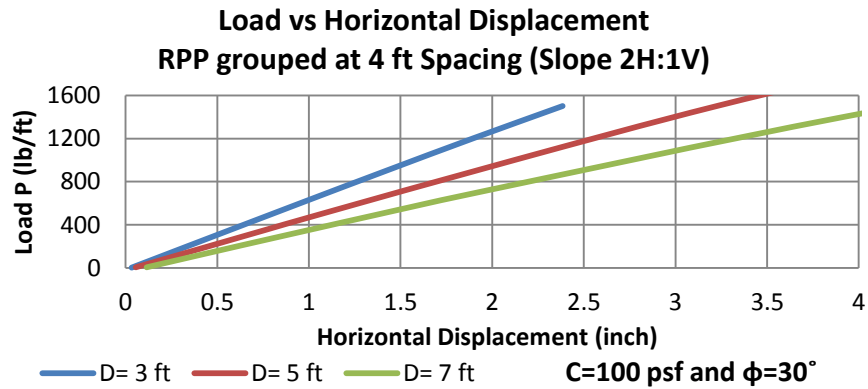


(c)

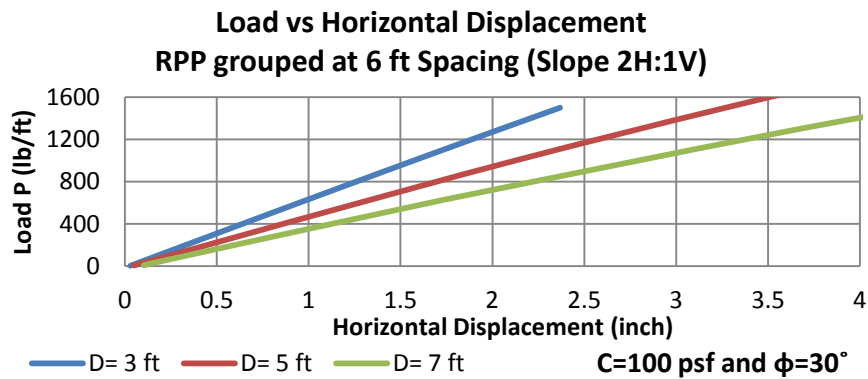
Figure B 2: Design Chart for Load versus Flexural Stress of RPP grouped at, a. 2-ft, b. 4-ft, c. 6-ft spacing for a soil of $c=100$ psf, $\phi=20^\circ$ and slope 2H:1V.



(a)



(b)



(c)

Figure B 3: Design Chart for Load versus Horizontal Displacement of RPP grouped at, a. 2-ft, b. 4-ft, c. 6-ft spacing for a soil of $c=100$ psf, $\phi=30^\circ$ and slope 2H:1V.

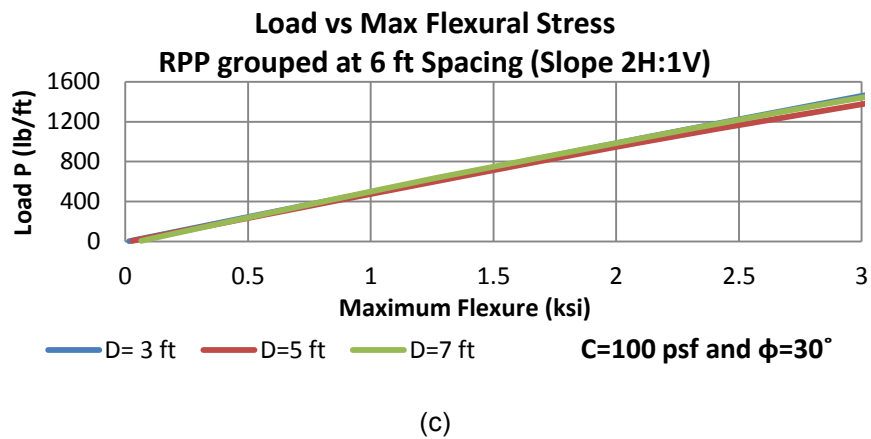
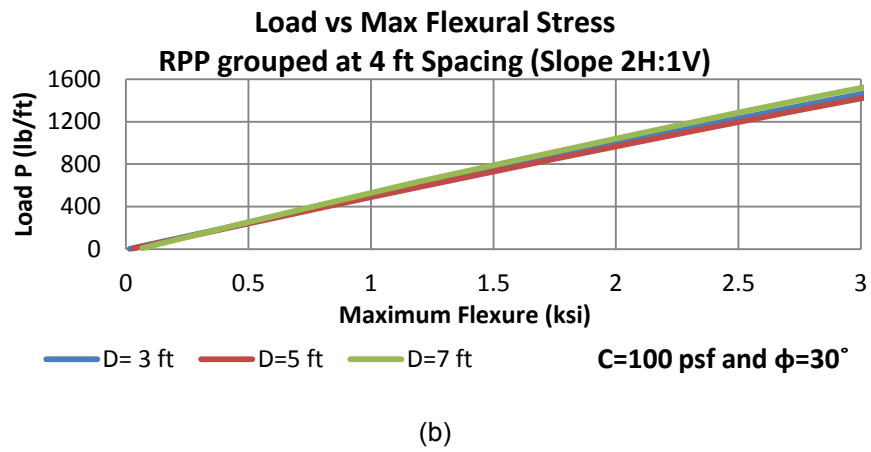
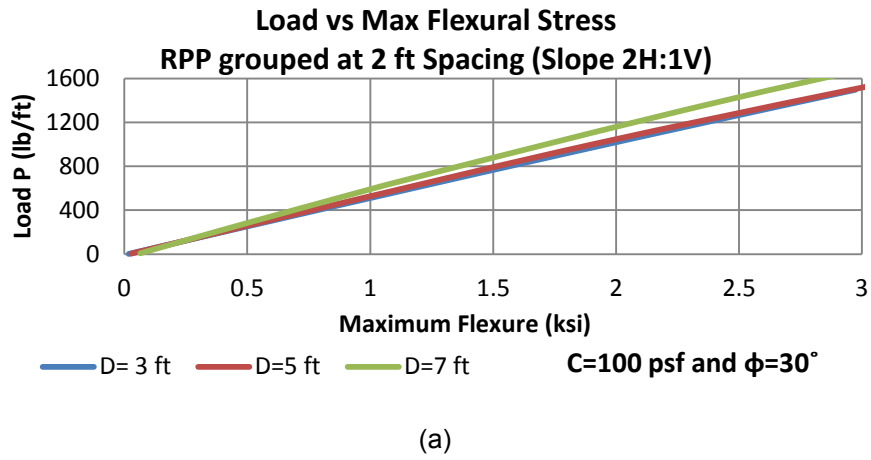
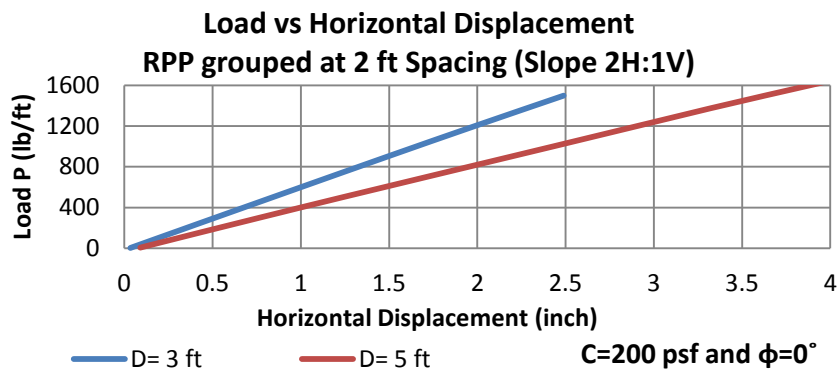
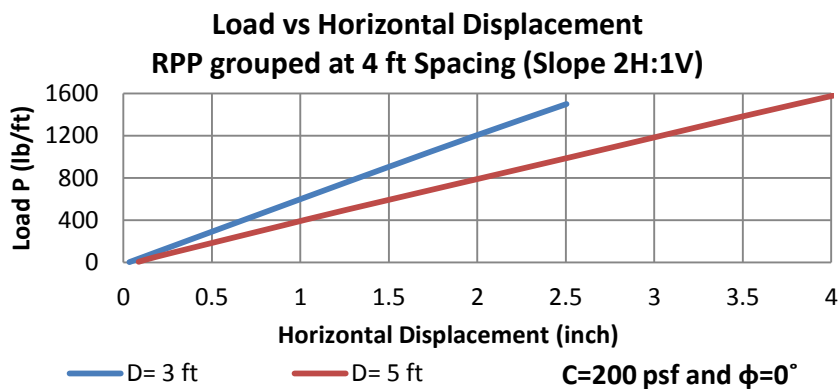


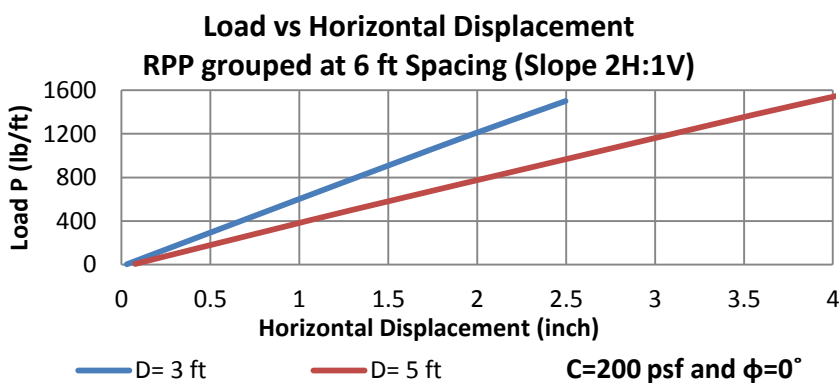
Figure B 4: Design Chart for Load versus Flexural Stress of RPP grouped at, a. 2-ft, b. 4-ft, c. 6-ft spacing for a soil of $c=100$ psf, $\phi=30^\circ$ and slope 2H:1V.



(a)

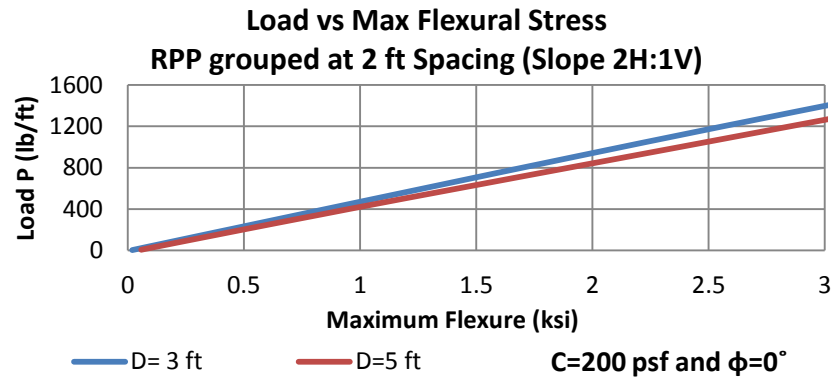


(b)

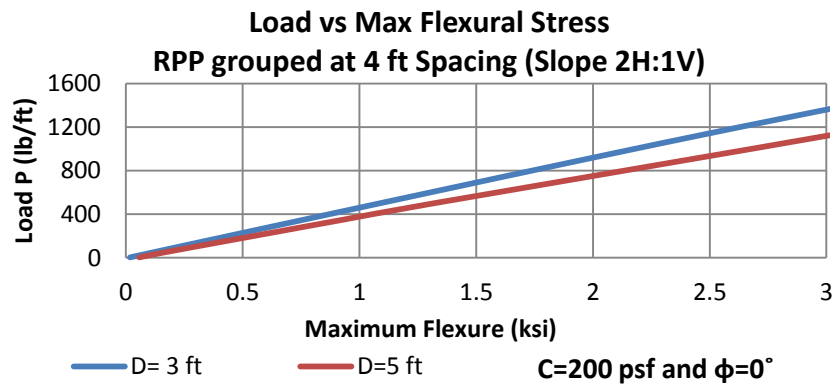


(c)

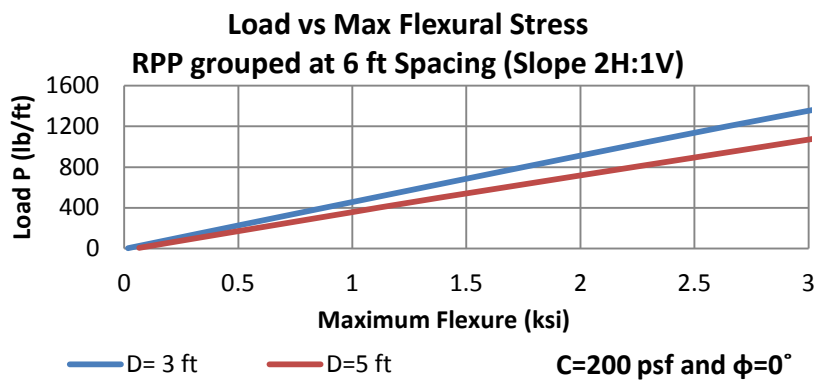
Figure B 5: Design Chart for Load versus Horizontal Displacement of RPP grouped at, a. 2-ft, b.4-ft, c. 6-ft spacing for a soil of $c=200$ psf, $\phi=0^\circ$ and slope 2H:1V.



(a)



(b)



(c)

Figure B 6: Design Chart for Load versus Flexural Stress of RPP grouped at, a. 2-ft, b. 4-ft, c. 6-ft spacing for a soil of $c=200$ psf, $\phi=0^\circ$ and slope 2H:1V.

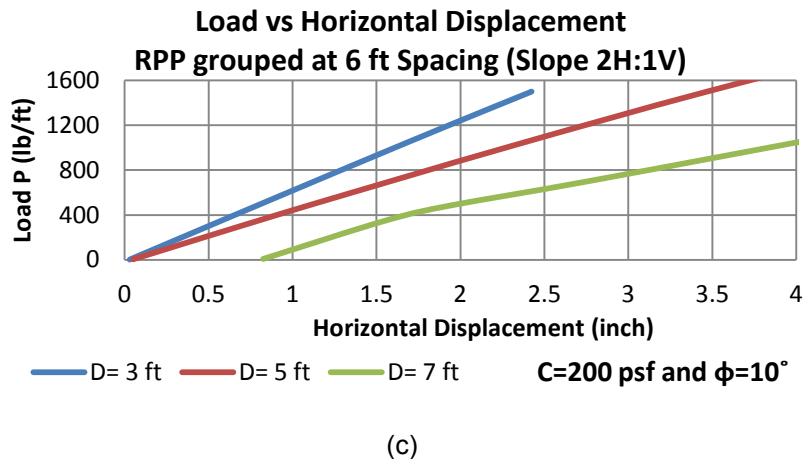
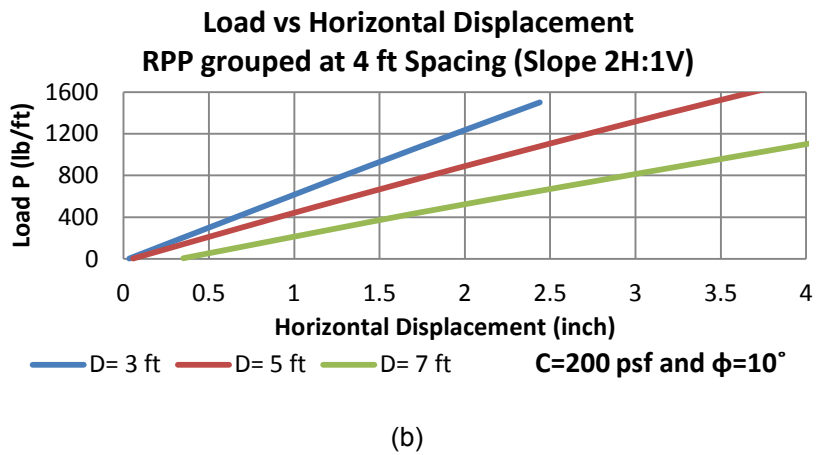
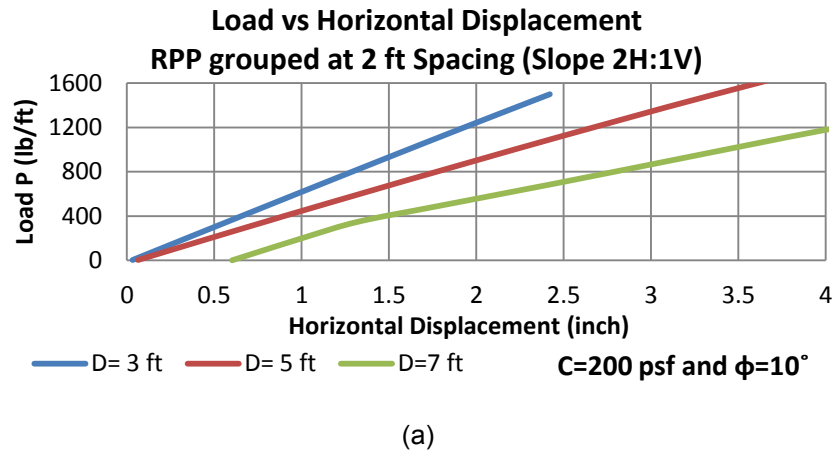
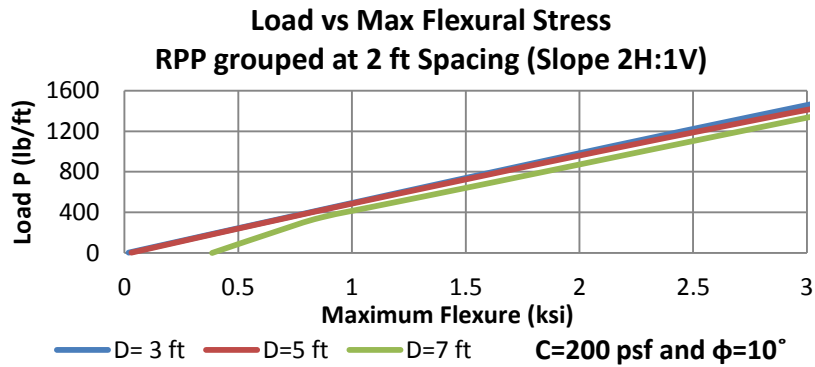
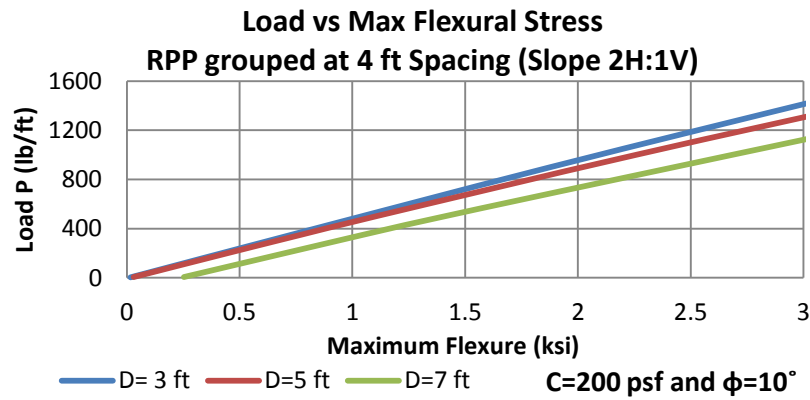


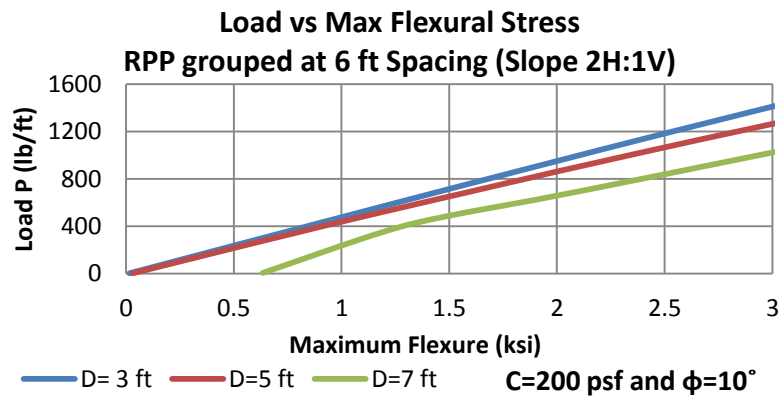
Figure B 7: Design Chart for Load versus Horizontal Displacement of RPP grouped at, a. 2-ft, b. 4-ft, c. 6-ft spacing for a soil of $c=200$ psf, $\phi=10^\circ$ and slope 2H:1V.



(a)

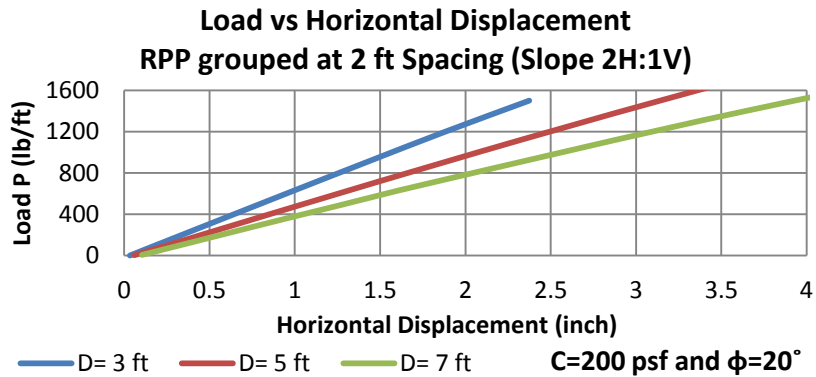


(b)

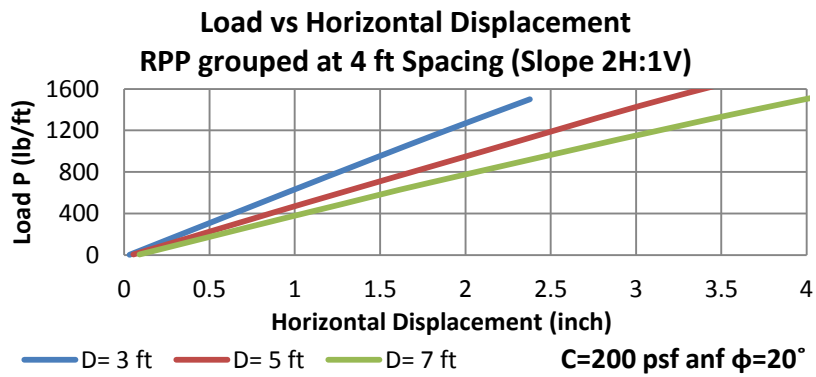


(c)

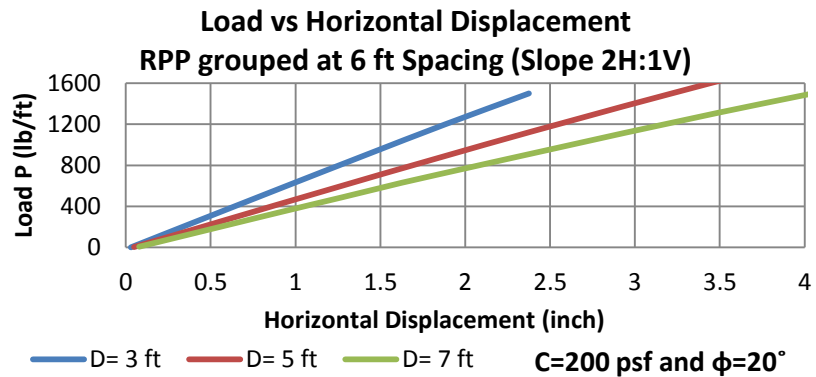
Figure B 8: Design Chart for Load versus Flexural Stress of RPP grouped at, a. 2-ft, b. 4-ft, c. 6-ft spacing for a soil of $c=200$ psf, $\phi=10^\circ$ and slope 2H:1V.



(a)

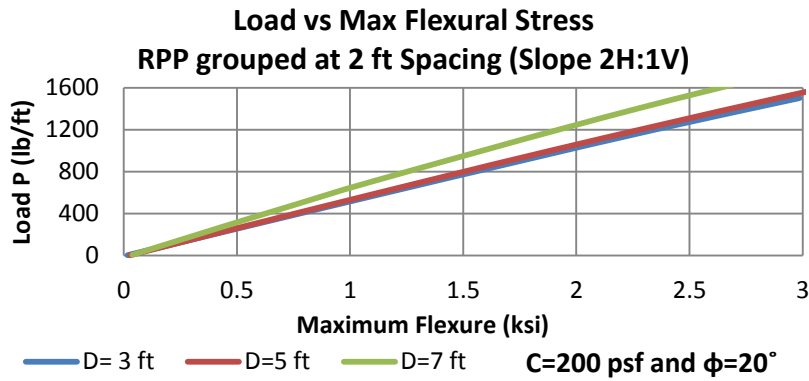


(b)

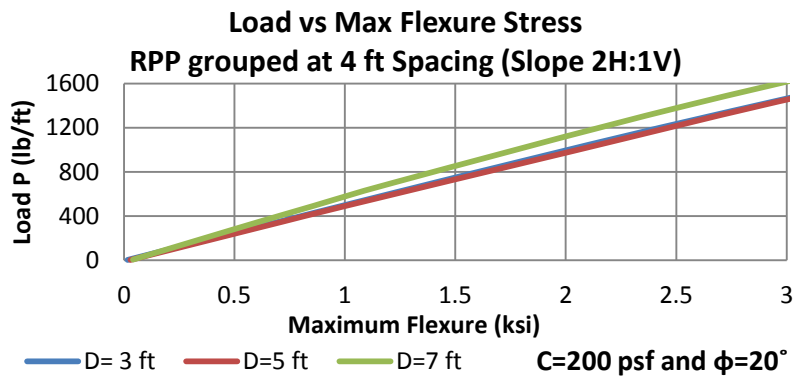


(c)

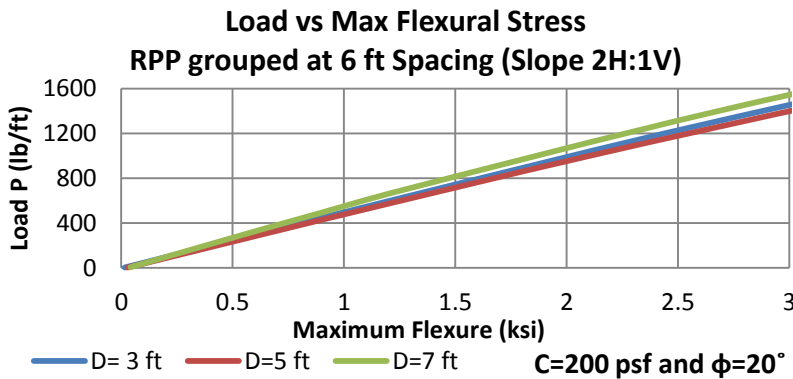
Figure B 9: Design Chart for Load versus Horizontal Displacement of RPP grouped at, a. 2-ft, b. 4-ft, c. 6-ft spacing for a soil of $c=200$ psf, $\phi=20^\circ$ and slope 2H:1V.



(a)

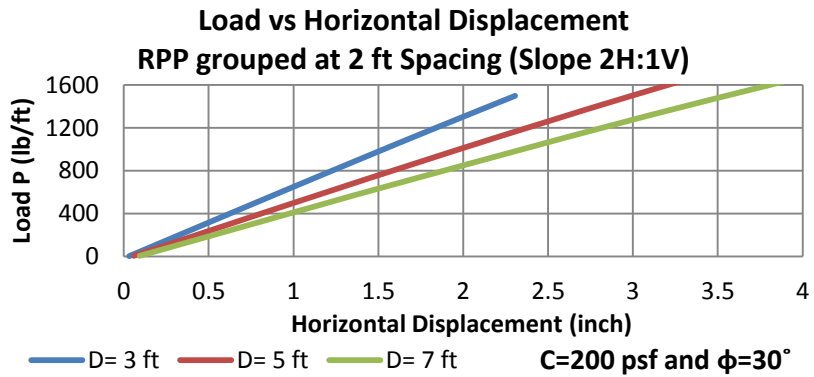


(b)

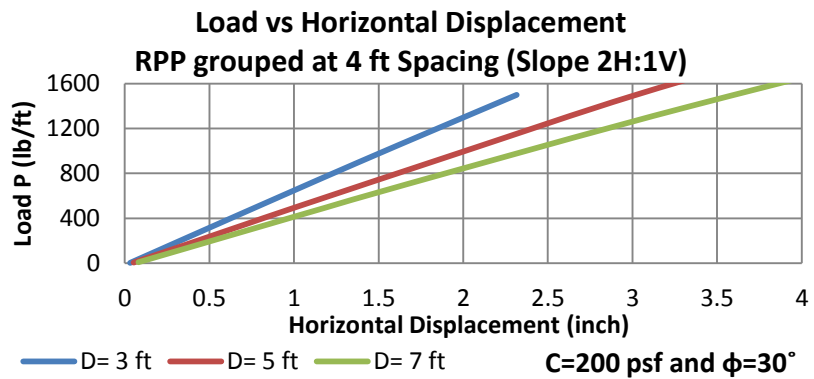


(c)

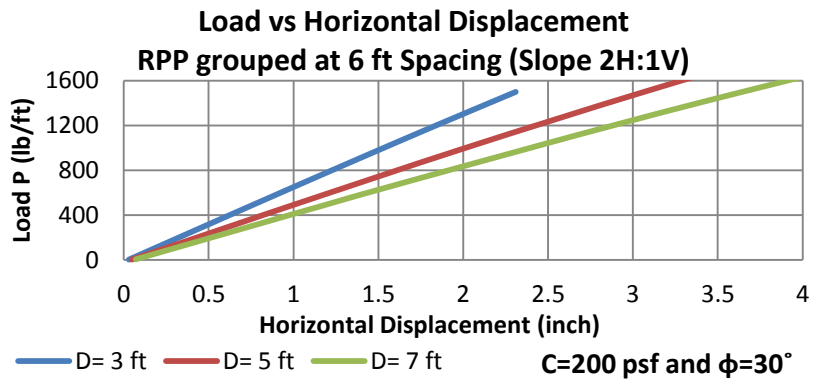
Figure B 10: Design Chart for Load versus Flexural Stress of RPP grouped at, a. 2-ft, b. 4-ft, c. 6-ft spacing for a soil of $c=200$ psf, $\phi=20^\circ$ and slope 2H:1V.



(a)

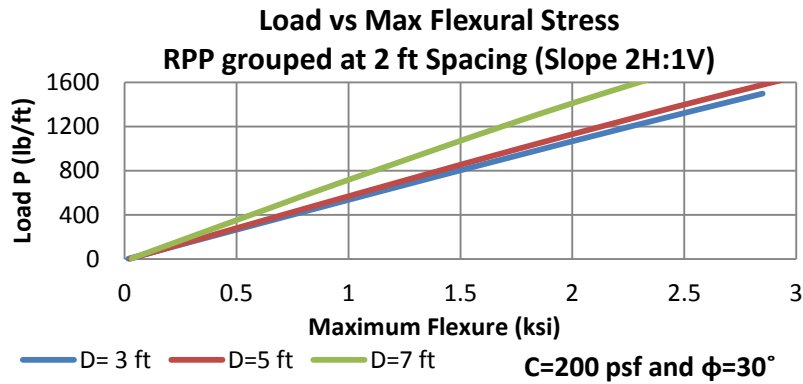


(b)

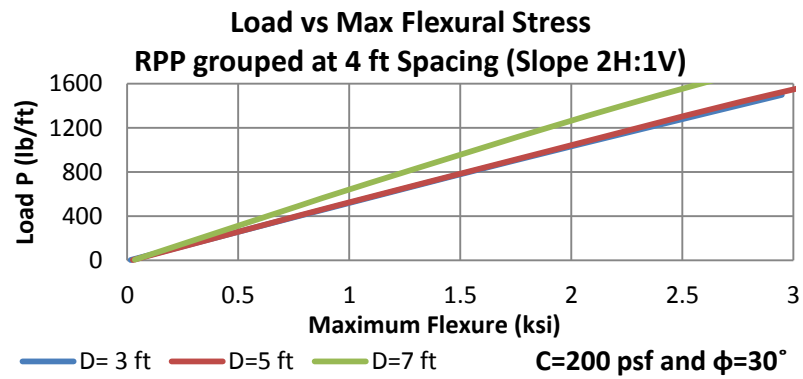


(c)

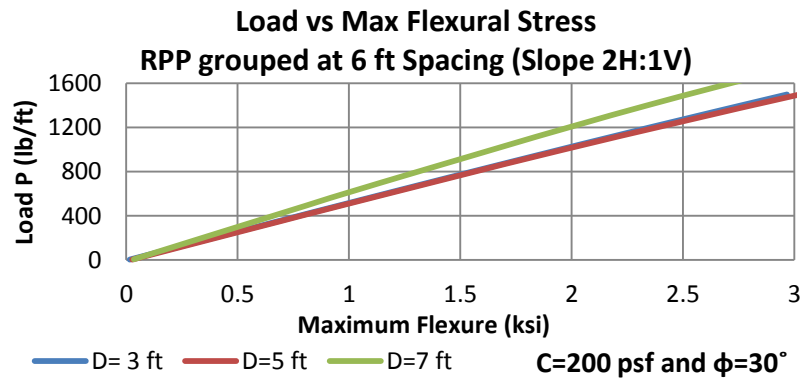
Figure B 11: Design Chart for Load versus Horizontal Displacement of RPP grouped at,
a. 2-ft, b. 4-ft, c. 6-ft spacing for a soil of $c=200$ psf, $\phi=30^\circ$ and slope 2H:1V.



(a)

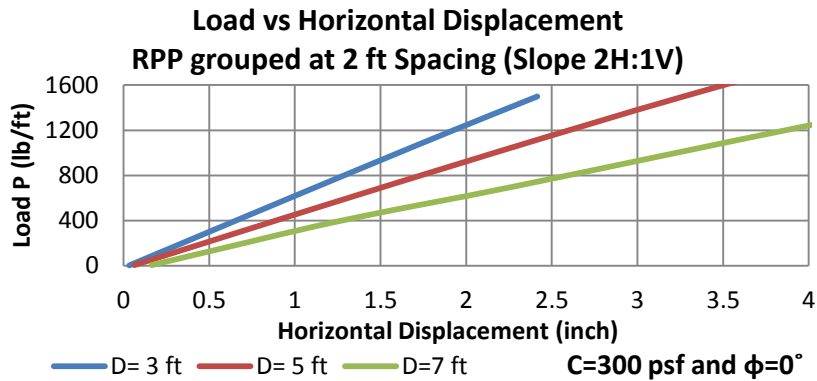


(b)

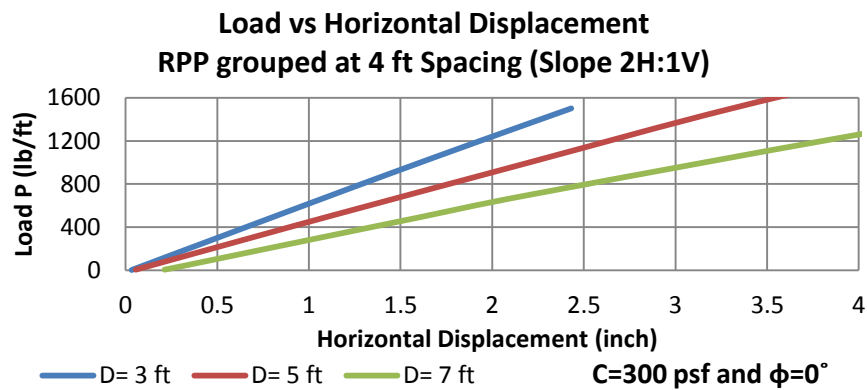


(c)

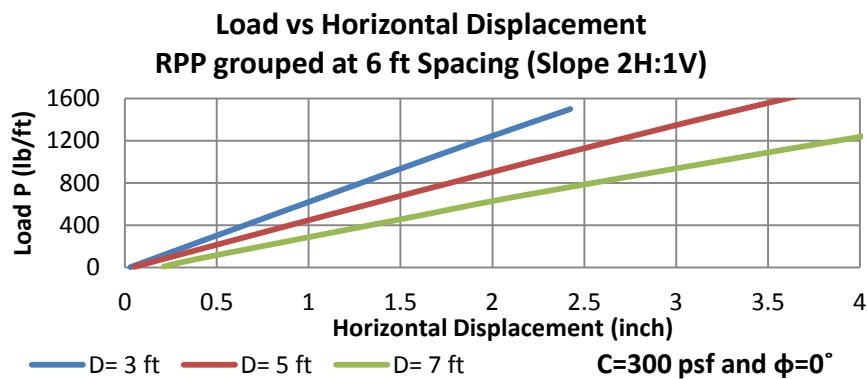
Figure B 12: Design Chart for Load versus Flexural Stress of RPP grouped at, a. 2-ft, b. 4-ft, c. 6-ft spacing for a soil of $c=200$ psf, $\phi=30^\circ$ and slope 2H:1V.



(a)

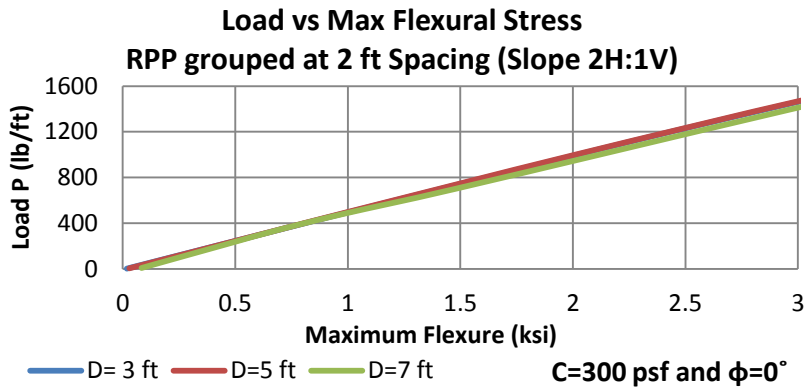


(b)

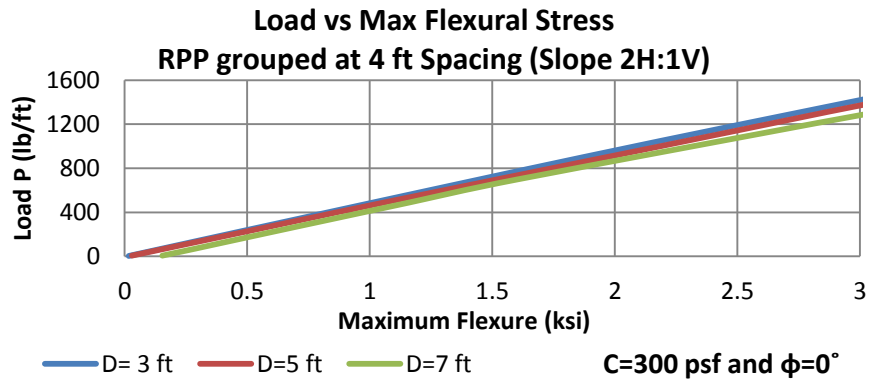


(c)

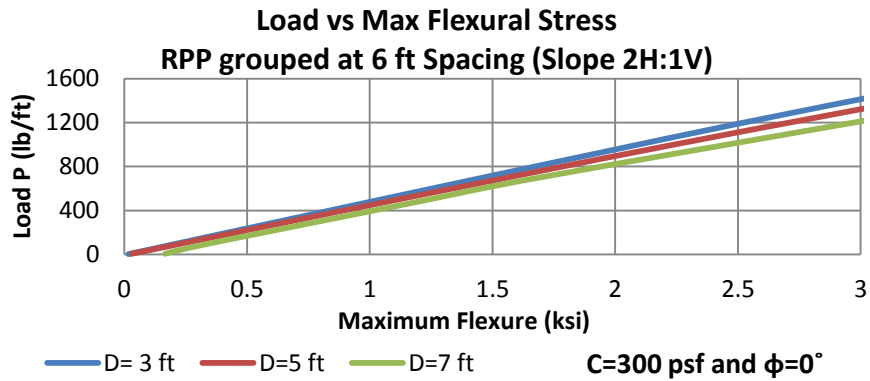
Figure B 13: Design Chart for Load versus Horizontal Displacement of RPP grouped at, a. 2-ft, b. 4-ft, c. 6-ft spacing for a soil of $c=300$ psf, $\phi=0^\circ$ and slope 2H:1V.



(a)

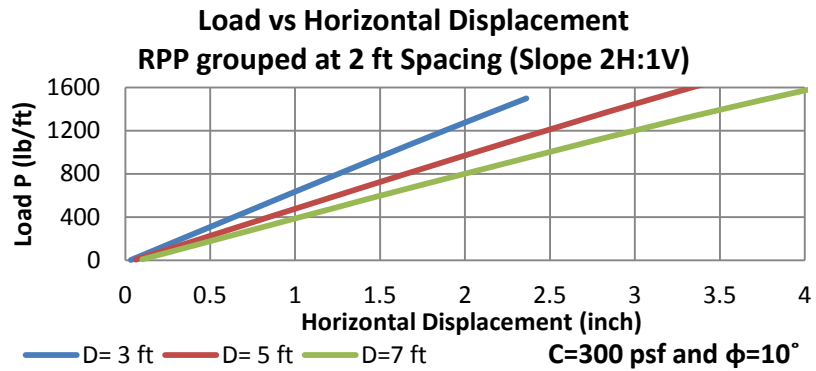


(b)

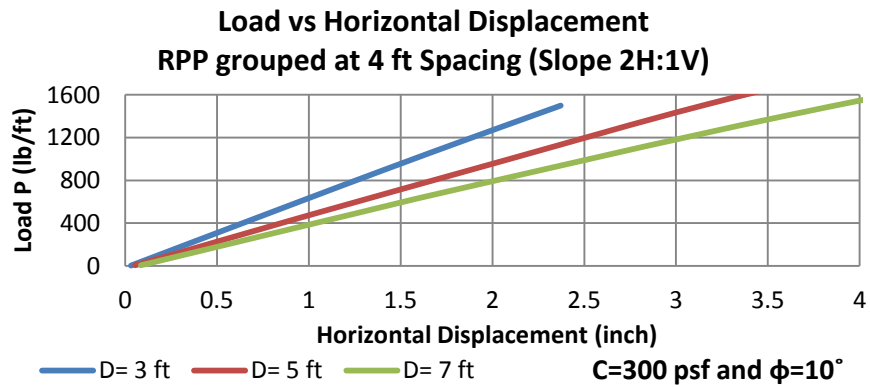


(c)

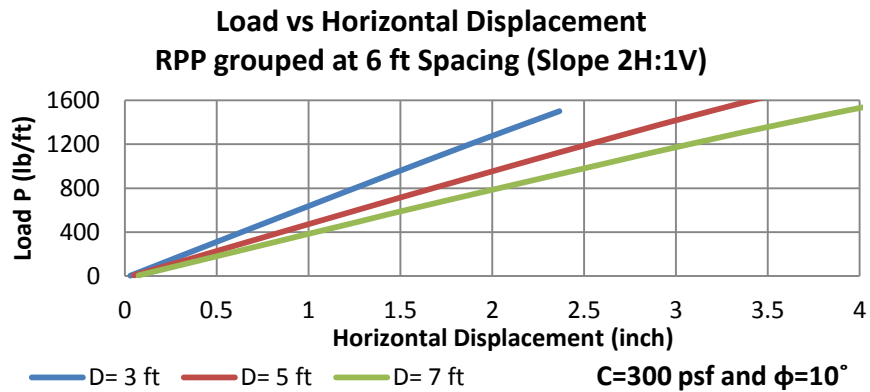
Figure B 14: Design Chart for Load versus Flexural Stress of RPP grouped at, a. 2-ft, b. 4-ft, c. 6-ft spacing for a soil of $c=300$ psf, $\phi=0^\circ$ and slope 2H:1V.



(a)

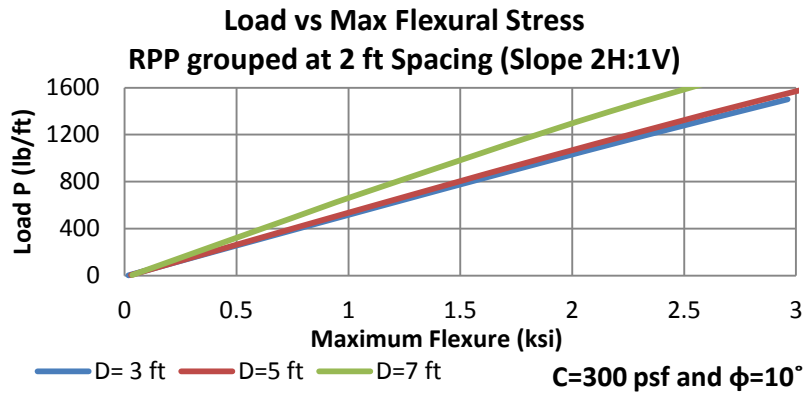


(b)

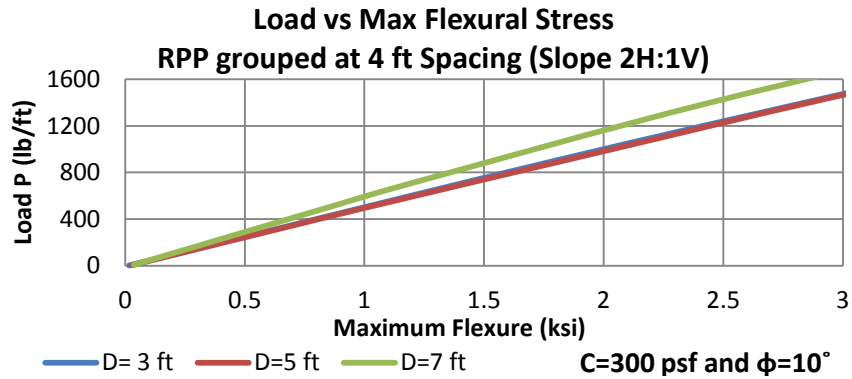


(c)

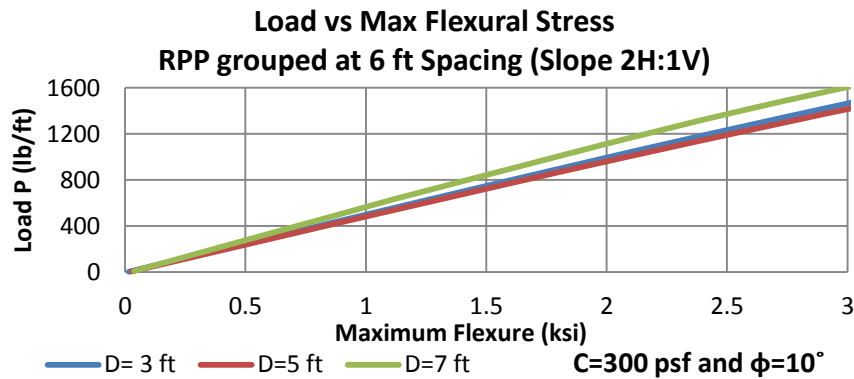
Figure B 15: Design Chart for Load versus Horizontal Displacement of RPP grouped at, a. 2-ft, b. 4-ft, c. 6-ft spacing for a soil of $c=300$ psf, $\phi=10^\circ$ and slope 2H:1V.



(a)

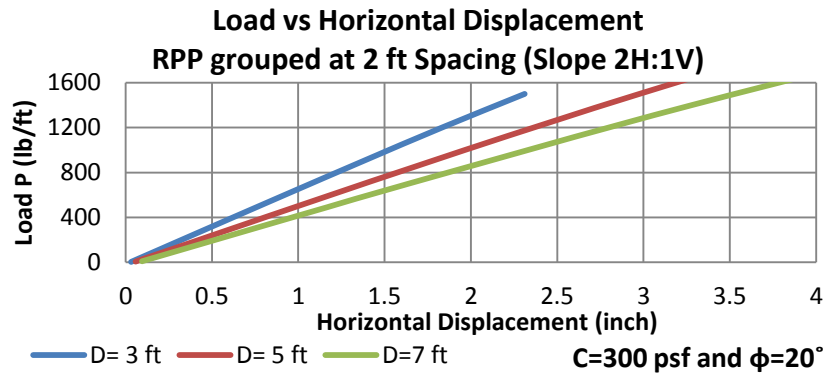


(b)

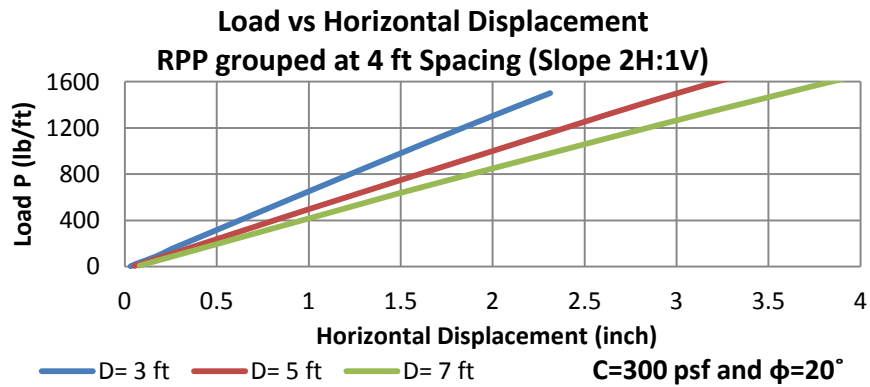


(c)

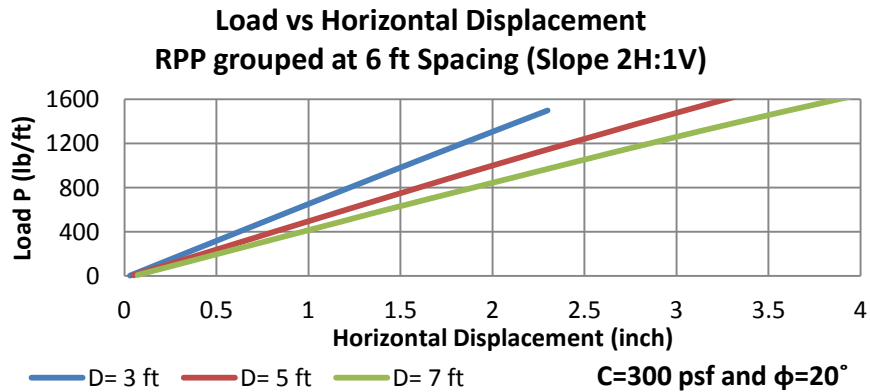
Figure B 16: Design Chart for Load versus Flexural Stress of RPP grouped at, a. 2-ft, b. 4-ft, c. 6-ft spacing for a soil of $c=300$ psf, $\phi=10^\circ$ and slope 2H:1V.



(a)

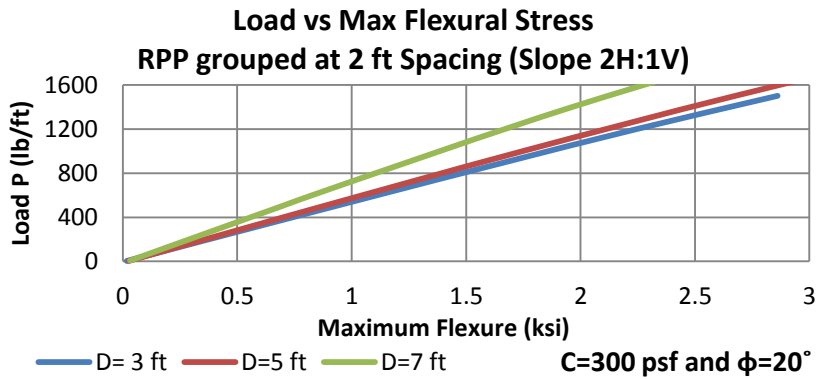


(b)

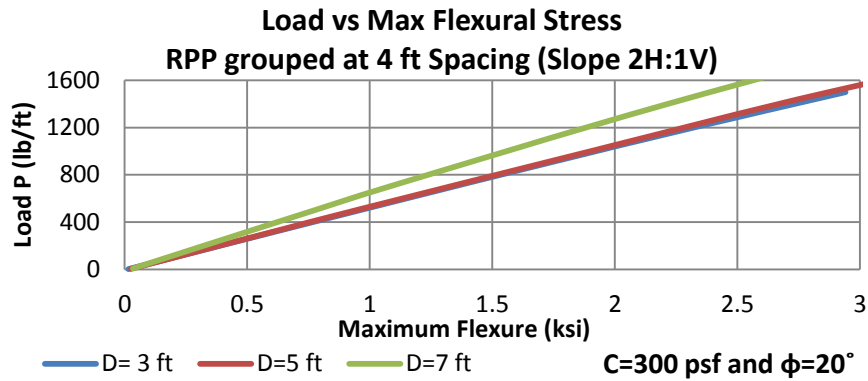


(c)

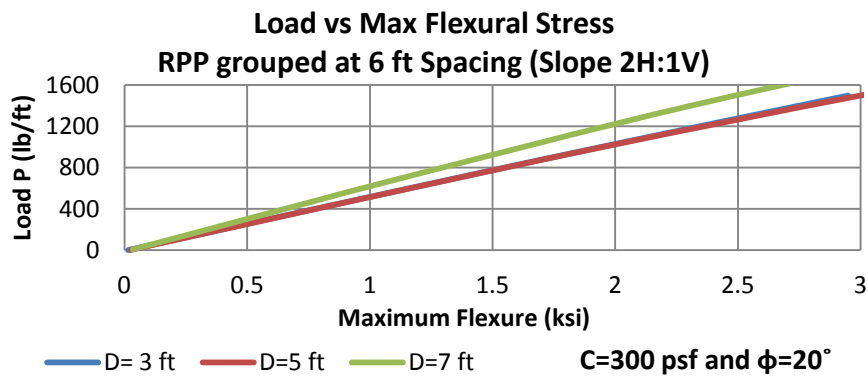
Figure B 17: Design Chart for Load versus Horizontal Displacement of RPP grouped at, a. 2-ft, b. 4-ft, c. 6-ft spacing for a soil of $c=300$ psf, $\phi=20^\circ$ and slope 2H:1V.



(a)

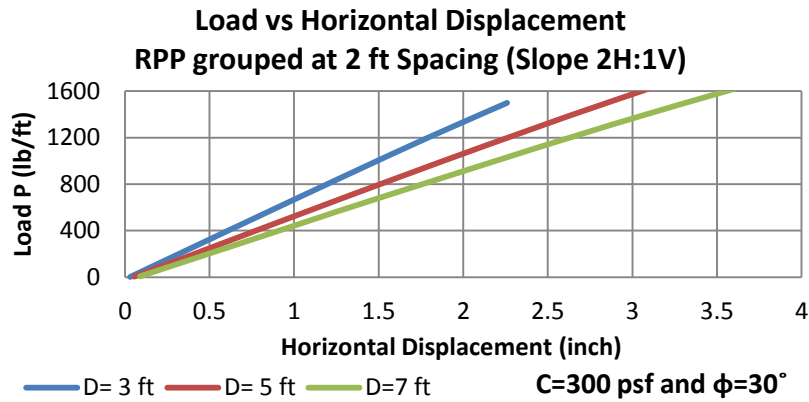


(b)

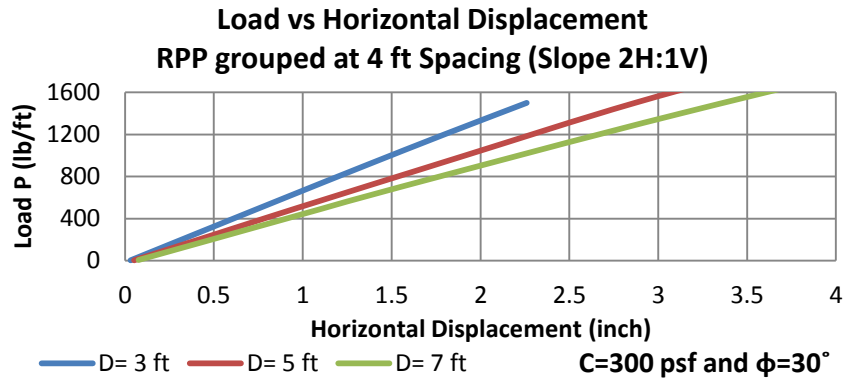


(c)

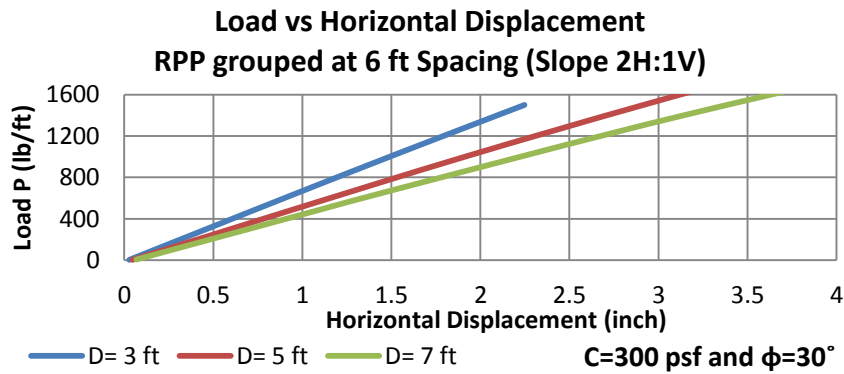
Figure B 18: Design Chart for Load versus Flexural Stress of RPP grouped at, a. 2-ft, b. 4-ft, c. 6-ft spacing for a soil of $c=300$ psf, $\phi=20^\circ$ and slope 2H:1V.



(a)

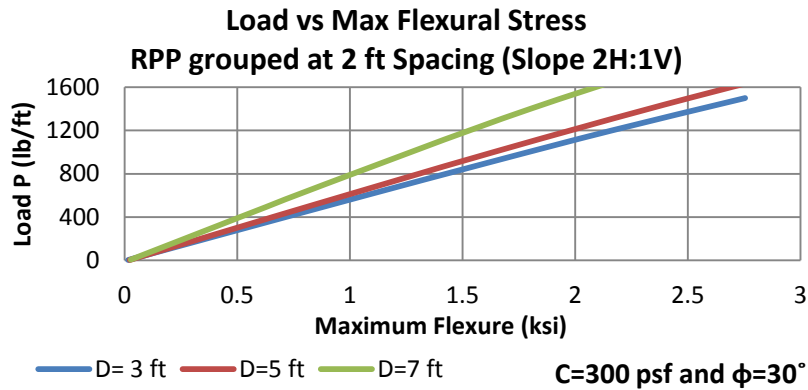


(b)

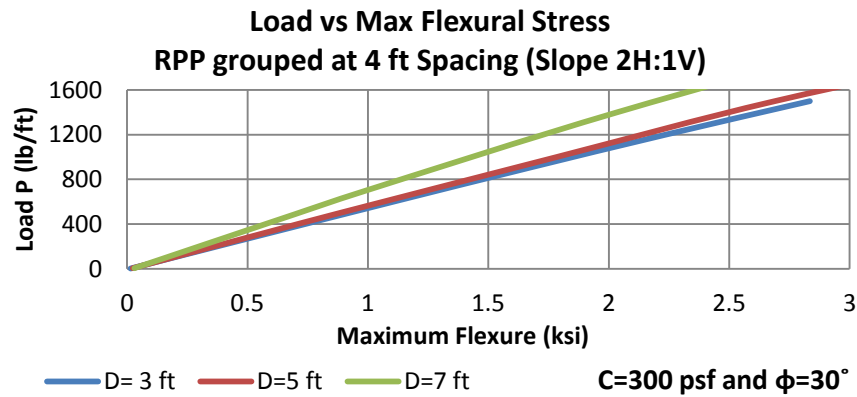


(c)

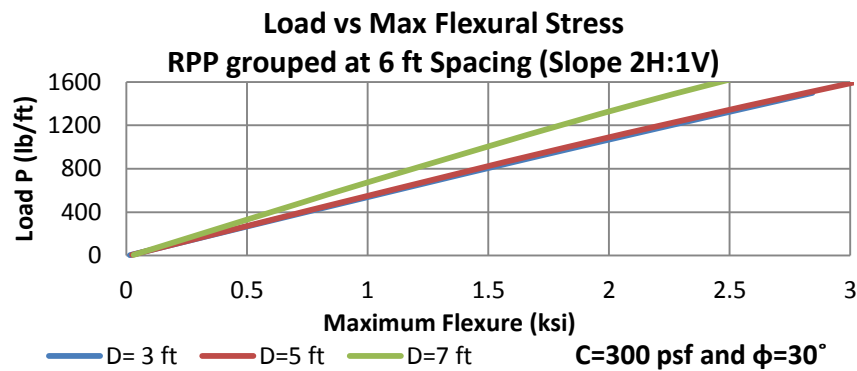
Figure B 19: Design Chart for Load versus Horizontal Displacement of RPP grouped at, a. 2-ft, b. 4-ft, c. 6-ft spacing for a soil of $c=300$ psf, $\phi=30^\circ$ and slope 2H:1V.



(a)

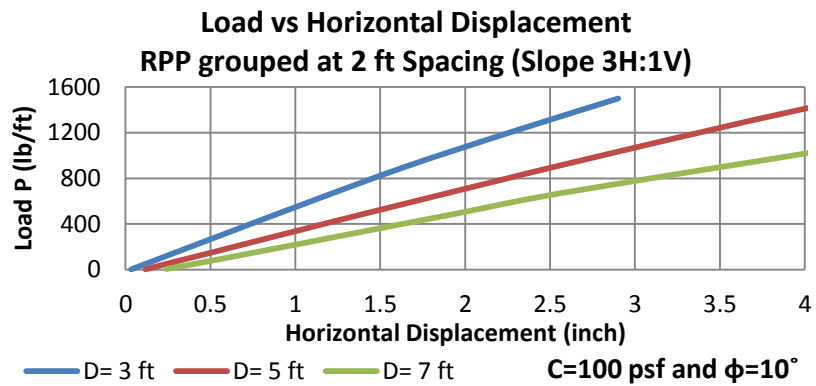


(b)

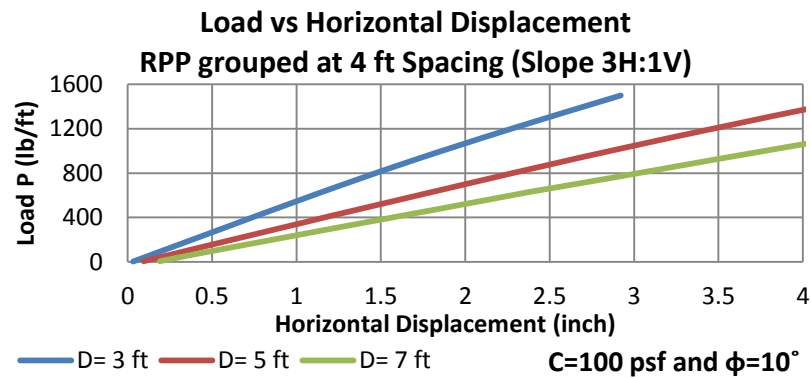


(c)

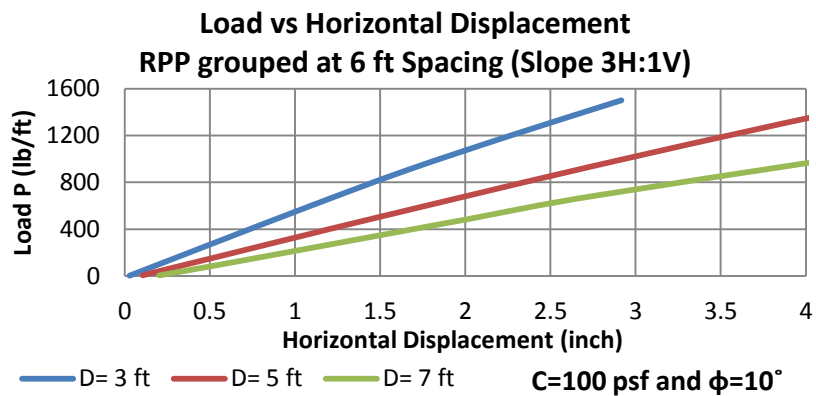
Figure B 20: Design Chart for Load versus Flexural Stress of RPP grouped at, a. 2-ft, b. 4-ft, c. 6-ft spacing for a soil of $c=300$ psf, $\phi=30^\circ$ and slope 2H:1V.



(a)

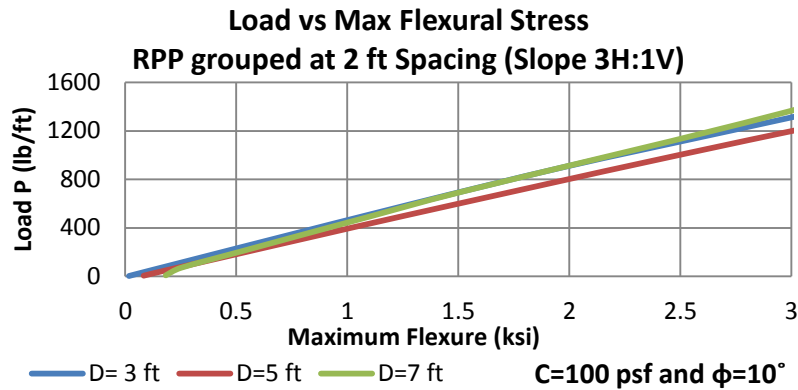


(b)

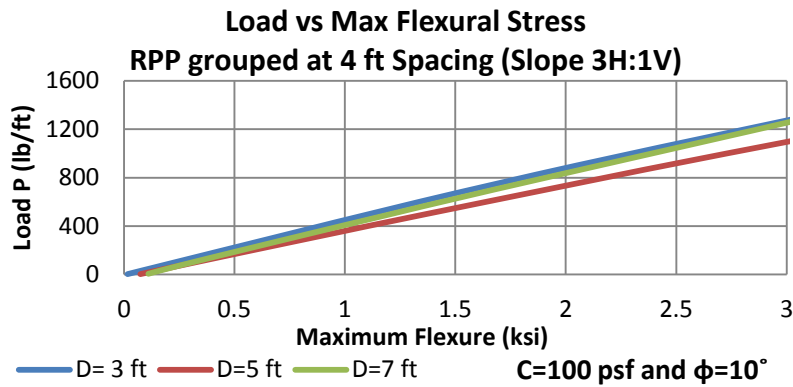


(c)

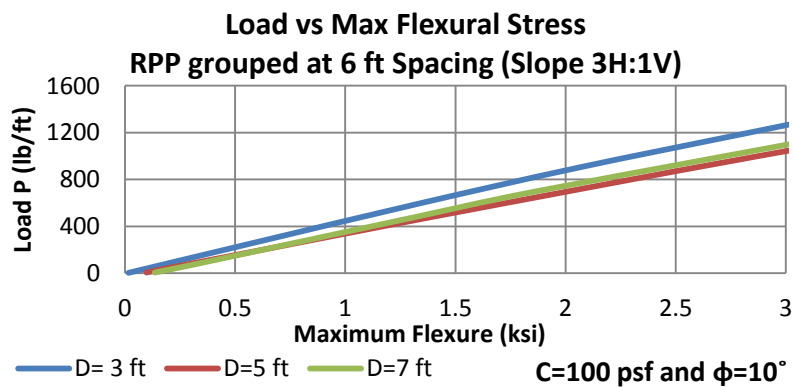
Figure B 21: Design Chart for Load versus Horizontal Displacement of RPP grouped at, a. 2-ft, b.4-ft, c. 6-ft spacing for a soil of $c=100$ psf, $\phi=10^\circ$ and slope 3H:1V.



(a)

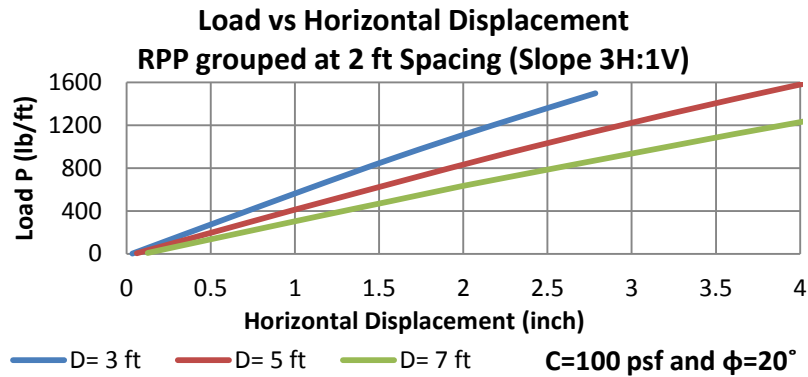


(b)

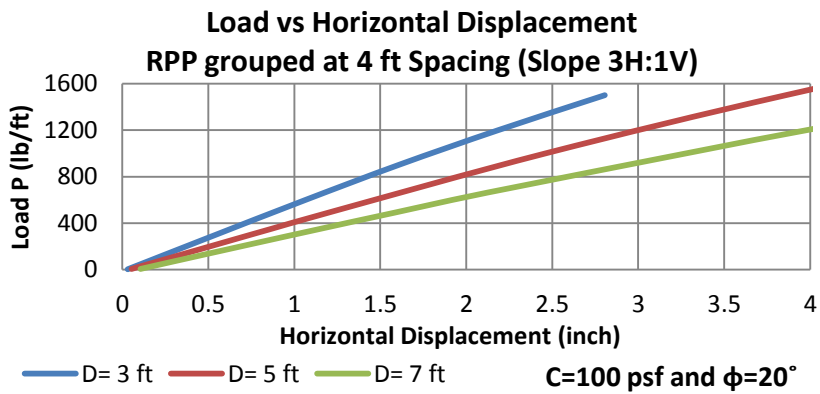


(c)

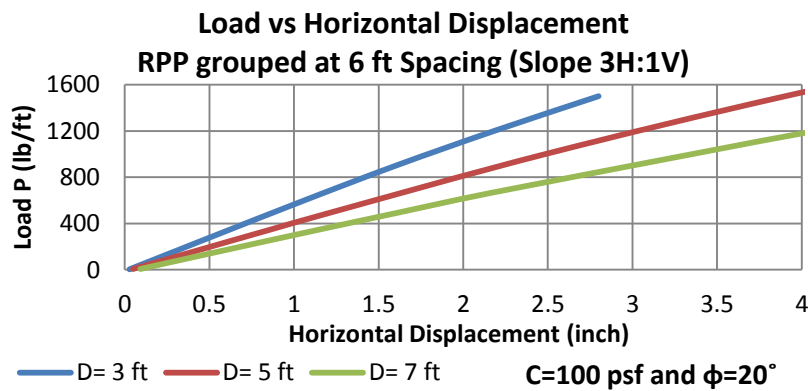
Figure B 22: Design Chart for Load versus Flexural Stress of RPP grouped at, a. 2-ft, b. 4-ft, c. 6-ft spacing for a soil of $c=100$ psf, $\phi=10^\circ$ and slope 3H:1V.



(a)

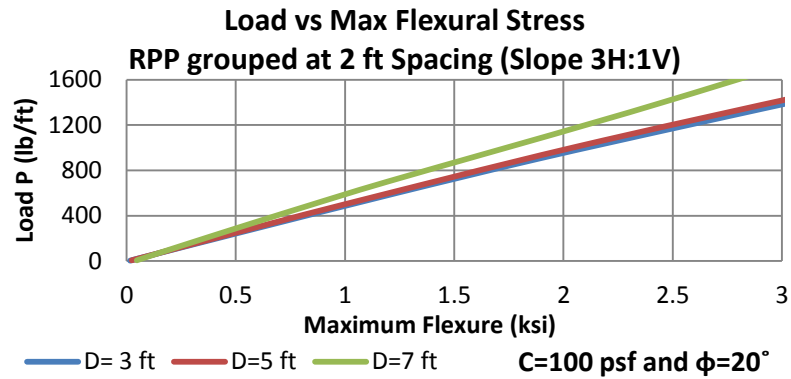


(b)

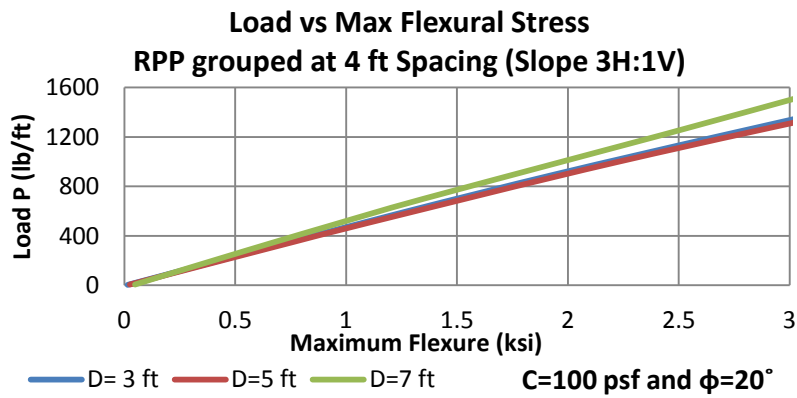


(c)

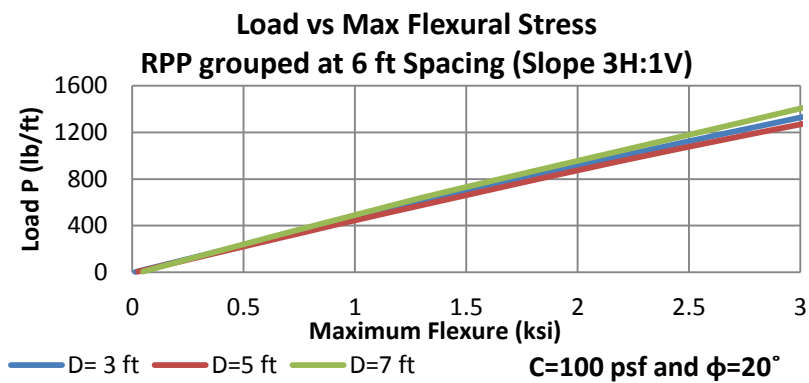
Figure B 23: Design Chart for Load versus Horizontal Displacement of RPP grouped at, a. 2-ft, b. 4-ft, c. 6-ft spacing for a soil of $c=100$ psf, $\phi=20^\circ$ and slope 3H:1V.



(a)

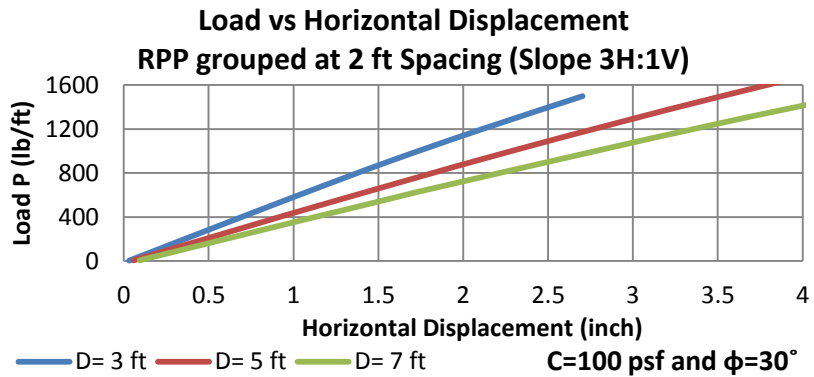


(b)

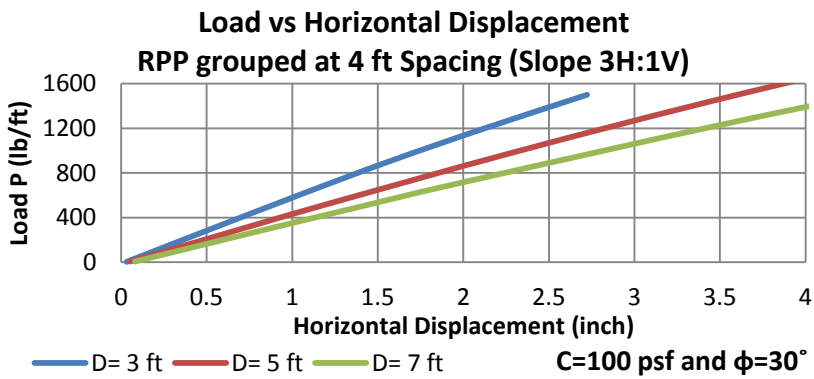


(c)

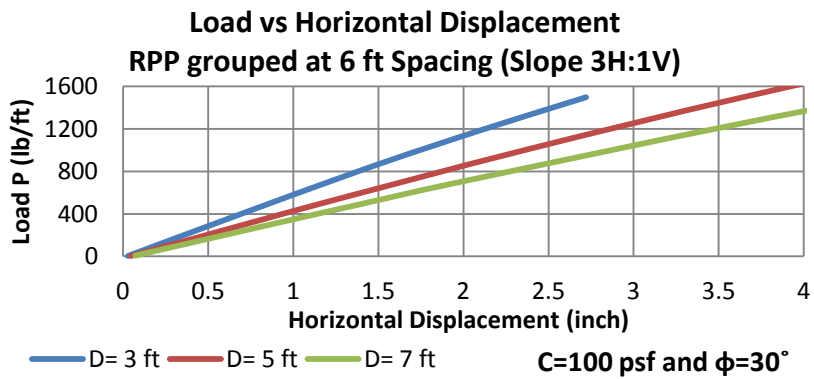
Figure B 24: Design Chart for Load versus Flexural Stress of RPP grouped at, a. 2-ft, b. 4-ft, c. 6-ft spacing for a soil of $c=100$ psf, $\phi=20^\circ$ and slope 3H:1V.



(a)

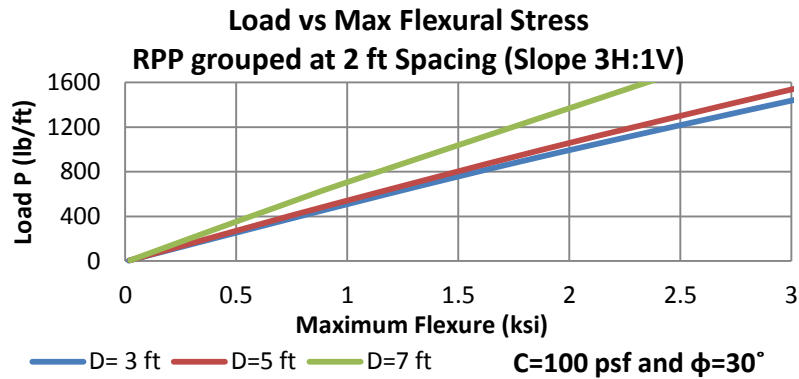


(b)

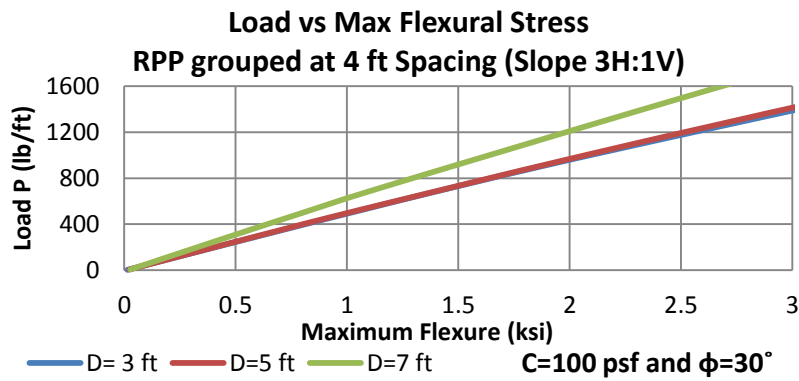


(c)

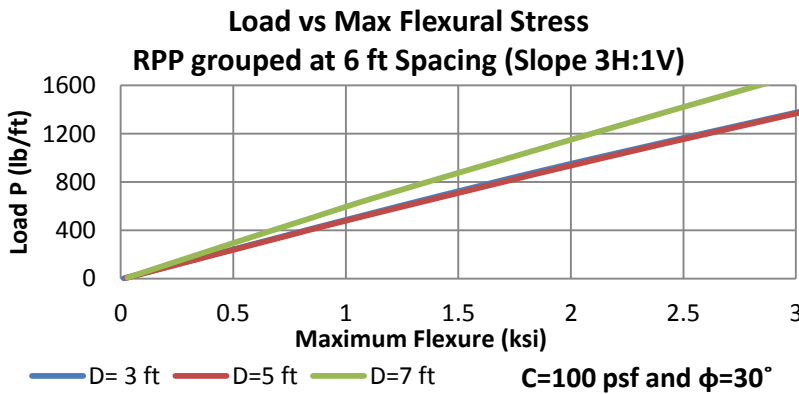
Figure B 25: Design Chart for Load versus Horizontal Displacement of RPP grouped at, a. 2-ft, b. 4-ft, c. 6-ft spacing for a soil of $c=100$ psf, $\phi=30^\circ$ and slope 3H:1V.



(a)

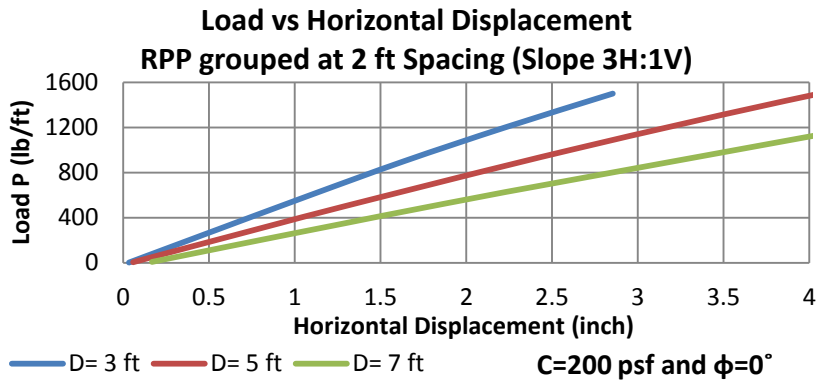


(b)

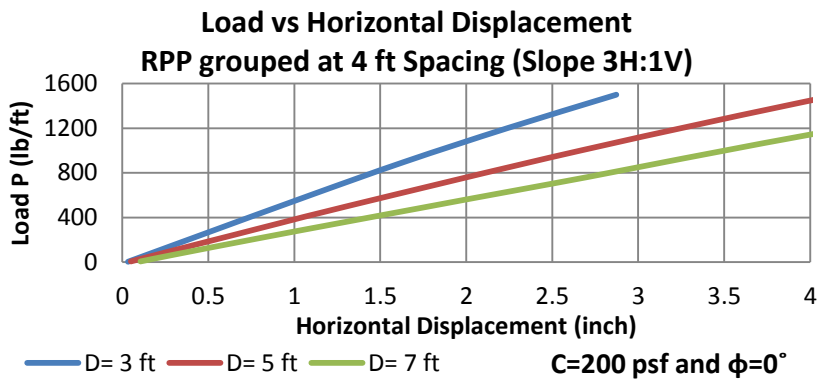


(c)

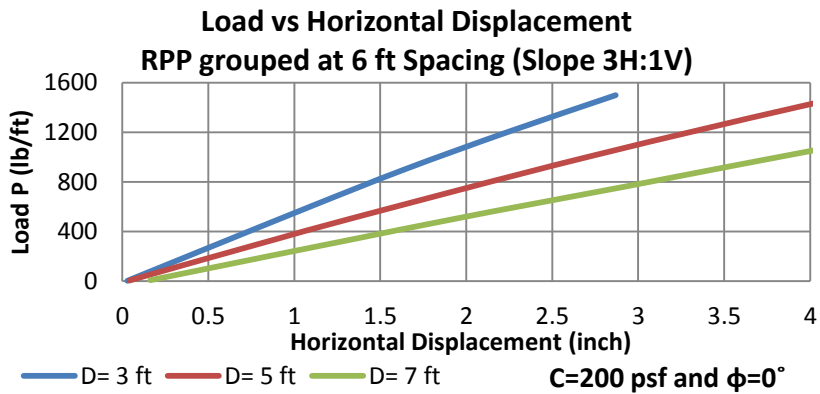
Figure B 26: Design Chart for Load versus Flexural Stress of RPP grouped at, a. 2-ft, b. 4-ft, c. 6-ft spacing for a soil of $c=100$ psf, $\phi=30^\circ$ and slope 3H:1V.



(a)

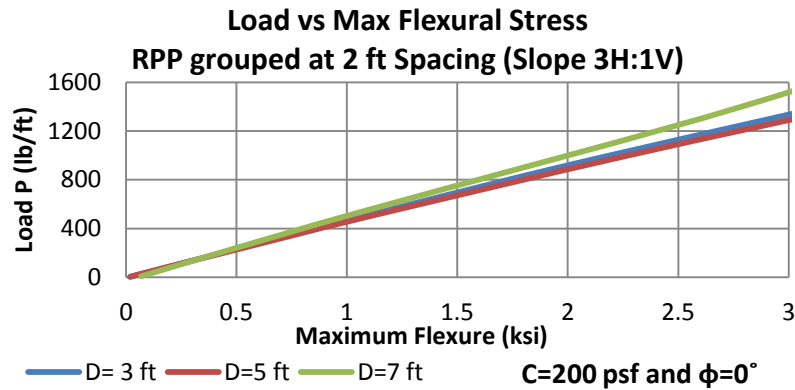


(b)

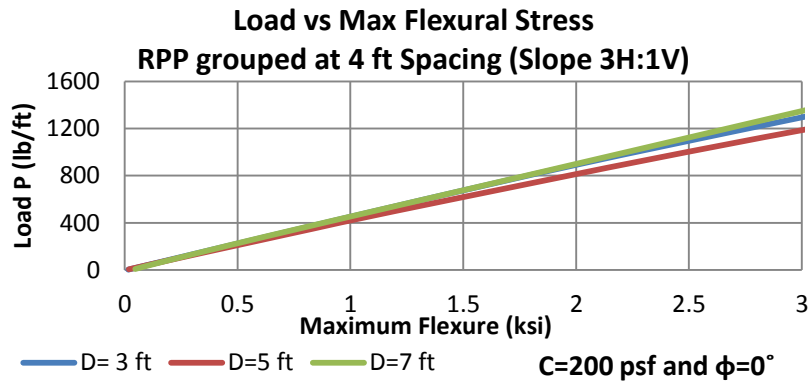


(c)

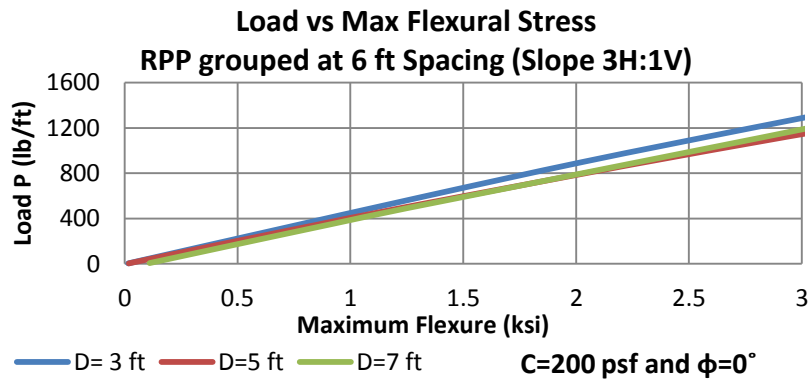
Figure B 27: Design Chart for Load versus Horizontal Displacement of RPP grouped at, a. 2-ft, b. 4-ft, c. 6-ft spacing for a soil of $c=200$ psf, $\phi=0^\circ$ and slope 3H:1V.



(a)

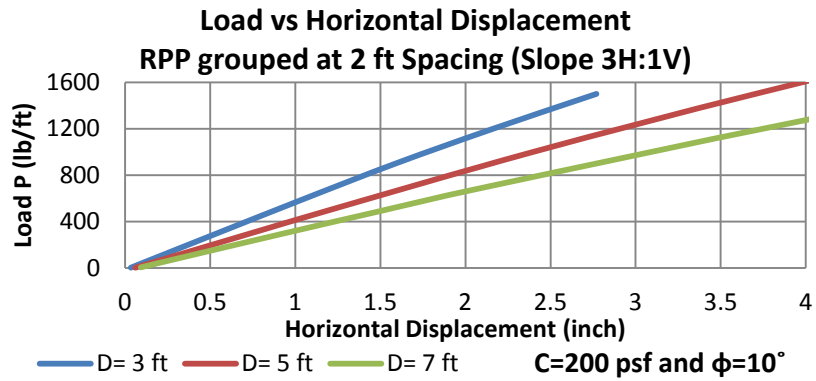


(b)

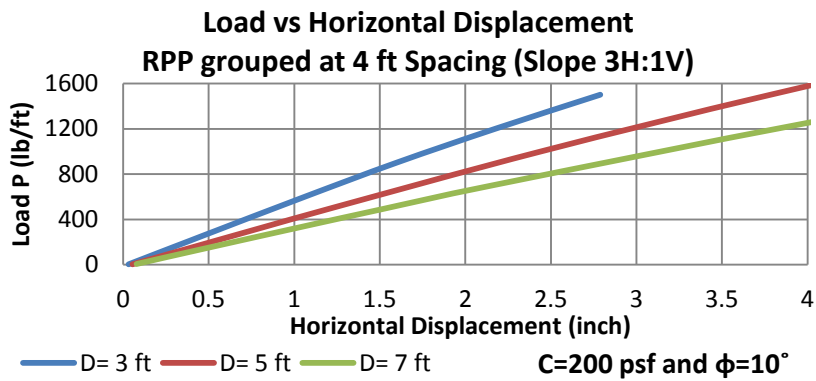


(c)

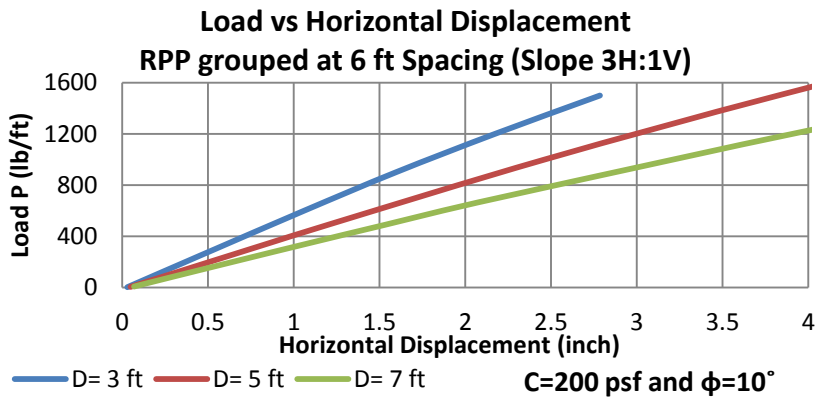
Figure B 28: Design Chart for Load versus Flexural Stress of RPP grouped at, a. 2-ft, b. 4-ft, c. 6-ft spacing for a soil of $c=200$ psf, $\phi=0^\circ$ and slope 3H:1V.



(a)

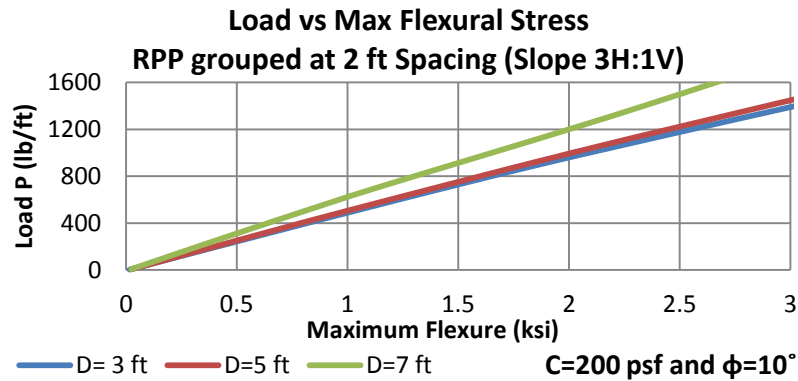


(b)

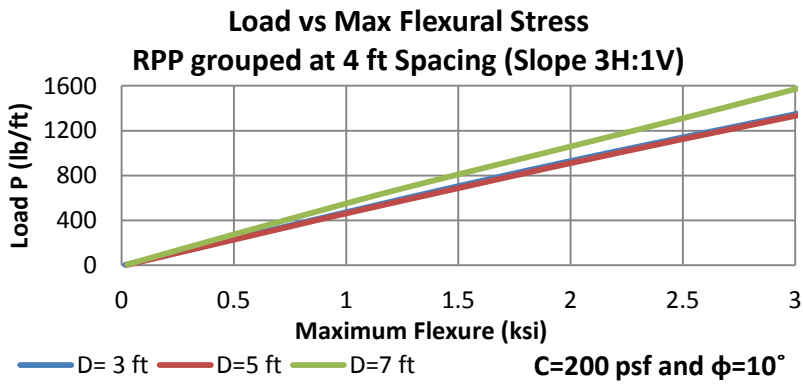


(c)

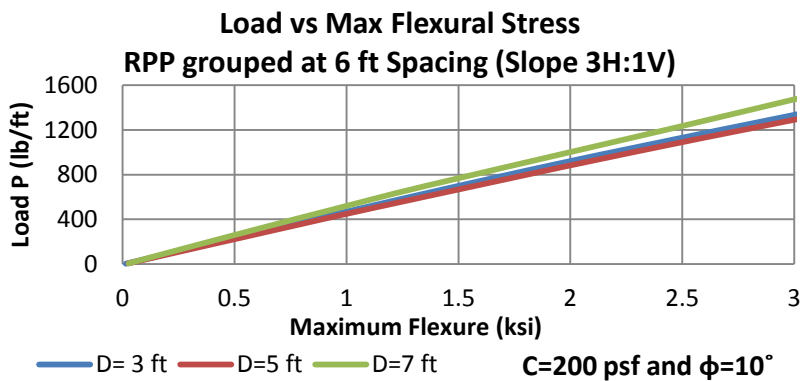
Figure B 29: Design Chart for Load versus Horizontal Displacement of RPP grouped at, a. 2-ft, b. 4-ft, c. 6-ft spacing for a soil of $c=200$ psf, $\phi=10^\circ$ and slope 3H:1V.



(a)

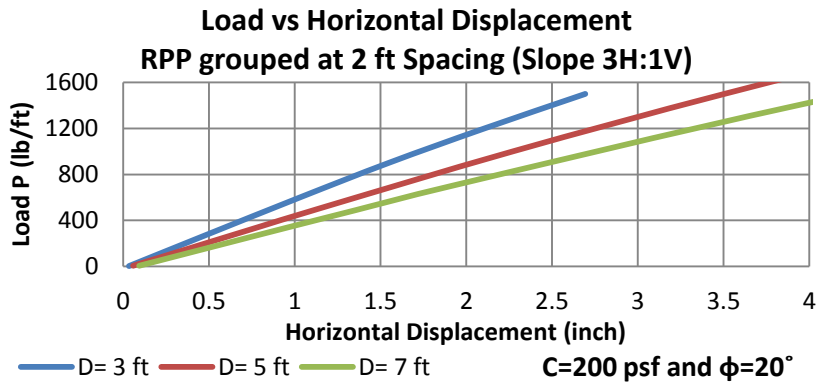


(b)

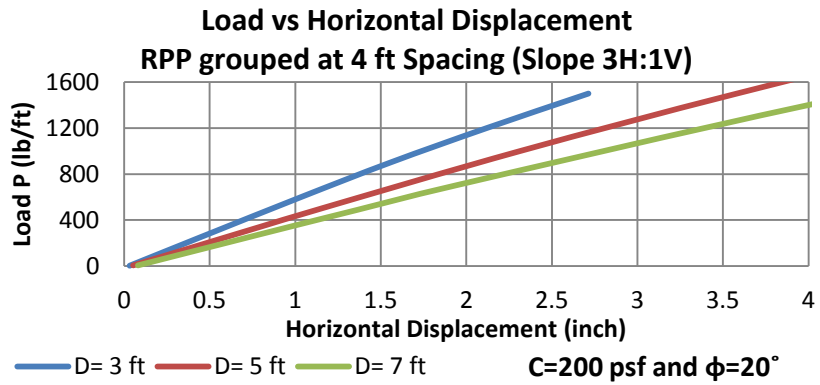


(c)

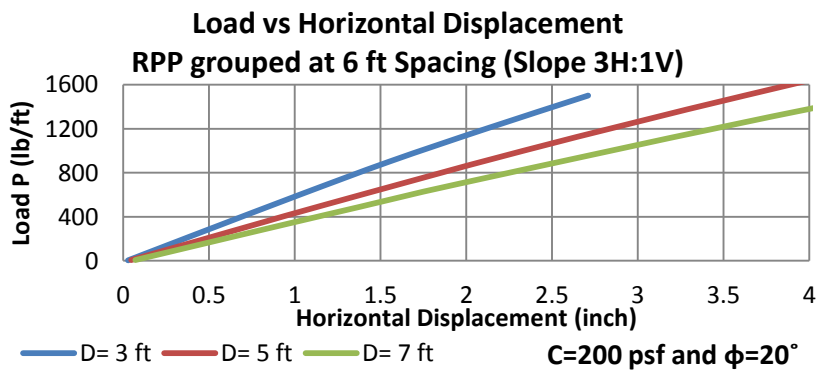
Figure B 30: Design Chart for Load versus Flexural Stress of RPP grouped at, a. 2-ft, b. 4-ft, c. 6-ft spacing for a soil of $c=200$ psf, $\phi=10^\circ$ and slope 3H:1V.



(a)

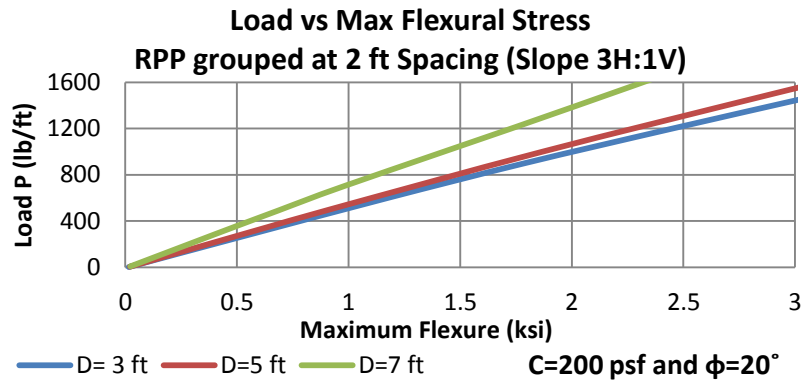


(b)

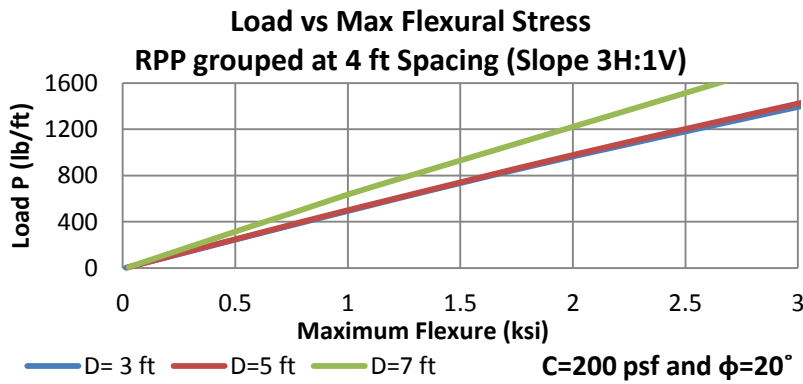


(c)

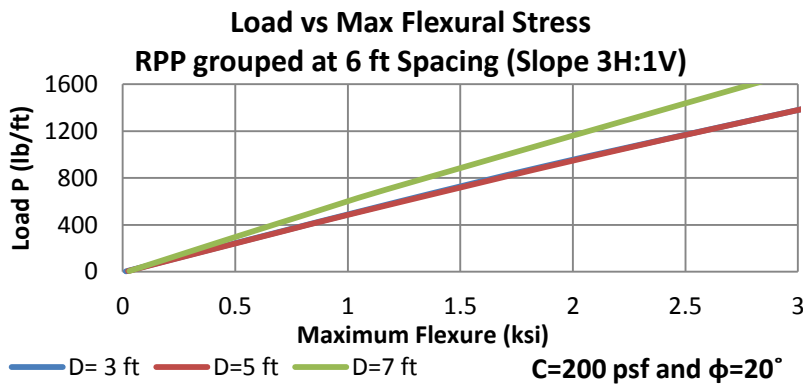
Figure B 31: Design Chart for Load versus Horizontal Displacement of RPP grouped at, a. 2-ft, b.4-ft, c. 6-ft spacing for a soil of $c=200$ psf, $\phi=20^\circ$ and slope 3H:1V.



(a)

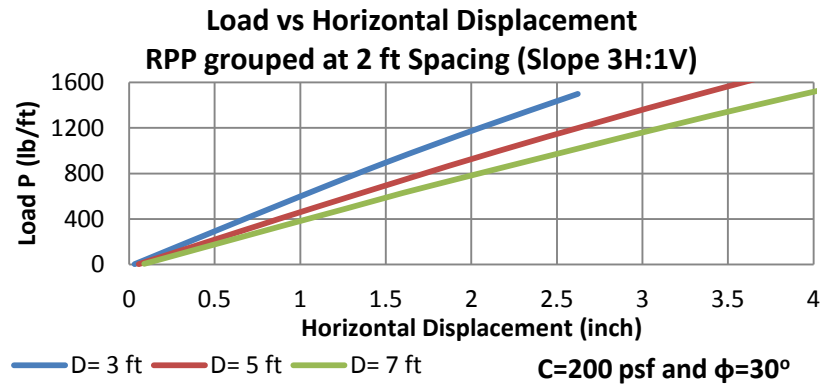


(b)

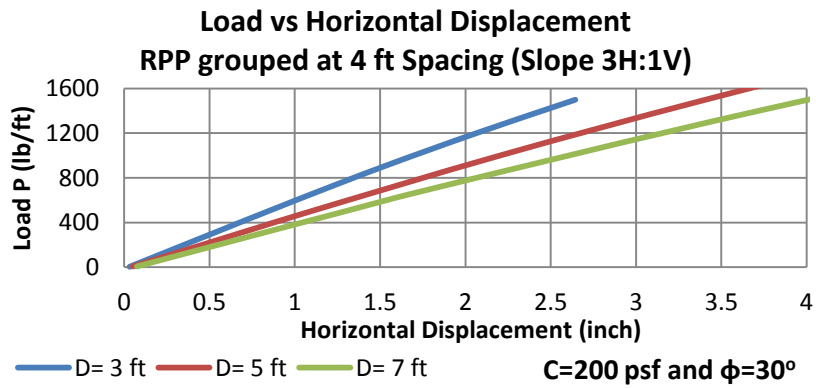


(c)

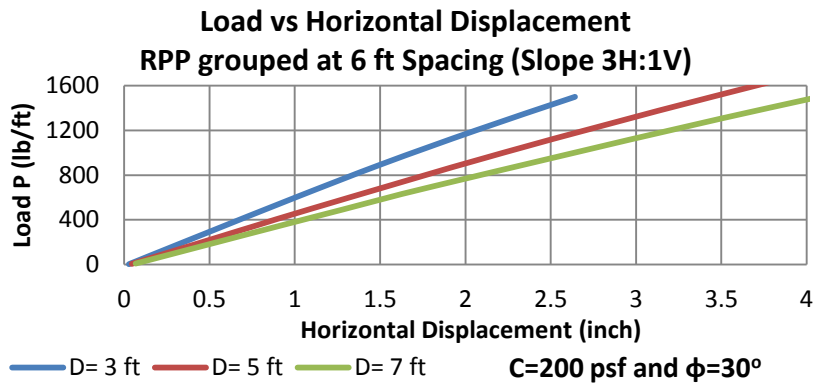
Figure B 32: Design Chart for Load versus Flexural Stress of RPP grouped at, a. 2-ft, b. 4-ft, c. 6-ft spacing for a soil of $c=200$ psf, $\phi=20^\circ$ and slope 3H:1V.



(a)

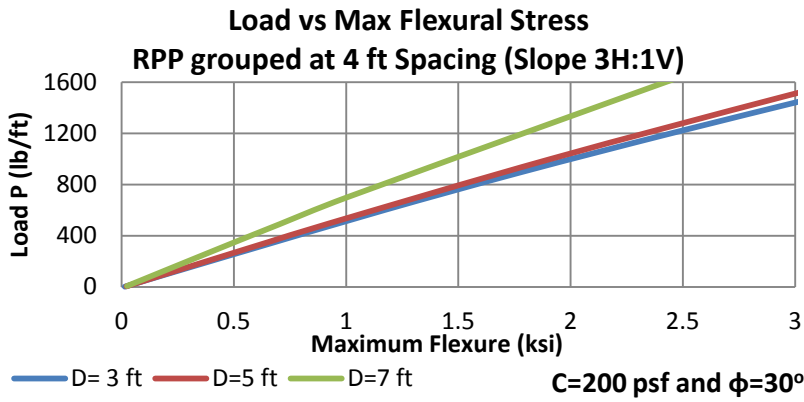
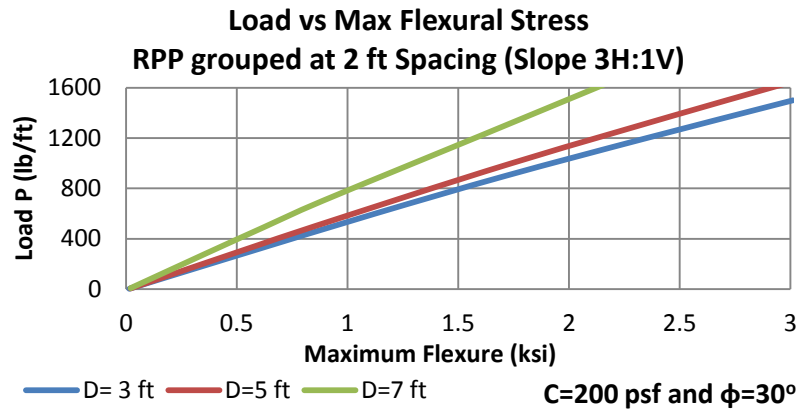


(b)

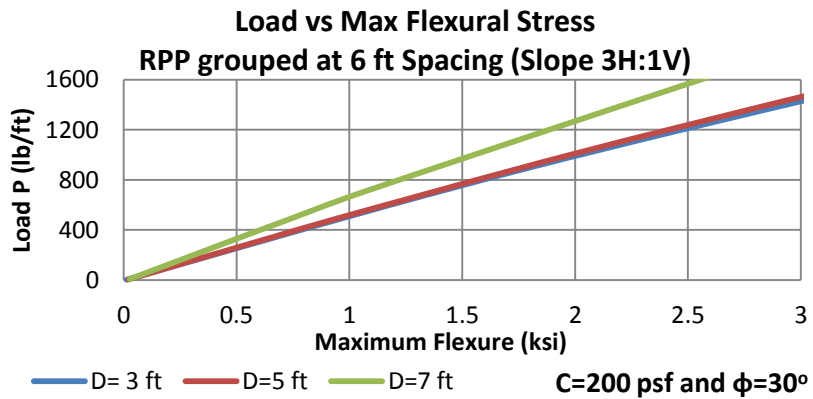


(c)

Figure B 33: Design Chart for Load versus Horizontal Displacement of RPP grouped at, a. 2-ft, b. 4-ft, c. 6-ft spacing for a soil of $c=200$ psf, $\phi=30^\circ$ and slope 3H:1V.

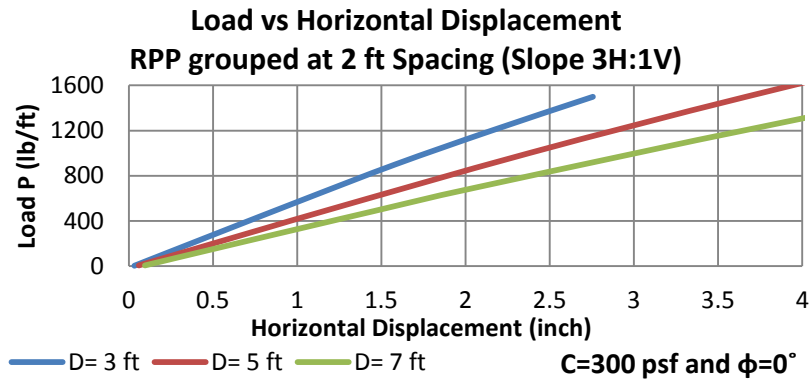


(b)

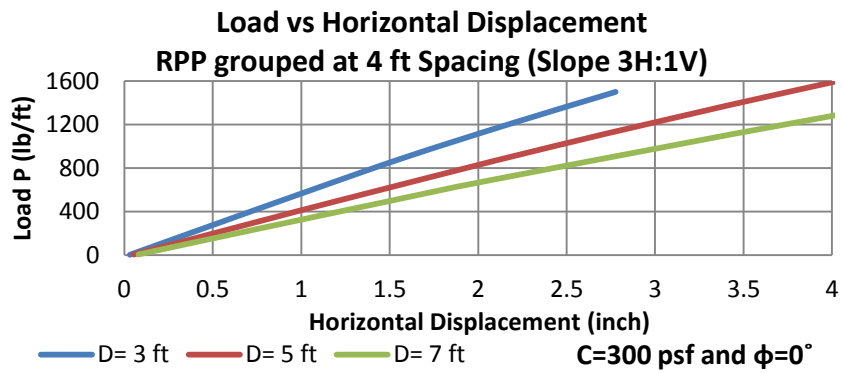


(c)

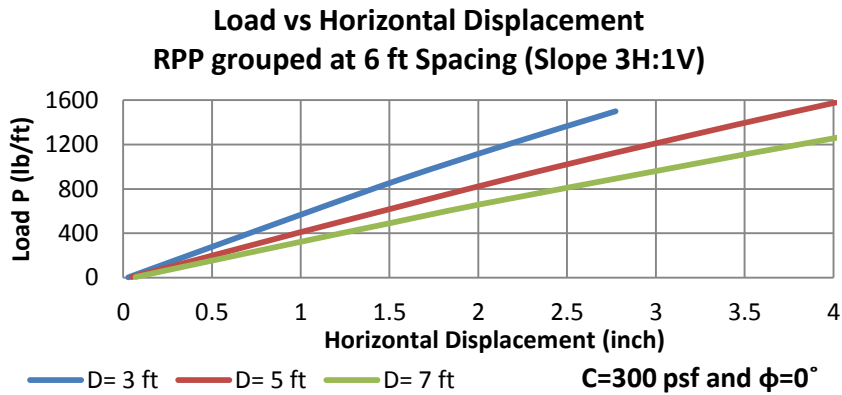
Figure B 34: Design Chart for Load versus Flexural Stress of RPP grouped at, a. 2-ft, b. 4-ft, c. 6-ft spacing for a soil of $c=200$ psf, $\phi=30^\circ$ and slope 3H:1V.



(a)

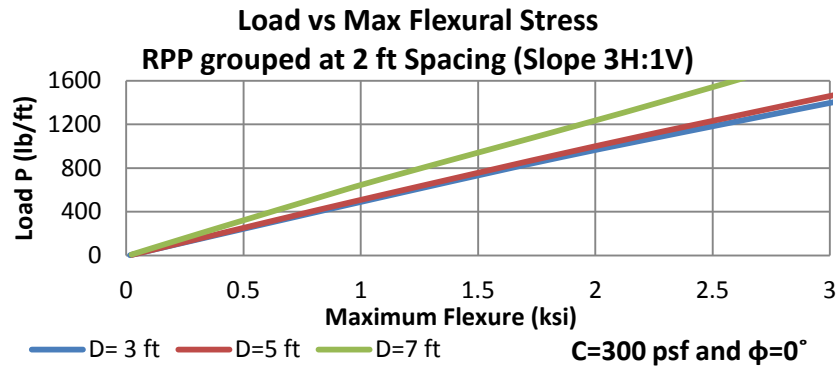


(b)

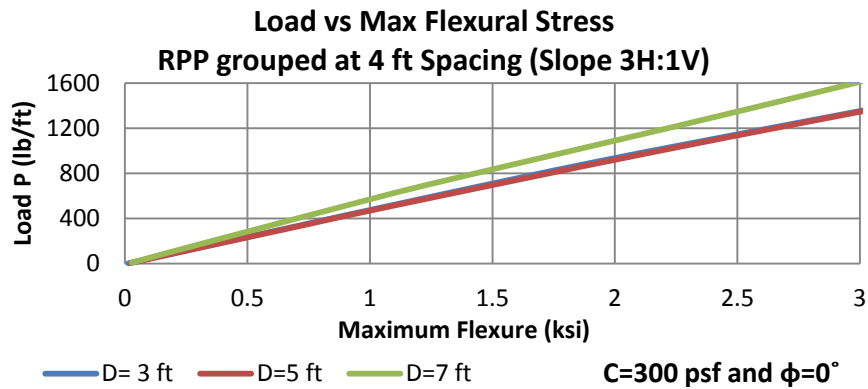


(c)

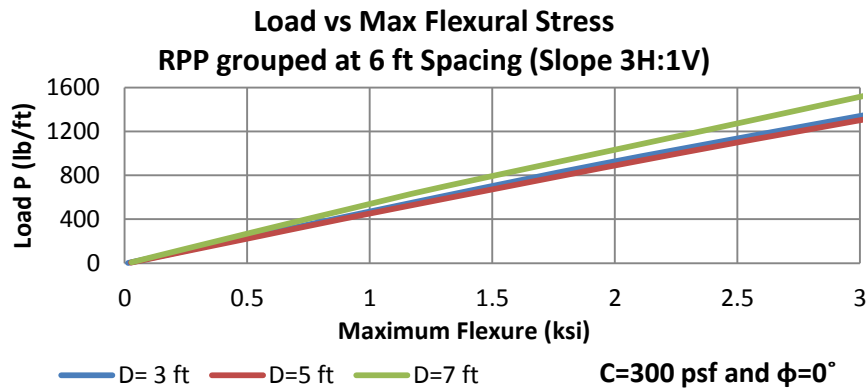
B 35: Design Chart for Load versus Horizontal Displacement of RPP grouped at, a. 2-ft, b. 4-ft, c. 6-ft spacing for a soil of $c=300$ psf, $\phi=0^\circ$ and slope 3H:1V.



(a)

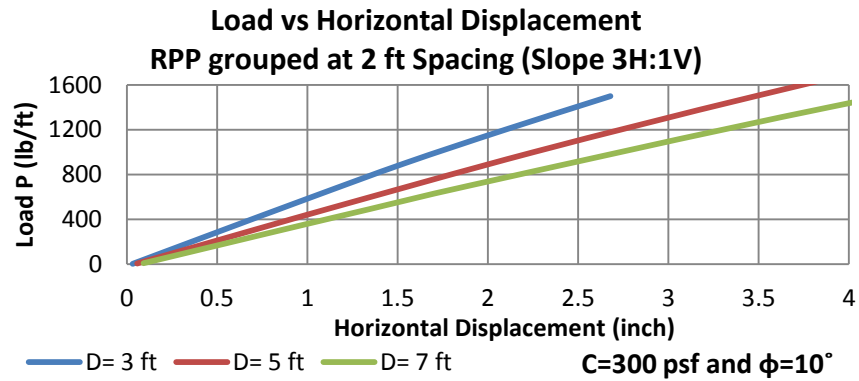


(b)

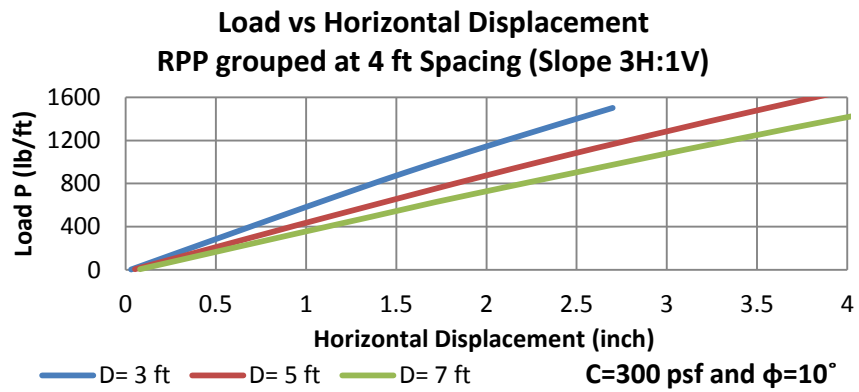


(c)

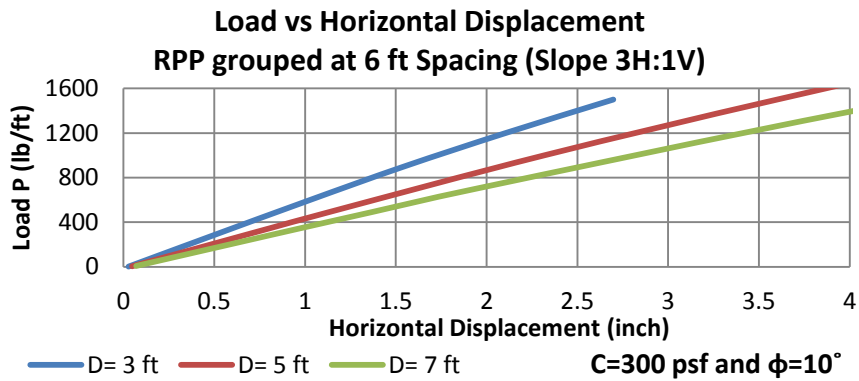
Figure B 36: Design Chart for Load versus Flexural Stress of RPP grouped at, a. 2-ft, b. 4-ft, c. 6-ft spacing for a soil of $c=300$ psf, $\phi=0^\circ$ and slope 3H:1V.



(a)

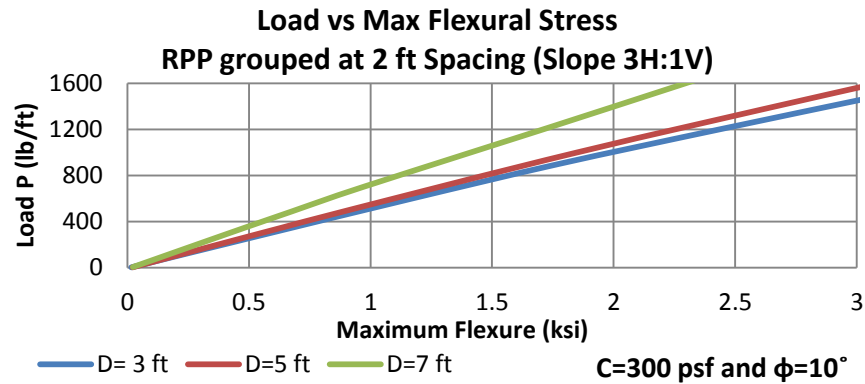


(b)

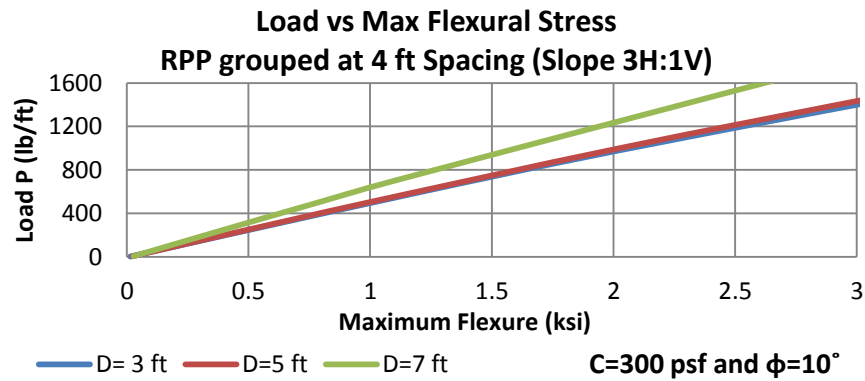


(c)

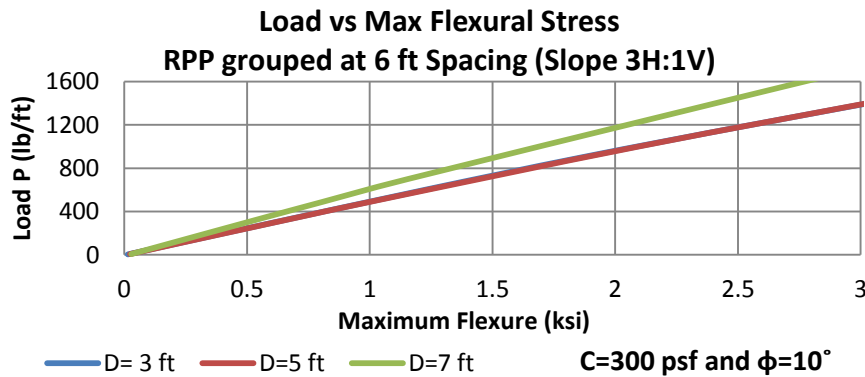
B 37: Design Chart for Load versus Horizontal Displacement of RPP grouped at, a. 2-ft, b. 4-ft, c. 6-ft spacing for a soil of $c=300$ psf, $\phi=10^\circ$ and slope 3H:1V.



(a)

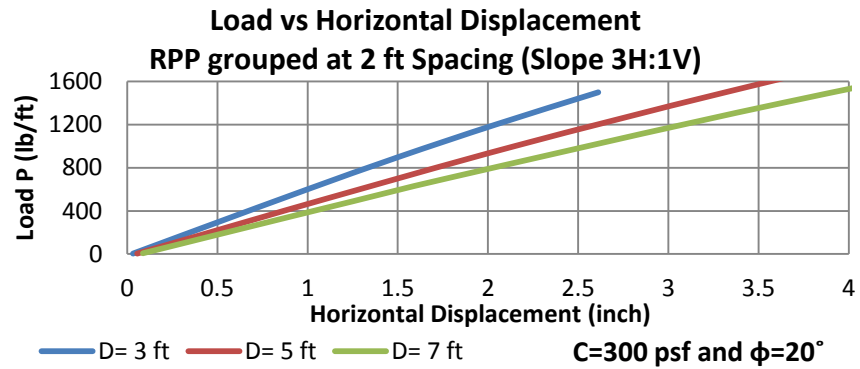


(b)

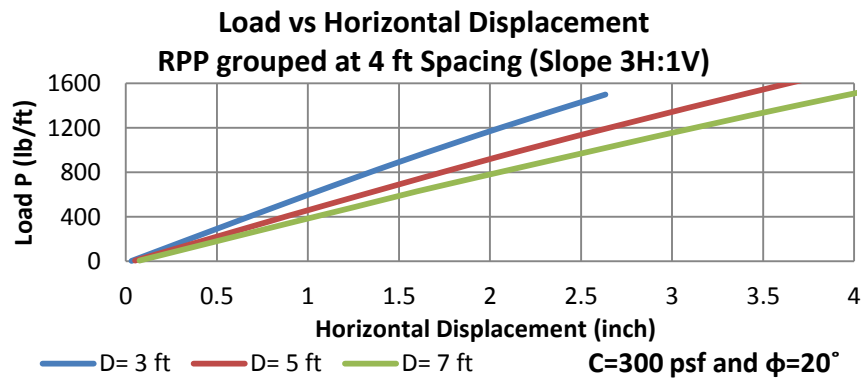


(c)

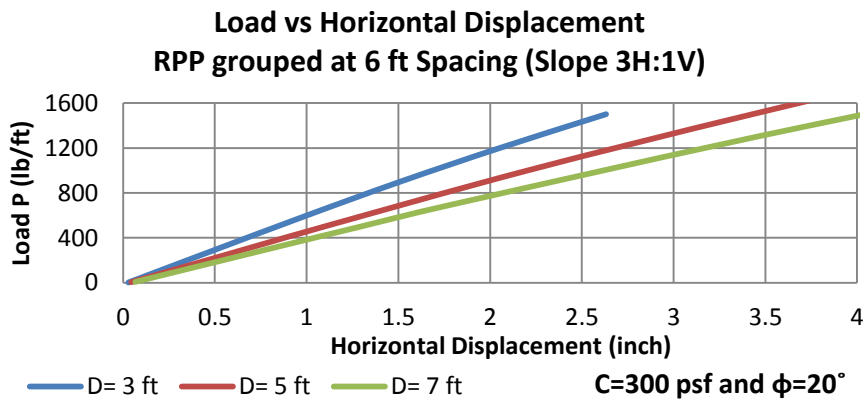
Figure B 38: Design Chart for Load versus Flexural Stress of RPP grouped at, a. 2-ft, b. 4-ft, c. 6-ft spacing for a soil of $c=300$ psf, $\phi=10^\circ$ and slope 3H:1V.



(a)

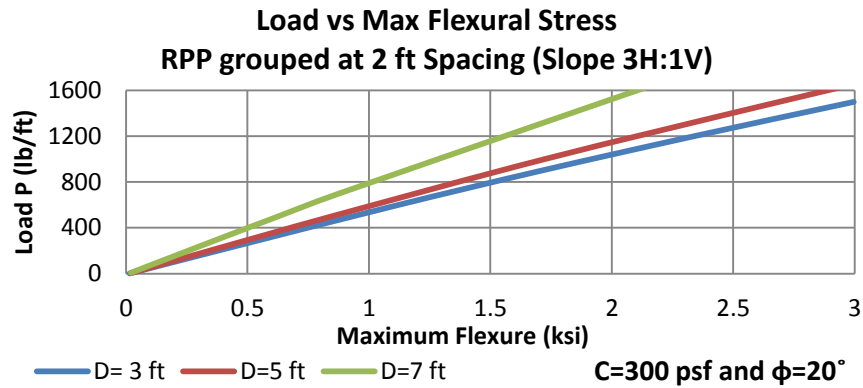


(b)

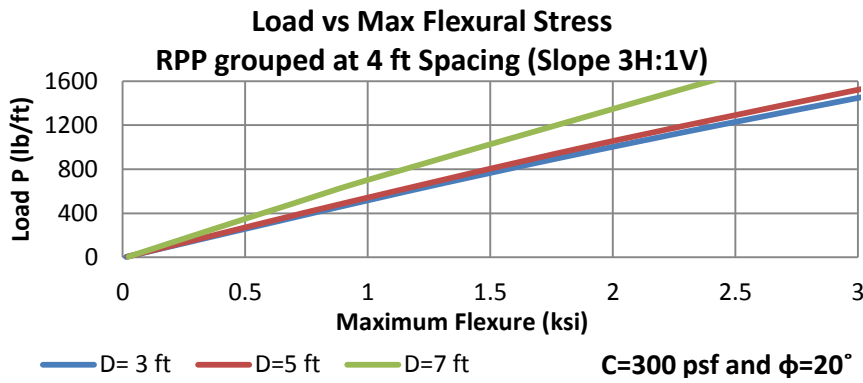


(c)

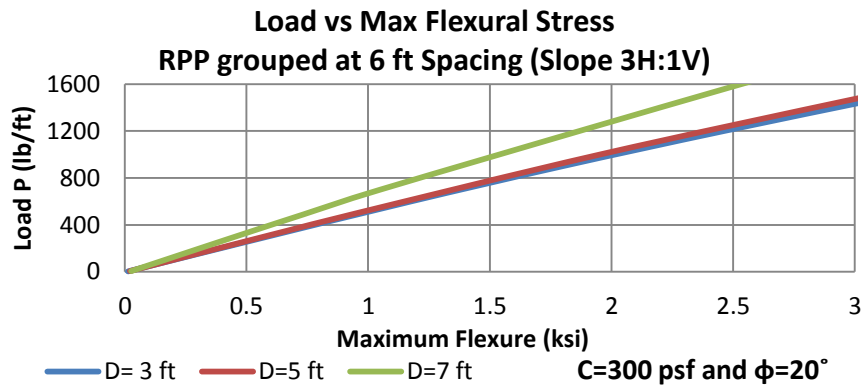
B 39: Design Chart for Load versus Horizontal Displacement of RPP grouped at, a. 2-ft, b. 4-ft, c. 6-ft spacing for a soil of $c=300$ psf, $\phi=20^\circ$ and slope 3H:1V.



(a)

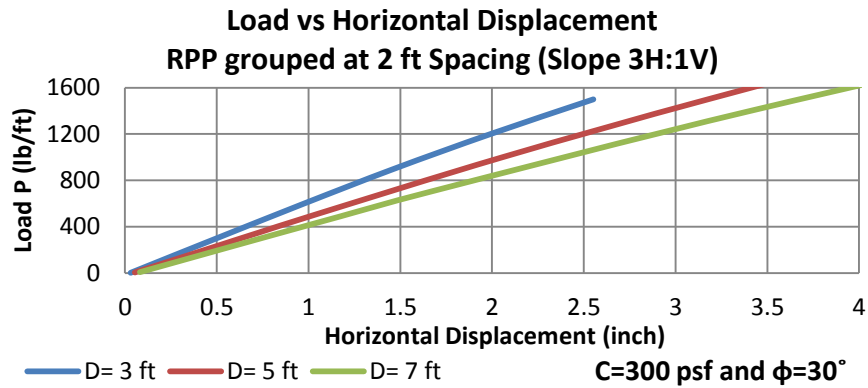


(b)

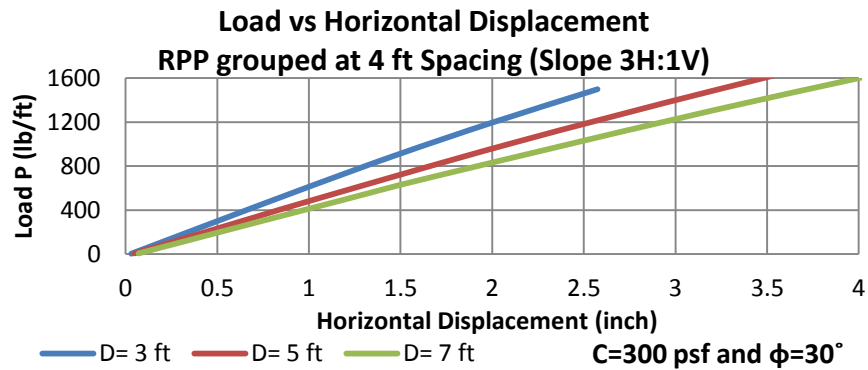


(c)

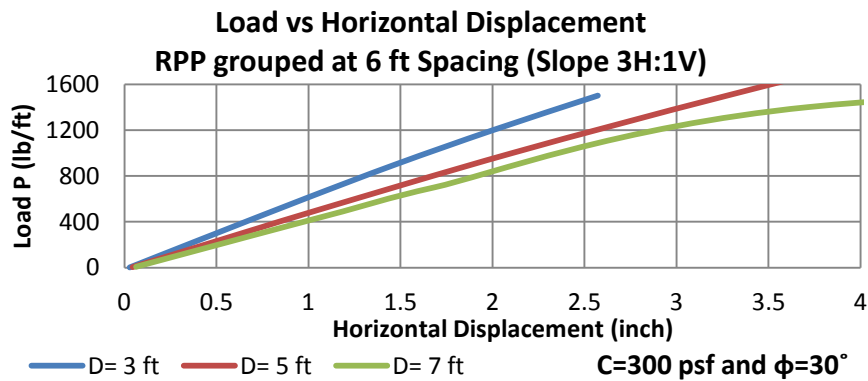
Figure B 40: Design Chart for Load versus Flexural Stress of RPP grouped at, a. 2-ft, b. 4-ft, c. 6-ft spacing for a soil of $c=300$ psf, $\phi=0^\circ$ and slope 3H:1V.



(a)

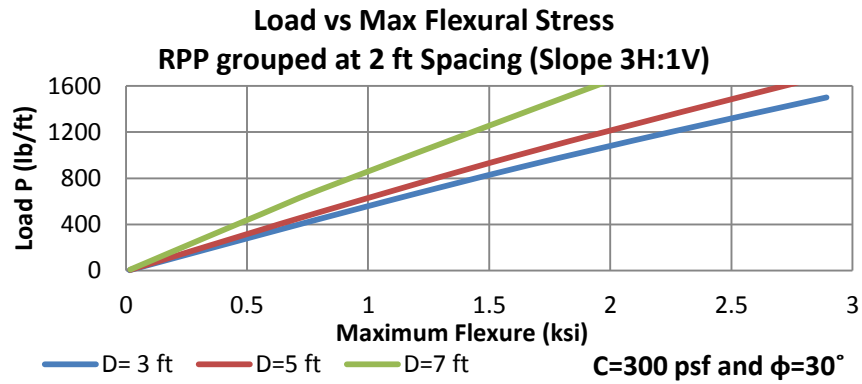


(b)

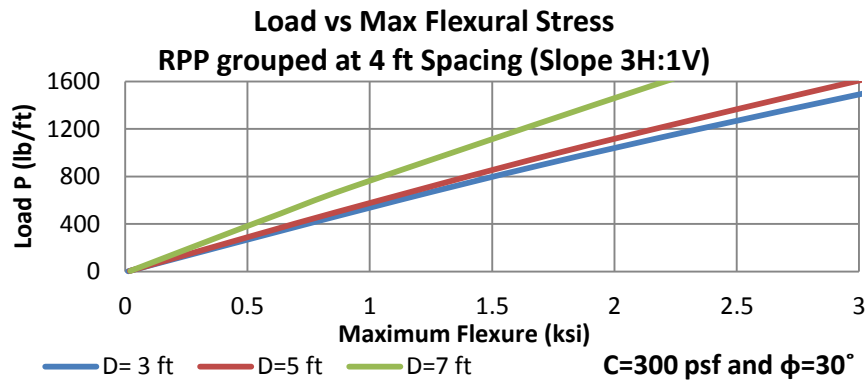


(c)

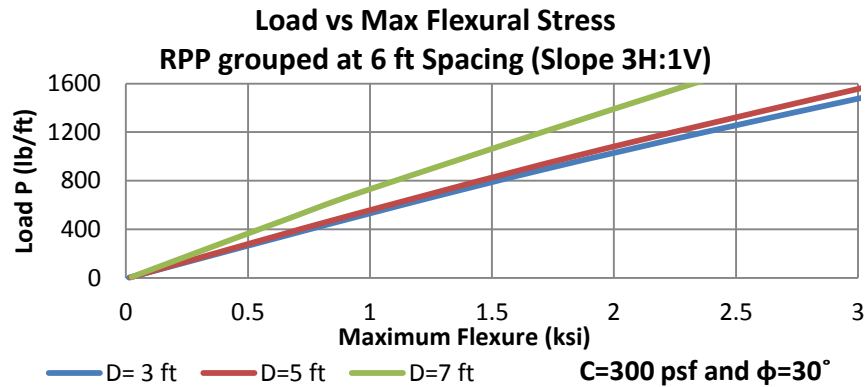
B 41: Design Chart for Load versus Horizontal Displacement of RPP grouped at, a. 2-ft, b. 4-ft, c. 6-ft spacing for a soil of $c=300$ psf, $\phi=30^\circ$ and slope 3H:1V.



(a)

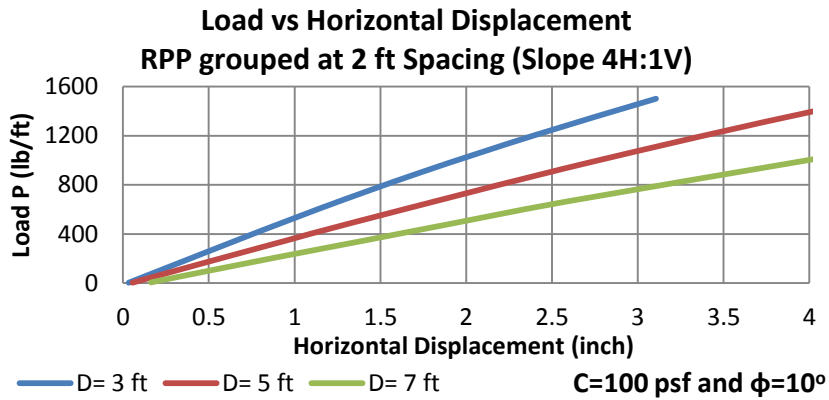


(b)

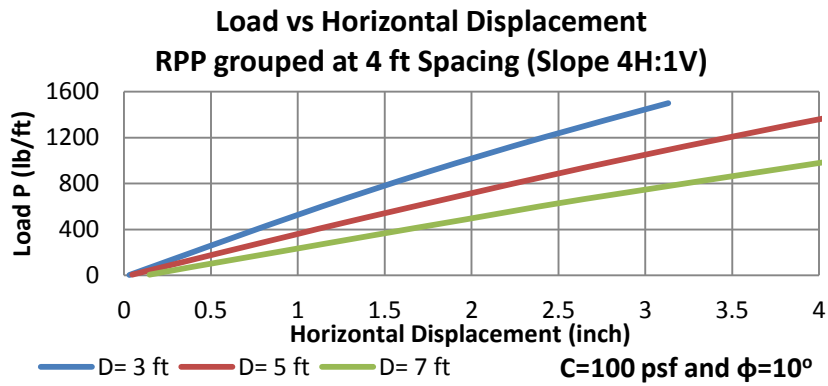


(c)

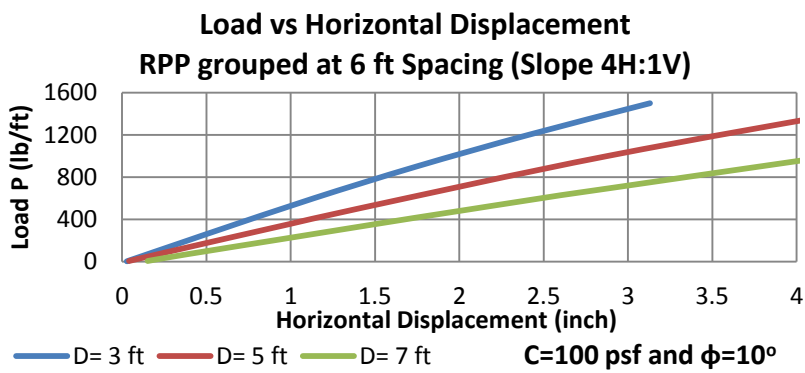
Figure B 42: Design Chart for Load versus Flexural Stress of RPP grouped at, a. 2-ft, b. 4-ft, c. 6-ft spacing for a soil of $c=300$ psf, $\phi=30^\circ$ and slope 3H:1V.



(a)

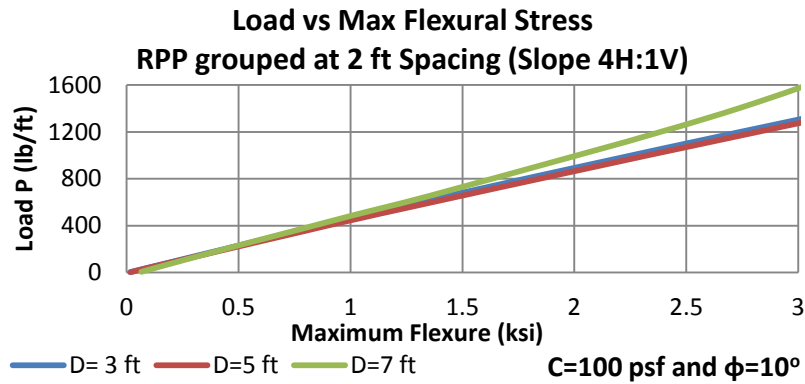


(b)

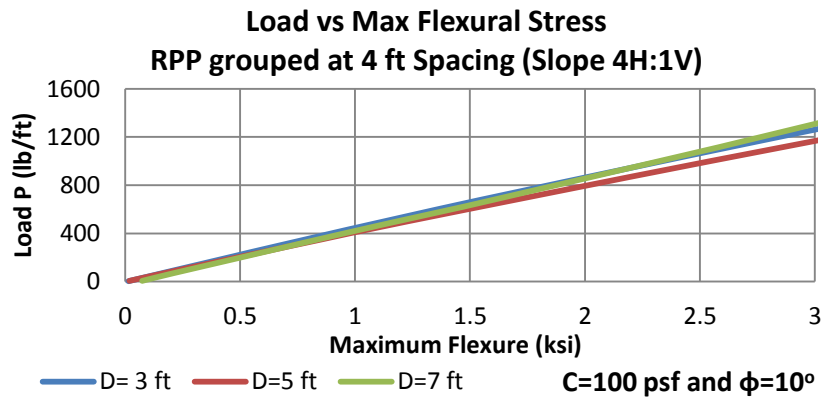


(c)

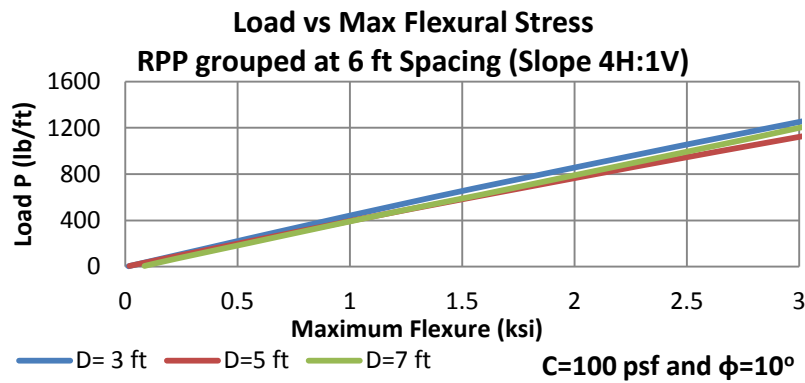
Figure B 43: Design Chart for Load versus Horizontal Displacement of RPP grouped at, a. 2-ft, b. 4-ft, c. 6-ft spacing for a soil of $c=100$ psf, $\phi=10^\circ$ and slope 4H:1V.



(a)

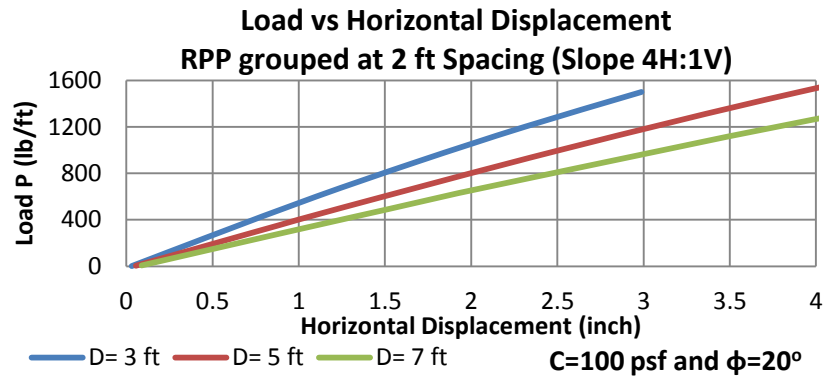


(b)

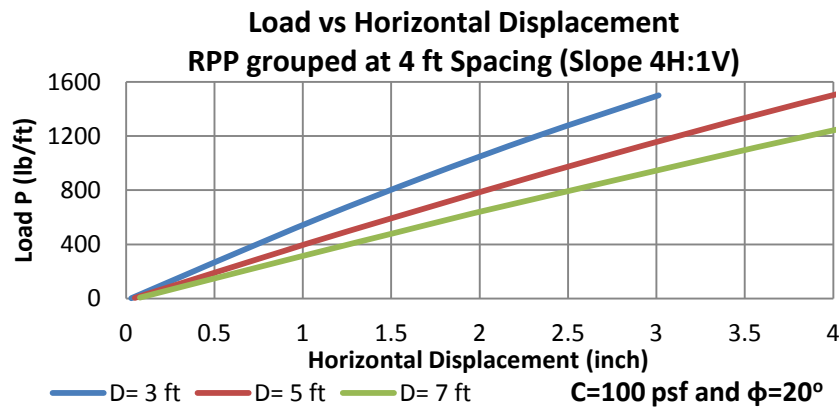


(c)

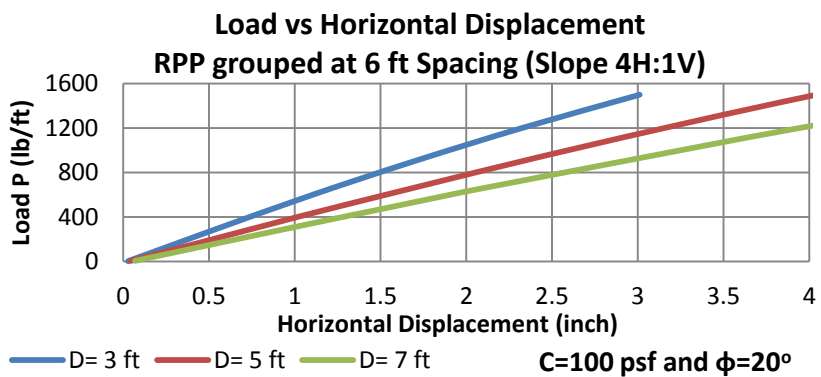
Figure B 44: Design Chart for Load versus Flexural Stress of RPP grouped at, a. 2-ft, b. 4-ft, c. 6-ft spacing for a soil of $c=100$ psf, $\phi=10^\circ$ and slope 4H:1V.



(a)

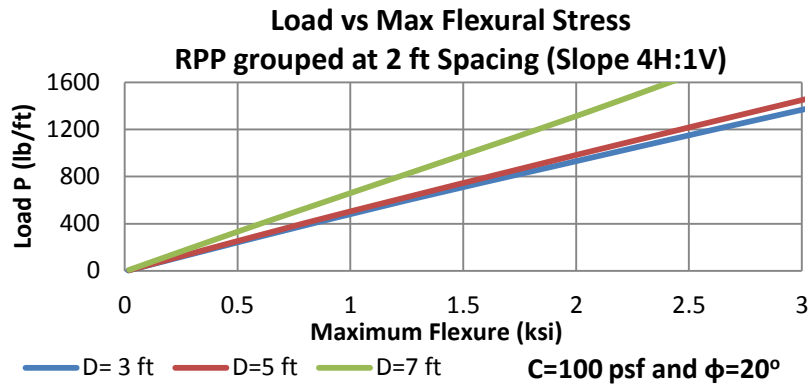


(b)

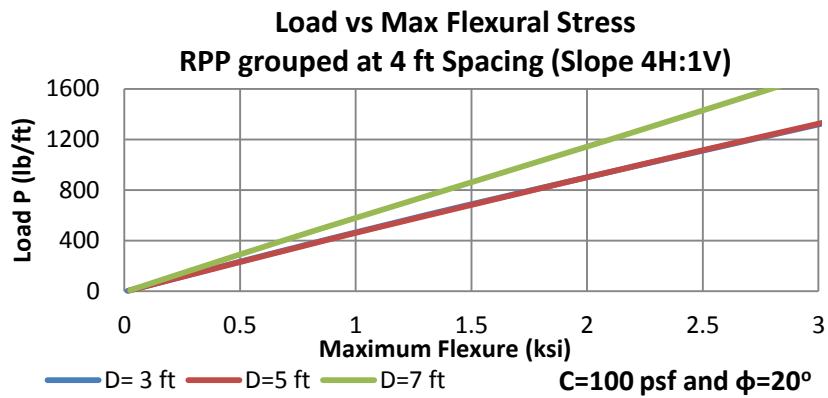


(c)

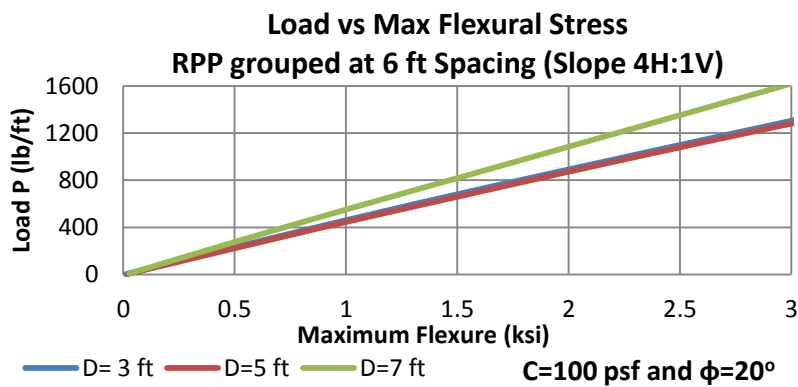
Figure B 45: Design Chart for Load versus Horizontal Displacement of RPP grouped at, a. 2-ft, b. 4-ft, c. 6-ft spacing for a soil of $c=100$ psf, $\phi=20^\circ$ and slope 4H:1V.



(a)

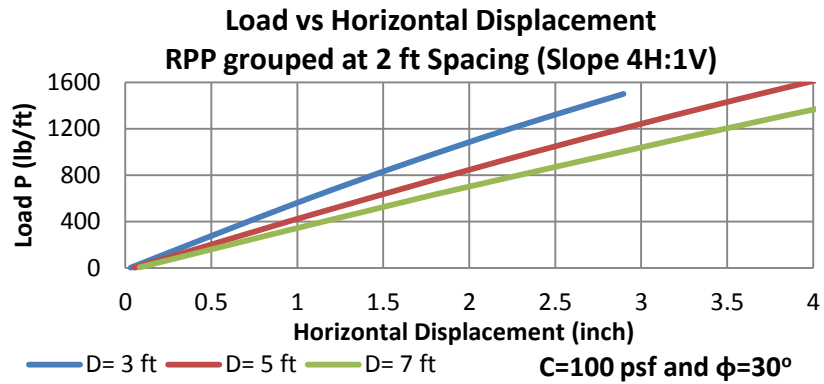


(b)

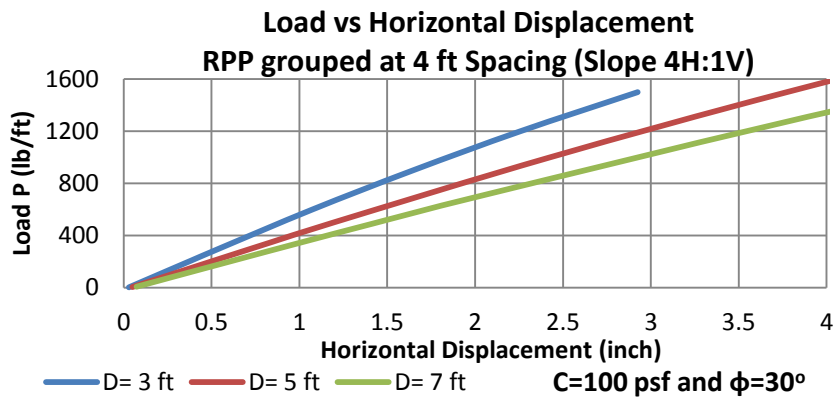


(c)

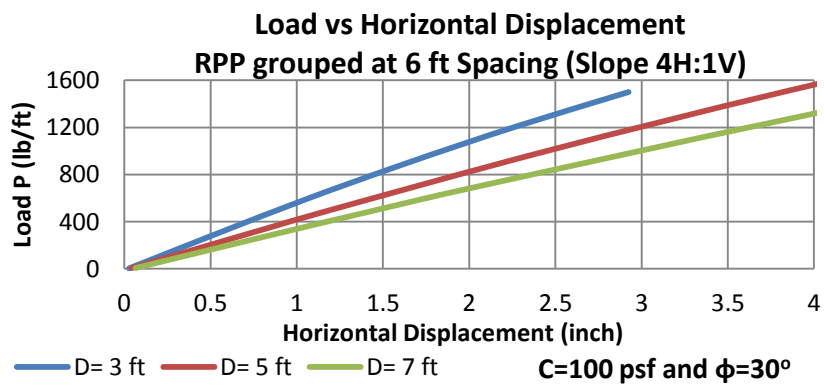
Figure B 46: Design Chart for Load versus Flexural Stress of RPP grouped at, a. 2-ft, b. 4-ft, c. 6-ft spacing for a soil of $c=100$ psf, $\phi=20^\circ$ and slope 4H:1V.



(a)

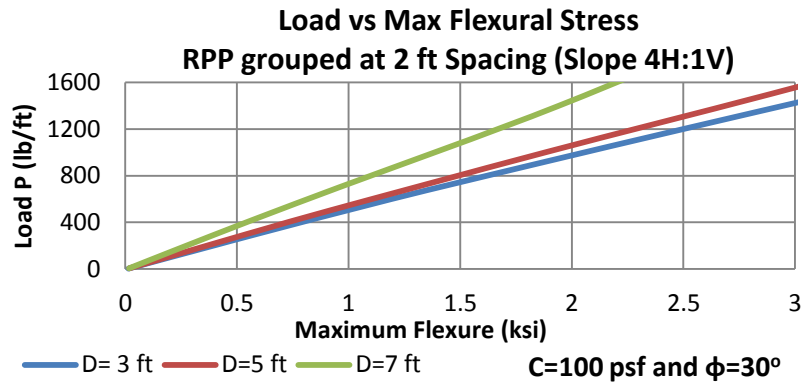


(b)

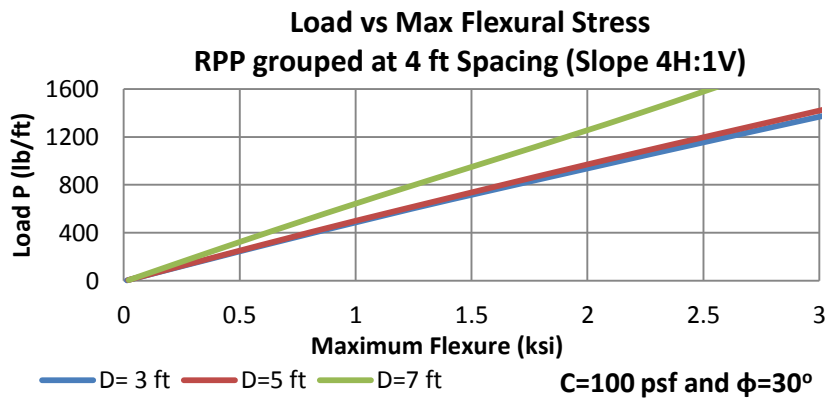


(c)

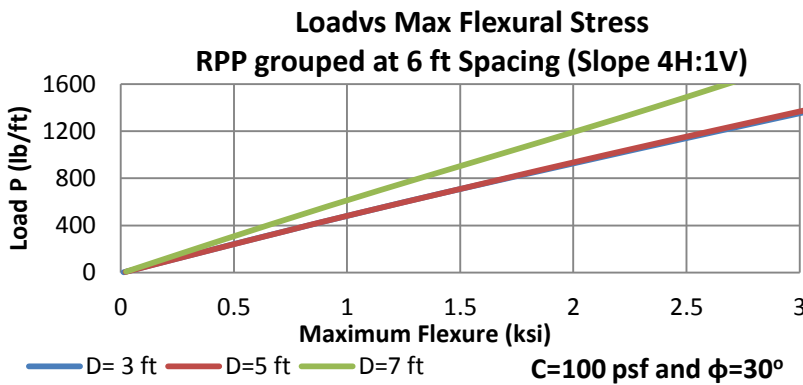
Figure B 47: Design Chart for Load versus Horizontal Displacement of RPP grouped at, a. 2-ft, b. 4-ft, c. 6-ft spacing for a soil of $c=100$ psf, $\phi=30^\circ$ and slope 4H:1V.



(a)

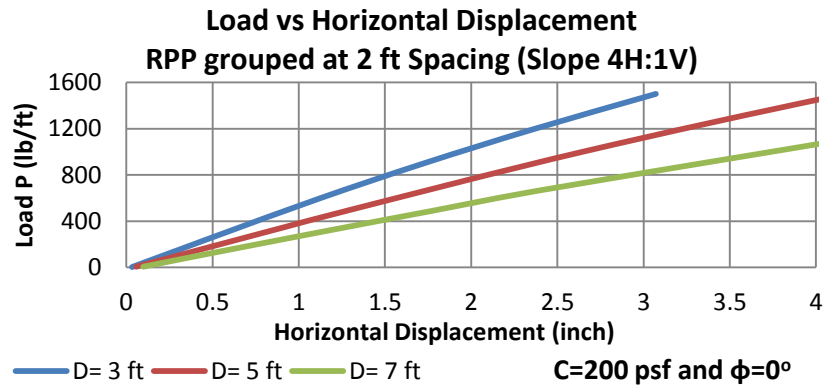


(b)

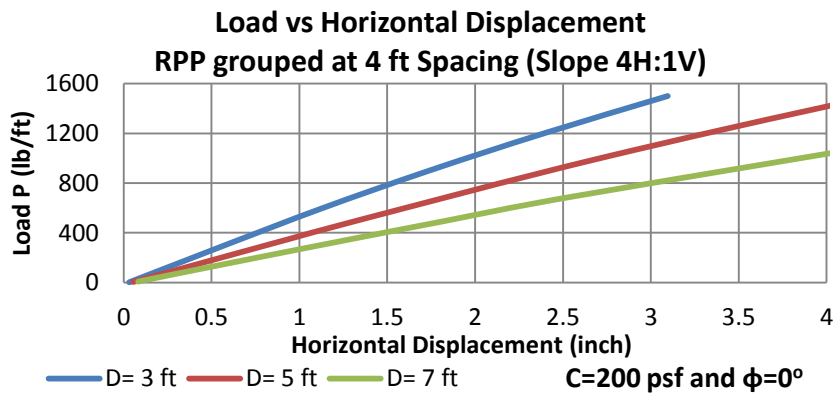


(c)

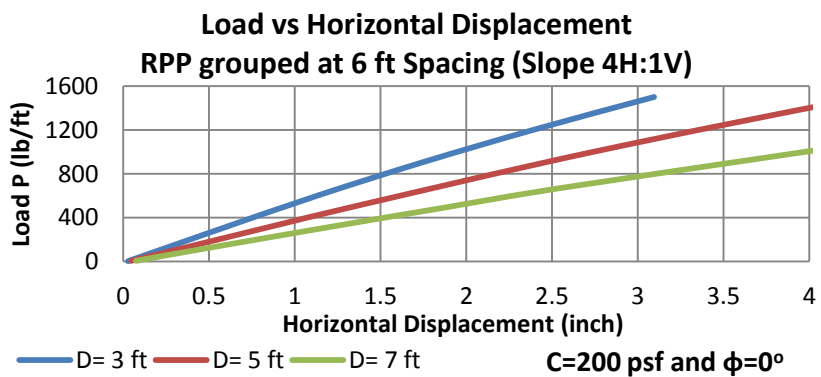
Figure B 48: Design Chart for Load versus Flexural Stress of RPP grouped at, a. 2-ft, b. 4-ft, c. 6-ft spacing for a soil of $c=100$ psf, $\phi=30^\circ$ and slope 4H:1V.



(a)

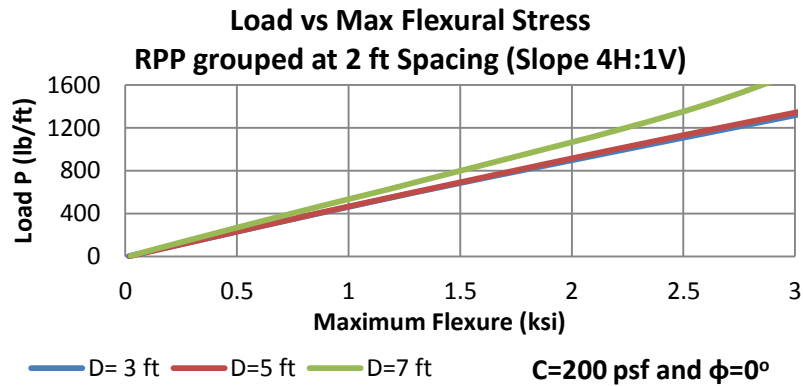


(b)

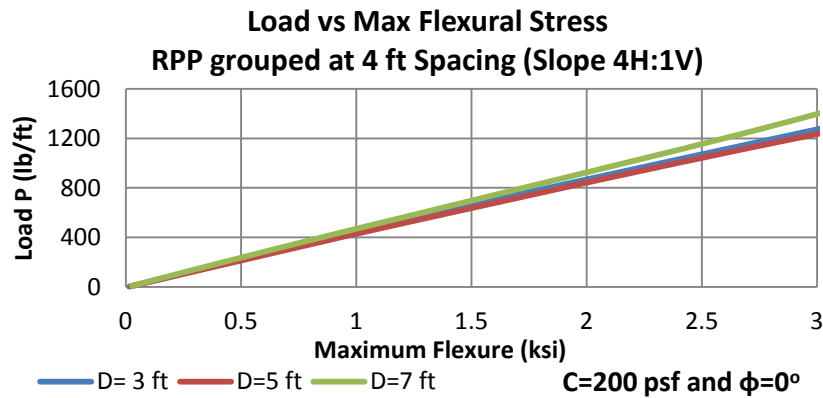


(c)

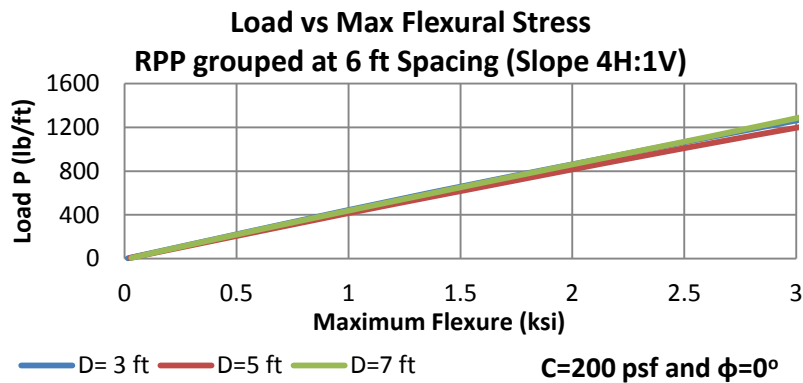
Figure B 49: Design Chart for Load versus Horizontal Displacement of RPP grouped at, a. 2-ft, b. 4-ft, c. 6-ft spacing for a soil of $c=200$ psf, $\phi=0^\circ$ and slope 4H:1V.



(a)

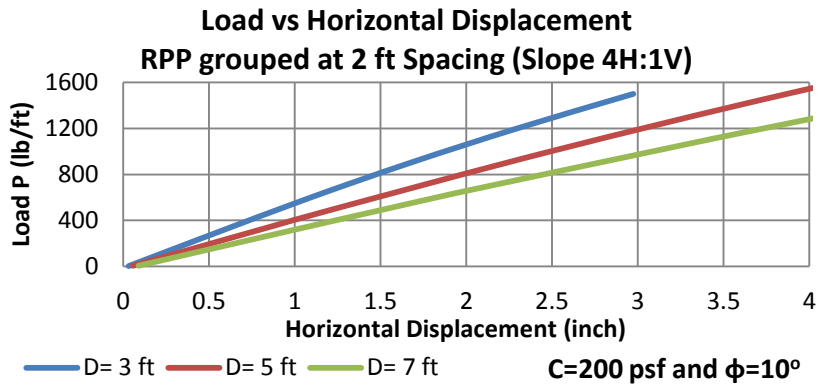


(b)

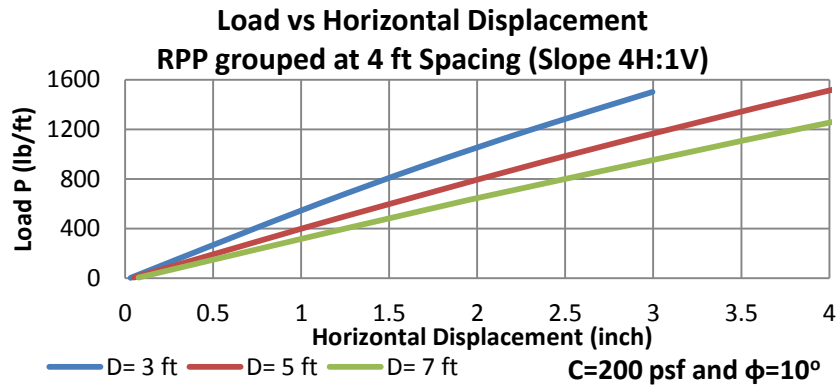


(c)

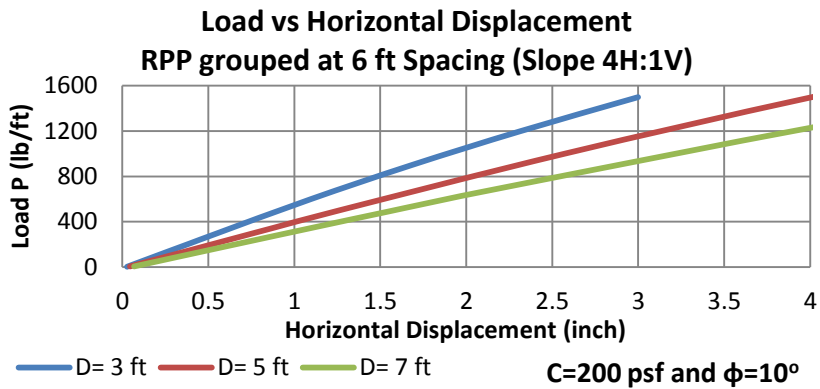
Figure B 50: Design Chart for Load versus Flexural Stress of RPP grouped at, a. 2-ft, b. 4-ft, c. 6-ft spacing for a soil of $c=200$ psf, $\phi=0^\circ$ and slope 4H:1V.



(a)

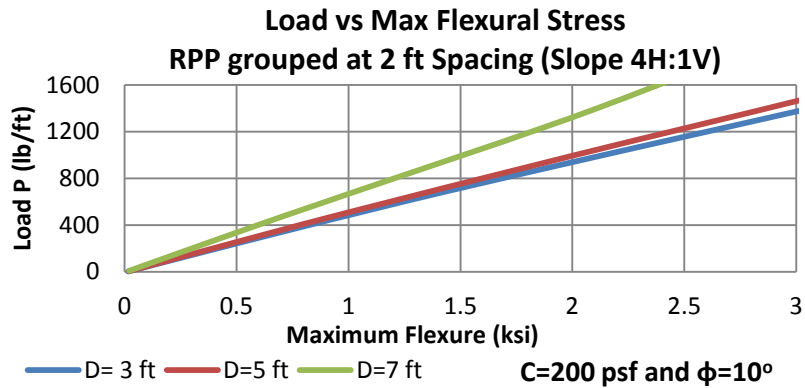


(b)

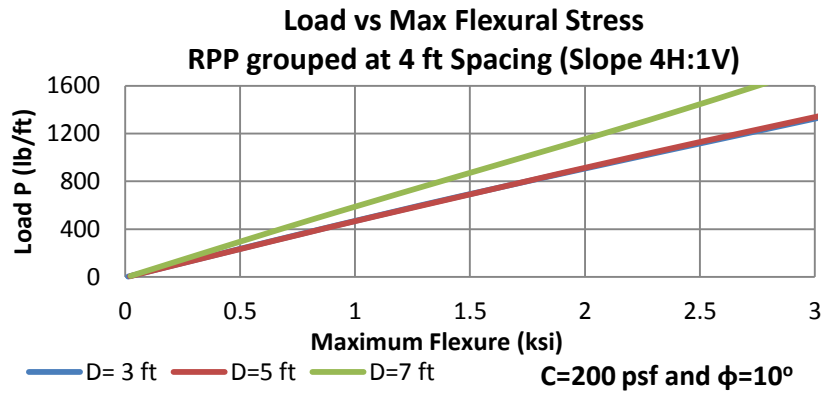


(c)

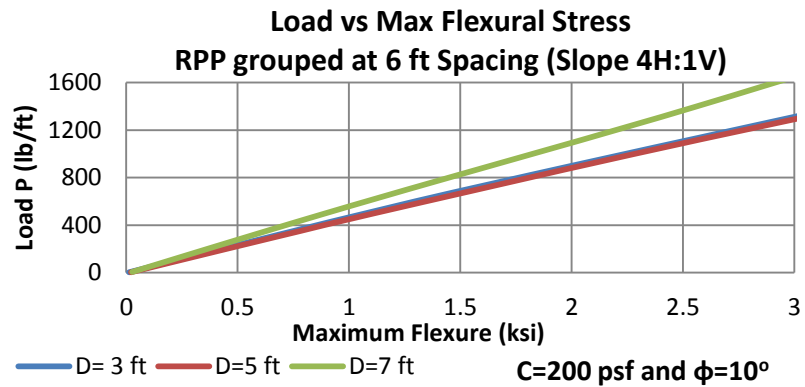
Figure B 51: Design Chart for Load versus Horizontal Displacement of RPP grouped at, a. 2-ft, b. 4-ft, c. 6-ft spacing for a soil of $c=200$ psf, $\phi=10^\circ$ and slope 4H:1V.



(a)

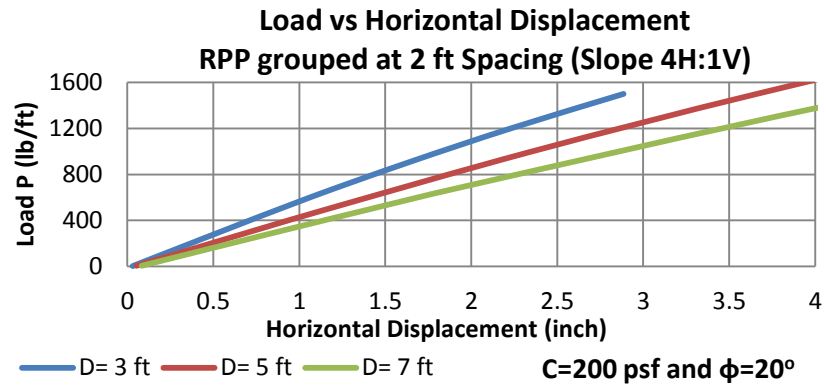


(b)

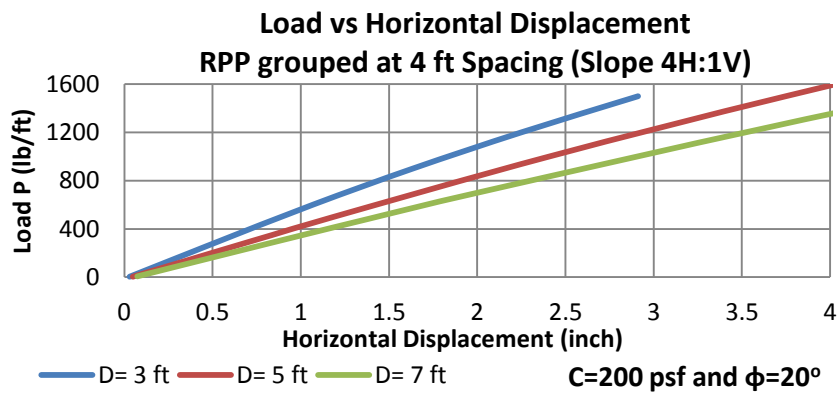


(c)

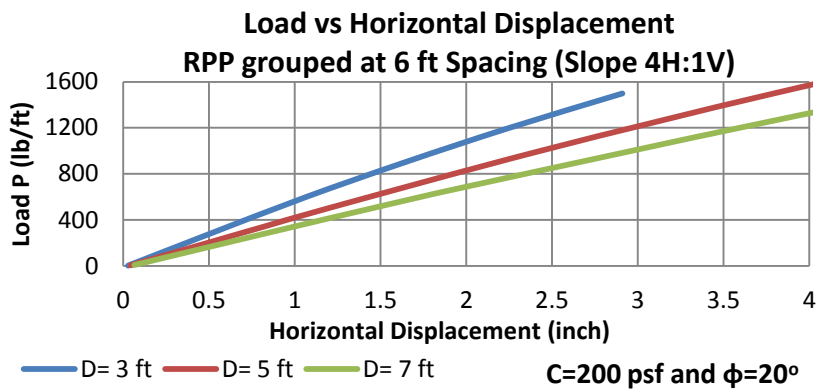
Figure B 50: Design Chart for Load versus Flexural Stress of RPP grouped at, a. 2-ft, b. 4-ft, c. 6-ft spacing for a soil of $c=200$ psf, $\phi=10^\circ$ and slope 4H:1V.



(a)

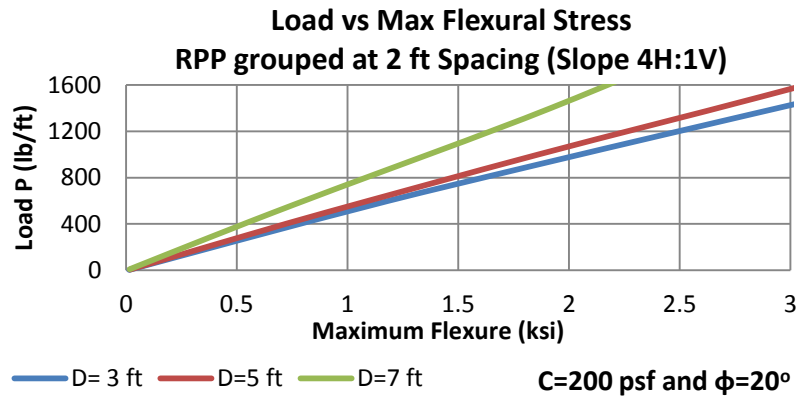


(b)

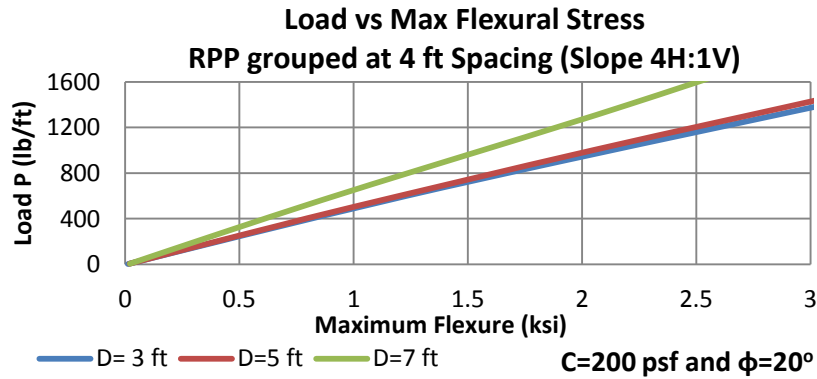


(c)

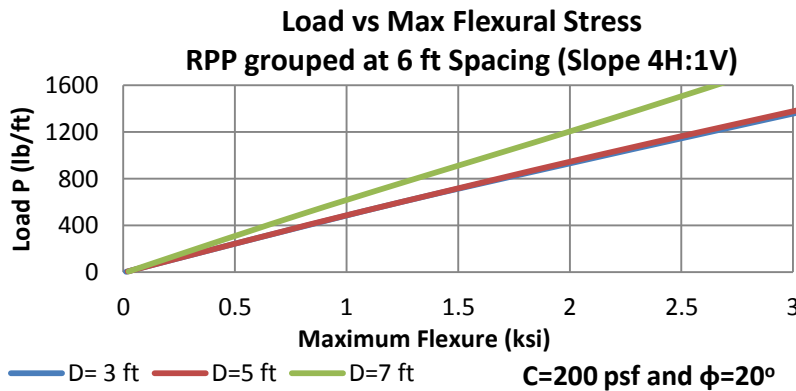
Figure B 53: Design Chart for Load versus Horizontal Displacement of RPP grouped at, a. 2-ft, b.4-ft, c. 6-ft spacing for a soil of $c=200$ psf, $\phi=20^\circ$ and slope 4H:1V.



(a)

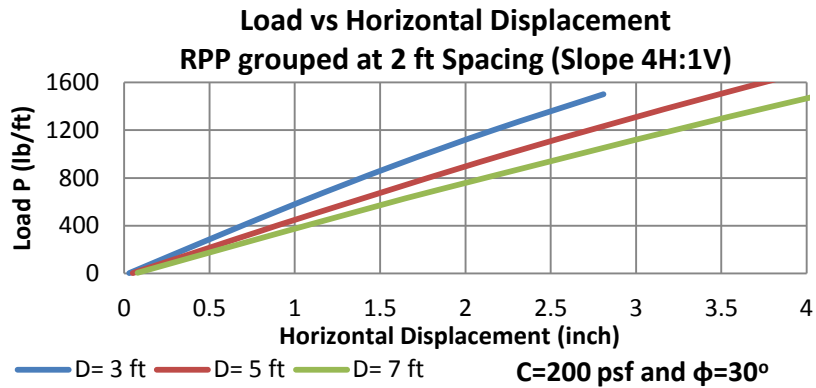


(b)

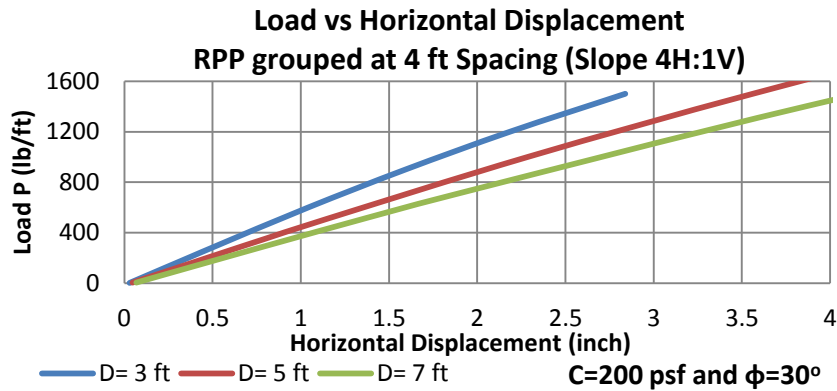


(c)

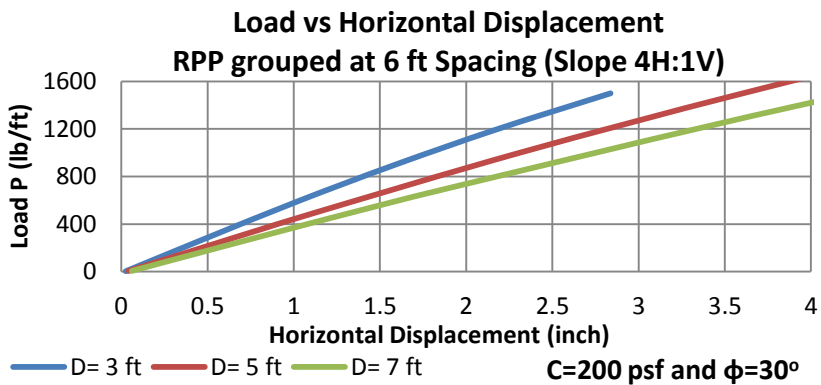
Figure B 54: Design Chart for Load versus Flexural Stress of RPP grouped at, a. 2-ft, b. 4-ft, c. 6-ft spacing for a soil of $c=200$ psf, $\phi=20^\circ$ and slope 4H:1V.



(a)

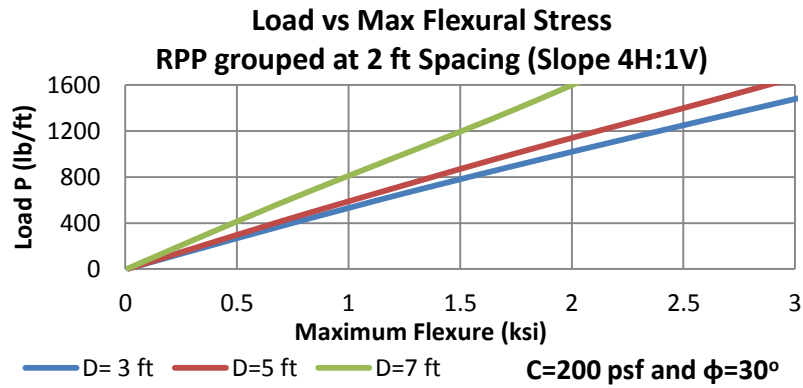


(b)

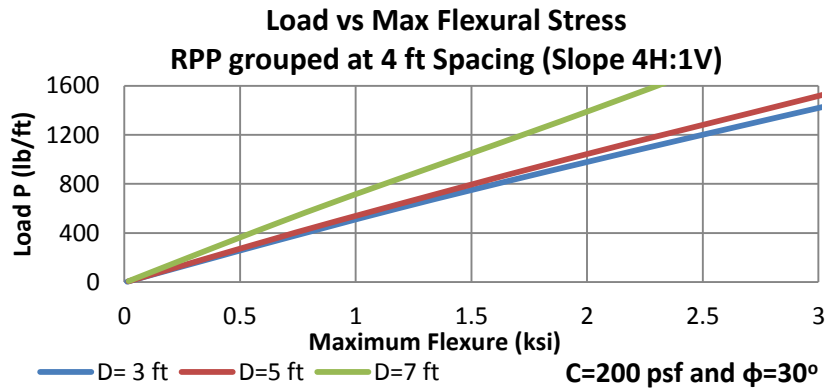


(c)

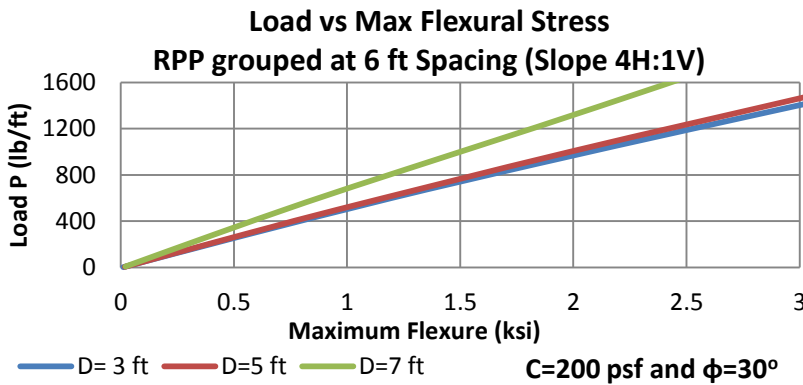
Figure B 55: Design Chart for Load Vs Horizontal Displacement of RPP grouped at, a. 2-ft, b. 4-ft, c. 6-ft spacing for a soil of $c=200$ psf, $\phi=30^\circ$ and slope 4H:1V.



(a)

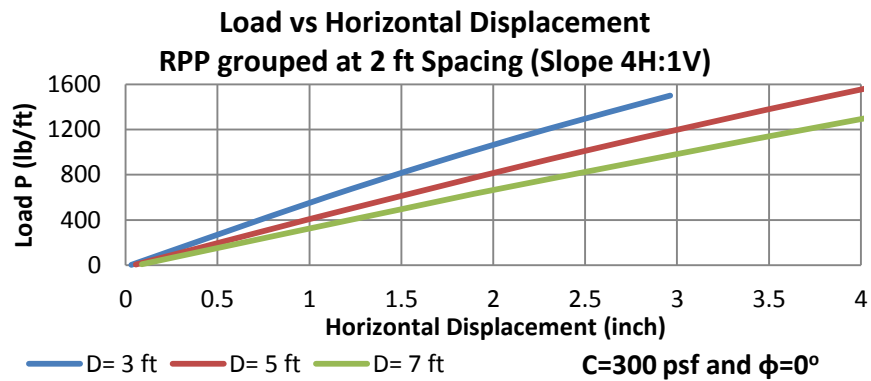


(b)

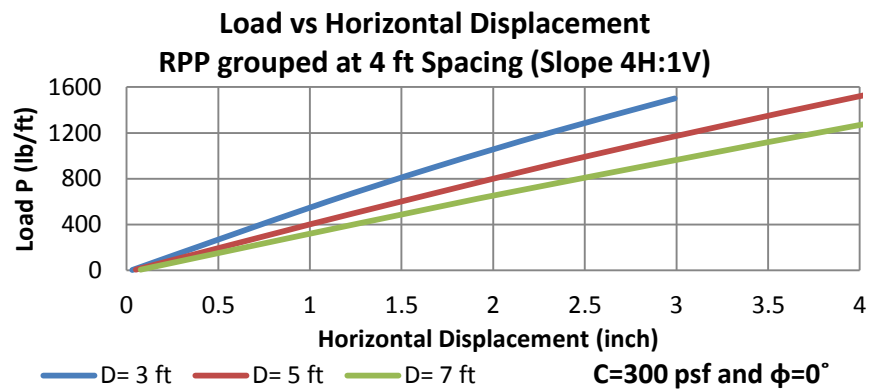


(c)

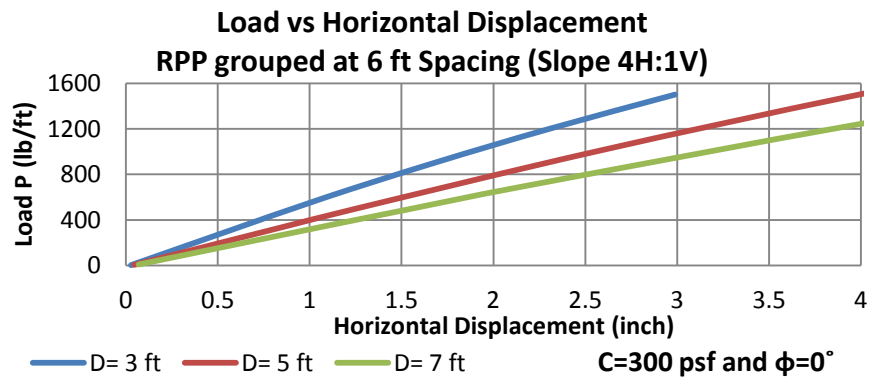
Figure B 56: Design Chart for Load versus Flexural Stress of RPP grouped at, a. 2-ft, b. 4-ft, c. 6-ft spacing for a soil of $c=200$ psf, $\phi=30^\circ$ and slope 4H:1V.



(a)

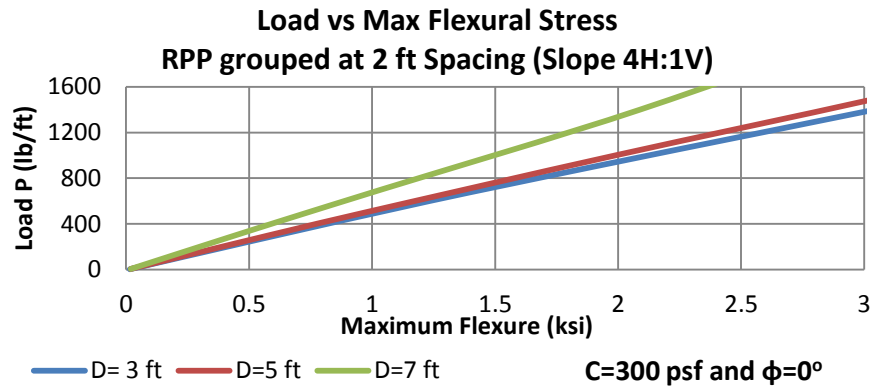


(b)

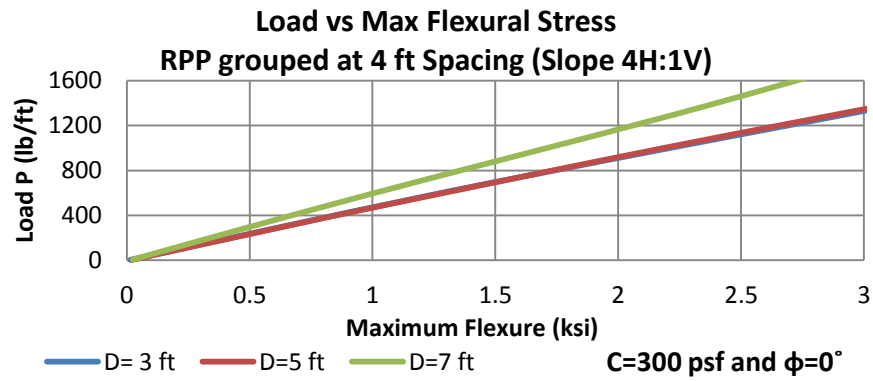


(c)

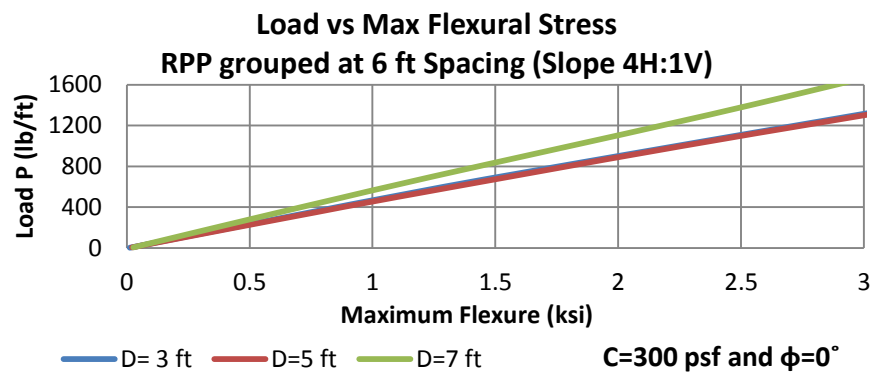
Figure B 57: Design Chart for Load versus Horizontal Displacement of RPP grouped at, a. 2-ft, b. 4-ft, c. 6-ft spacing for a soil of $c=300$ psf, $\phi=0^\circ$ and slope 4H:1V.



(a)

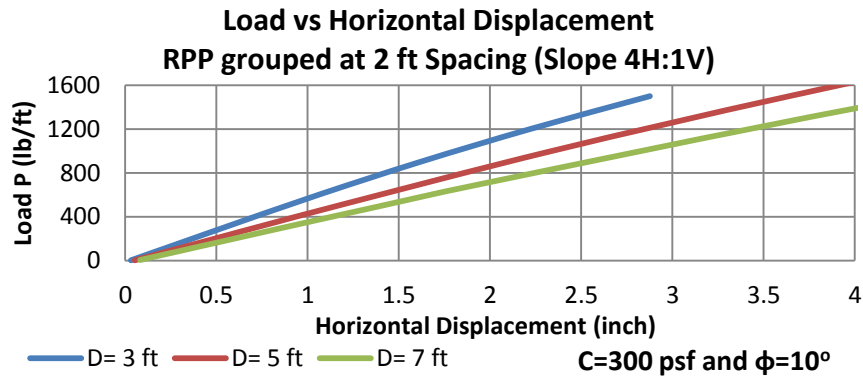


(b)

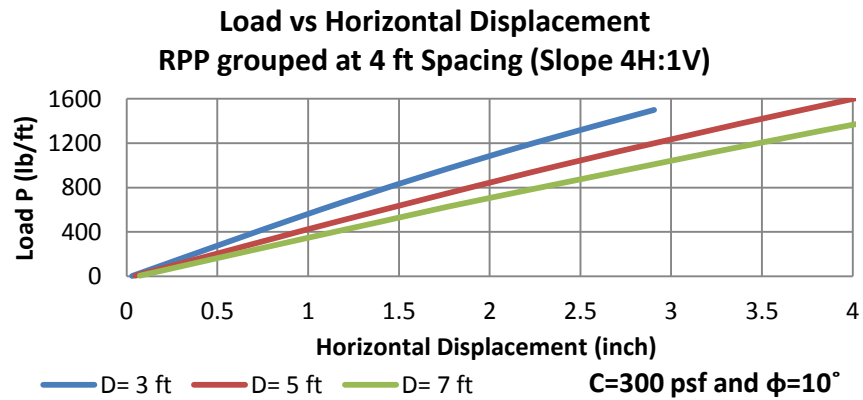


(c)

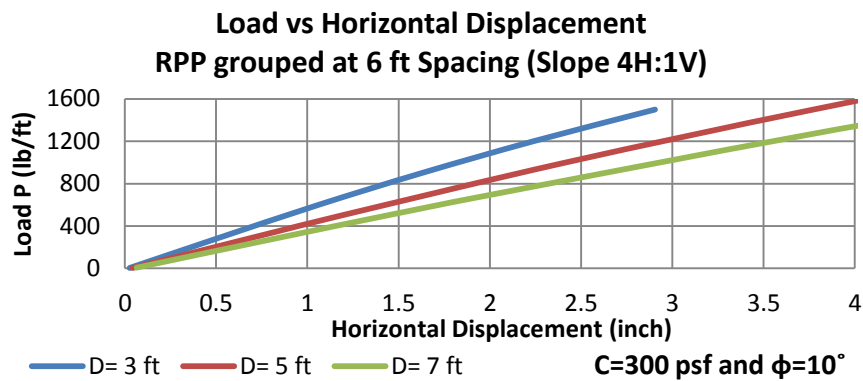
Figure B 58: Design Chart for Load versus Flexural Stress of RPP grouped at, a. 2-ft, b. 4-ft, c. 6-ft spacing for a soil of $c=300$ psf, $\phi=0^\circ$ and slope 4H:1V.



(a)

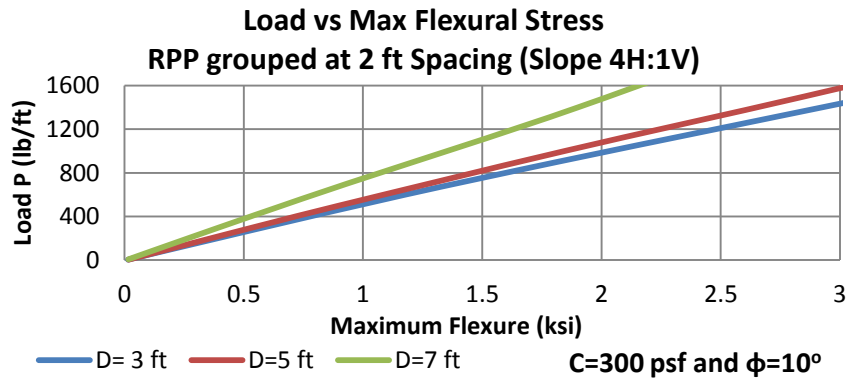


(b)

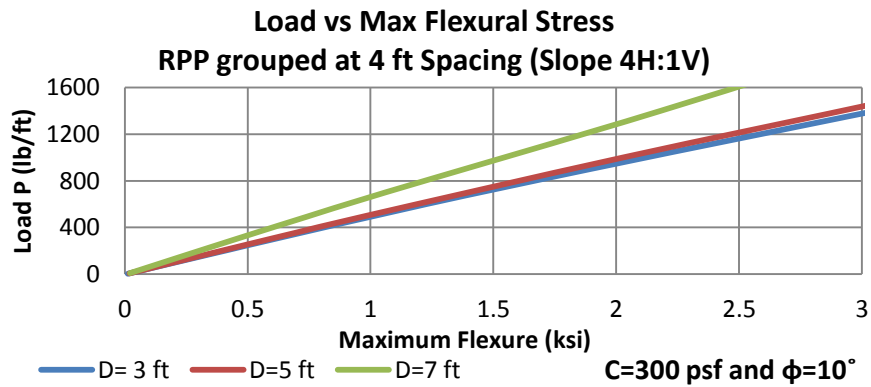


(c)

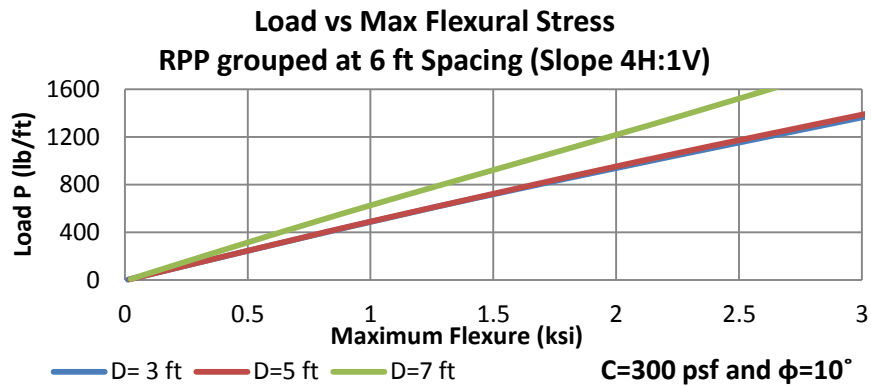
Figure B 59: Design Chart for Load versus Horizontal Displacement of RPP grouped at, a. 2-ft, b. 4-ft, c. 6-ft spacing for a soil of $c=300$ psf, $\phi=10^\circ$ and slope 4H:1V.



(a)

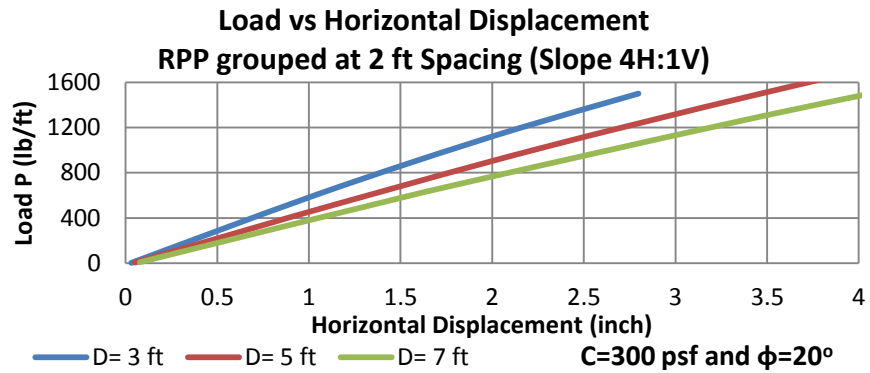


(b)

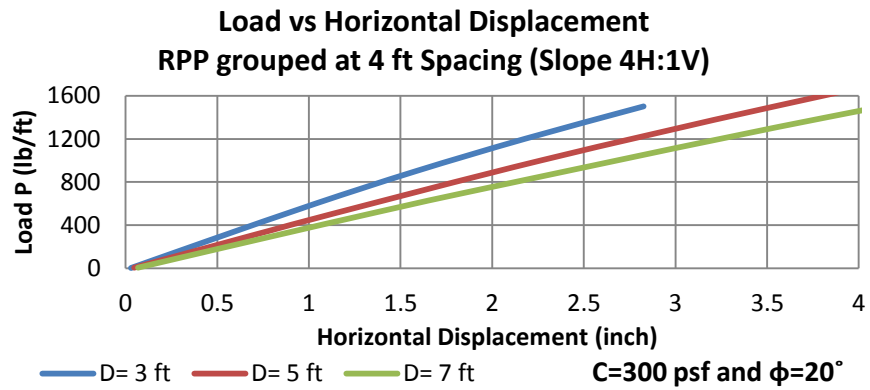


(c)

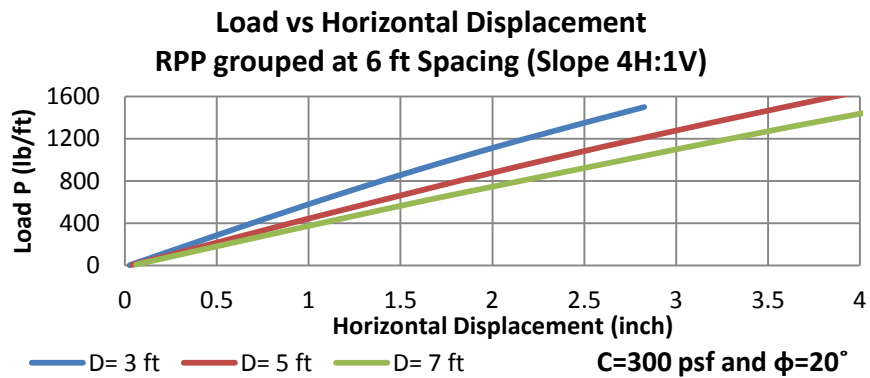
Figure B 60: Design Chart for Load versus Flexural Stress of RPP grouped at, a. 2-ft, b. 4-ft, c. 6-ft spacing for a soil of $c=300$ psf, $\phi=10^\circ$ and slope 4H:1V.



(a)

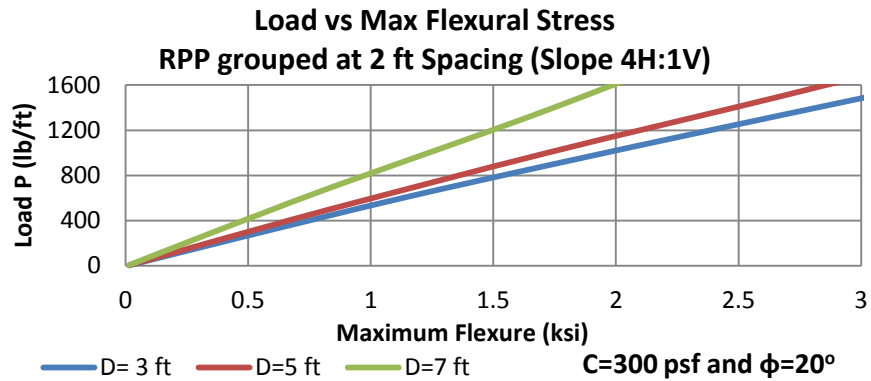


(b)

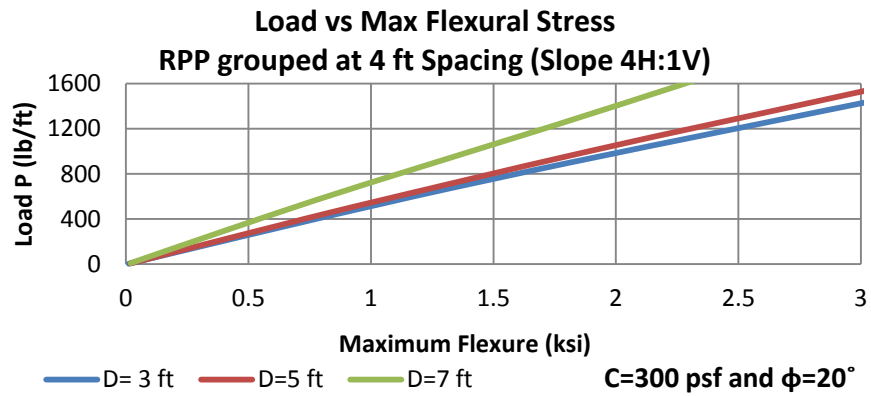


(c)

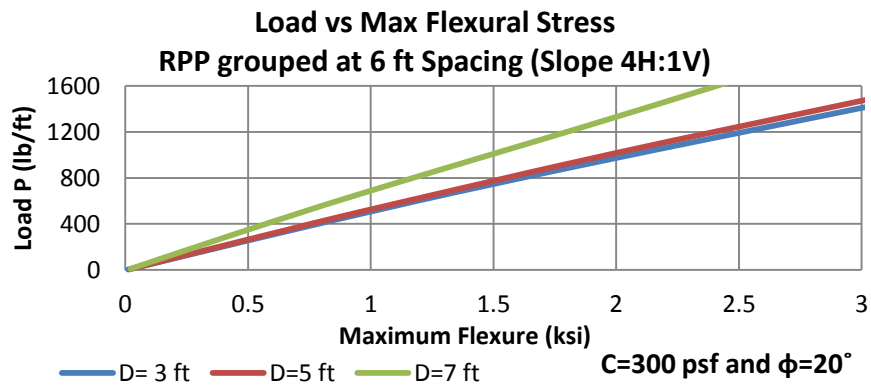
Figure B 61: Design Chart for Load versus Horizontal Displacement of RPP grouped at, a. 2-ft, b. 4-ft, c. 6-ft spacing for a soil of $c=300$ psf, $\phi=20^\circ$ and slope 4H:1V.



(a)

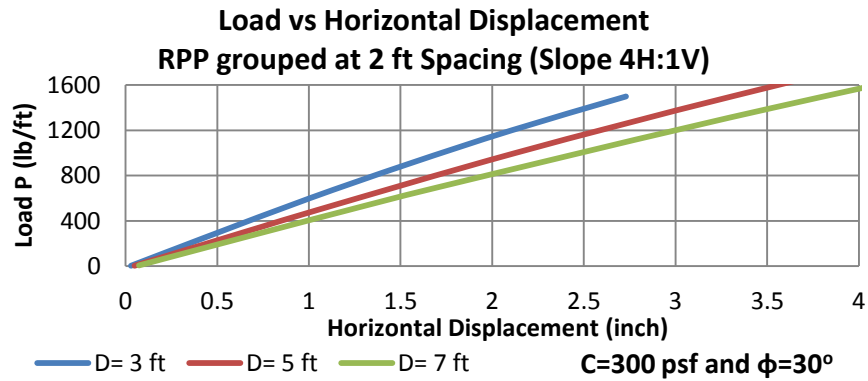


(b)

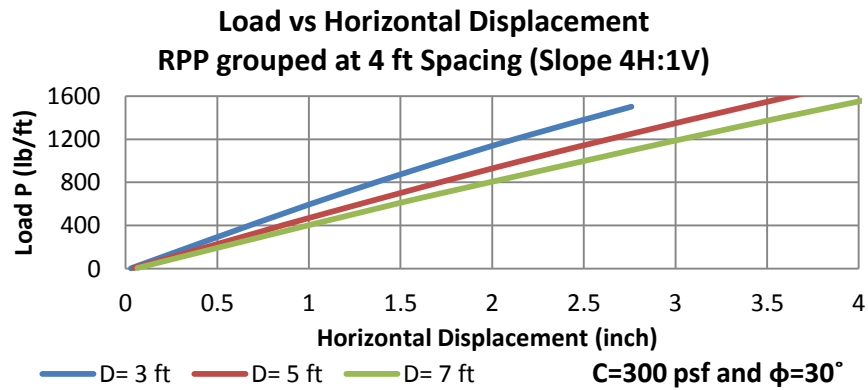


(c)

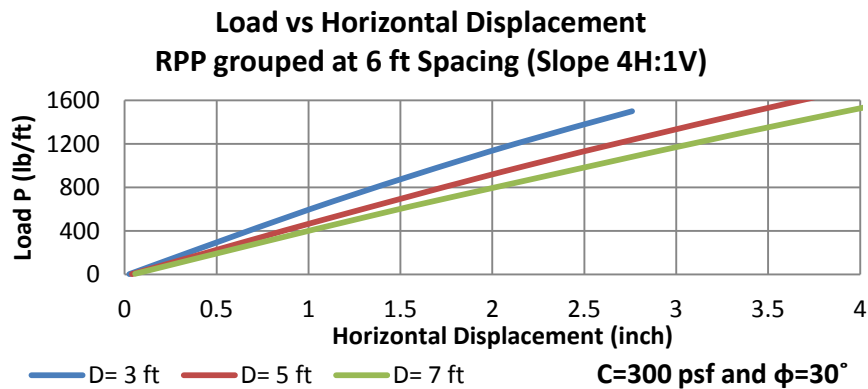
Figure B 62: Design Chart for Load versus Flexural Stress of RPP grouped at, a. 2-ft, b. 4-ft, c. 6-ft spacing for a soil of $c=300$ psf, $\phi=20^\circ$ and slope 4H:1V.



(a)

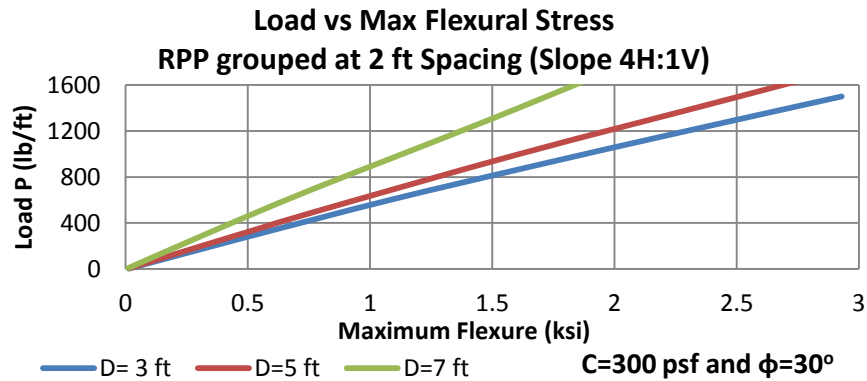


(b)

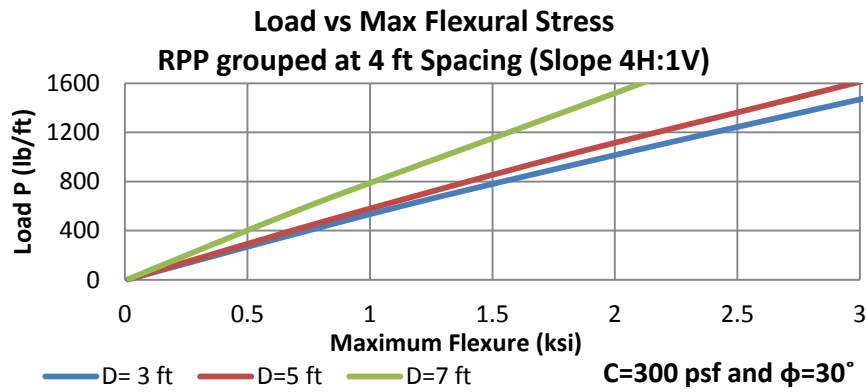


(c)

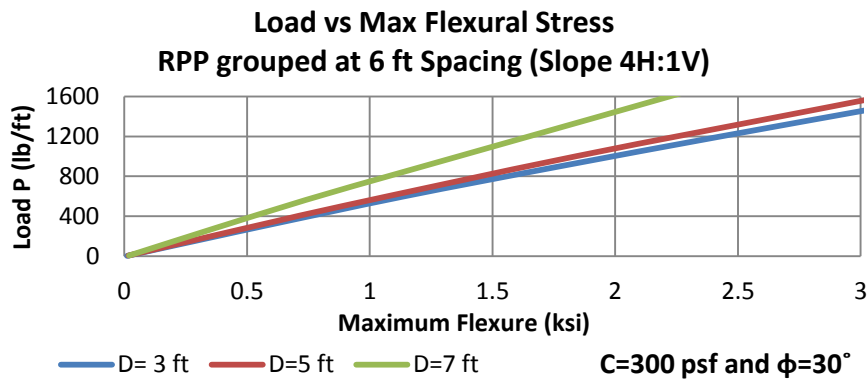
Figure B 63: Design Chart for Load versus Horizontal Displacement of RPP grouped at, a. 2-ft, b. 4-ft, c. 6-ft spacing for a soil of $c=300$ psf, $\phi=30^\circ$ and slope 4H:1V.



(a)



(b)



(c)

Figure B 64: Design Chart for Load versus Flexural Stress of RPP grouped at, a. 2-ft, b. 4-ft, c. 6-ft spacing for a soil of $c=300$ psf, $\phi=30^\circ$ and slope 4H:1V.

Appendix C

Multiplication Factors for Horizontal Displacement and Flexural stress

List of Tables

Table Number	Multiplication Factors	Slope Ratio
C 1	Horizontal Displacement	2H:1V
C 2	Horizontal Displacement	3H:1V
C 3	Horizontal Displacement	4H:1V
C 4	Flexural Stress	2H:1V
C 5	Flexural Stress	3H:1V
C 6	Flexural Stress	4H:1V

**C 1: Multiplication Factors for Horizontal Displacement between RPP Grouped at
Different Spacing versus Single RPP for Slope Ratio of 2H:1V**

Slip Surface Soil Parameters	Allowable Horizontal Displacement (in)	Multiplication Factor for Horizontal Displacement (Single RPP vs Grouped RPP)								
		Depth of Slip Surface 3 ft			Depth of Slip Surface 5 ft			Depth of Slip Surface 7 ft		
		Spacing of RPP 2 ft	Spacing of RPP 4 ft	Spacing of RPP 6 ft	Spacing of RPP 2 ft	Spacing of RPP 4 ft	Spacing of RPP 6 ft	Spacing of RPP 2 ft	Spacing of RPP 4 ft	Spacing of RPP 6 ft
C=100 psf and $\phi=20^\circ$	1	1	1	1	1.09	1.06	1.03	1.28	1.20	1.13
	2	1	1	1	1.09	1.07	1.04	1.27	1.18	1.14
	3	1	1	1	1.1	1.07	1.05	1.26	1.19	1.14
	4				1.09	1.07	1.05	1.27	1.21	1.15
C=100 psf and $\phi=30^\circ$	1	1	1	1	1.04	1.02	1	1	1	1
	2	1	1	1	1.03	1.02	1.01	1.05	1.04	1.04
	3	1	1	1	1.04	1.02	1.01	1.08	1.07	1.04
	4				1.03	1.01	1	1.09	1.08	1.05
C=200 psf and $\phi=0^\circ$	1	1	1	1	1.10	1.06	1.04			
	2	1	1	1	1.11	1.06	1.03			
	3	1	1	1	1.11	1.07	1.04			
	4				1.13	1.09	1.06			
C=200 psf and $\phi=10^\circ$	1	1	1	1	1	1	1	1.21	1.14	1.10
	2	1	1	1	1.03	1.02	1	1.22	1.13	1.10
	3	1	1	1	1.04	1.02	1	1.23	1.15	1.11
	4				1.04	1.02	1	1.23	1.15	1.11
C=200 psf and $\phi=20^\circ$	1	1	1	1	1	1	1	1	1	1
	2	1	1	1	1	1	1	1	1	1
	3	1	1	1	1.03	1.02	1	1.05	1.05	1.02
	4				1.03	1	1	1.06	1.04	1.03
C=200 psf and $\phi=30^\circ$	1	1	1	1	1	1	1	1	1	1
	2	1	1	1	1	1	1	1	1	1
	3	1	1	1	1.03	1	1	1.05	1.04	1
	4				1.03	1	1	1.05	1.03	1.02
C=300 psf and $\phi=0^\circ$	1	1	1	1	1	1	1	1.32	1.13	1.05
	2	1	1	1	1.03	1.02	1	1.28	1.11	1.04
	3	1	1	1	1.04	1.03	1	1.29	1.12	1.05
	4				1.04	1.03	1	1.29	1.11	1.06
C=300 psf and $\phi=10^\circ$	1	1	1	1	1	1	1	1	1	1.02
	2	1	1	1	1.04	1.03	1	1.04	1.03	1.02
	3	1	1	1	1.04	1.03	1	1.04	1.03	1.02
	4				1.04	1.03	1	1.05	1.03	1.02

Table C 1-Continued

C=300 psf and $\phi=20^\circ$	1	1	1	1	1	1	1	1	1	1
	2	1	1	1	1.04	1	1	1.04	1.03	1
	3	1	1	1	1.04	1	1	1.04	1.03	1.02
	4				1.04	1	1	1.04	1.03	1.02
C=300 psf and $\phi=30^\circ$	1	1	1	1	1.03	1	1	1	1	1
	2	1	1	1	1.03	1	1	1.04	1	1
	3	1	1	1	1.03	1	1	1.04	1.03	1.02
	4				1.03	1	1	1.04	1.03	1.02

Table C 2: Multiplication Factor for Horizontal Displacement between RPP Grouped at
Different Spacing versus Single RPP for Slope Ratio of 3H:1V.

Slip Surface Soil Parameters	Allowable Horizontal Displacement (in)	Multiplication Factor for Horizontal Displacement (Single RPP vs Grouped RPP)								
		Depth of Slip Surface 3 ft			Depth of Slip Surface 5 ft			Depth of Slip Surface 7 ft		
		Spacing of RPP 2 ft	Spacing of RPP 4 ft	Spacing of RPP 6 ft	Spacing of RPP 2 ft	Spacing of RPP 4 ft	Spacing of RPP 6 ft	Spacing of RPP 2 ft	Spacing of RPP 4 ft	Spacing of RPP 6 ft
C=100 psf and $\phi=10^\circ$	1	1	1	1	1.11	1.10	1.06	1.28	1.15	1.08
	2	1	1	1	1.10	1.08	1.05	1.27	1.16	1.09
	3	1	1	1	1.11	1.08	1.06	1.29	1.18	1.11
	4				1.13	1.09	1.07	1.34	1.21	1.13
C=100 psf and $\phi=20^\circ$	1	1	1	1	1	1	1	1	1	1
	2	1	1	1	1.04	1	1	1.08	1.05	1.03
	3	1	1	1	1.05	1.03	1	1.09	1.07	1.04
	4				1.04	1	1	1.10	1.08	1.04
C=100 psf and $\phi=30^\circ$	1	1	1	1	1	1	1	1	1	1
	2	1	1	1	1.04	1.02	1	1.06	1.04	1
	3	1	1	1	1.04	1.02	1	1.07	1.04	1
	4				1.04	1.02	1	1.07	1.05	1.03
C=200 psf and $\phi=0^\circ$	1	1	1	1	1	1	1	1.51	1.41	1.24
	2	1	1	1	1.06	1.04	1	1.32	1.29	1.21
	3	1	1	1	1.06	1.05	1	1.39	1.35	1.26
	4				1.06	1.04	1	1.48	1.44	1.35
C=200 psf and $\phi=10^\circ$	1	1	1	1	1	1	1	1.07	1.04	1.02
	2	1	1	1	1.04	1	1	1.08	1.05	1.02
	3	1	1	1	1.04	1.03	1	1.09	1.07	1.03
	4				1.04	1.03	1	1.09	1.07	1.04
C=200 psf and $\phi=20^\circ$	1	1	1	1	1	1	1	1	1	1
	2	1	1	1	1.06	1.04	1	1.06	1.05	1.02
	3	1	1	1	1.04	1.02	1	1.06	1.05	1.02
	4				1.04	1.02	1	1.06	1.04	1.02
C=200 psf and $\phi=30^\circ$	1	1	1	1	1	1	1	1	1	1
	2	1	1	1	1.04	1.02	1	1.05	1.03	1
	3	1	1	1	1.04	1.02	1	1.05	1.04	1.02
	4				1.04	1.02	1	1.06	1.04	1.02
C=300 psf and $\phi=0^\circ$	1	1	1	1	1	1	1	1	1	1
	2	1	1	1	1.04	1.02	1	1.08	1.06	1.03
	3	1	1	1	1.04	1.02	1	1.08	1.06	1.03
	4				1.04	1.02	1	1.08	1.06	1.03

Table C 2-Continued

C=300 psf and $\phi=10^\circ$	1	1	1	1	1.04	1	1	1	1	1
	2	1	1	1	1.05	1.02	1	1.06	1.04	1.02
	3	1	1	1	1.05	1.02	1	1.06	1.04	1.02
	4				1.05	1.02	1	1.06	1.04	1.02
C=300 psf and $\phi=20^\circ$	1	1	1	1	1	1	1	1	1	1
	2	1	1	1	1.04	1.02	1	1.05	1.04	1.02
	3	1	1	1	1.04	1.02	1	1.05	1.04	1.02
	4				1.04	1.02	1	1.05	1.04	1.02
C=300 psf and $\phi=30^\circ$	1	1	1	1	1	1	1	1	1	1
	2	1	1	1	1.04	1	1	1.04	1.03	1
	3	1	1	1	1.03	1.02	1	1.05	1.03	1
	4				1.03	1.02	1	1.05	1.03	1

Table C 3 Multiplication Factor for Horizontal Displacement between RPP Grouped at
Different Spacing versus Single RPP for Slope Ratio of 4H:1V.

Slip Surface Soil Parameters	Allowable Horizontal Displacement (in)	Multiplication Factor for Horizontal Displacement (Single RPP vs Grouped RPP)								
		Depth of Slip Surface 3 ft			Depth of Slip Surface 5 ft			Depth of Slip Surface 7 ft		
		Spacing of RPP 2 ft	Spacing of RPP 4 ft	Spacing of RPP 6 ft	Spacing of RPP 2 ft	Spacing of RPP 4 ft	Spacing of RPP 6 ft	Spacing of RPP 2 ft	Spacing of RPP 4 ft	Spacing of RPP 6 ft
C=100 psf and $\phi=10^\circ$	1	1	1	1	1.06	1.04	1.03	1.15	1.07	1.04
	2	1	1	1	1.06	1.04	1.03	1.17	1.09	1.07
	3	1	1	1	1.07	1.04	1.03	1.16	1.10	1.06
	4				1.07	1.04	1.02	1.18	1.10	1.08
C=100 psf and $\phi=20^\circ$	1	1	1	1	1.04	1.03	1	1.07	1.05	1.03
	2	1	1	1	1.05	1.03	1	1.07	1.05	1.02
	3	1	1	1	1.05	1.03	1	1.08	1.06	1.02
	4				1.04	1.02	1	1.07	1.05	1.03
C=100 psf and $\phi=30^\circ$	1	1	1	1	1.05	1.02	1	1.07	1.05	1.03
	2	1	1	1	1.04	1.03	1	1.07	1.05	1.04
	3	1	1	1	1.05	1.03	1	1.07	1.05	1.04
	4				1.04	1.02	1	1.07	1.05	1.03
C=200 psf and $\phi=0^\circ$	1	1	1	1	1.04	1.03	1	1.12	1.10	1.08
	2	1	1	1	1.05	1.03	1	1.14	1.10	1.06
	3	1	1	1	1.05	1.04	1	1.16	1.12	1.09
	4				1.05	1.03	1	1.18	1.16	1.11
C=200 psf and $\phi=10^\circ$	1	1	1	1	1.05	1.03	1	1.07	1.06	1
	2	1	1	1	1.05	1.03	1	1.07	1.06	1.03
	3	1	1	1	1.05	1.04	1	1.07	1.06	1.02
	4				1.05	1.03	1	1.08	1.05	1.03
C=200 psf and $\phi=20^\circ$	1	1	1	1	1.04	1.03	1	1.07	1.04	1.02
	2	1	1	1	1.05	1.03	1	1.06	1.04	1.03
	3	1	1	1	1.05	1.03	1	1.07	1.05	1.03
	4				1.05	1.03	1	1.07	1.05	1.02
C=200 psf and $\phi=30^\circ$	1	1	1	1	1.05	1.03	1	1.05	1.03	1
	2	1	1	1	1.05	1.03	1	1.05	1.04	1.02
	3	1	1	1	1.04	1.03	1	1.06	1.04	1.02
	4				1.04	1.02	1	1.06	1.04	1.02
C=300 psf and $\phi=0^\circ$	1	1	1	1	1.04	1.02	1	1.05	1	1
	2	1	1	1	1.04	1.03	1	1.06	1.05	1.03
	3	1	1	1	1.05	1.02	1	1.07	1.05	1.03
	4				1.04	1.02	1	1.07	1.05	1.03

Table C 3-Continued

C=300 psf and $\phi=10^\circ$	1	1	1	1	1	1	1	1.06	1.04	1
	2	1	1	1	1.04	1.02	1	1.06	1.04	1.02
	3	1	1	1	1.04	1.02	1	1.06	1.05	1.03
	4				1.04	1.02	1	1.07	1.05	1.03
C=300 psf and $\phi=20^\circ$	1	1	1	1	1	1	1	1.06	1	1
	2	1	1	1	1.04	1.02	1	1.06	1.03	1.02
	3	1	1	1	1.04	1.02	1	1.06	1.04	1.02
	4				1.04	1.03	1	1.06	1.04	1.03
C=300 psf and $\phi=30^\circ$	1	1	1	1	1	1	1	1	1	1
	2	1	1	1	1.04	1.02	1	1.04	1.03	1
	3	1	1	1	1.04	1.02	1	1.05	1.04	1.02
	4				1.04	1.02	1	1.05	1.04	1.02

**C 4: Multiplication Factors for Flexural Stress between RPP Grouped at Different Spacing
versus Single RPP for Slope Ratio of 2H:1V**

Slip Surface Soil Parameters	Allowable Flexural Stress (ksi)	Multiplication Factor for Flexural Stress (Single RPP vs Grouped RPP)								
		Depth of Slip Surface 3 ft			Depth of Slip Surface 5 ft			Depth of Slip Surface 7 ft		
		Spacing of RPP 2 ft	Spacing of RPP 4 ft	Spacing of RPP 6 ft	Spacing of RPP 2 ft	Spacing of RPP 4 ft	Spacing of RPP 6 ft	Spacing of RPP 2 ft	Spacing of RPP 4 ft	Spacing of RPP 6 ft
C=100 psf and $\phi=20^\circ$	1	1.04	1	1	1.27	1.13	1.07	1.55	1.42	1.28
	2	1.04	1	1	1.27	1.15	1.09	1.54	1.36	1.24
	3	1.04	1	1	1.27	1.15	1.09	1.54	1.38	1.26
C=100 psf and $\phi=30^\circ$	1	1.04	1	1	1.14	1.05	1	1.26	1.14	1.08
	2	1.04	1	1	1.12	1.04	1	1.26	1.14	1.08
	3	1.04	1	1	1.12	1.05	1.02	1.26	1.14	1.09
C=200 psf and $\phi=0^\circ$	1	1.07	1	1	1.20	1.08	1.04			
	2	1.05	1	1	1.23	1.10	1.05			
	3	1.05	1	1	1.26	1.11	1.06			
C=200 psf and $\phi=10^\circ$	1	1.04	1	1	1.14	1.05	1.03	1.56	1.30	1.20
	2	1.04	1	1	1.14	1.06	1.03	1.51	1.29	1.20
	3	1.04	1	1	1.14	1.06	1.03	1.50	1.31	1.23
C=200 psf and $\phi=20^\circ$	1	1.04	1	1	1.14	1.06	1.03	1.23	1.12	1.05
	2	1.04	1	1	1.14	1.06	1.03	1.22	1.10	1.05
	3	1.04	1	1	1.14	1.07	1.02	1.22	1.10	1.05
C=200 psf and $\phi=30^\circ$	1	1.07	1	1	1.14	1.05	1	1.22	1.08	1.03
	2	1.06	1	1	1.13	1.05	1	1.22	1.09	1.03
	3	1.06	1	1	1.13	1.05	1	1.22	1.08	1.04
C=300 psf and $\phi=0^\circ$	1	1.06	1	1	1.12	1.05	1.02	1.61	1.35	1.13
	2	1.05	1	1	1.13	1.05	1.02	1.58	1.29	1.10
	3	1.04	1	1	1.13	1.05	1.02	1.57	1.30	1.11
C=300 psf and $\phi=10^\circ$	1	1.07	1	1	1.16	1.07	1.03	1.23	1.10	1.04
	2	1.06	1	1	1.15	1.06	1.03	1.23	1.09	1.04
	3	1.06	1	1	1.14	1.06	1.03	1.22	1.08	1.04
C=300 psf and $\phi=20^\circ$	1	1.06	1	1	1.16	1.06	1.03	1.22	1.09	1.04
	2	1.06	1	1	1.15	1.05	1.03	1.22	1.09	1.04
	3	1.05	1	1	1.15	1.06	1.03	1.21	1.10	1.04
C=300 psf and $\phi=30^\circ$	1	1.06	1	1	1.14	1.06	1	1.22	1.09	1.04
	2	1.06	1	1	1.14	1.06	1	1.21	1.09	1.04
	3	1.05	1	1	1.14	1.06	1	1.21	1.08	1.03

**C 5: Multiplication Factors for Flexural Stress between RPP Grouped at Different Spacing
versus Single RPP for Slope Ratio of 3H:1V**

Slip Surface Soil Parameters	Allowable Flexural Stress (ksi)	Multiplication Factor for Flexural Stress (Single RPP vs Grouped RPP)								
		Depth of Slip Surface 3 ft			Depth of Slip Surface 5 ft			Depth of Slip Surface 7 ft		
		Spacing of RPP 2 ft	Spacing of RPP 4 ft	Spacing of RPP 6 ft	Spacing of RPP 2 ft	Spacing of RPP 4 ft	Spacing of RPP 6 ft	Spacing of RPP 2 ft	Spacing of RPP 4 ft	Spacing of RPP 6 ft
C=100 psf and $\phi=10^\circ$	1	1.06	1	1	1.28	1.16	1.09	1.55	1.32	1.16
	2	1.06	1	1	1.27	1.15	1.09	1.49	1.34	1.19
	3	1.05	1	1	1.27	1.15	1.09	1.51	1.37	1.20
C=100 psf and $\phi=20^\circ$	1	1.05	1	1	1.17	1.07	1.04	1.33	1.15	1.08
	2	1.05	1	1	1.17	1.06	1.03	1.33	1.15	1.08
	3	1.05	1	1	1.16	1.06	1.03	1.33	1.16	1.08
C=100 psf and $\phi=30^\circ$	1	1.05	1	1	1.16	1.04	1	1.23	1.11	1.05
	2	1.05	1	1	1.16	1.05	1.02	1.25	1.10	1.04
	3	1.05	1	1	1.16	1.06	1.02	1.28	1.11	1.04
C=200 psf and $\phi=0^\circ$	1	1.06	1	1	1.18	1.08	1.04	1.88	1.54	1.37
	2	1.06	1	1	1.18	1.08	1.04	1.81	1.55	1.35
	3	1.06	1	1	1.18	1.09	1.05	1.78	1.52	1.34
C=200 psf and $\phi=10^\circ$	1	1.05	1	1	1.17	1.08	1.03	1.28	1.12	1.06
	2	1.05	1	1	1.16	1.07	1.04	1.30	1.13	1.08
	3	1.05	1	1	1.16	1.06	1.03	1.32	1.15	1.08
C=200 psf and $\phi=20^\circ$	1	1.05	1	1	1.16	1.07	1.03	1.26	1.10	1.04
	2	1.05	1	1	1.16	1.05	1.03	1.26	1.11	1.05
	3	1.05	1	1	1.16	1.06	1.03	1.27	1.10	1.04
C=200 psf and $\phi=30^\circ$	1	1.06	1	1	1.16	1.06	1.03	1.25	1.09	1.05
	2	1.06	1	1	1.15	1.06	1.03	1.25	1.10	1.05
	3	1.06	1	1	1.15	1.06	1.03	1.27	1.11	1.05
C=300 psf and $\phi=0^\circ$	1	1.06	1	1	1.15	1.06	1.02	1.26	1.13	1.06
	2	1.05	1	1	1.15	1.06	1.02	1.27	1.14	1.07
	3	1.05	1	1	1.15	1.06	1.02	1.31	1.15	1.07
C=300 psf and $\phi=10^\circ$	1	1.05	1	1	1.15	1.07	1.03	1.23	1.09	1.04
	2	1.05	1	1	1.15	1.07	1.03	1.24	1.10	1.04
	3	1.05	1	1	1.15	1.06	1.03	1.26	1.10	1.04
C=300 psf and $\phi=20^\circ$	1	1.06	1	1	1.16	1.06	1.03	1.25	1.09	1.04
	2	1.06	1	1	1.15	1.06	1.03	1.25	1.10	1.05
	3	1.06	1	1	1.15	1.06	1.03	1.27	1.10	1.04
C=300 psf and $\phi=30^\circ$	1	1.06	1	1	1.17	1.06	1.02	1.24	1.10	1.04
	2	1.06	1	1	1.16	1.06	1.03	1.24	1.10	1.04
	3	1.06	1	1	1.16	1.06	1.02	1.26	1.10	1.04

**C 6: Multiplication Factors for Flexural Stress between RPP Grouped at Different Spacing
versus Single RPP for Slope Ratio of 4H:1V**

Slip Surface Soil Parameters	Allowable Flexural Stress (ksi)	Multiplication Factor for Flexural Stress (Single RPP vs Grouped RPP)								
		Depth of Slip Surface 3 ft			Depth of Slip Surface 5 ft			Depth of Slip Surface 7 ft		
		Spacing of RPP 2 ft	Spacing of RPP 4 ft	Spacing of RPP 6 ft	Spacing of RPP 2 ft	Spacing of RPP 4 ft	Spacing of RPP 6 ft	Spacing of RPP 2 ft	Spacing of RPP 4 ft	Spacing of RPP 6 ft
C=100 psf and $\phi=10^\circ$	1	1.05	1	1	1.17	1.09	1.05	1.39	1.19	1.13
	2	1.05	1	1	1.19	1.09	1.04	1.43	1.24	1.15
	3	1.05	1	1	1.19	1.09	1.05	1.52	1.27	1.17
C=100 psf and $\phi=20^\circ$	1	1.04	1	1	1.16	1.07	1.03	1.26	1.13	1.06
	2	1.05	1	1	1.16	1.06	1.03	1.27	1.11	1.06
	3	1.05	1	1	1.16	1.06	1.03	1.32	1.13	1.06
C=100 psf and $\phi=30^\circ$	1	1.04	1	1	1.17	1.06	1.03	1.24	1.12	1.06
	2	1.05	1	1	1.17	1.07	1.03	1.28	1.12	1.06
	3	1.05	1	1	1.18	1.06	1.03	1.33	1.13	1.06
C=200 psf and $\phi=0^\circ$	1	1.05	1	1	1.16	1.06	1.03	1.36	1.21	1.14
	2	1.05	1	1	1.16	1.06	1.03	1.45	1.24	1.16
	3	1.05	1	1	1.16	1.06	1.03	1.58	1.29	1.19
C=200 psf and $\phi=10^\circ$	1	1.04	1	1	1.16	1.06	1.03	1.25	1.12	1.07
	2	1.04	1	1	1.16	1.06	1.03	1.27	1.12	1.06
	3	1.04	1	1	1.16	1.06	1.03	1.34	1.13	1.06
C=200 psf and $\phi=20^\circ$	1	1.04	1	1	1.15	1.07	1.03	1.26	1.11	1.06
	2	1.05	1	1	1.16	1.07	1.03	1.28	1.11	1.06
	3	1.05	1	1	1.17	1.07	1.03	1.34	1.13	1.06
C=200 psf and $\phi=30^\circ$	1	1.05	1	1	1.16	1.07	1.03	1.25	1.11	1.05
	2	1.05	1	1	1.16	1.06	1.02	1.27	1.11	1.05
	3	1.05	1	1	1.17	1.06	1.02	1.34	1.12	1.05
C=300 psf and $\phi=0^\circ$	1	1.06	1	1	1.17	1.06	1.03	1.28	1.10	1.05
	2	1.06	1	1	1.17	1.06	1.03	1.30	1.10	1.05
	3	1.06	1	1	1.17	1.07	1.03	1.34	1.13	1.06
C=300 psf and $\phi=10^\circ$	1	1.04	1	1	1.16	1.06	1.03	1.25	1.12	1.06
	2	1.04	1	1	1.17	1.06	1.03	1.27	1.12	1.06
	3	1.05	1	1	1.17	1.06	1.03	1.34	1.12	1.06
C=300 psf and $\phi=20^\circ$	1	1.05	1	1	1.16	1.06	1.03	1.24	1.10	1.05
	2	1.05	1	1	1.16	1.06	1.03	1.26	1.11	1.06
	3	1.05	1	1	1.17	1.06	1.02	1.34	1.12	1.06
C=300 psf and $\phi=30^\circ$	1	1.04	1	1	1.17	1.06	1.02	1.24	1.10	1.05
	2	1.05	1	1	1.16	1.06	1.02	1.27	1.10	1.04
	3	1.05	1	1	1.17	1.06	1.02	1.33	1.12	1.05

Appendix D

Calculation of Factor of Safety for RPP Reinforced Slope using Multiplication Factors

Given,

Soil Type	Slope Height (ft)	Top Soil			Foundation Soil		
		c (psf)	ϕ (degree)	Y (pcf)	c (psf)	ϕ (degree)	Y (pcf)
Slope ratio 3H:1V	40	250	10	125	400	10	125

Depth of slip surface (perpendicular to slope surface) , D=7 ft

Length of slip surface, $L = [40^2 + (3 \cdot 40)^2]^{(0.5)} = 126.5$ ft

Slope inclination, $\beta = 18.43^\circ$

Unit weight of top soil, $Y' = 125$ pcf

Unit weight of saturated soil, $Y_{sat} = 125$ pcf

Depth of slip surface (vertically), $h = D / \cos \beta = 7 / \cos 18.43^\circ = 7.38$ ft

RPP spacing, $s = 3$ -ft

Mobilized load, $P = 725$ lb/ft (Khan, 2013)

Multiplication Factor for RPP at 3-ft spacing, $MF = 1.06$ (from table 4.6)

Factor of Safety of Reinforced Slope considering 2 inch allowable horizontal displacement,

$$FS = \frac{c' L + h L Y' \cos^2 \beta \tan \phi' + \left(\frac{L}{s} + 1\right) * MF * P}{h L \sin \beta \cos \beta Y_{sat}}$$

$$FS = \frac{250 * 126.5 + 7.38 * 126.5 * 125 * \cos^2 18.43^\circ \tan 10^\circ + \left(\frac{126.5}{3} + 1\right) * 1.06 * 725}{7.38 * 126.5 * \sin 18.43^\circ \cos 18.43^\circ * 125}$$

$$FS = 2.38$$

Appendix E

Calculation of Factor of Safety for RPP Reinforced Slope using Group Resistance Design

Charts

List of Figures

Figure No	Types of Design Chart	Cohesion (psf)	Friction Angle (Degree)	Slope Ratio
E 1	Load vs Horizontal Displacement	200	10	3H:1V
E 2	Load vs Horizontal Displacement	300	10	3H:1V

Given,

Soil Type	Slope Height (ft)	Top Soil			Foundation Soil		
		c (psf)	ϕ (degree)	Y (pcf)	c (psf)	ϕ (degree)	Y (pcf)
Slope ratio 3H:1V	40	250	10	125	400	10	125

Depth of slip surface (perpendicular to slope surface) , $D=7$ ft

Length of slip surface, $L = [40^2 + (3 \cdot 40)^2]^{(0.5)} = 126.5$ ft

Slope inclination, $\beta = 18.43^\circ$

Unit weight of top soil, $Y' = 125$ pcf

Unit weight of saturated soil, $Y_{sat} = 125$ pcf

Depth of slip surface (vertically), $h = D / \cos \beta = 7 / \cos 18.43^\circ = 7.38$ ft

RPP spacing, $s=3$ -ft

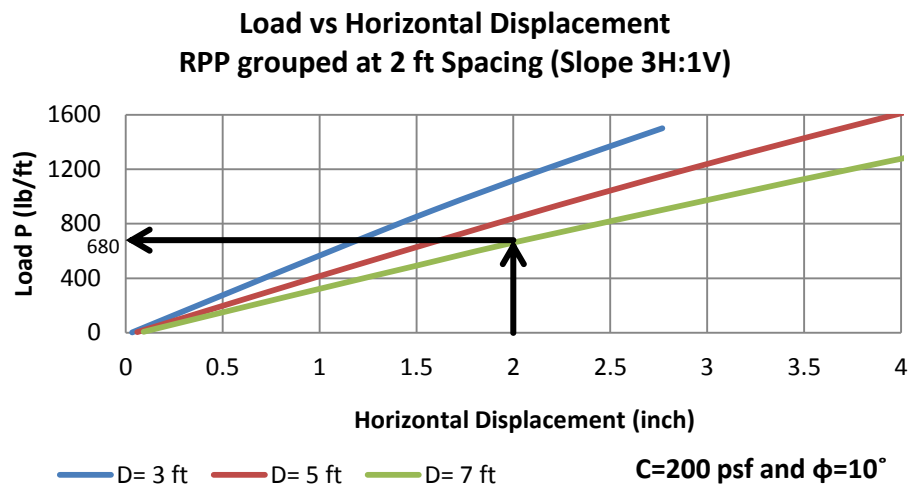
Mobilized load (for $c=250$ psf and $\phi=10^\circ$), $P' = (680+660+730+715)/4 = 696.25$ lb/ft (from figure E 1 and E 2, shown below)

Factor of Safety of Reinforced Slope considering 2 inch allowable horizontal displacement,

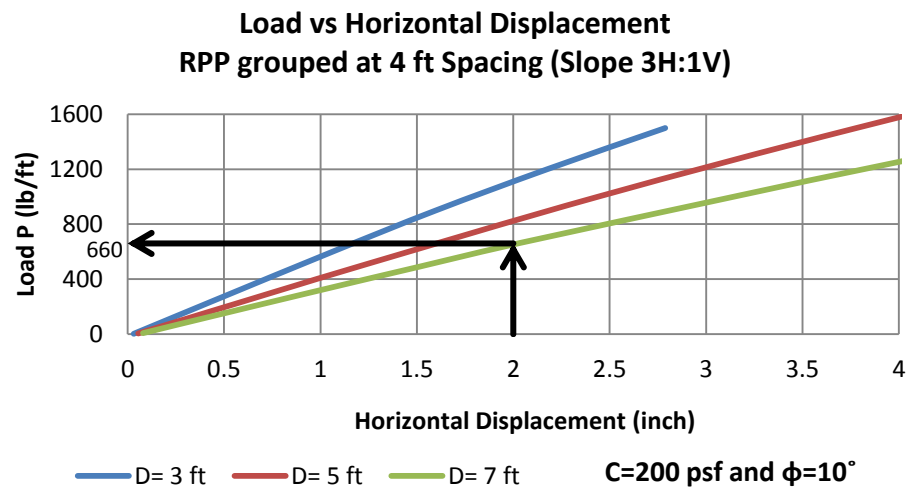
$$FS = \frac{c' L + h L Y' \cos^2 \beta \tan \phi' + \left(\frac{L}{s} + 1\right) P'}{h L \sin \beta \cos \beta Y_{sat}}$$

$$FS = \frac{250 \cdot 126.5 + 7.38 \cdot 126.5 \cdot 125 \cdot \cos^2 18.43^\circ \tan 10^\circ + \left(\frac{126.5}{3} + 1\right) \cdot 696.25}{7.38 \cdot 126.5 \cdot \sin 18.43^\circ \cos 18.43^\circ \cdot 125}$$

FS= 2.29

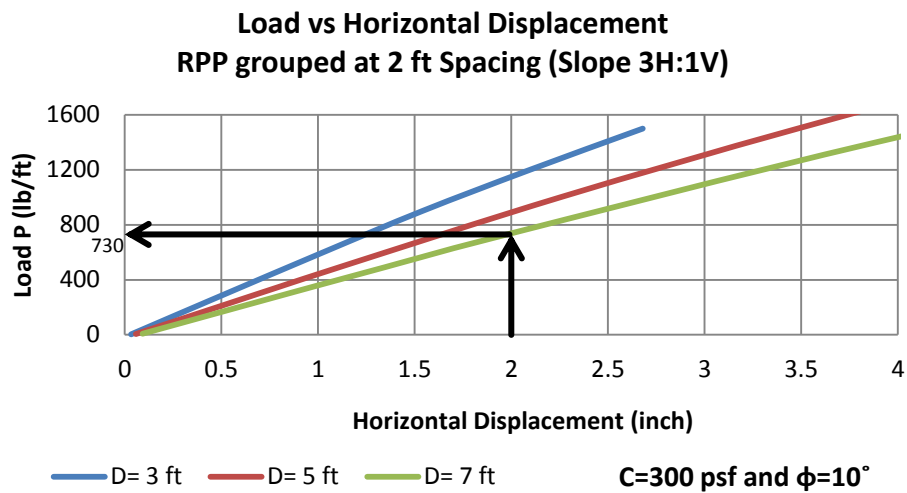


(a)

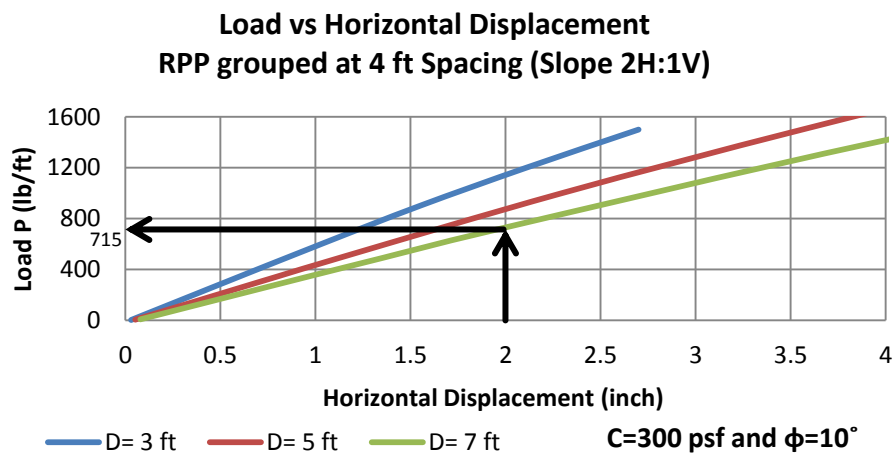


(b)

Figure E 1: Design Chart for Load versus Horizontal Displacement of RPP grouped at,
a. 2-ft, b. 4-ft, spacing for a soil of $c=200$ psf, $\phi=10^\circ$ and slope 3H:1V.



(a)



(b)

Figure E 2: Design Chart for Load versus Horizontal Displacement of RPP grouped at,
a. 2-ft, b. 4-ft, spacing for a soil of $c=300$ psf, $\phi=10^\circ$ and slope 3H:1V.

References

- Abramson, L., Lee, t., Sharma, S., and Boyce, G., (2002). "Stability and Stabilization Methods." John Wiley, New York.
- Bachus, R. C., and R. D. (Barksdale, 1989). "Design methodology for foundations on stone columns." foundation engineering congress, Evanston, Illinois, pp. 244-257, June.
- Beles, A. A., and Stanculescu, I. I. (1958). "Thermal treatment as a means of improving the stability of earth masses." *Geotechnique*, Vol. 8, No. 4, pp. 158-165.
- Birley, A.W., Haworth, B., and Bachelor, J. (1991). "Physics of Plastics." Oxford University Press, New York.
- Bowders, J. J., Loehr, J. E., Salim, h., and Chen, C. W. (2003). "Engineering properties of recycled plastic pins for slope stabilization." *Transportation Research Record: Journal of the Transportation Research Board*, 1849(1), 39-46.
- Broms, B. B. (1991). "Stabilization of soil with lime columns". *Foundation Engineering Handbook*, Second Edition, H. Y. Fang, Ed. New York: Van Nostrand Reinhold, Chapter 24, pp. 833-855.
- Chen, C. W., Salim, H., Bowders, J. J., Loehr, E., and Owen, J. (2007). "Creep behavior of recycled plastic lumber in slope stabilization applications." *J. Mater. Civ. Eng.*, 19(2), 130-138.
- Day, R. W., and Axten, G. W. (1989). "Surficial stability of compacted clay slopes." *Journal of Geotechnical Engineering*, 115(4), 577-580.

Elias, V., B. Christopher, and R. Berg, (2001). "Mechanically stabilized earth walls and reinforced soil slopes design and construction guidelines." Report FHWA-NHI-00-043, Federal Highway Administration, Washington, D.C., 2001.

Fay, L., Akin, M., and Shi, X. (2012). "Cost-effective and sustainable road slope stabilization and erosion control." Transportation Research Board, (Vol. 430).

Hausmann, M. R. (1990). "Engineering Principles of Ground Modification." New York: McGraw-Hill.

Khan, M. S. (2013). "Sustainable slope stabilization using recycled plastic pin." Ph. D. Dissertation, The University of Texas at Arlington, Arlington, Texas.

Krishnaswamy, P. and Francini, R. (2000), "long term durability of recycled plastic lumber in structural application",
<http://www.environmental-expert.com/Files/0/articles/2183/2183.pdf> Feb 12, 2014.

Lizzi, F. (1985). "Pali Radice" (Root Piles) and "Reticulated Pali Radice, Underpinning." S. Thorburn and J. F. Hutchison, Eds. Glasgow and London: Surrey University Press, Chapter 4.

Loehr, J. E. and Bowders, J. J. (2007). "Slopes stabilization using recycled plastic pins-Phase III." Final Report RI98-007D, Missouri Department of Transportation, Jefferson City, Missouri.

Loehr, J. E., Bowders, J. J., Owen, J. W., Sommers, L., and Liew, W. (2000). "Stabilization of slopes using recycled plastic pins." Journal of the Transportation Research Board, 1-8.

McCormick, W., and Short, R. (2006). "Cost effective stabilization of clay slopes and failure using plate piles" Proc., IAEG2006, The Geological Society of London, London, United Kingdom, 1-7.

McLaren, M. G. (1995). "Recycled plastic lumber and shapes, design and specifications." Proc., 13th Structures Congress, Vol. 1, ASCE, New York, 819-833.

Nusbaum, P. J., and B. E. Colley (1971). "Dam Construction and facing with soil cement." Portland Cement Association.

Titi, H., and Helwany, S. (2007). "Investigation of vertical members to resist surficial slope instabilities." Wisconsin Department of Transportation, Madison, WI.

Wisconsin Department of Transportation (2003). "Standard specifications for highway and structure construction."

Biographical Information

Mohammad Rezaul Haque Bhuiyan was born in Bangladesh, a small country with idyllic beauty. He received his Bachelor of Science degree in Civil Engineering from Military Institute of Science and Technology, Dhaka, Bangladesh in 2006. . He then spent the following year in Liberia as a project engineer under United Nations and till June 2010 worked in Corps of Engineers of Bangladesh Army as a Major. He got admitted in the University of Texas at Arlington in Fall 2011 as a part time student and received his Master's degree in civil engineering with emphasis on geotechnical engineering in Spring 2014. His aim is to become an efficient geotechnical engineer by gaining industrial experience.